Coordination of late stages of cytokinesis by the inhibitor of apoptosis protein BRUCE

Dissertation der
Fakultät für Biologie der
Ludwig-Maximilians-Universität
München

Vorgelegt von
Diplom-Biochemiker
Christian Pohl

Juli 2008

Ehrenwörtliche Erklärung

Hiermit erkläre ich, dass ich die vorliegende Dissertation selbständig und ohne unerlaubte Hilfe angefertigt habe. Ich habe weder anderweitig versucht, eine Dissertation einzureichen oder eine Doktorprüfung durchzuführen, noch habe ich diese Dissertation oder Teile derselben einer anderen Prüfungskommission vorgelegt.

München, Februar 2008

Die vorliegende Arbeit wurde zwischen Februar 2003 und Oktober 2007 unter der Anleitung von Prof. Dr. Stefan Jentsch am Max-Planck-Institut für Biochemie, Martinsried, durchgeführt.

Wesentliche Teile dieser Arbeit sind veröffentlicht in:

Bartke T, **Pohl C**, Pyrowolakis G, and Jentsch S. (2004). Dual Role of BRUCE as an Antiapoptotic IAP and a Chimeric E2/E3 Ubiquitin Ligase. *Mol. Cell* **14**, 801-811.

Pohl C, Jentsch S. (2008). Final Stages of Cytokinesis and Midbody Ring Formation are Controlled by BRUCE. *Cell*, **132**, 832-845.

Teile dieser Arbeit (Text und Abbildungen) sind daher diesen Veröffentlichungen entlehnt.

Promotionsgesuch eingereicht am: 18. März 2008

Tag der mündlichen Prüfung: 16. Juli 2008

Erster Gutachter: Prof. Dr. Stefan Jentsch

Zweiter Gutachter: Prof. Dr. Michael Schleicher

Contents

1 Summary

Cell division entails the segregation of replicated chromosomes during mitosis and the separation of the cytoplasm and its organellar content in cytokinesis to yield two daughter cells. During cytokinesis a circumferential furrow is established on the surface of a dividing cell that deepens perpendicular to the axis of the mitotic spindle. The furrow differentiates into the intercellular bridge, which contains a specialized organelle, the midbody, lying in its centre. At the midbody, membrane insertion allows sealing of the cytoplasmic channel that interconnects the daughter cells and results in their separation. High fidelity in cytokinesis regulation is an essential mechanism to prevent aberrant divisions and, in consequence, multinucleation and accumulation of centrioles that can lead to unwanted cell transformation.

This study demonstrates that BRUCE (baculovirus inhibitor of apoptosis repeat containing ubiquitin-conjugating enzyme), a huge 528 kDa anti-apoptotic protein with ubiquitin-conjugating activity, is a regulator of cytokinesis. Depletion of BRUCE from cultured mammalian cells leads to the formation of elongated syncytia and to cytokinesis-associated apoptosis. Furthermore, BRUCE is required for proper midbody structure and formation of its central part, the midbody ring.

It is shown that BRUCE can serve as a multifunctional scaffold by interacting with the vesicle targeting machinery and mitotic regulators. Upon mitotic exit, BRUCE is targeted to the midbody ring *via* its C-terminus binding to MKLP1 (mitotic kinesin-like protein 1), which is a core component of the midbody ring. Additionally, this study identifies BRUCE as a component of tubular endosomes in interphase cells and it is demonstrated that this compartment is utilized as a pool for membrane insertion in late cytokinesis. Hence, the molecular basis of the phenotypes seen after BRUCE depletion are a failure of membrane delivery and defective recruitment of mitotic regulators to the midbody ring. Notably, these phenotypes resemble those seen in cells depleted of centriolin, a protein necessary for the localization of membrane tethering factors to the midbody ring.

Additionally, it is demonstrated that ubiquitin itself shows a dynamic pattern of localization first highly concentrated on midbody microtubules and later on the midbody ring after constriction of the intercellular connection. Upon BRUCE depletion, this localization pattern of ubiquitin is lost and midbody rings are lost concomitantly. Both BRUCE and MKLP1 are ubiquitylated and UBPY (ubiquitin-specific protease Y) is shown to serve as their de-ubiquitylating enzyme. Preventing de-ubiquitylation by a dominant negative mutant of UBPY leads to the accumulation of binucleate cells and mislocalization of MKLP1.

BRUCE can therefore serve as a factor linking the ubiquitin-proteasome system to membrane traffic thereby ensuring proper abscission during cytokinesis.

2 Introduction

2.1 Cytokinesis as the final process in cell division

Animal cell division is usually divided in five discernible phases, the first four of which (prophase, metaphase, anaphase and telophase) ensure segregation of the genetic material into the two daughter cells. The fifth phase – cytokinesis – representing the final and irreversible step of division, separates the cytoplasmic volumes of the daughter cells by sealing the intercellular bridge, which connects them (Figure 1).

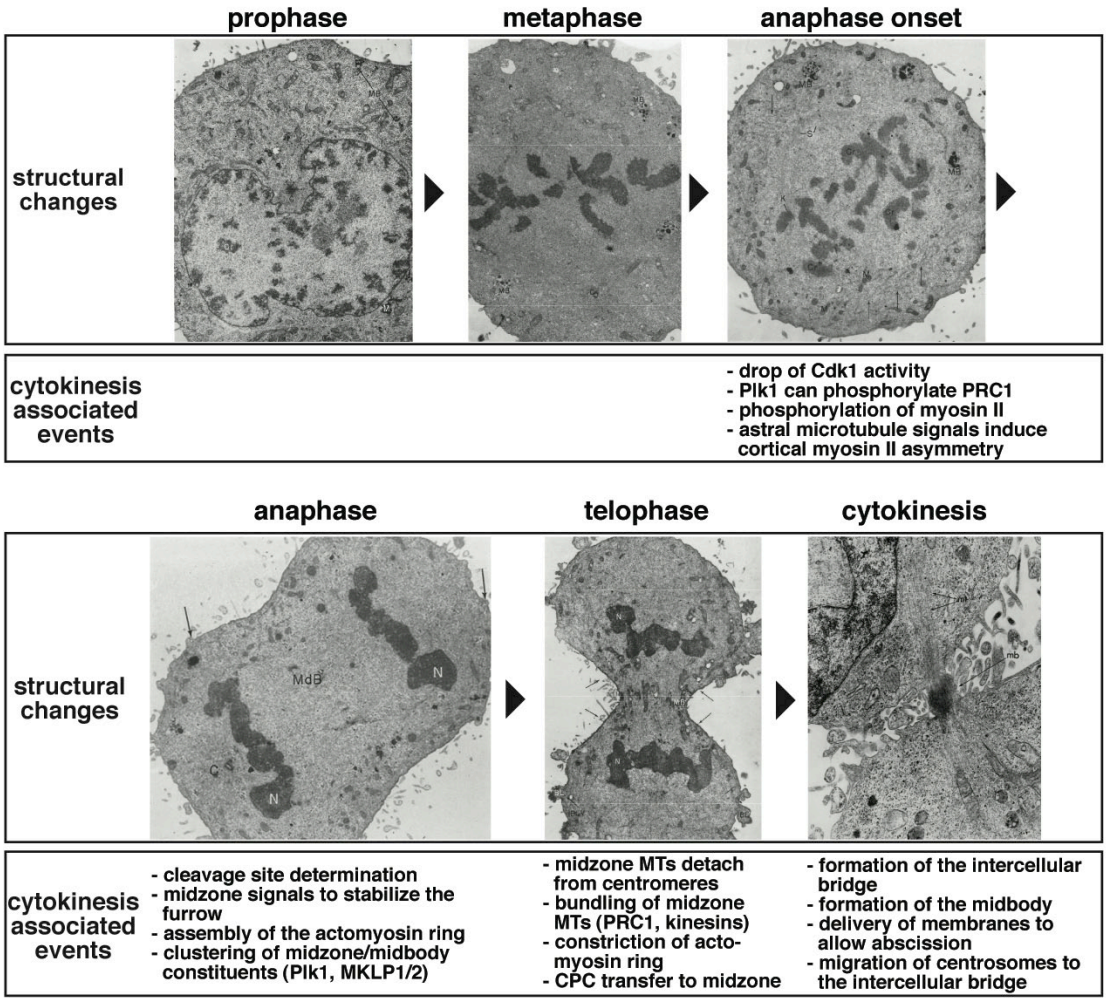

Figure 1. Cell cycle stages and the corresponding events leading to cytokinesis.
Images depicting electron micrographs of HeLa cells during the cell cycle show ultrastructural details at 6000-18000-fold magnification. Images were taken from Robbins and Gonatas,1964 and Byers and Abramson, 1968. (MT = microtubule)

As early as in 1891, Flemming described specialized structures in lung epithelial cells of salamander larva that were only visible late during cell division (Flemming, 1891). He speculated that these might represent the vertebrate equivalent of the plant cell plate. Notably,

he discovered a densely stained body at the site of abscission, 1-1.5 μm in size, naming it 'Zwischenkörper' (midbody) which he could also trace in cells that had finally separated. According to his perception the 'Zwischenkörper' then vanished at the cell boundary. Furthermore, he perceived that the 'Verbindungsfäden' (connecting threads) are constricted at the site of abscission coming from both daughter cells and ending in the 'Zwischenkörper' on either side. He also recognized an 'eigenthümliche Differenzirung' (strange differentiation) of stainable bodies earlier when the site of furrowing is first discernible and concluded that this might represent the structures that transform into the 'Zwischenkörper'. Flemming's observations and other early reports on cell division lead to the widely accepted concept that the mitotic apparatus is important for both transport of chromosomes to opposite poles and for the division of the cytoplasmic mass (Belar, 1929a; Belar 1929b; Inoue 1953).

Cytokinesis is usually described by four timely and morphologically distinct sub-processes. Already overlapping with anaphase, signals derived from the mitotic spindle specify the cleavage plane and thereby cortical sites for furrowing. This is preceded by furrow ingression mediated by a plasma membrane anchored ring consisting of actin and myosin II. Beneath this ring, microtubule remodeling and protein relocalization from spindle poles and centromeres leads to the formation of the midzone holding the half-spindles apart. Constriction of the cell cortex subsequently leads to the formation of a narrow intercellular channel that contains the midbody consisting of tightly bundled anti-parallel microtubules originating from the midzone that embrace a phase-dense structure called midbody ring. Finally, during abscission, vesicular material is delivered along midbody microtubules to the midbody ring. Homo- and probably heterotypic fusion events of vesicles seal the intercellular connection, thereby separating the two daughter cells (Glotzer, 2001; Eggert et al., 2006).

In this study, BRUCE is introduced as a novel factor acting during late stages of cytokinesis. The following outline will describe the molecular mechanisms of cytokinesis, its links to the cell cycle machinery, membrane traffic and ubiquitin-dependent regulation to allow a classification of BRUCE in the context of late stages of cell division. The outline will focus on animal cells and the mammalian nomenclature for genes and proteins unless noted otherwise.

2.2 The timing of cytokinesis

The existence of a time window during the cell cycle in which cytokinesis can occur was first demonstrated in experiments by Rappaport (Rappaport, 1975; Rappaport and Rappaport, 1993) and this phase was later termed C-phase (Canman et al., 2000). C-phase timing, like any other cell cycle stage, relies on cyclin-dependent kinases (Cdks), which drive cells through mitosis in cooperation with several other protein kinases such as those of the Polo and Aurora

families (Nigg, 2001). Cdks are only active when bound to their cognate cyclin cofactor. Fluctuations in cyclin levels due to synthesis and regulated destruction therefore allow Cdk activity to be restricted to certain phases of the cell cycle. Evidence from several experimental systems suggests that Cdk1 activity has to drop to allow cytokinesis and that the spindle must be assembled properly (Wheatley et al., 1997; Canman et al., 2000). These two prerequisites must also be met in order to allow anaphase onset and mitotic exit (Peters, 2006). The cell cycle oscillator therefore dictates the timing of cytokinesis by ensuring the coordination of chromosome segregation with separation of the cytoplasm. Interestingly, the inhibition of Cdk1 after anaphase onset alone is sufficient to induce cytokinesis without chromosome segregation (Niiya et al., 2005). Apart from Cdk1, another cell cycle-regulated kinase, Polo-like kinase 1 (Plk1), represents a key component of mitotic and cytokinetic events (Barr et al., 2004). Its activity rises during mitosis and Plk1 subsequently phosphorylates several components needed for midzone and midbody formation (see below). Moreover, Plk1 can dock to pre-phosphorylated proteins and thereby reach subcellular sites where its activity is needed e.g. centrosomes, the midzone, and the midbody. These pre-phosphorylated sites are often created by Cdk1 (Elia et al., 2003). Cdk1 and Plk1 action can hence be considered a hand-over mechanism.

Furthermore, cytokinesis timing is connected to the phosphorylation of myosin II which is elementary for the proper formation and function of the contractile actomyosin ring, although the kinase necessary for this process is not yet unambiguously identified (Komatsu et al., 1997a; Komatsu et al., 1997b; Kosako et al., 2000; Komaba et al., 2001; Murata-Hori et al., 2000; Murata-Hori et al., 2001; Suizu et al., 2002; Yamashiro et al., 2003; Batchelder et al., 2007). Nonetheless, several of the kinases implicated are also found to be regulated by upstream kinases, which are in turn cell cycle-dependent. Additionally, inhibiting ubiquitin-dependent protein degradation prevents or slows down cytokinesis (Shuster and Burgess, 2002; Straight et al., 2003; and see below). This could be explained by a stabilization of cyclin B, the activating cofactor for Cdk1, thereby keeping its activity high. Altogether, kinase signaling governed by the cell cycle starting from the point of anaphase onset represents the up-most layer of temporal regulation in cytokinesis.

2.3 Cleavage site specification

Establishing the cleavage site represents the first step in cytokinesis, which is subject to both temporal regulation – coupling it to the cell cycle – and spatial regulation – coupling it to spindle position (Glotzer, 2001; Eggert et al., 2006). Since the classical experiments performed by Rappoport in the 1960ies (Rappaport, 1996), it has become clear that cues originating from

the spindle apparatus can induce furrowing, the first morphologically distinct event in cytokinesis, by modulation of cortical actin (Bray and White, 1988; see Figure 1). Nonetheless, until recently, the contributions from astral microtubules (the radial non-spindle microtubules originating from centrosomes) *vs.* spindle midzone microtubules (anti-parallel microtubules from the spindle remaining after chromosome separation) were unclear. Spatial separation of asters and midzones using laser-dissection showed that the furrow is first positioned by an astral signal and subsequently by a second midzone-derived signal (Bringmann and Hyman, 2005). Several factors were identified that are either needed for both furrowing activities (components of the contractile ring), or are needed primarily for the midzone-induced furrowing (kinases, microtubule bundling factors, kinesin transport protein, see below). The astral pathway seems to negatively regulate cortical myosin II recruitment, thereby inducing a break in symmetry that allows equatorial furrowing by coalescence of cortical contractile elements (Werner et al., 2007). Strikingly, there is an additional layer of asymmetry in many cell types in that unilateral furrowing can be observed: Cells first initiate a symmetric circumferential furrow, but then one of its edges stops furrowing while the furrow associated with the opposing edge continues (Savoian et al., 1999). This suggests that individual furrowing units can work independently and that the contractile ring does not function like a 'purse string' as previously envisioned. Recent data supports these ideas and shows that asymmetry might originate from anillin (an actin filament cross linker) and septins (filamentous components of the contractile ring). These proteins allow unilateral instead of circumferential symmetry of furrowing, thereby ensuring robustness of cytokinesis and adaptability to developmentally demanded asymmetric ingression (Maddox et al., 2007).

The molecular requirements that specify the site of furrowing are mainly attributed to signaling *via* Rho GTPases (Piekny et al., 2005). Rho cooperates with its guanine nucleotide exchange factor (GEF) Ect2 and its GTPase activating protein (GAP) MgcRacGAP to coordinate contractile ring assembly. Downstream targets for Rho are kinases implicated in myosin II phosphorylation (citron kinase, Rho kinase ROCK), myosin phosphatase, and formin family proteins that promote actin polymerization. Recently, the initial event for Rho activation has been elucidated (Burkard et al., 2007; Petronczki et al., 2007; Brennan et al., 2007). The key mitotic kinase Plk1 phosphorylates Ect2, which only then can bind to MgcRacGAP at the spindle midzone from where it reaches cortical sites. Here, this protein complex can act on Rho to induce contractile ring formation. Surprisingly, the Plk1-dependent mechanism for Rho localization seems to be conserved in yeast where cytokinesis apparently utilizes different mechanisms (Yoshida et al., 2006). In contrast to the current notion, it was also recently shown that Ect2 serves mainly to restrict activated Rho to the midzone/furrow and that a newly

discovered GEF, GEF-H1, is needed for persistent Rho activation, probably superseding Ect2 as the major GEF for Rho (Birkenfeld et al., 2007).

2.4 The spindle midzone and the formation of the midbody

Concomitant with the formation of the cortical actomyosin ring, large rearrangements take place in the spindle midzone. Elongated overlapping microtubules underneath the contractile ring that were formerly attached to the spindle become gradually self-organized and bundled. They also lose contact with centromeres and their organizing centers, lying in the cytoplasm, at this point also contain γ-tubulin (Julian et al., 1993; Shu et al., 1995). The micotubules of the midzone keep the two genomes separate and deliver proteins that trigger the second signal for furrow formation. Bundling of midzone microtubules is achieved by the joint action of microtubule associated proteins (MAP) and kinesin motor proteins. The function of the spindle midzone was already outlined in the stembody hypothesis by Belar (Belar, 1929a; Belar, 1929b), who described 'Stemmfasern' (pushing threads, microtubules) that help to further push spindle poles apart in order to support chromosome segregation and cell elongation,

PRC1 (protein required for cytokinesis 1) represents a major microtubule-bundling factor in the midzone as demonstrated *in vivo* and *in vitro* (Mollinari et al., 2002). It is tightly regulated by cell cycle-dependent kinases (Jiang et al., 1998; Zhu and Jiang, 2005). PRC1 can only interact with kinesin motor proteins like KIF4, which travel on midzone microtubules, if its Cdk1-dependent phosphorylation is lost. Furthermore, Cdk1 phosphorylation of PRC1 in metaphase is thought to prevent Plk1 binding. After anaphase onset, Cdk1 activity drops and Plk1 can phosphorylate PRC1, thereby creating its own docking site. PRC1 then in turn delivers Plk1 to the midzone/midbody (Neef et al., 2007). In addition, there seems to be an interdependency of localization: on the one hand, PRC1 interacts with several kinesins needed for cytokinesis (KIF4, KIF14, MKLP1/2) and is needed for their proper localization as well as for the localization of their cargo e.g. citron kinase (Gruneberg et al., 2006). On the other hand, depletion of mitotic kinesins MKLP1/2 also leads to a block in midzone assembly and a loss of PRC1 at that site (Matuliene and Kuriyama, 2002; Gruneberg et al., 2004). Recently it has been shown that at least 15 kinesins are involved in mitosis/cytokinesis regulation (Zhu et al., 2005). Among these are Eg5, KIF2A and KIFC1 which are needed for spindle formation, MCAK, CENP-E, KIF14, KIF18 and KID required for chromosome alignment, and KIF3A, KIF4A/B, KIF12, MPP1 and MKLP1/2 essential for cytokinesis (Abaza et al., 2003; Zhu et al., 2005; D'Avino et al., 2007; Chen et al., 2007).

A core component at the midzone besides PRC1 is the plus-end-directed motor protein mitotic kinesin-like protein 1 (MKLP1 or KIF23) (Nislow et al., 1992). In interphase cells,

MKLP1 localizes exclusively to the nucleus. In cytokinesis, MKLP1 is first associated with the midzone and then with the midbody ring (Adams et al., 1998). MKLP1 persistently associates with the midbody ring also when it is taken up as a division remnant (Nislow et al., 1990; Powers et al., 1998; Raich et al., 1998). In all animal systems tested, MKLP1 is essential for the persistence of the contractile ring, midzone assembly and completion of cytokinesis. MKLP1 co-purifies on the one hand with Plk1 and on the other hand with MgcRacGAP in a complex called centralspindlin from *C. elegans* embryos and human cells, most likely in a 2:2 stoichiometry (Liu et al., 2004; Mishima et al., 2002; Yuce et al., 2005). This configuration might allow bridging of anti-parallel microtubules. Additionally, this complex binds the Rho GEF Ect2. Hence, the centralspindlin complex represents an integrating element allowing midzone-derived furrowing activity by mediating a crosstalk of actomysosin ring regulators and activities that support midbody formation.

In order to function in cytokinesis, MKLP1 needs to be de-phosphorylated at sites that were phosphorylated by Cdk1 in metaphase and has in turn to be phosphorylated by Aurora B, the kinase component of the chromosomal passenger complex (Guse et al., 2005; Neef et al., 2006; see below). Aurora B phosphorylation thereby inactivates a bipartite nuclear localization signal preventing premature nuclear re-import of MKLP1. Interestingly, transfer of Aurora B from centromeres to the midzone requires a functionally related kinesin, MKLP2 (Hill et al., 2000; Neef et al., 2006). Moreover, both MKLP1 and MKLP2 bind to and are phosphorylated by Plk1 (Lee et al., 1995; Adams et al., 1998; Neef et al., 2003) and the modifications are probably also important for proper cytokinesis. MKLP1 possesses an alternatively spliced isoform, called CHO1, that includes exon 18 (Kuriyama et al., 2002). The domain encoded by exon 18 allows CHO1 to additionally bind actin, arguing for a direct link of the midzone to the cortical actomyosin ring and divergent functions of the two isoforms at the midzone. Notably, MKLP1 also plays a role in postmitotic cells. It has been found in dendritic processes where it establishes the pattern of non-uniform microtubule polarity (Sharp et al., 1997).

Another factor that can interact both with mitotic kinesins and bundle microtubules, is Cep55 (Fabbro et al., 2005; Zhao et al., 2006). Cep55 binds to the centralspindlin complex and also to Tsg101, a component of the 'endosomal sorting complex required for transport' (ESCRT) (Zhao et al., 2006; Carlton and Martin-Serrano, 2007). The role of ESCRT in cytokinesis will be described below. Notably, Cep55 was identified as a centrosomal protein where it interacts with γ-tubulin ring complex anchoring proteins (Fabbro et al., 2005). To participate in cytokinesis, Cep55 is first phosphorylated by Erk2/Cdk1, which creates a docking site for Plk1, which in turn adds another phosphorylation allowing Cep55 to travel to the midzone. Here, it is needed for proper formation of the midbody by localizing PRC1 and

MKLP2, as well as for membrane-mediated abscission by controlling the SNARE proteins endobrevin and syntaxin-2 (Zhao et al., 2006). Hence, Cep55 represents a direct link of centrosomes and the midbody (Doxsey, 2005). There are also several other proteins, like Cdc14A, Lats1/2 and centriolin that localize to centrosomes and translocate to the midbody in cytokinesis (see below; Doxsey, 2005; Doxsey et al., 2005).

The idea of molecular contacts mediated by proteins translocating from centrosomes to midbodies is supported by findings in HeLa cells, demonstrating a post-anaphase repositioning of centrosomes towards the midbody (Piel et al., 2001). Piel et al. concluded that only when the mother centriole moved to the midbody and then back to the cell center, cells finally separate. They also provide evidence that the function of the centrosome is to release midbody microtubules to proceed with abscission.

A central element that serves to connect the above mentioned events of midzone and midbody formation to the dynamics of the mitotic spindle is a protein complex known as the chromosomal passenger complex (CPC). It consists of the kinase Aurora B, the inner centromere protein INCENP, the small baculovirus inhibitor of apoptosis repeat (BIR)-containing protein survivin, and borealin (Ruchaud et al., 2007). In metaphase, CPC is concentrated on inner centromeres by the interdependent binding of INCENP and survivin to a not yet unambiguously identified centromere-receptor. A contribution of centromeric histones CENP-A and H2A.Z to CPC recruitment is suggested (Zeitlin et al., 2001; Kunitoku et al., 2003; Rangasamy et al., 2003). At this stage, Aurora B phosphorylates histone H3 and condensin subunits, probably leading to altered chromosome structures (Giet and Glover, 2001). Subsequently, CPC is crucial for the release of arm cohesion, kinetochore maturation and proper spindle assembly. After anaphase onset, CPC transfers from centromeres to the midzone and the midbody. This transfer is at least in part dependent on MKLP2 (Gruneberg et al., 2004; see above). Besides this, Aurora B phosphorylates multiple other proteins (MgcRacGAP, MKLP1, myosin II) whose modification positively affects cytokinesis.

Similar to mitotic kinesins and their respective cargo, there seems to be a great extend of interdependencies as far as localization of CPC components and substrates is concerned. A putative CPC-function at the interface of chromosome segregation and cytokinesis is suggested by the so-called NoCut pathway in *S. cerevisiae*, where the Aurora B-homolog Ipl1 regulates the localization of two anillin-like proteins, Boi1/2, negative regulators of cytokinesis (Norden et al., 2006). Boi1/2 are removed from the bud neck only when chromosome separation is completed and Ipl1 is inactive. A similar process is not yet described for higher eukaryotes.

Figure 2 summarizes the molecular inventory of cytokinesis described so far by grouping proteins in three main classes: Regulators, structural components of the actomyosin ring, and components of the central spindle necessary for midbody formation.

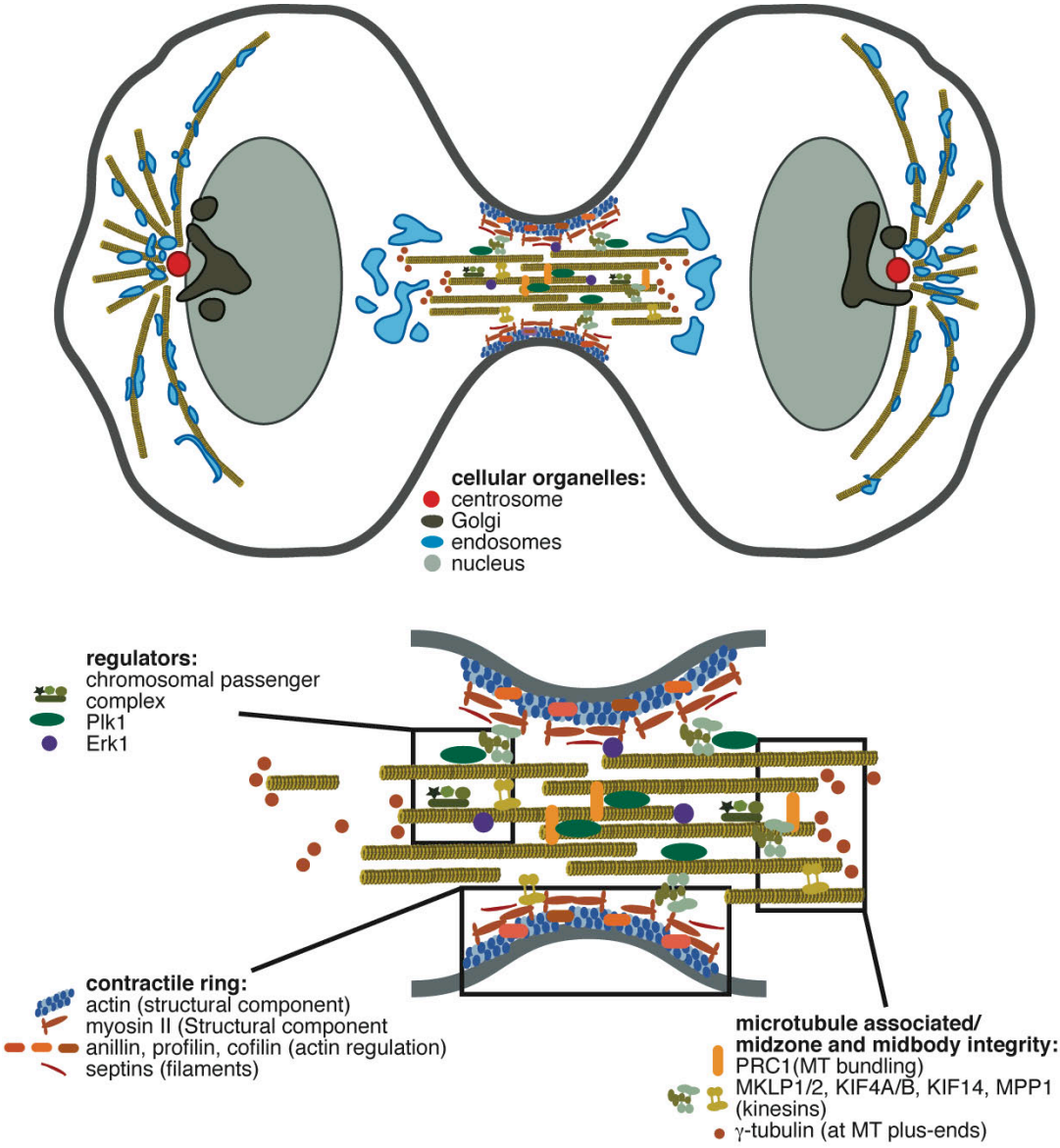

Figure 2. The inventory of cytokinesis.
Schematic drawing of a cell in late telophase/cytokinesis. The actomyosin ring is still found at the furrow and the midzone has already constricted. The lower panel shows the enlarged midzone region. Only three major classes of proteins involved in cytokinesis are shown.

2.5 Links between mitotic exit and cytokinesis

As detailed above, there are multiple lines of evidence that suggest first a coupling of mitotic exit to the licensing of cytokinesis and second an involvement of centrosomes or centrosomal proteins in cytokinesis. This demands a comparison to the elaborate networks that govern mitotic exit in yeast, the mitotic exit network (MEN) in *S. cerevisiae* and the septation initiation

network (SIN) in *S. pombe*. (Krapp et al., 2004; Bosl and Li, 2005; Doxsey et al., 2005). The yeast equivalents of centrosomes, the spindle pole bodies (SPBs), constitute the organizing platforms of both networks. Like in animal cell cytokinesis, these networks ensure cell division after completion of chromosome separation with an interphase-like state of Cdk1/Cdc2 activity. The core of both networks is a GTPase system that monitors the position of the anaphase spindle. Interestingly, SIN and MEN are organized asymmetrically. In fission yeast SIN, inhibitory components are localized to the old SPB. In budding yeast, the old SPB translocates into the bud and activators bind on this SPB.

This asymmetry in SIN and MEN might be needed to prevent premature activation before anaphase. Notably, similar asymmetries are also found in animal cell cytokinesis, e.g. asymmetric centrosome movement (Piel et al., 2001) and asymmetric delivery of membranes to the midbody (Gromley et al., 2005; see below). If the spindle is positioned improperly, SIN/MEN can delay anaphase onset. Additionally, in budding yeast, MEN is coupled to mitotic exit by the Cdc14 early anaphase release (FEAR). Cdc14, a phosphoprotein phosphatase, drives mitotic exit by dephosphorylating and thereby activating anaphase promoting complex (APC) activators and Cdk inhibitors. Cdc14 is only transiently released in early anaphase and MEN activation later allows sustained release leading to a second wave of cyclin degradation, mitotic exit and cytokinesis. Notably, Cdc14 localization is affected by the yeast Plk1 homolog Cdc5 (Visintin et al., 2003).

Due to the general differences between yeast and animal cells – e.g. closed *vs.* open mitosis, budding before spindle alignment, etc. – a similar regulation like FEAR/MEN in higher eukaryotes is not directly extrapolatable. Nevertheless, several components that could either act as the scaffold homologs (yeast Nud1 *vs*. mammalian centriolin), activating kinases (yeast Dbf2 *vs*. mammalian Lats1/2) or phosphatases (yeast Cdc14 *vs*. mammalian Cdc14A/B) are also found in mammals. However, there is no evidence yet for a centrosome-organized mitotic exit or a checkpoint-like delay in cytokinesis in animal cells.

Data from higher eukaryotes provide evidence that there is not a unique decisive substrate that, when phosphorylated by Cdk1, prevents mitotic exit or cytokinesis on its own (Pines, 2006). It seems more likely that multiple targets need to be dephosphorylated in order to drive different sub-processes, leading to mitotic exit and cytokinesis. Several lines of evidence also disfavor the existence of a positive-feedback loop that would accelerate exit from mitosis once Cdk activity is low, limiting the similarities of mammalian mitotic exit to the networks in budding and fission yeast (Straight et al., 2003; Potapova et al., 2006).

The plethora of regulatory principles and interdependencies that can be found during cytokinesis allow to conclude that a multitude of events, like degradation of cell cycle

regulators, cytoskeletal rearrangements and membrane traffic converge on the midbody. Therefore, the following chapters will describe the contributions of membrane traffic and of processes regulated by the ubiquitin-proteasome system to cytokinesis.

2.6 Membrane traffic and its role in cell division

In animal cells, it has become clear that plasma membrane remodeling is an integral element of abscission, the final event that takes place on the midbody (Straight and Field, 2000; Finger and White, 2002; Otegui et al., 2005; Albertson et al., 2005; Matheson et al., 2005; Baluska et al., 2006). It requires coordination by several regulators of vesicle trafficking that will be discussed below.

Observing *X. laevis* eggs during cleavage, it has been found more than 30 years ago that new membrane is formed prior to cleavage (Bluemink and de Laat, 1973). Concerning the timing of this membrane delivery, the authors concluded that membrane insertion in cytokinesis is a late event, which is separable from furrow ingression. Furthermore, it has been shown during the process of cellularization in *D. melanogaster* that new membrane is inserted from intracellular pools (Lecuit and Wieschaus, 2000). During the first 13 divisions in *Drosophila* development, cells divide in a syncytium with only partially ingressing furrows in divisions 10-13. During the 14th division, for the first time in the process of cellularization, full cytokinesis occurs for all cells (Mazumdar and Mazumdar, 2002).

Concerning the origin of membranes that are inserted in the cleavage furrow, several lines of evidence suggest that Golgi-derived exocytic membranes contribute to cytokinesis. *Drosophila* cellularization, in contrast to cleavages in *C. elegans* and sea urchins, is sensitive to inhibition of GTPases regulating protein secretion by Brefeldin A (BFA) (Shuster and Burgess, 2002; Sisson et al., 2000) and the Golgi membrane proteins strabismus (Lee et al., 2003) and lava lamp (Sisson et al., 2000; Papoulas et al., 2005) are both required for cellularization. Lava lamp has also been shown to regulate targeted membrane insertion by dynein-based Golgi-movements (Papoulas et al., 2005). Besides exocytosis, endocytosis is also needed for membrane remodeling at the furrow. Both processes depend on small GTPases of the Rab and Arf/Arl families. Rab proteins are general regulators of organelle identity that specify the targeting of incoming membranes to the right acceptor membrane (Chavrier et al., 1990; Huber et al., 1993; Lombardi et al., 1993; Casanova et al., 1999; Sönnichsen et al., 2000; Zerial and McBride, 2001; Grigoriev et al., 2007). In the initial step of membrane fusion, the specific pairing of membrane zipping SNARE proteins (soluble NSF attachment protein receptors) between the two bilayers ensures selection of the right donor and acceptor membrane (Chen and Scheller, 2001). During this process Rabs define a second

layer of control preventing erroneous SNARE-mediated fusions. SNARE proteins syntaxin 2 and endobrevin/VAMP8 themselves were found to be essential for cytokinesis (Low et al., 2003). Rab proteins, like the related Arf/Arl proteins (Gillingham and Munro, 2007), are small GTPases. They switch between a GDP- and a GTP-bound state and this change is interconnected to a cycle of reversible attachment to membranes. After delivery to their target membranes, Rabs are activated by exchange of GDP to GTP, allowing interaction with an effector molecule. After completion of downstream events and GTP hydrolysis, Rabs are retrieved by GDI (GDP dissociation inhibitor) and delivered to their starting compartment (Goody et al., 2005). Besides SNARE proteins a multitude of Rab effector proteins are known to transduce information to downstream targets on their respective organelle.

D. melanogaster mutants in endocytosis (Rab5 and dynamin GTPases) show impaired cellularization and, in the case of a dynamin mutant, accumulation of secretory cargo in recycling endosomes that contain Rab11 (Pelissier et al., 2003). This is explained by the fact that the large GTPase dynamin is not only important for endocytosis but also for vesiculation at intracellular organelles like the *trans*-Golgi network (TGN) and also Rab11 recycling endosomes. *D. melanogaster* expressing a dominant-negative version of Rab11 cannot perform cellularization. This phenotype resembles that of the nuclear-fallout (Nuf) mutant (Strickland and Burgess, 2004). In the Nuf mutant, actin and membrane remodeling at the furrow are impaired. Notably, the human Nuf homolog arfophilin-2/FIP4 binds to both Rab11 and the small GTPase Arf5 in a GTP-dependent manner (Hickson et al., 2003). Recent data suggest that Nuf/FIP4 regulates the timing of Rab11 recycling endosome delivery to the cleavage furrow. FIP4 is concentrated around centrosomes only while Rab11 translocates to the furrow (Riggs et al., 2007). This mechanism of traffic regulation may constitute another example of centrosome-organized events in cytokinesis (see above).

Further reports identified a whole family of Rab11/25-interacting proteins (FIPs), which all possess a C-terminal Rab-binding domain (Prekeris et al., 2000; Prekeris et al., 2001; Lindsay and McCaffrey, 2002; Hales et al., 2002). As mentioned above for FIP4, FIP3 can also bind to Arf GTPases. This dual Rab/Arf interaction plays a major role in the regulation of cytokinesis. It has been demonstrated that a dominant-negative form of Rab11 (Rab11-S25N) can induce multinucleation and that FIP3, FIP4 and Rab11 all localize to the midbody (Wilson et al., 2005). Disruption of the interaction of FIP3 with Rab11 led to cytokinesis failure and induced multinucleation. The recruitment of FIP3/4 to the midbody in turn depends on their interaction with Arf6 (Fielding et al., 2005). On the midbody, FIP3/4 serve as connectors between Arf6/Exo70 and Rab11 to allow vesicle tethering prior to fusion (Fielding et al., 2005).

In addition to Arf6, there are probably contributions from other Arf-family members like Arf1 and Arl1 to cytokinesis (Altan-Bonnet et al., 2003; Skop et al., 2004).

Systematic approaches to elucidate the role of other Rab proteins in cytokinesis yielded partially contradictory data. Yu and colleagues (Yu et al., 2007) claim that only Rab11 is involved in cytokinesis. In contrast, Kouranti and coworkers (Kouranti et al., 2006) show that interfering with Rab35 induced substantial binucleation. HeLa cells expressing dominant negative Rab35 S22N mislocalize the septin SEPT2/Nedd5 and the membrane lipid $PI(4,5)P_2$ (Kouranti et al., 2006). For $PI(4,5)P_2$ the function at the cleavage furrow is mainly to recruit lipid-binding proteins containing PH-domains like PLCδ (Naito et al., 2006) and to tether the contractile ring to the plasma membrane (Field et al., 2005).

An additional example highlighting the importance of regulators of targeted membrane insertion for cytokinesis is represented by the recently demonstrated cooperation of the exocyst complex with the large coiled-coil centrosomal protein centriolin. In a screen for scleroderma pigmentosa autoantigens, Gromley and colleagues identified centriolin, which is found on the maternal centriole and, interestingly, also on the midbody (Gromley et al., 2003). They could show that centriolin depletion induces a rather unique failure in cytokinesis. Cells form regular furrows but never separate and form long intercellular bridges. Apart from extensive coiled-coils, centriolin also harbors a Nud1/Cdc11 domain. Cdc11 represents the scaffold of the above mentioned *S. cerevisiae* mitotic exit network. Overexpression of this isolated domain also elicits a failure in cytokinesis. Surprisingly, interconnected cells generated by centriolin depletion can undergo mitosis with a seemingly normal progeny. Centriolin has been found to interact with membrane targeting factors Snapin, a SNARE-associated protein and components of the exocyst complex namely Sec5, 8 and 15 (Gromley et al., 2005, see below). Cytokinetic centriolin localization has been pinned down further to the midbody ring. In addition, it was shown that Snapin and every single subunit of the exocyst localize to the midbody ring and that their localization to this site depends on centriolin. As a consequence, cells fail to undergo abscission and secretory vesicles accumulate adjacent to the midbody ring when cells are depleted of centriolin. Notably, Gromley et al. present evidence that some part of membrane material is delivered to the midbody only from one side.

The exocyst, an evolutionarily conserved vesicle tethering complex, was originally identified in yeast (Novick et al., 1980; Novick et al., 1981; TerBush et al., 1996; Hsu et al., 2004). Mutants in exocyst genes accumulate post-Golgi vesicles and it has been demonstrated that exocyst subunits localize to sites of polarized exocytosis. The mammalian complex has a size of 600-700 kDa and consists of Sec3, Sec5, Sec8, Sec10, Sec15, Exo70 and Exo84. Interestingly, in mammals, the exocyst complex co-purifies with a septin-complex

(Hsu et al., 1998). The exocyst is implicated in various processes mediating constitutive secretion from the TGN to the plasma membrane. It also plays a central role in targeting vesicles to the midbody ring (Gromley et al., 2005). During cytokinesis, the exocyst relocalizes from a pericentrosomal site to the midbody. During this relocalization it also transfers another GTPase, RalA, to the midbody (Chen et al., 2006). Disruption of the RalA-exocyst functions on either side causes late stage cytokinesis failure like binucleation but also formation of two- to four-cell syncytia interconnected by elongated bridges filled with microtubule bundles. This phenotype in turn resembles the one of centriolin depletion arguing that this reflects an epistatic relationship.

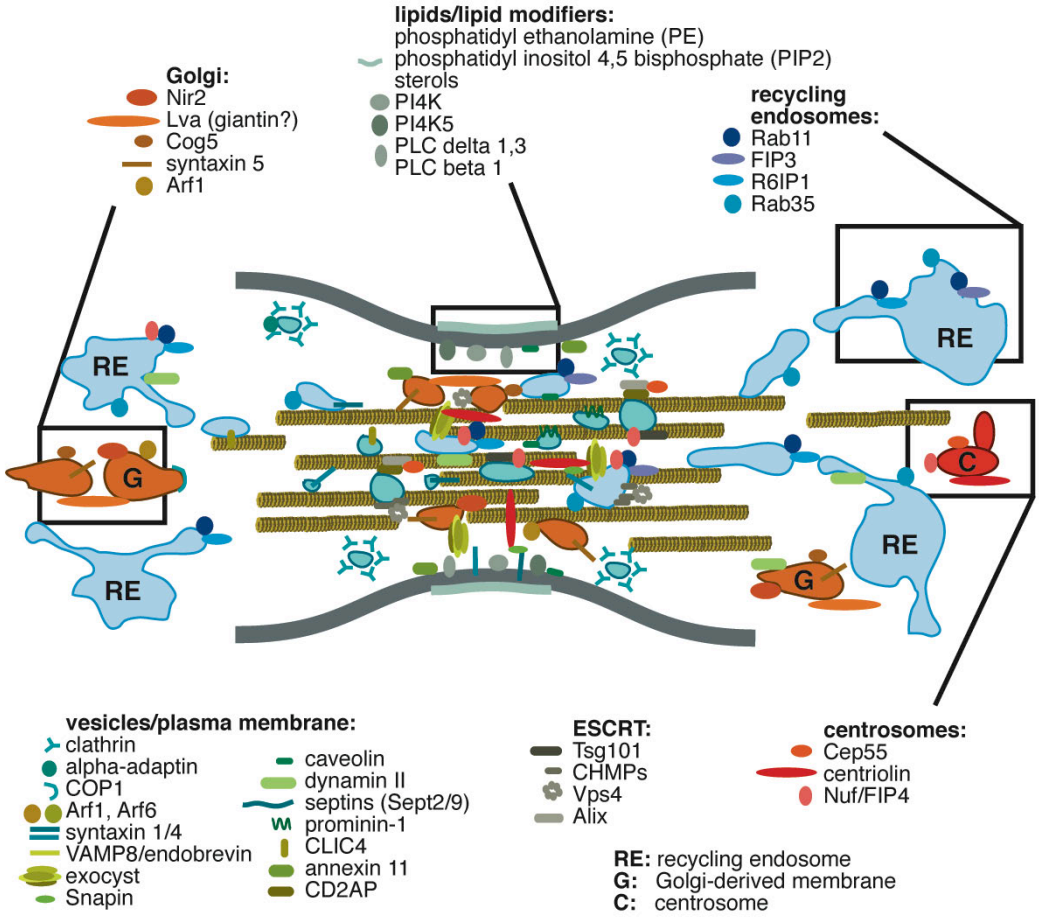

Figure 3. Membrane traffic in cytokinesis.
Schematic drawing of the intercellular bridge in late cytokinesis. The cortical plasma membrane is enriched for PE, PIP2 and sterols. Membraneous carriers from recycling endosomes and Golgi arrive at the midbody ring and are targeted for fusion by numerous factors grouped here in six categories: Golgi proteins, lipids and lipid modifiers, recycling endosomal proteins, vesicular and plasma membrane proteins, ESCRT components, and centrosomal proteins.

Several reports (Nislow et al., 1990; Powers et al., 1998; Raich et al., 1998; Gromley et al., 2005) demonstrated that part of the midbody – the midbody ring and adhering microtubules – are in fact taken up by one of the daughter cells after abscission. Consequently, this uptake

generates asymmetry, probably the only inherent asymmetric feature in cell division besides unilateral membrane delivery. However, there are also cases where asymmetry needs to be avoided (see also discussion). To maintain an initially undifferentiated state, progenitor cells have to divide symmetrically. A scenario that meets these requirements has been found in neuroepithelial cells. In these cells a transmembrane protein and somatic stem cell marker CD133/prominin-1 is clustered on midbodies that form at the apical side of the epithelium facing the neural tube (Dubreuil et al., 2007). To avoid asymmetric inheritance of the stem cell marker, cells release prominin-1-containing midbodies into the neural tube fluid.

Figure 3 summarizes the molecular inventory of membrane traffic in cytokinesis as described above by grouping individual factors in six categories: Golgi proteins, lipids and lipid modifiers, recycling endosomal proteins, vesicular and plasma membrane proteins, ESCRT components, and centrosomal proteins. Several of these factors are regulated by ubiquitin, which will be discussed in the following paragraph.

2.7 Post-translational modification of proteins with ubiquitin

The covalent attachment of ubiquitin to target proteins constitutes a post-translational modification, which serves multiple purposes like protein degradation by the ubiquitin-proteasome system (UPS) or modulation of protein function and/or localization (Figure 4). Protein modification with ubiquitin involves an enzymatic cascade of at least three steps (Jentsch, 1992; Kerscher et al., 2006). Ubiquitin is first synthesized as a poly-ubiquitin protein (3-5 ubiquitin units from the UbB gene and 9-10 ubiquitin units from the UbC gene) or as a fusion protein to the N-termini of ribosomal proteins (ribosomal protein L40 in the case of the UbA52 gene and ribosomal protein S27a in the case of the UbA80 gene) (Finley et al., 1989; Chan et al., 1995). These fusion proteins are then cleaved into their monomeric components by ubiquitin C-terminal hydrolases (UCHs) (Rose and Warms, 1983; Pickart and Rose, 1985). Hereafter, ubiquitin is activated by an E1 ubiquitin-activating enzyme that uses ATP to adenylate ubiquitin at its C-terminus. This ubiquitin-AMP is rapidly attacked by an internal sulfhydryl group in the E1 leading to an ubiquitin-E1 thioester (Ciechanover et al., 1982; Haas et al., 1982, Haas et al., 1983). The thioester is then transferred to an E2 ubiquitin-conjugating enzyme and transferred to the target protein by the help of an E3 ubiquitin ligase forming an isopeptide bond between the C-terminal carboxyl group in ubiquitin and the ε-amino group of an internal lysine in the target (Hershko et al., 1986). E3 ligases of the RING-type (really interesting new gene) bring the E2 and the substrate into close proximity to allow ubiquitylation from the E2-thioester. In the case of HECT-type (homologous to E6-AP carboxy terminus) E3 ligases, the E2-ubiquitin thioester is transferred onto a cystein in the E3 HECT domain and

then transfered to the substrate which is bound by the HECT E3 (Pickart, 2001). Selection in substrate modification is conferred by this final step at the level of the E3 ubiquitin ligase. This is also illustrated by the number of proteins known for each class of enzymes. So far only two E1 enzymes are known, while there are 33 E2 enzymes and 500-1000 E3 enzymes in mammalian cells (Kaiser and Fon, 2007; Jin et al., 2007; Pelzer et al., 2007). The computational analysis for the human genome is predicting even higher numbers (Semple et al., 2003).

Attachment of ubiquitin to an internal lysine onto an already covalently coupled ubiquitin leads to the formation of ubiquitin chains. During chain elongation another class of proteins, called E4, can act as auxiliary factors to allow efficient extension of the chain (Koegl et al., 1999). Mass spectrometry has shown that any of the seven internal lysines in ubiquitin can be used for chain formation with a relative abundance order of K48, K11, K63, K6, K27, K29 and K33 based on semi-quantitative estimation from spectral counts (Xu and Peng, 2006). Furthermore, different linkages can occur in one chain resulting in so-called barbed or forked chains (Peng et al., 2003; Tagwerker et al., 2006). The type of ubiquitin modification, e.g. mono-ubiquitylation, multiple mono-ubiquitylation or poly-ubiquitylation with different chain topologies, results in different fates for the substrate: Ubiquitin modifications are recognized by specific receptors harboring ubiquitin-binding domains that can differentiate between chain length and/or chain linkage (Pickart and Fushman, 2004; Figure 4). At least 14 different ubiquitin binding domains (UBDs) are known until now (Hurley et al., 2006). These domains are structurally divergent but most of them interact with a hydrophobic patch around I44 of ubiquitin (Hicke et al., 2005). They show low affinities to monomeric ubiquitin but increased binding to polymeric ubiquitin.

Proteins modified with ubiquitin are subsequently transferred to the proteasome, if chains are linked *via* internal lysine 48 of ubiquitin. For certain substrates transfer to the proteasome also depends on the sequential action of ubiquitin-binding factors that work in a hand-over mechanism (Richly et al., 2005). Furthermore, the length of the K48-linked chain critically influences the affinity for the proteasome (Thrower et al., 2000). At the proteasome, a multi-subunit assembly with an inner cavity lined with proteolytic sites, ubiquitin chains are trimmed off. Hereafter, the target protein is dragged into the cavity and degraded into small peptides in an ATP-dependent manner.

In contrast, mono-ubiquitylation or modification with chains through internal lysine 63 of ubiquitin are considered modifications that normally do not lead to proteasomal degradation but serve a wide range of other processes, like endocytosis, protein sorting, membrane traffic, transcription, DNA repair, ribosomal protein synthesis or cell cycle regulation (Pickart and

Fushman, 2004). These modifications on the one hand can signal *via* interaction with proteins containing UBDs. An obvious model in this case is that the linkage of a poly-ubiquitin chain determines its function either by presenting a specific pattern of hydrophobic sites or by restricting the chain's ability to adopt certain conformations. The specificity of a given ligand's interaction would then be dictated by its ability to select one chain conformation over another or to discriminate between different conformations. On the other hand, ubiquitylation might mask a binding site and therefore prevent interaction with ligands. A third possibility besides the modulation of binary protein-protein contacts is the formation or dissolution of protein complexes by ubiquitylation, which seems especially relevant for patho-physiological processes like neurodegenerative diseases.

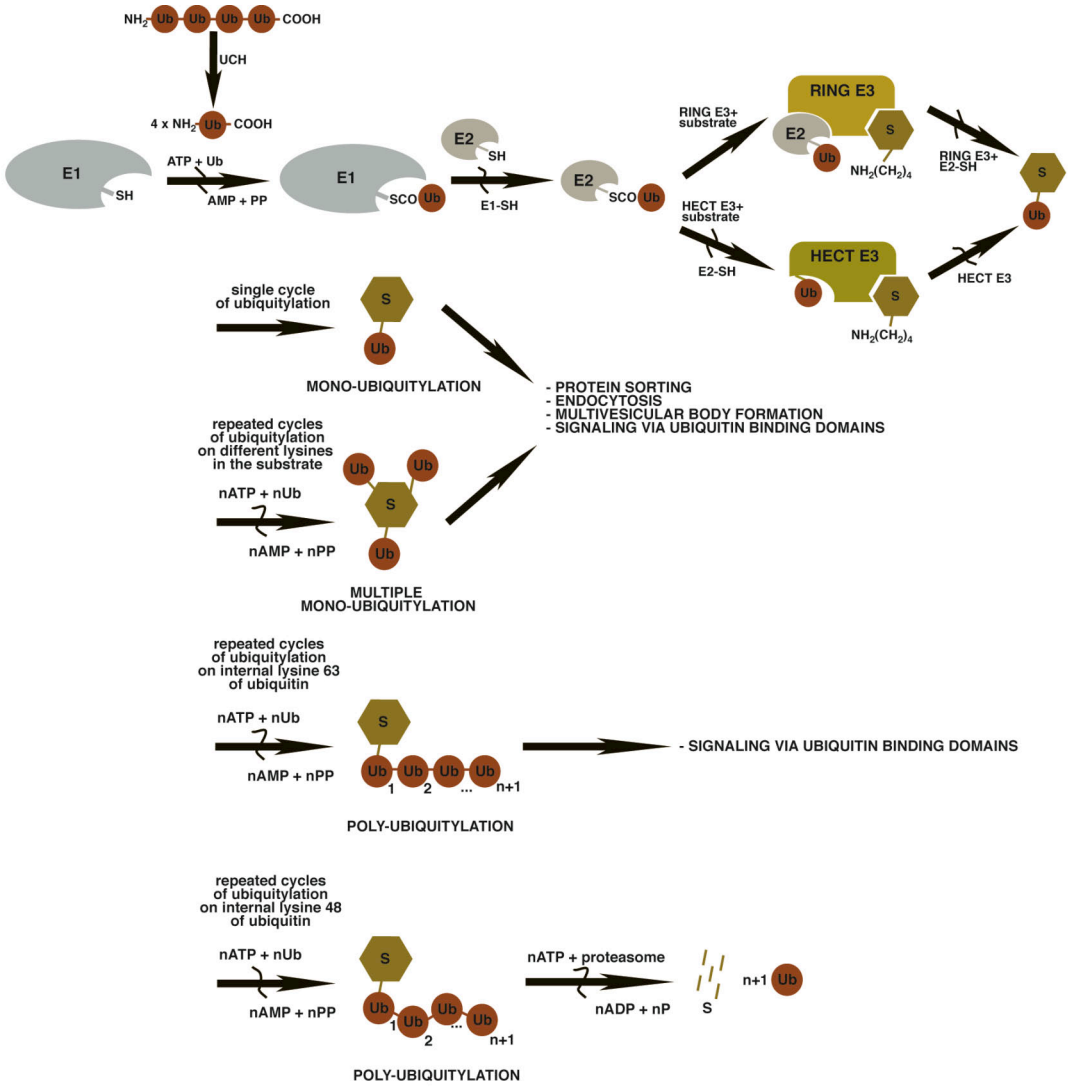

Figure 4. Ubiquitylation pathway and fates of ubiquitylated substrates.
Cartoon depicting the stepwise mechanism of ubiquitin activation and transfer. Mono-ubiquitylation, multiple mono-ubiquitylation and poly-ubiquitylation via internal lysine 48 and 63 of ubiquitin can have different consequences for the substrate protein.

Furthermore, numerous de-ubiquitylating enzymes (DUBs) allow rapid de-modification and regulation/timing of the post-translational modification. DUBs can be grouped in five subfamilies. Four of these subfamilies comprise cysteine proteases: Ubiquitin-specific proteases (UBP), ubiquitin C-terminal hydrolases (UCH), Josephine domain proteins and ovarian tumor-related proteases (OUT). The fifth subfamily are metalloproteases containing a JAMM/MPN+ domain (Amerik and Hochstrasser, 2004). DUBs can proofread ubiquitin-protein conjugates, remove ubiquitin from cellular adducts and keep the proteasome free of inhibitory ubiquitin chains thereby coupling de-ubiquitylation to degradation (Amerik and Hochstrasser, 2004). Additionally, DUBs are required for the regulation of gene silencing, inflammatory signaling and the maturation of late endosomes into multivesicular bodies (MVB) (see below).

Ubiquitylation besides its 'canonical' role in protein degradation through its reversibility represents a versatile post-translational modification to regulate protein activity, location and conformation. Interestingly, there is increasing evidence demonstrating a crosstalk between ubiquitylation and other post-translational modifications like phosphorylation or modification by ubiquitin-like proteins such as SUMO (small ubiquitin-like modifier) (Hunter, 2007).

2.8 Ubiquitin-dependent cell cycle transitions and the regulation of cytokinesis

A central role for ubiquitin lies in the turnover of cyclin proteins, which are the key elements driving the cell cycle by activating cell cycle dependent kinases (Cdks) (Glotzer et al., 1991; see above). Besides cyclins a great number of other proteins need to be degraded during the cell cycle by the UPS (Pines, 2006). Modification of cyclins and other cell-cycle regulated proteins is carried out mostly by two classes of multi-subunit ubiquitin ligases. The most prominent is the anaphase-promoting complex/cyclosome (APC/C), which consists of at least 11 subunits that assemble on a scaffold (Apc2), a RING-finger protein (Apc11) and a subunit that is important for substrate recognition and extension of the poly-ubiquitin chain (Doc1/Apc10) (Peters, 2006). Substrate selection during the cell cycle requires the binding to one of two activating WD40-domain proteins known as Cdc20 and Cdh1 (Figure 5). Cdc20 exclusively binds to APC/C if phosphorylated by Cdk1, and the assembled APC^{Cdc20} primarily recognizes proteins that harbor destruction boxes (a R/KXXL/I/M/V sequence). APC^{Cdc20} is therefore active only until anaphase onset: At this point Cdk1 activity drops because its cyclin B activator is degraded and thus also phosphorylation of Cdc20 stops. Substrates for APC^{Cdc20} are proteins that need to be degraded in prometa- and metaphase (e.g. cyclin A, Nek2 kinase). In early M-phase and probably already in interphase (Di Fiore and Pines, 2007) APC^{Cdc20} is kept inactive by binding to the inhibitor Emi1 (Machida and Dutta, 2007). Emi1 needs to be

phosphorylated by Plk1 to be ubiquitylated by another E3 ligase complex, $SCF^{\beta TrCP}$ (see below). However, the main inhibition of APC^{Cdc20} takes place on the level of spindle assembly. APC^{Cdc20} is active only if all kinetochores are attached to spindle microtubules. This scenario is also called spindle assembly checkpoint (Peters, 2006). At unattached kinetochores, the checkpoint proteins Mad2 and BubR1 build complexes with Cdc20 or APC^{Cdc20} as long as unattached kinetochores are present. It has been suggested that the Mad2/Cdc20 and BubR1/Cdc20 complexes might sequester Cdc20 away from the APC/C and thereby keep it inactive (Peters, 2006). A similar mechanism involving the inhibitor Emi1 has recently been described (Ban et al., 2007). Emi1 binds the spindle-organizing NuMA/dynein-dynactin complex to anchor and inhibit the APC/C at spindle poles, probably limiting destruction of spindle-associated cyclin B.

When all kinetochores are finally attached, APC^{Cdc20} can drive cell cycle progression by ubiquitylation of cyclin B leading to inactivation of Cdk1. Furthermore, APC^{Cdc20} also promotes degradation of securin which in turn activates separase, a protease that mediates sister chromatid separation. Due to the decrease in Cdk1 activity, the affinity of Cdc20 for the APC/C decreases and Cdh1, at anaphase onset, can bind to the APC/C as it is now hypo-phosphorylated, and Emi1, which also sequesters Cdh1 away from the APC/C, is now phosphorylated by Plk1 and degraded (Moshe et al., 2004; Hansen et al., 2004). The APC^{Cdh1} modifies targets different from those recognized by APC^{Cdc20}, which include functional components of mitosis- and cytokinesis structures (kinetochores, spindle, contractile ring, midbody) to convert cells back into an interphase state. These comprise the spindle midzone protein PRC1 and the contractile ring regulators anillin (Zhao and Fang, 2005) and Ect2 (see above) (Pines, 2006). Furthermore, APC^{Cdh1} drives degradation of mitotic regulators survivin, Aurora A and Plk1 (Castro et al., 2002; Lindon and Pines, 2004). Preventing Plk1 degradation at the end of mitosis interferes with the coordination of spindle relative to cleavage furrow position and, in consequence, results in cytokinesis failure (Lindon and Pines, 2004).

Another class of multi-subunit ubiquitin ligases with roles in mitosis are Skp1-Cullin-F-box (SCF) ligases. They are composed of a scaffolding cullin, a RING-finger protein (Rbx1), an adaptor protein (Skp1), and a substrate-interacting F-box protein. Approximately 70 F-box proteins are identified in humans so far allowing to accommodate for a wide range of substrates. In contrast to the APC/C, SCF-ligases recognize phospho-degrons in target proteins and therefore the recognition of SCF-substrates does not depend on the modification of the ligase itself but on the modification of the substrate. As described above, the $SCF^{\beta TrCP}$ is crucial for cell cycle progression by degrading APC/C inhibitors like Emi1 (Moshe et al., 2004; Hansen et al., 2004). An SCF complex with the F-box protein Skp1 (SCF^{Skp1}) has been found

to localize on the midbody where it mediates ubiquitylation of a kinesin important for chromosome movement and midzone establishment, CENP-E (Liu et al., 2006).

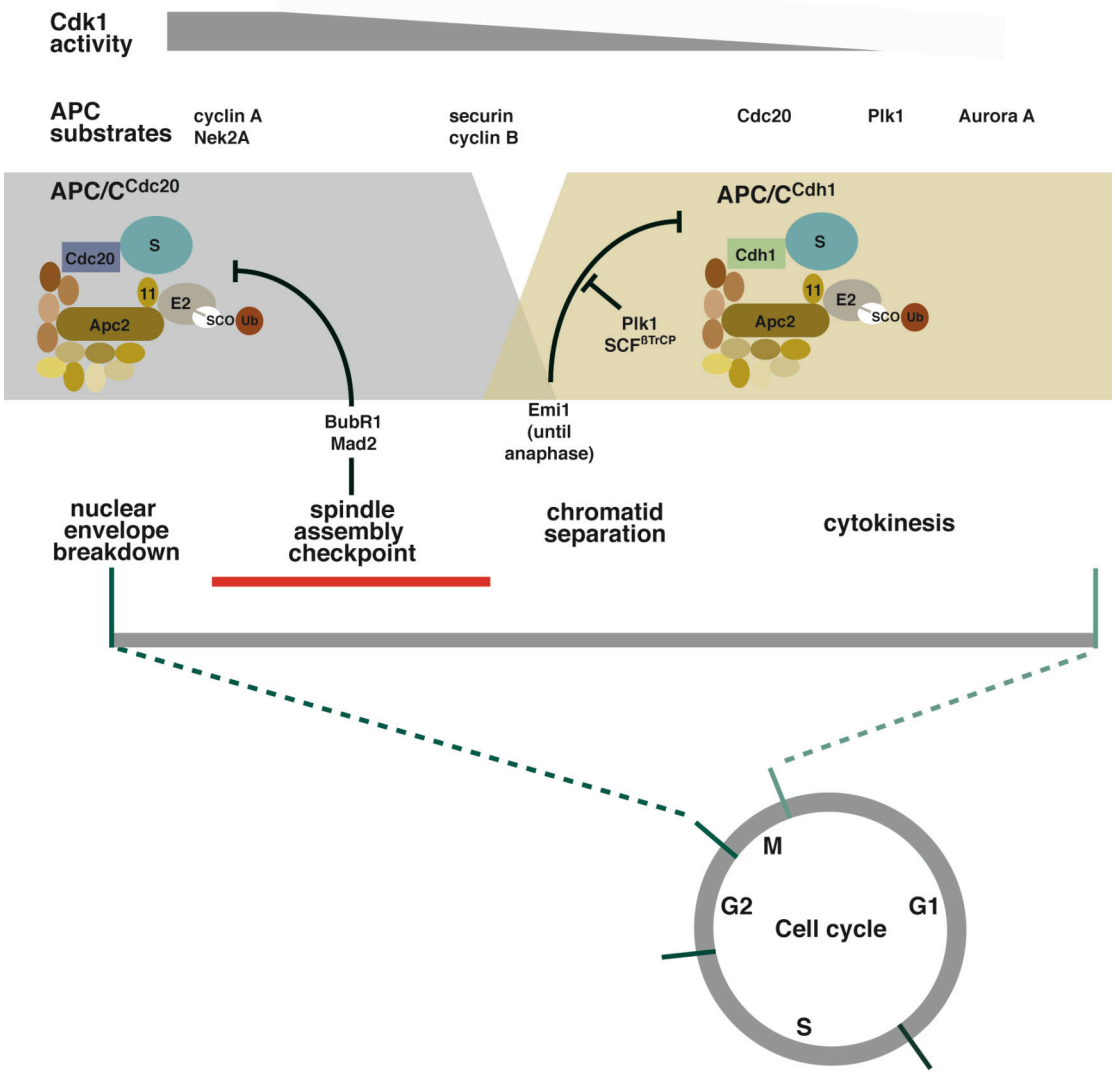

Figure 5. The cell cycle and its regulatory proteins degraded by the APC/C and the ubiquitin proteasome pathway.
Cartoon depicting the cell cycle and the timing of APC/C activation and degradation of different substrates. The inhibition of APC/C^{Cdc20} by the spindle assembly checkpoint and the inhibition of APC/C^{Cdh1} by Emi1 are shown (S = APC/C substrate; 11 = Apc11).

Besides F-box proteins there are also proteins of the BTB-family (Bric-a-brac/Tramtrack/Broad complex) that can act as substrate recruiting factors in complex with cullin 3. Complexes of Cul3 with the BTB proteins KLHL9 and KLHL13 are required for chromosome alignment and midzone/midbody formation (Sumara et al., 2007). These complexes remove the CPC component Aurora B from chromosomes and allow transport to the midzone by mediating Aurora B ubiquitylation.

As outlined above, exit from mitosis requires the degradation of cell cycle regulators by the ubiquitin proteasome system. Several observations allow to conclude that ubiquitin-dependent processes are also spatially linked to cytokinesis: Components of the UPS like the ubiquitin activating enzyme E1 and the proteasome itself are both concentrated on midbodies (Grenfell et al., 1994; Wojcik et al., 1995). Furthermore, the chromosomal passenger proteins survivin and Aurora B (Zhao et al., 2000; Sumara et al., 2007) as well as Plk1 (Lindon and Pines, 2004) are degraded most likely on midbody microtubules. Also the core APC/C subunit Doc1/Apc10 was found on the midbody (Kurasawa and Todokoro, 1999). In addition, proteasomal inhibition after anaphase onset revealed that cells fail to complete cytokinesis when ubiquitin-dependent degradation is shut down (Straight et al., 2003). Recent findings extend this view showing that a combination of Cdk1 and proteasomal inhibition can revert late cytokinetic stages to a pre-anaphase state (Potapova et al., 2006).

2.9 A role for components of multivesicular body formation in cytokinesis

Apart from ubiquitin-mediated degradation by the proteasome there is a second type of ubiquitin-dependent degradation by targeting proteins to proteolytic organelles like the vacuole or lysosomes. Most substrates of this pathway are either cell surface transmembrane proteins that are endocytosed or biosynthetic cargo originating from the *trans* Golgi network. Both types of substrates are often mono-ubiquitylated at their cytoplasmic domains. The best characterized ubiquitin-dependent step in this pathway is the maturation of endosomes into multivesicular bodies. These MVBs form through invagination of the limiting membrane of endosomes.

The ‘endosomal sorting complex required for transport’ (ESCRT), which consists of four multi-subunit protein complexes ESCRT-0 to –III, drives ubiquitin-dependent sorting and the formation of multi-vesicular bodies (MVB). ESCRT components are known to recognize specific membrane lipids on the one hand and ubiquitylated transmembrane proteins on the other hand (Hurley and Emr, 2006). Dual recognition allows sequential recruitment of ESCRT subcomplexes and leads to the clustering and sorting of proteins but can also lead to inward budding of membrane domains into the lumen of endosomes. Lysosomal hydrolases can then digest the luminal content.

Recently, this well-established pathway for sorting of ubiquitylated membrane proteins at endosomes has been found to be involved in cytokinesis regulation as well (Spitzer et al., 2006; Carlton and Martin-Serrano, 2007; Morita et al., 2007). Several members of ESCRT were described to be essential for cytokinesis. During the abscission step in cytokinesis a problem similar to the one in enveloped virus egress is encountered. Thin membrane tubules

have to be resolved from within a cell to yield separate membranes. This led to the speculation that cytokinesis and viral budding might make use of a similar molecular machinery. Intriguingly, the recruitment of ESCRT components to the midbody seems to be brought about by the centrosomal protein Cep55 (see above). Cep55 binds to the ESCRT-I component Tsg101 and to another protein Alix, both found to be needed for viral budding (Garrus et al., 2001; Strack et al., 2003). Additionally, Tsg101 can bind the Rho-associated kinase ROCK (see above) and IQGAP1, a factor probably involved in actin remodeling during cytokinesis (Machesky, 1998).

Furthermore, late ESCRT components like ESCRT-III CHMPs and Vps4, an AAA-ATPase that is implicated in ESCRT disassembly and membrane modulation, localize to the midbody and overexpression of CHMPs and expression of dominant negative Vps4(K173Q) give rise to cytokinesis failure (Carlton and Martin-Serrano, 2007; Morita et al., 2007).

The involvement of ESCRT components in the regulation of cytokinesis additionally represents an emerging link between membrane traffic and the ubiquitin-proteasome system in cytokinesis. The ESCRT machinery contains several ubiquitin-binding modules: In ESCRT-0 the multidomain protein Vps27/Hrs can bind to ubiquitylated proteins *via* an ubiquitin interaction motif (UIM), in ESCRT-I Vps23/Tsg101 can bind *via* an ubiquitin E2-variant domain (UEV) and in ESCRT-II Vps36 can bind *via* the GRAM-like ubiquitin-binding in EAP45 domain (GLUE) (Hurley and Emr, 2006; Williams and Urbé, 2007). Whether in cytokinesis ESCRT complexes function in a conveyor belt-like mechanism that involves a stepwise hand-over of ubiquitylated proteins from one ESCRT subcomplex to the other or rather in the fashion of a gradually assembling concentric ring, is still unknown (Nickerson et al., 2007).

This outline so far described cytokinesis regulation and the specific contributions from different cellular pathways. The data presented in this study focuses on the role of BRUCE in membrane transport and ubiquitylation during cytokinesis. The following chapter will thus give information on the current knowledge about BRUCE.

2.10 BRUCE represents an unusual BIRP

Programmed cell death or apoptosis is driven by caspases, the proteases executing proteolytic cleavage of the cell inventory (Salvesen and Duckett, 2002). Proteolytic activity of caspases can be inhibited by so-called BIRPs, proteins that harbor a baculovirus inhibitor of apoptosis repeat (BIR). BIRPs also protect cells from apoptosis by ubiquitylation and degradation of pro-apoptotic factors (Verhagen et al., 2001). The BIR domain represents a zinc-binding fold of approximately 70 amino acids harboring a $CX_2CX_6WX_3DX_5HX_6C$ consensus sequence (Hinds et al., 1999). Notably, linker sequences at the boundaries of BIR domains have been shown to

bind to activated caspases thereby sterically preventing access to substrates (Riedl et al., 2001; Huang et al., 2001; Chai et al., 2001).

In mammalian cells, after loss of mitochondrial integrity, apoptosis-inducing factors like Smac and the serine protease HtrA2 are released through permeability transition pores. These factors can bind to BIRPs *via* a short N-terminal sequence on the same surfaces where caspases bind. This results in a competition of Smac/HtrA2 and caspases for BIRP binding. Therefore, as soon as the cytoplasmic concentration of Smac/HtrA2 rises above a critical level, caspases are relieved from repression by BIRPs and can initiate apoptosis (Ditzel and Meier, 2002).

BRUCE is an unusual BIRP, firstly due to its size of 528 kDa and secondly due to the fact that it contains a single BIR-domain and an ubiquitin-conjugating enzyme (UBC) E2-domain, whereas most other BIRPs contain several BIR-domains and a C-terminal RING finger domain. BRUCE was discovered in a screen using degenerate primers for ubiquitin-conjugating (UBC) enzymes (the E2 enzymes of the ubiquitin conjugation pathway, see above) (Hauser, 1992). *In vitro* BRUCE can form a thioester with ubiquitin and can transfer ubiquitin to substrate proteins demonstrating that it possesses a functional UBC domain (Hauser et al., 1998; Bartke et al., 2004; Hao et al., 2004). Cell fractionation and membrane flotation experiments revealed that BRUCE is a peripherally membrane associated protein (Bardroff, 1997). Furthermore, BRUCE was found to localize mainly to the TGN and perinuclear vesicles. It was also demonstrated that cancer cells expressing high levels of BRUCE are resistant to apoptosis-inducing agents and that conversely downregulating BRUCE results in sensitivity to these agents (Chen et al., 1999).

Notably, analysis of the ortholog of BRUCE in *Drosophila*, dBRUCE, showed that it is in fact involved in apoptosis regulation. dBRUCE could inhibit apoptosis executed *via* the Smac/HtrA2-related pro-apoptotic factors Reaper and Grim but not apoptosis induced *via* a third related factor, Hid (Vernooy et al., 2002). This argued for a role of dBRUCE in specialized pathways leading to cell death. Indeed, during the final step of spermatogenesis in *Drosophila*, spermatids remove their bulk cytoplasm in the process of spermatid individualization. This process is accompanied by an apoptosis-like caspase activation which has to be restricted locally and temporally (Arama et al., 2003). Strikingly, in dbruce -/- flies, which are male sterile, spermatids acquire hyper-condensed nuclei and finally degenerate, indicating uncontrolled or excessive apoptosis. There is also evidence that spermatogenesis in mammals involves transient caspase activation and, in consequence, there might be a need for the anti-apoptotic potential of BRUCE (Arama et al., 2003).

In addition, BRUCE functions as an inhibitor of apoptosis protein in mammalian cells (Bartke et al., 2004; Hao et al., 2004). It can bind and inhibit activated initiator caspases-8 and -9 and executioner caspases-3, -6 and -7. Furthermore, both Smac and HtrA2 are able to compete for BRUCE-bound caspases. Interestingly, BRUCE is also a substrate of caspases and the serine protease HtrA2, pointing to a role in regulating apoptosis at early stages when proteolytic activity mediated by these enzymes is still low. Furthermore, BRUCE can ubiquitylate both Smac and HtrA2 and probably also caspase-9, a caspase initiating apoptosis after mitochondrial permeabilization (Bartke et al., 2004; Hao et al., 2004). Although only a mono-ubiquitylationon the substrate Smac was observed *in vitro*, BRUCE might collaborate with other E3 ligases for poly-ubiquitylation and proteasomal degradation. This is likely also the case for the other BRUCE substrates HtrA2 or caspases. The anti-apoptotic function is probably further restricted to certain subcellular structures, e.g. the TGN and endosomes, where BRUCE localizes (Hauser et al., 1998). Besides the regulation of caspases/pro-apoptotic factors, BRUCE itself seems to be regulated *via* ubiquitin-dependent degradation. Nrdp1/FLRF (neuregulin degrading protein 1/fetal liver ring finger), a RING finger containing ubiquitin ligase initially found to be involved in the degradation of the receptor tyrosine kinase ErbB3/4 (Diamonti et al., 2002; Qiu and Goldberg, 2002), can act as an ubiquitin ligase for BRUCE leading to its proteasome-dependent degradation (Qiu et al., 2004). Overexpression of Nrdp1 was shown to decrease cellular levels of BRUCE and to induce apoptosis by an uncharacterized mechanism. Notably, Nrdp1 also interacts with a de-ubiquitlyating enzyme USP8/UBPY (ubiquitin-specific protease 8 or Y) (Wu et al., 2004). UBPY is a cysteine protease with highest similarity to yeast Doa4. It is implicated in cell cycle regulation, efficient downregulation of the EGF receptor and stability regulation of ESCRT-0 components Hrs and STAM2 (Clague and Urbé, 2006). Depletion of UBPY leads to an increase in size and number of MVBs and accumulation of ubiquitin on their surface (Row et al., 2006). UBPY knockout in mice results in embryonic lethality and knockout in adult animals leads to a severe liver failure (Niendorf et al., 2007). Apart from the UBPY-Nrdp1-BRUCE complex there is a UBPY-OTU1-GRAIL complex described with OTU1 (ovarian tumor 1), representing a member of the ovarian tumor gene DUBs, and GRAIL, an ubiquitin E3 ligase crucial for the induction of anergy in CD4 T-cells (Soares et al., 2004).

Depletion of BRUCE in cultured cells results in sensitization to apoptotic stimuli and finally cell death (Qiu et al., 2004; Hao et al., 2004; Ren et al., 2005). Additionally, depletion in the lung cancer cell line H460 seemingly led to a stabilization of the p53 tumor suppressor, which might be specifically accompanied by mitochondrial-triggered apoptosis (Ren et al., 2005). BRUCE-deficient mice die perinatally due to impaired placental development that can

be attributed to insufficient differentiation (Lotz et al., 2004). However, in contrast to data obtained in cultured cells and to gene-trap mice where N-terminal truncated forms of BRUCE are fused to a ß-galactosidase-neomycin cassette, no signs for elevated apoptosis in the knockout embryos could be observed (Lotz et al., 2004; Hitz et al., 2005, Ren et al., 2005). In the case of gene-trap mice, where insertion of the trap occurred in intron 45 (Hitz et al., 2005) or in intron 30 (Ren et al., 2005), the apoptotic phenotype might be explained by the fact that the artificially created fusion proteins behave more like dominant negative versions. The reason might be that out of the two functional domains characterized so far only the UBC domain is inactivated. Figure 6 depicts BRUCE in a schematic network of protein-protein interactions as described above.

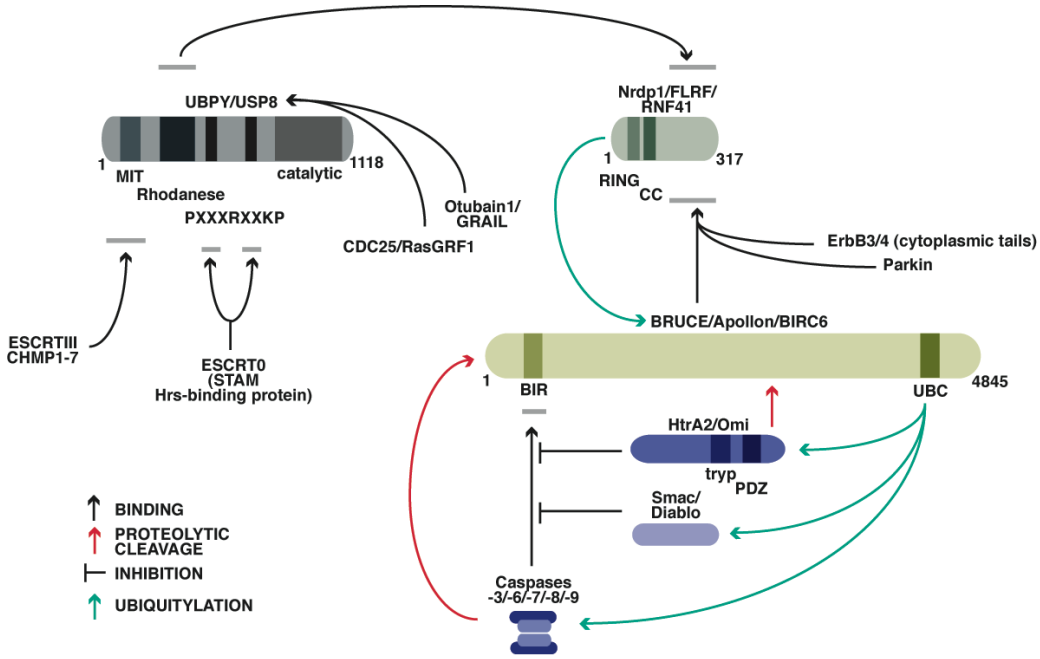

Figure 6. Protein interaction network for BRUCE.
Cartoon depicting the bi-functional IAP/E2 BRUCE, the RING E3-ligase Nrdp1 and the de-ubiquitylating enzyme UBPY. The domain architecture for each protein and the protein length in numbers of amino acids are shown. Furthermore, selected protein-protein interactions are depicted. (tryp = trypsin domain; CC = coiled-coil; MIT = domain in microtubule interacting and trafficking proteins; BIR = baculovirus inhibitor of apoptosis repeat; UBC = ubiquitin conjugating enzyme domain; ESCRT = endosomal sorting complex required for transport; PXXXRXXKP = peptide in UBPY binding to SH3 domains)

Besides apoptosis regulation, BIRPs like survivin (Li et al., 1999) and cIAP1 (Samuel et al., 2005) are also known to participate in cell cycle events and cytokinesis. Notably, with respect to its BIR-domain, BRUCE is most closely related to survivin. Survivin represents a 17 kDa protein which harbors an N-terminal BIR domain and a C-terminal coiled-coil domain. It constitutes a core component of the chromosomal passenger complex and is therefore also essential for cytokinesis (see above). Survivin was described to bind to $p34^{cdc2}$ which

phosphorylates Thr_{34} in survivin, thus enabling it to inhibit caspase-9 specifically when cells pass trough cytokinesis (O'Connor et al., 2000). Similar to BRUCE, survivin can firmly bind to Smac but shows only limited potential in inhibiting caspases *in vivo* (Song et al., 2003; Banks et al., 2000). The C-terminal coiled-coil domain was shown to bind microtubules (Reed and Bischoff, 2000). Furthermore, overexpression of survivin led to reduced centrosomal microtubule nucleation and reduced microtubule dynamics in spindles and midbodies (Rosa et al., 2006).

cIAP1, a predominantly nuclear protein in interphase, has recently been described to participate in cell cycle regulation (Samuel et al., 2005). After nuclear re-accumulation in telophase, a small pool of cIAP1 associates with the midbody in a complex with survivin. Cells overexpressing cIAP1 exhibit an accumulation in G2/M, grow slower and show cytokinesis defects.

Intriguingly, the single BIR proteins of *C. elegans* BIR-1 and *S. cerevisiae* Bir1p do not inhibit apoptosis but instead are involved in cell cycle regulation (Fraser et al., 1999; Uren et al., 1999). Taken together, this suggests that the ancestral funtion of BIRPs may be to control cell cycle events and that regulation of apoptosis as a specific pathway that emerged in multicellular organisms was accompanied by BIR gene duplication.

3 Aim of this study

Several recent reports demonstrated that, besides their roles in apoptosis regulation, BIRP proteins are also utilized by other cellular pathways. The subject of this study, the giant multi-functional ubiquitin-conjugating enzyme BRUCE, is classified as an anti-apoptotic BIRP (Bartke et al., 2004; Hao et al., 2004). However, previous work suggested that BRUCE, besides directly affecting apoptosis, can also act as a general survival factor (Bartke, 2004; Lotz, 2004).

The aim of this study is to investigate the functions of BRUCE in mammalian tissue culture cells and to discover functions that link BRUCE's anti-apoptotic activity to specific cellular processes. To this objective, depletion of BRUCE from cells by RNA interference was established and truncation constructs were generated that are able to mimic the effect of BRUCE depletion. The resulting phenotypes were analyzed biochemically and by microcopy techniques such as life-cell imaging to delineate the underlying molecular basis. Additionally, this study describes novel interactors of BRUCE to allow a better understanding of the various pathways this multi-functional protein is implicated in.

Beyond this initial scope, a general involvement of the ubiquitin-proteasome system in cytokinesis regulation is described with a focus on BRUCE and UBPY, an enzyme with de-ubiquitylating activity. Additionally, a search for proteins that might become ubiquitylated during cytokinesis revealed that the mitotic kinesin MKLP1 is a target for this modification.

4 Results

4.1 BRUCE localizes to the midbody ring and associates with mitotic regulators

Previous reports demonstrated that BRUCE is a cytosolic protein, which is peripherally associated with endomembranes (Hauser et al., 1998). In search for a physiological role of BRUCE in unchallenged cells, the subcellular distribution of BRUCE was re-examined using antibodies that detect the endogenous protein. By using three different polyclonal antibodies directed against N- or C-terminal regions of BRUCE (Bartke et al., 2004; Hauser et al., 1998) (Figure 7A), a comparable staining pattern is detected (Figure 7B) and cells depleted of BRUCE show virtually no staining (Figure 7C).

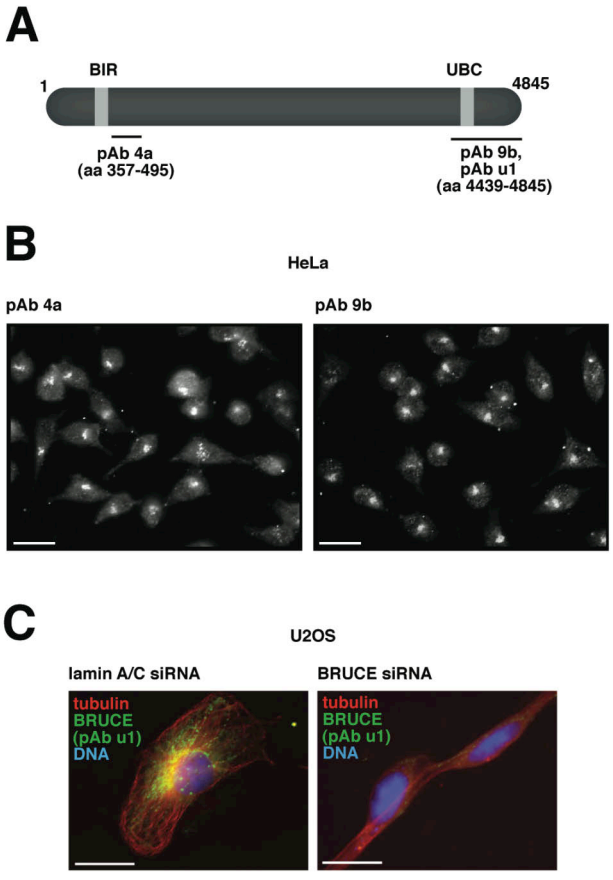

Figure 7. Specificity of BRUCE polyclonal antisera.
(A) Schematic representation of the antigens used to generate BRUCE antisera in rabbits.
(B) Different BRUCE antisera give similar staining patterns. HeLa cells were fixed and stained with two different antisera raised against the N- or C-terminus of BRUCE (pAb 4a and pAb 9b,respectively, scale bar = 20 μm).
(C) anti-BRUCE serum pAb u1 does not stain BRUCE siRNA-treated cells. U2OS cells were treated with siRNAs targeting lamin A/C or BRUCE, fixed after 3 days and stained with anti-α-tubulin (red), anti-BRUCE pAb u1 (green), and DAPI (blue) (scale bar = 20 μm).

In both HeLa and U2OS cells BRUCE relocalizes considerably during the cell cycle (Figure 8 and 9). It concentrates in a pericentriolar compartment in interphase, moves partially to spindle poles in metaphase, and finally localizes to the spindle midzone and the midbody in telophase and during cytokinesis (Figure 8A and Figure 9A). On the midbody, BRUCE localizes in a characteristic ring-like arrangement that is embraced by Aurora B and

microtubules (Figure 8B and 8C), indicating that BRUCE is associated with the midbody ring (Gromley et al., 2005).

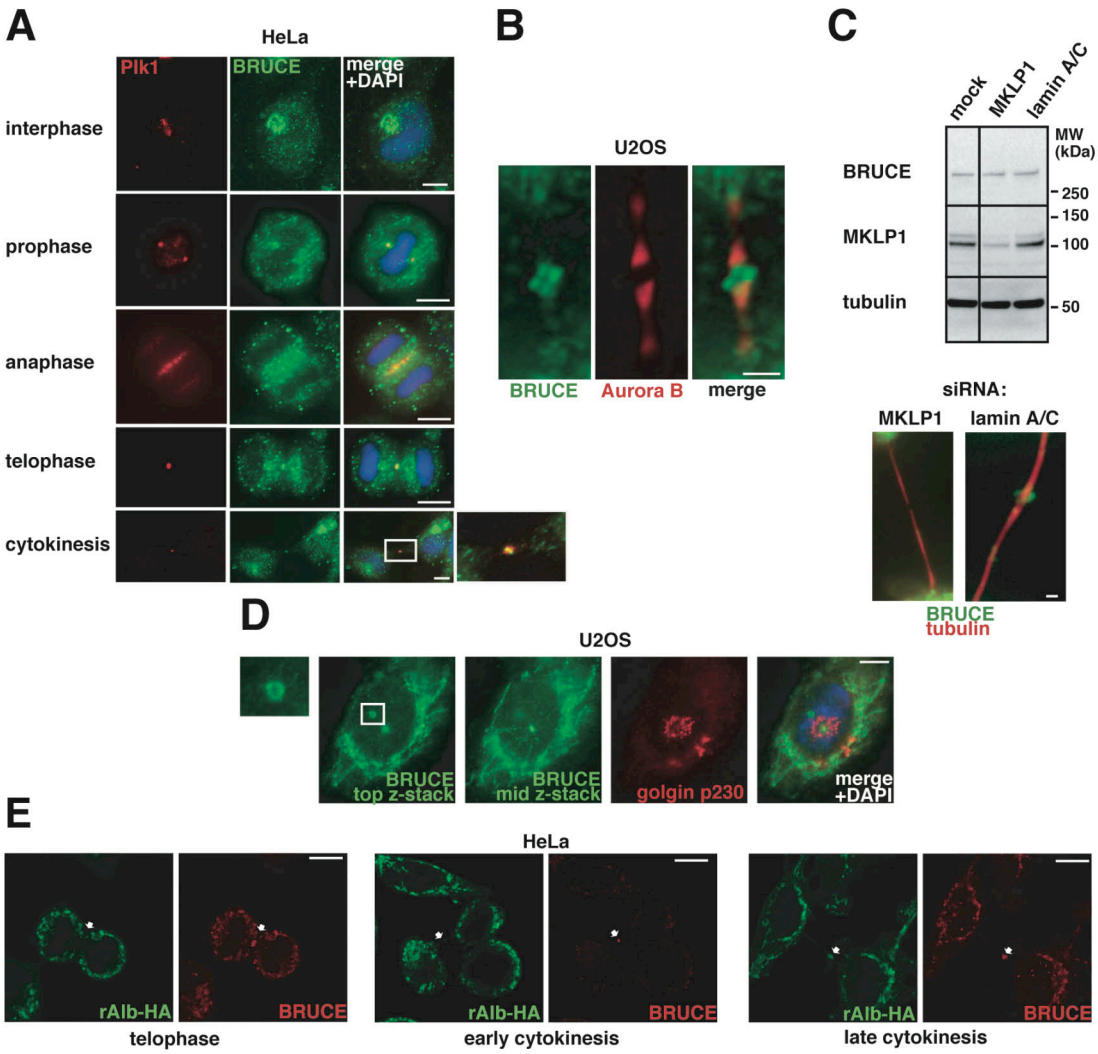

Figure 8. BRUCE shows a cell cycle-dependent localization.
(A) BRUCE localizes to mitotic structures. Immunofluorescence (IF) of HeLa cells stained with anti-Plk1 (red) and anti-BRUCE (green) and DAPI to visualize DNA. The box outlined in white shows the enlarged midbody region of the cytokinesis merge (scale bar = 10 μm).
(B) BRUCE localizes to the midbody ring of U2OS cells. The midbody region is shown with anti-Aurora B (red) and anti-BRUCE (green) staining (scale bar = 1 μm).
(C) Localization of BRUCE to the midbody ring depends on MKLP1. Top: Lysates from HeLa cells transfected with 100 nM siRNAs for three days were analyzed by BRUCE, MKLP1, and α-tubulin immunoblotting. Bottom: Midbodies of siRNA-treated cells are shown stained with anti-α-tubulin (red) and anti-BRUCE (green) (scale bar = 1 μm).
(D) BRUCE is found on midbody ring remnants. U2OS cells were fixed and stained with anti-BRUCE (green) and anti-golgin p230 (red), and DAPI (blue) (scale bar = 10 μm). The top z-stack on the left shows a midbody ring remnant in the plane of the plasma membrane (shown enlarged on the left).
(E) Relationship between BRUCE and constitutive secretory cargo. HeLa cells stably expressing HA-albumin are shown in different cell cycle stages with anti-HA (green) and anti-BRUCE (red) staining (scale bar = 10 μm). The arrow shows the position of the midbody ring.

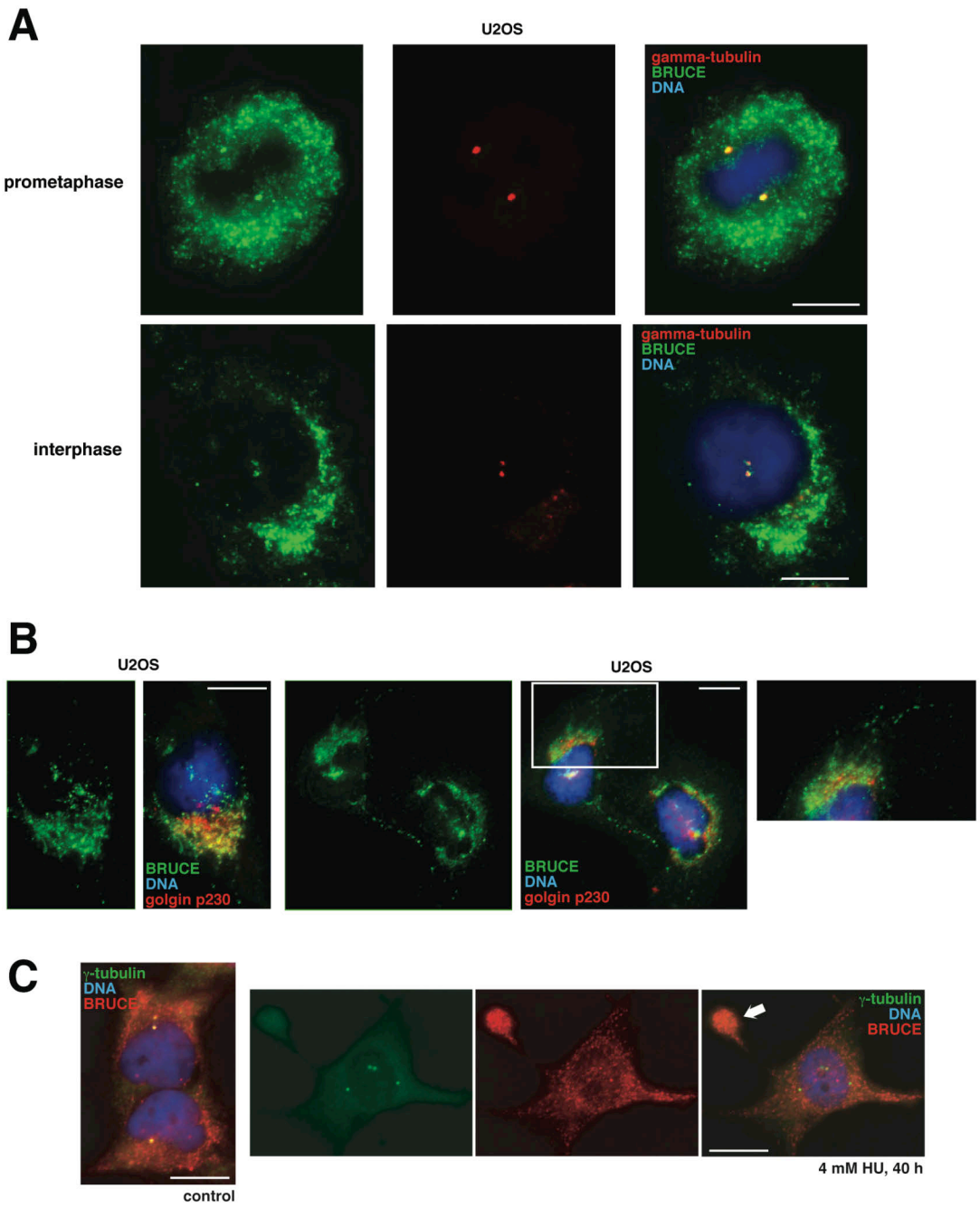

Figure 9. BRUCE partially localizes to spindle poles and centrosomes and is found on perinuclear endosomes in U2OS cells.
(A) BRUCE localizes to spindle poles and centrosomes of U2OS cells. Cells were fixed and stained with anti-γ-tubulin (red), anti-BRUCE (green) and DAPI (blue, DNA, scale bar = 10 μm).
(B) BRUCE is distributed to the TGN and additional vesicular structures. U2OS cells were fixed and stained with anti-p230 (red), anti-BRUCE (green) and DAPI (blue) (scale bar = 10 μm). The amplified area on the right is boxed.
(C) BRUCE is mislocalized after artificial centrosome amplification. U2OS cells were either left untreated (left panel, control) or were grown in culture medium supplemented with 4 mM hydroxyurea (HU) for 40 h. Cells were fixed and stained with anti-γ-tubulin (red), anti-BRUCE (green) and DAPI (blue, DNA, scale bar = 10 μm). The arrow points to a cellular protrusion that contains accumulated BRUCE-positive tubular endosomes.

By using siRNAs targeting MKLP1, a mitotic kinesin essential for the formation of the midbody matrix (Matuliene and Kuriyama, 2002), complete loss of BRUCE at the midbody ring

can be observed in midbody-forming cells (Figure 8C). In untreated cells, BRUCE localizes to the midbody ring as soon as this structure first appears in telophase, and BRUCE persists on the ring even after its uptake by one of the daughter cells after completion of abscission (Figure 8D and 8E).

Notably, midbody ring remnants taken up by one of the daughter cells following cytokinesis are almost exclusively found in the plane of the plasma membrane (Figure 8D). Following the concept that the midbody ring might serve as the site for membrane-mediated abscission, a HeLa cell line expressing HA-epitope tagged albumin was constructed, which allows to investigate membrane traffic and to trace vesicles containing constitutively secreted cargo. Localization of secretory vesicles on the midbody ring is visible only in late cytokinesis when the intercellular bridge has constricted to about 1 μm in diameter, whereas BRUCE, as an apparent firm resident of the midbody ring, localizes to the midbody ring much earlier, concurrent with its formation (Figure 8E).

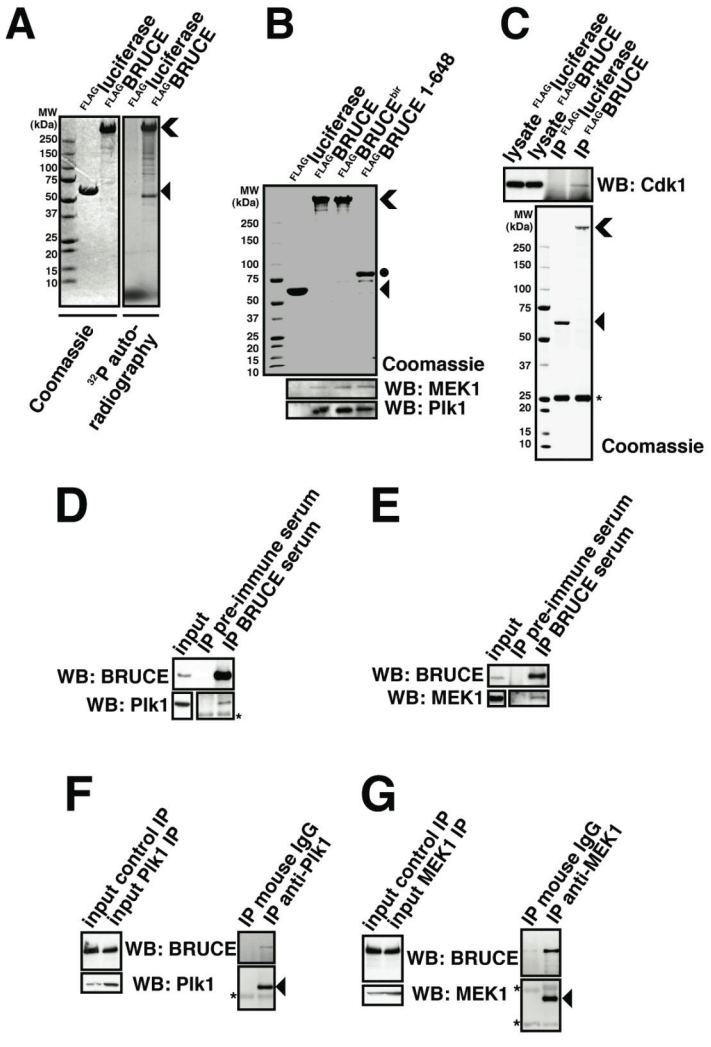

Figure 10. BRUCE is phosphorylated by co-purifying kinases.
(A) BRUCE is phosphorylated by co-purifying factors. Luciferase and BRUCE were expressed in HEK 293T cells, purified via their FLAG epitope tag, peptide-eluted from the affinity matrix, and incubated with ^{32}P-γ-ATP. Proteins were resolved by SDS-PAGE and either stained with Coomassie, or gels were dried and radio-labeled proteins were detected by autoradiography. Open arrowheads mark BRUCE, closed arrowheads luciferase.
(B) and (C) BRUCE associates with mitotic kinases Plk1, MEK1, and Cdk1. FLAG-tagged fusion proteins were purified as in (A) and assayed for associated proteins by immunoblotting (WB).
(D) to (G) Plk1 and MEK1 coprecipitate with BRUCE at endogenous levels. Lysates of HEK 293T cells were subjected to immunoprecipitation and immunoblotting using a pre-immune serum or an antiserum (pAb u1) raised against the C-terminus of BRUCE [(D) and (E)], or unspecific mouse IgGs or anti-Plk1 or anti-MEK1 antibodies, respectively [(F) and (G)]. The asterisks mark the signals corresponding to antibody light or heavy chains.

Given its highly dynamic localization pattern during cell division, a search for binding partners was performed also investigating whether BRUCE might be a target for mitotic phosphorylation. Indeed, BRUCE is particularly phosphorylated in S-phase extracts (data not shown) and immunopurified BRUCE is also phosphorylated by co-purified factors whereas a control protein purified by the same method is not (Figure 10A). By immunopurification (IP) of FLAG-tagged BRUCE, or immunoprecipitation of the endogenous protein, BRUCE associates with the mitotic kinases Cdk1, MEK1, and Plk1 (Figures 10B-10G). In order to characterize the binding site in BRUCE for kinases, FLAG-tagged BRUCE, the BIR-domain mutant (^{FLAG}BRUCE^{bir}), an N-terminal fragment that is normally created by caspase cleavage (^{FLAG}BRUCE 1-648) and a control protein (^{FLAG}luciferase) were immunopurified (Figure 10B). Whereas the control protein shows no binding to either MEK1 or Plk1, all BRUCE constructs bind to both kinases. This indicates that the N-terminus of BRUCE is required for kinase interaction and that a functional BIR-domain is dispensable.

Recently, a mixed IAP-IAP complex of survivin and XIAP was identified (Dohi et al., 2004). The midzone and midbody localization of BRUCE might allow an interaction with survivin, which is also enriched there. Hence, complex formation between BRUCE and survivin was investigated. When overexpressed, survivin can indeed co-precipitate BRUCE and *vice versa* (Figure 11A and 11B). In addition, BRUCE is able to mono-ubiquitylate survivin *in vitro* (Figure 11C), arguing for a regulatory modification or a priming ubiquitylation for the degradation of survivin later on in cytokinesis. These data indicate that the two BIRPs may indeed cooperate at the midzone or the midbody, where both proteins are found (Figure 8A) (Ruchaud et al., 2007).

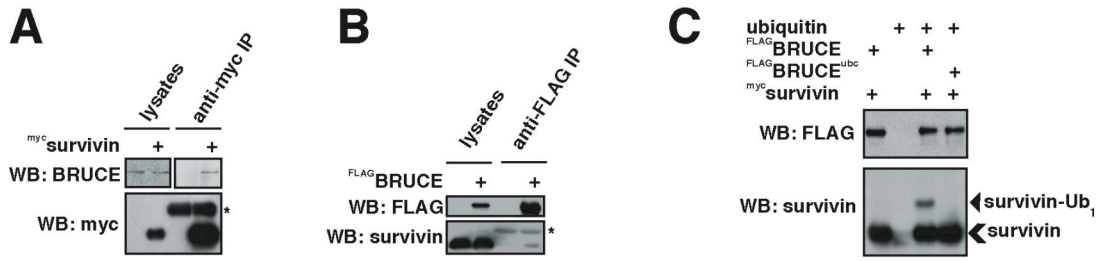

Figure 11. BRUCE interacts with and modifies survivin.
(A) Survivin can co-precipitate BRUCE. HEK 293T cells were transfected with empty vector or myc-survivin. Immunoprecipitation with anti-myc antibodies was carried out and lysates and precipitated material were probed by immunoblotting (WB) for surivin (myc) and BRUCE.
(B) BRUCE can co-precipitate survivin. HEK 293T cells were transfected with empty vector or FLAG-BRUCE. Immunoprecipitation with anti-FLAG antibodies was carried out and lysates and precipitated material were probed by immunoblotted for surivin and BRUCE (FLAG).
(C) In vitro ubiquitylation of survivin by BRUCE. BRUCE and survivin were purified from HEK 293T cells via their epitope tags. As a control, a UBC-domain mutant of BRUCE which cannot support thioester formation, was also purified. Proteins were incubated in the indicated combinations in assay mix containing ubiquitin activating enzyme E1 and ATP.

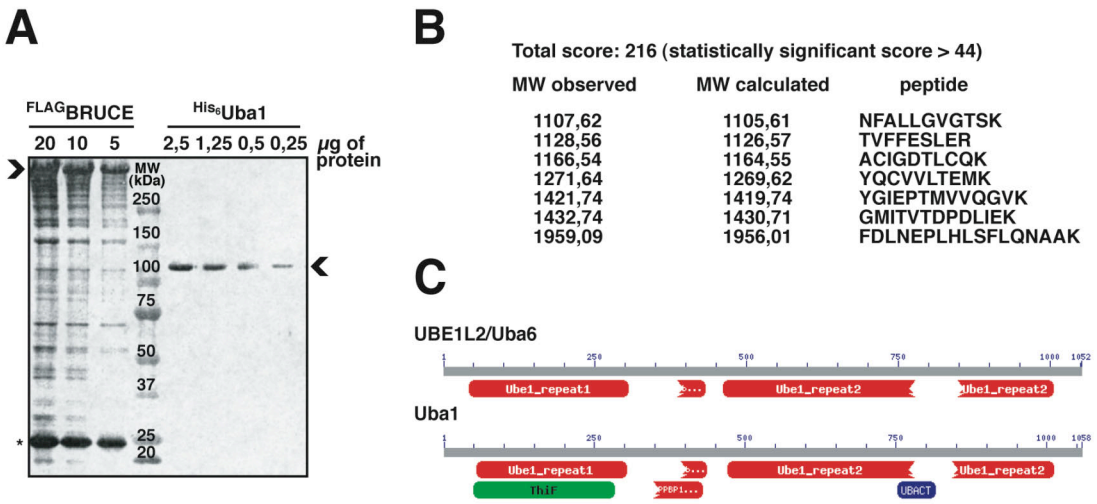

Figure 12. Identification of UBE1L2 in BRUCE purifications.
(A) UBE1L2 co-purifies with BRUCE. HEK 293T cells were transfected with a ^{FLAG}BRUCE expression vector. Cells were harvested and lysed. BRUCE was purified on an anti-FLAG immunoaffinity resin. To estimate the molecular weight of co-purified bands, His_6-epitope tagged wheat Uba1 purified from bacteria was also loaded on the same gel. Amounts of proteins loaded are indicated. Open arrowheads indicate BRUCE and Uba1, respectively. The asterisk indicates the light chain of the affinity resin's antibody.
(B) Peptides of UBE1L2 recovered in BRUCE immunopurifications. The band at the molecular weight of Uba1 was excised and analysed by mass spectrometry. The peptides recovered for UBE1L2 are shown.
(C) UBE1L2 and Uba1 show the same domain architecture.

Interestingly, when performing *in vitro* ubiquitylation reactions, it was frequently observed that reactions containing BRUCE, however not supplemented with ubiquitin activating enzyme E1, can support ubiquitylation (data not shown). Immunopurified BRUCE was therefore analyzed for co-purifying E1 activity (Figure 12A). Strikingly, peptides corresponding to a protein called UBE1L2/Uba6/E1-L2 were recovered in mass spectrometric analysis (Figure 12B). This protein has only recently been found to be a functional E1 for ubiquitin and probably also for the ubiquitin-like modifier FAT10 (Jin et al., 2007; Chiu et al., 2007; Pelzer et al., 2007). UBE1L2 shows an identical domain composition to Uba1 with varying identities of 30-60% in each domain (Figure 12C). UBE1L2 is probably a specialized E1 that can only transfer ubiquitin to a small number of E2s like e.g. UBE2Z/Use1 and probably BRUCE. The putative association of UBE1L2 with BRUCE might argue for an Uba1-independent loading of BRUCE with ubiquitin by this newly identified ortholog. Further testing will be needed to conclude whether BRUCE is an E2 that specifically functions together with UBE1L2.

4.2 BRUCE is a component of tubular and recycling endosomes and associates with the exocyst

In order to further characterize the vesicular system where BRUCE resides, cells were stained with anti-α-tubulin and anti-BRUCE antibodies. Indirect immunofluorescence revealed that endomembranes containing BRUCE cluster around centrosomes (Figure 13A). Furthermore, peripheral vesicles decorated with BRUCE are collinear with microtubules, suggesting the presence of a vesicular system that utilizes the microtubule network for transport processes (Figure 13C). When testing an association of BRUCE with additional factors on endogenous levels, α-tubulin can be specifically co-precipitated with an anti-BRUCE serum (Figure 13C). BRUCE can therefore be characterized as a resident of membranous organelles that travel on microtubules and BRUCE might mediate or modulate contacts with tubulin. Additionally, BRUCE localization along microtubules seems to depend on functional centrosomes. In a setting of artificially amplified centrosomes by treating U2OS cells with hydroxyurea (Meraldi et al., 1999), BRUCE-stained structures accumulate in strange cellular protrusions (Figure 9C). This indicates that when microtubule organization is disrupted BRUCE localization is also affected.

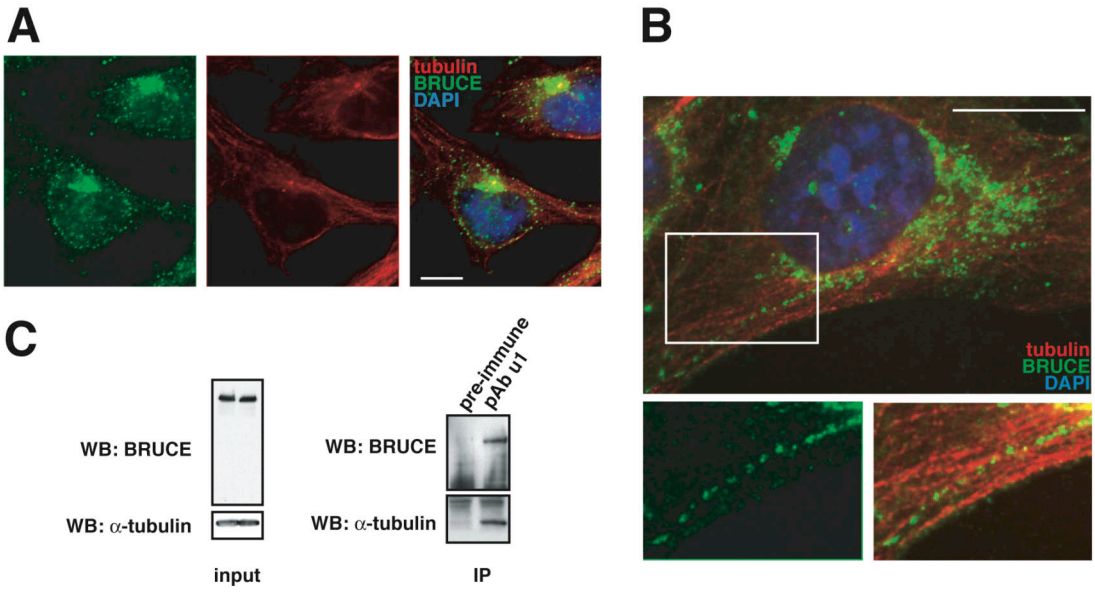

Figure 13. BRUCE is concentrated in a pericentrosomal compartment and is associated with microtubules.
(A) and (B) BRUCE is concentrated in a pericentriolar compartment and is found on tubular vesicles along microtubules. HeLa (A) or U2OS cells (B) were fixed and stained with anti-α-tubulin (red), anti-BRUCE (green) and DAPI to stain DNA (blue) (scale bar = 10 μm). The box outlined in white in (B) is shown enlarged in the lower panels.
(C) BRUCE interacts with α-tubulin. HEK 293T cells were lysed and immunoprecipitations with pre-immune serum or anti-BRUCE u1 serum were carried out. Lysates and precipitated material were analyzed by SDS-PAGE and immunoblotting.

To elucidate whether the peripheral carriers that contain BRUCE are responsible for endocytosis or exocytosis, a transferrin uptake experiment was performed (Figure 14A). Co-localization of BRUCE with transferrin can be observed after a chase of 15 min when most of the transferrin is either already re-exocytosed *via* a quick recycling route (Hopkins, 1983) or reaches the pericentrosomal recycling compartment. At this point, the highest degree of co-localization can be detected, arguing for an association of BRUCE with recycling endosomes.

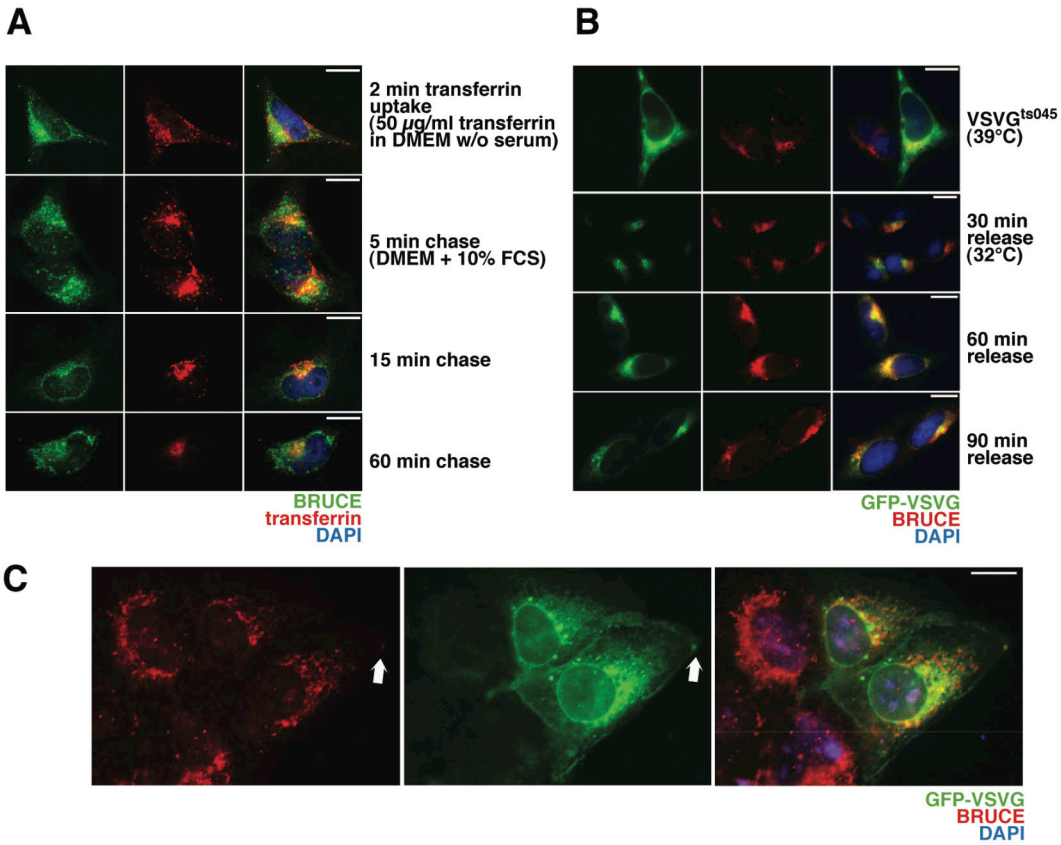

Figure 14. BRUCE is a component of exocytic but not endocytic carriers.
(A) BRUCE co-localizes with transferrin only at sites of recycling. HeLa cells were incubated in DMEM without serum but containing 50 µg/ml TRITC-labeled transferrin for 2 min. Subsequently, the medium was replaced by chase medium consisting of DMEM supplemented with 10% FCS. Cells were fixed at the indicated timepoints to follow the intracelluar fate of the transferrin that was endocytosed. Fixed cells were additionally stained with anti-BRUCE (green) and DNA was stained with DAPI (blue) (scale bars = 10 µm).
(B) BRUCE co-localizes with VSVG when it reaches the sorting compartment. HeLa cells were transfected with an expression vector coding for a temperature sensitive folding mutant of GFP-tagged VSVG (green). After transfection, cells were grown at the non-permissive temperature of 39°C for one day. VSVG transport was initiated by shifting cells to the permissive temperature of 32°C. During transport, cycloheximide was added (2.5 µg/ml). Cells were fixed at the indicated timepoints to follow intracelluar fate of VSVG. Fixed cells were additionally stained with anti-BRUCE (red) and DNA was stained with DAPI (blue) (scale bars = 10 µm).
(C) BRUCE is found on peripheral transport containers harboring exocytic cargo. The experiment was performed in U2OS cells as described in (B). Cells were fixed 120 min after shifting to the permissive temperature. The arrow points to a transport container that has almost reached the plasma membrane (scale bar = 10 µm).

Additionally, exocytosis was examined by the use of a temperature-sensitive folding mutant of the vesicular stomatitis virus glycoprotein (VSVG^{tsO45}) (Flamand, 1970; Gallione and Rose, 1985).

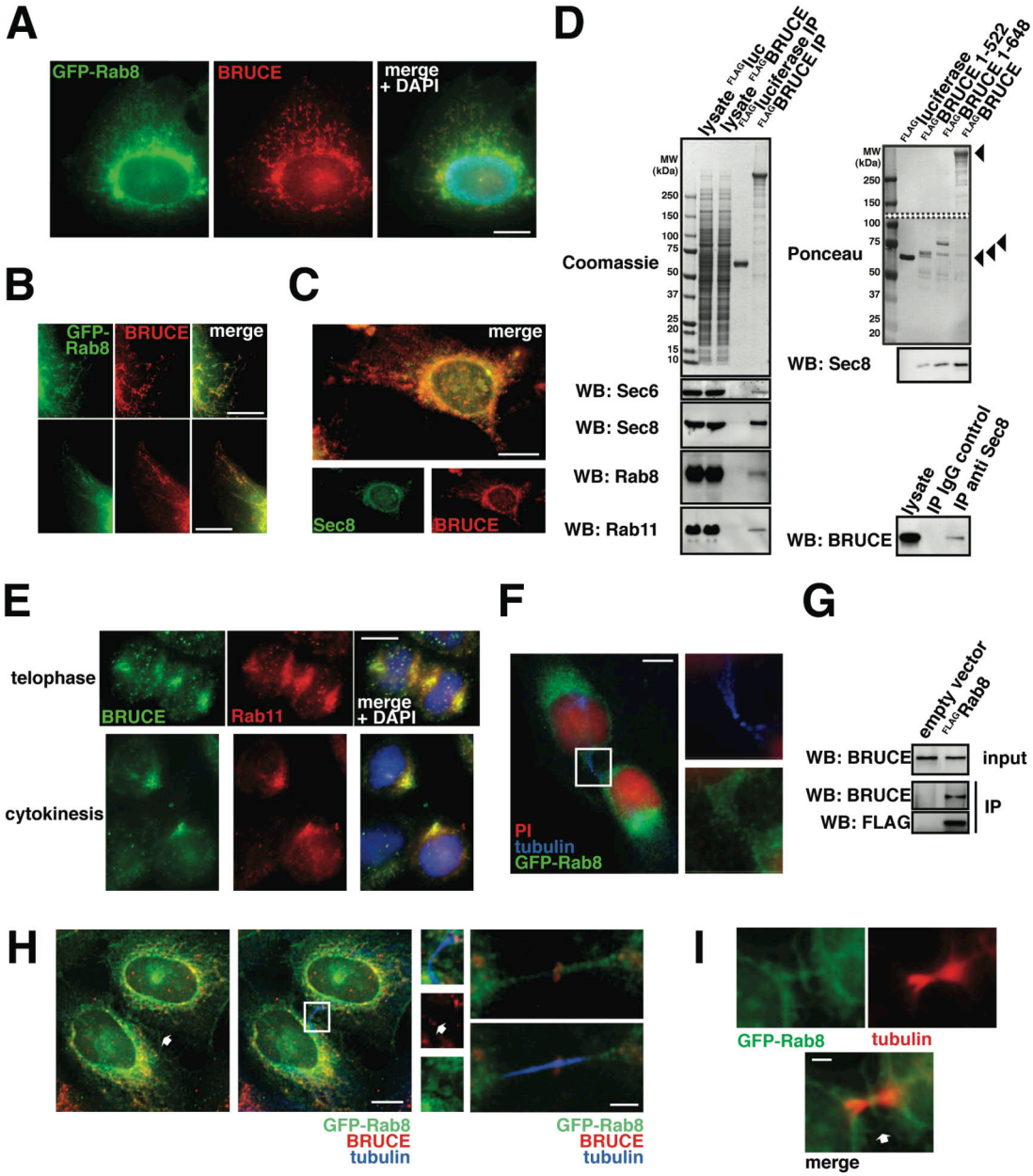

Figure 15. BRUCE is a component of tubular endosomes and interacts with membrane targeting factors.
(A) and (B) BRUCE localizes to Rab8 tubular endosomes in interphase cells. U2OS cells stably expressing GFP-Rab8 (green) were fixed and stained with anti-BRUCE (red) and DAPI (blue) (scale bar = 10 μm). (B) shows magnified areas of cellular protrusions with tubular endosomes (scale bar = 5 μm).
(C) BRUCE co-localizes with the exocyst component Sec8 in a perinuclear compartment. Fixed U2OS cells; anti-BRUCE (red), anti-Sec8 (green) (scale bar = 15 μm).
(D) BRUCE co-purifies with exocyst components Sec6, Sec8, and endosomal GTPases Rab8, Rab11. Left panel: HEK 293T cells were transfected with either FLAG-epitope tagged luciferase (luc) or BRUCE. Cells were lysed and FLAG-fusion proteins purified. Bound material was eluted with FLAG peptide and analyzed by Western blots (WB).

VSVG is first inserted into the ER membrane, glycosylated and further trimmed at the Golgi where it is packaged into transport containers that travel to the plasma membrane. The Orsay strain revertant ts45 (tsO45) is characterized by three amino acid exchanges that trap the protein in the ER at the non-permissive temperature of 39°C due to a folding problem. Secretion can be triggered by shifting cells to the permissive temperature of 32°C. Following the transport route of $VSVG^{tsO45}$ after release of the temperature block, co-localization with BRUCE at the point when most of the VSVG reaches the Golgi/TGN interface can be observed (Figure 14B). Strikingly, BRUCE is still found on VSVG-containing carriers right before they reach the plasma membrane (Figure 14C, carrier marked by an arrow). The pericentrosomal localization, the co-localization with recycled cargo at sites of late recycling and the association of BRUCE with traffic containers for exocytic cargo allows to conclude that BRUCE is associated with recycling and secretory endosomes. To characterize BRUCE localization further, co-localization with markers of the vesicular system was tested. Only partial co-localization with the TGN markers golgin p230 and TGN38 can be found (Figure 9B) (Hauser et al., 1998).

However, for a more detailed analysis, U2OS cells were generated that stably express GFP-Rab8 and GFP-Rab11, respectively. In these cells, a substantial co-localization with both endosomal GTPases Rab8 and Rab11 can be observed, even with Rab8-positive, peripheral tubular endosomes (Figure 15A, 15B and 15E). Besides Rab GTPases that define the recycling compartment, other factors for membrane tethering like the exocyst complex are also found here. This is also reflected by the co-localization of BRUCE with the exocyst subunit Sec8 (Figure 15C).

Figure 15 continued
Upper right panel: The N-terminus of BRUCE mediates interaction with Sec8. HEK 293T cells were transfected to express the indicated FLAG-fusion proteins which were subsequently purified and eluted. The length of the BRUCE constructs is given in amino acid residue numbers; the arrow heads point to the BRUCE constructs. Lower right panel: Sec8 and BRUCE interact when expressed at endogenous levels. HEK 293T cells were lysed and either incubated with mouse IgGs or anti-Sec8-antibodies. Material bound to protein-A-sepharose was analyzed by anti-BRUCE immunoblotting.
(E) Co-localization of BRUCE with Rab11 recycling endosomes in cytokinesis. Fixed HeLa cells; anti-Rab11 (red), anti-BRUCE (green), DAPI (blue) (scale bar = 15 μm).
(F) Rab8 tubular endosomes are found in the midbody region. Fixed U2OS cells; anti-α-tubulin (blue), propidium iodide DNA staining (red) (scale bar = 10 μm).
(G) BRUCE interacts with Rab8. HEK 293T cells were transfected with either FLAG-epitope tagged Rab8. Cells were lysed and FLAG-fusion proteins purified. Bound material was analyzed by Western blots (WB).
(H) and (I) Rab8 is found at the midbody ring and at the newly formed plasma membrane in-between dividing cells. Fixed U2OS cells; arrowheads indicate the site of the newly formed plasma membrane [scale bar (H) = 10 μm, (I) = 2 μm]. The smaller figures are enlargements of the framed areas. The position of the midbody ring is indicated by an arrow.

Importantly, Rab8 and Rab11, as well as the exocyst subunits Sec6 and Sec8, physically associate with BRUCE, as demonstrated by immunoprecipitations (Figure 15D and 15G). Similar to the mitotic kinases (Figure 10B), the binding site for the exocyst seems to lie within the N-terminal region of BRUCE (Figure 15D, upper right panel) and thus involves a different region in BRUCE than the one used for midbody ring interaction (see below). Notably, similar to exocyst subunit Exo70 (Vega and Hsu, 2001), BRUCE also relocalizes to growth cones in neuronally differentiated cells (Figure 16), strongly indicating that BRUCE is firmly connected to the exocyst and plays a more general role in targeted membrane delivery.

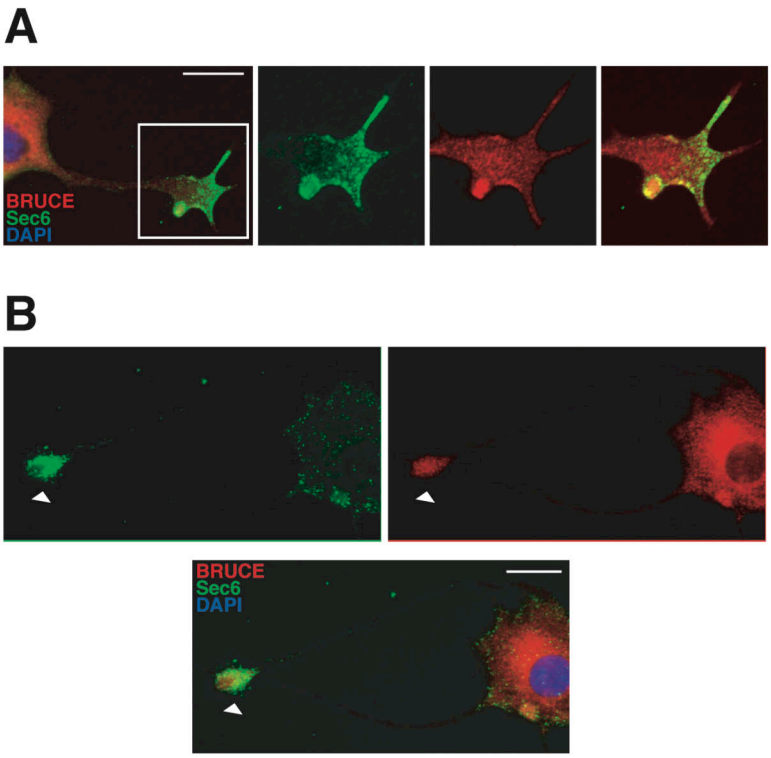

Figure 16. BRUCE re-localizes to growth cones in NGF-differentiated rat PC12 phaeochromocytoma cells.
(A) and (B) Exocyst subunit Sec6 and BRUCE are targeted to growth cones. Neurite outgrowth of PC12 cells was induced by treatment with NGF and cells were fixed after 3 days and stained with anti-BRUCE (red), anti-Sec6 (green),and DAPI (blue) (scale bar = 10 μm). The growth cones exhibit protrusions, which concentrate membranous pools that contain BRUCE and Sec6 (magnified in (A) and marked by arrowheads in (B)).

4.3 Rab11- and Rab8-endosomes are sources of membrane material in cytokinesis and the midbody ring acts as a barrier

Due to the finding that BRUCE associates with the midbody ring (Figure 8) and is also found on recycling and secretory vesicles (Figure 8, Figure 14 and Figure 15) the question emerged whether vesicles containing BRUCE participate in cytokinesis. Experiments shown here could confirm previous observations (Fielding et al., 2005) that suggested a role for recycling Rab11-endosomes in cytokinesis. Two pools of Rab11-endosomes are found on both sides of the intercellular bridge during cytokinesis, and a small fraction also seems to reach the midbody

ring (Figure 15E). However, in contrast to a recent report on HeLa cells (Yu et al., 2007), in engineered U2OS cells GFP-Rab8 staining at the midbody can be found (Figure 15F and 15H) and also at the newly formed plasma membrane at the contact site of dividing cells (Figure 15I). Indeed, live cell imaging suggests that Rab8-endosomes are delivered to the midbody ring and that this supplied material then diffuses at the plasma membrane laterally (Figure 17A). Remarkably, by using photobleaching experiments, it can be shown that Rab8-endosomes are unable to move freely from one perspective daughter cell to the other once the midbody ring has been assembled in telophase (Figure 17B), which differs from the otherwise mobile behavior of these vesicles during interphase.

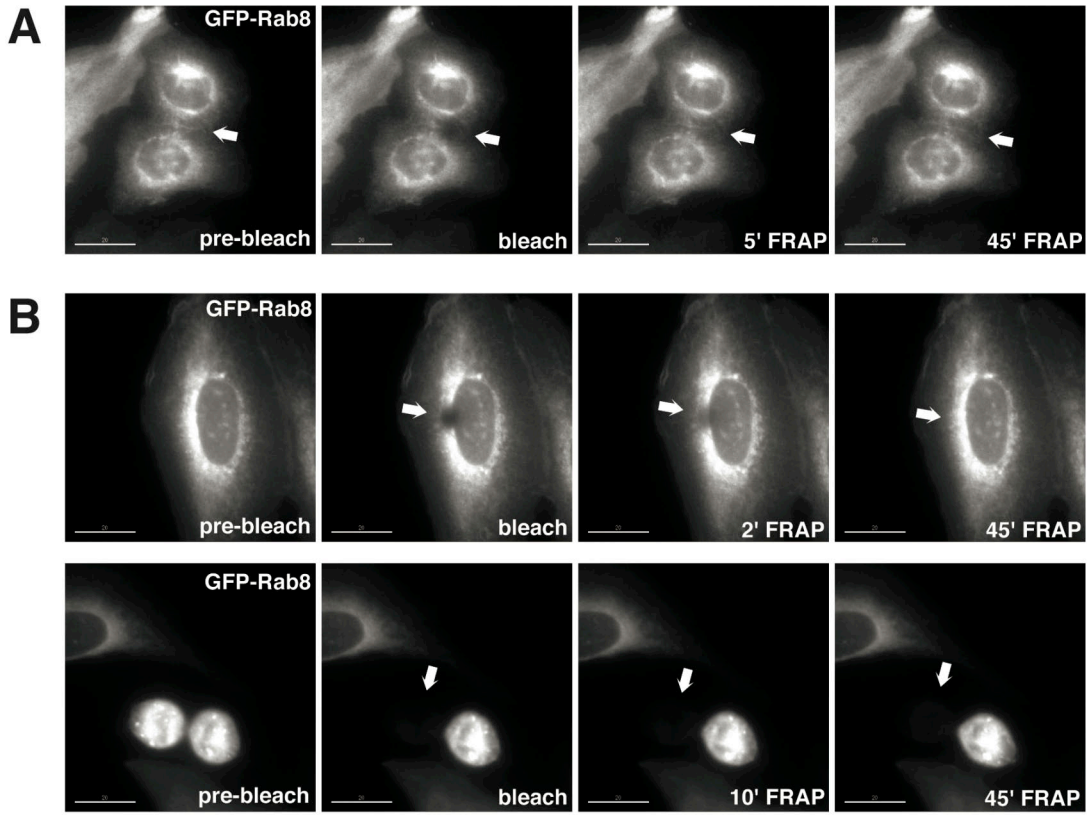

Figure 17. Rab8 dynamics during cytokinesis.
(A) Rab8 is found at the plasma membrane at the contact site of sibling cells in cytokinesis. U2OS cells that stably express GFP-Rab8 were analyzed by time lapse video microscopy. During cytokinesis, an area at the contact site of the plasma membrane of sibling cells was bleached by a short laser pulse and recovery of fluorescence was recorded (see arrows, scale bars = 20 μm).
(B) Rab8 endosomes cannot traverse the cleavage furrow. U2OS cells that stably express GFP-Rab8 were analyzed by time lapse video microscopy. To monitor interphase dynamics of Rab8 endosomes, an area in the perinuclear region was bleached by a short laser pulse and recovery of fluorescence was recorded (upper panel, arrows point to the bleached area). To monitor dynamics of Rab8 endosomes in cytokinesis, one of two sibling cells was completely bleached (lower panel, arrows point to the bleached cell, scale bars = 20 μm). Note that there is essentially no fluorescence recovery.

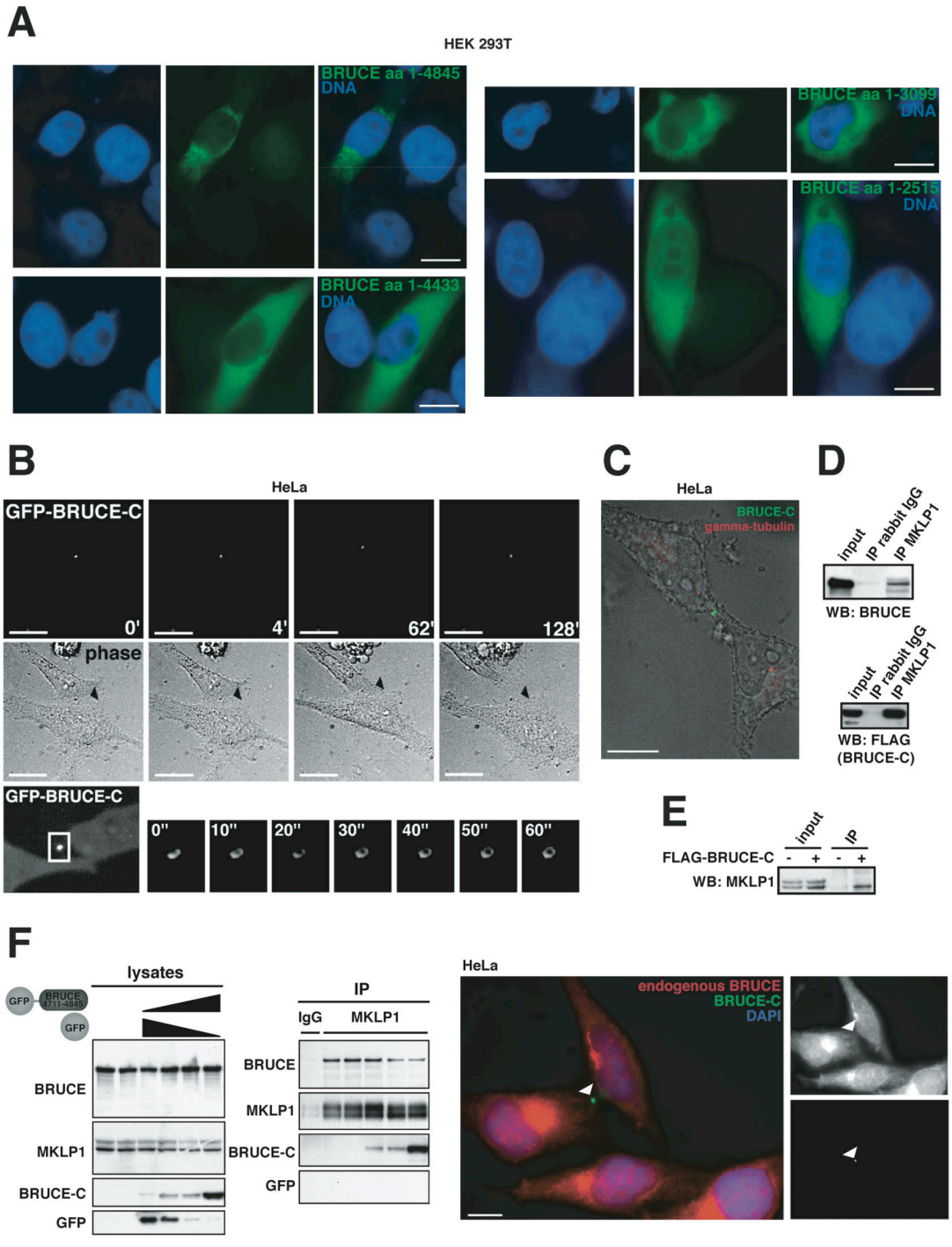

Figure 18. The C-terminus of BRUCE represents a midbody ring-targeting domain.
(A) BRUCE C-terminus mediates interaction with endomembranes. HEK 293T cells were transfected with GFP-fusions with the N-terminus of BRUCE (green). The length of the BRUCE constructs is given in residue numbers. Cells were fixed and stained with DAPI to visualize DNA (blue, scale bars = 10 μm).
(B) GFP fused to the C-terminus of BRUCE (amino acids 4711-4845, GFP-BRUCE-C) is localized to the midbody ring. The movie stills show GFP-BRUCE-C on the midbody ring of HeLa cells (scale bar = 15 μm).
(C) Localization of BRUCE-C relative to centrosomes. HeLa cells transfected with GFP-BRUCE-C (green) were stained with anti-γ-tubulin (red). The image shows a merge with the bright-field channel (scale bar = 15 μm).
(D) The midbody ring-targeting domain of BRUCE interacts with MKLP1. Top: Lysates of HEK 293T cells were immunoprecipitated (IP) with either rabbit IgGs or anti-MKLP1 antibodies and analyzed by anti-BRUCE WB. Bottom: HEK 293T cells transfected with GFP-FLAG-BRUCE-C were lysed and proteins immunoprecipitated with rabbit IgG (control) or anti-MKLP1 IgGs. Input and precipitates (IP) were analyzed by anti-FLAG blots (WB) detecting BRUCE-C.

This finding considerably substantiates the idea that midbody rings, in addition to acting as the site for membrane delivery, may play a role as a diffusion barrier in-between the two prospective daughter cells (Schmidt and Nichols, 2004). Apparently, this barrier does not only prevent intercellular exchange of plasma membrane-associated material as shown before (Schmidt and Nichols, 2004), but also of endosomal vesicles.

It should be emphasized that cytokinesis in U2OS cells probably demands for more plasma membrane remodeling than cytokinesis in HeLa cells because of the intercellular bridge in U2OS being rather short and often appearing to lie on top of the cells instead of being continuous with the cell protrusion generated by the cleavage furrow as can be seen for HeLa cells.

4.4 BRUCE harbors a midbody ring-targeting domain

The distinctive and dynamic localization of BRUCE suggested the presence of dedicated targeting domains. The use of BRUCE truncation constructs that comprise N-terminal portions of the protein reveals that the typical localization of BRUCE at sorting compartments requires its C-terminal region (Figure 18A). Hence, a fusion of GFP to the C-terminal 145 amino acids containing also the last 20 amino acids of the UBC domain was constructed (referred to as BRUCE-C). Surprisingly, this construct does not localize to pericentriolar endosomes but localizes to the phase-dense midbody ring that also contains MKLP1 (Figure 18B, 18C, 20B and 20C). Time-lapse video microscopy demonstrates that the BRUCE-C-labeled ring-like structure shows a degree of mobility and tilting characteristic for the midbody ring, and that it is taken up by one of the daughter cells following abscission (Figure 18B and Figure 19A). Prior to the uptake, the midbody ring moves along the intercellular bridge and contacts the plasma membrane of one cell (Figure 20A). As the localization of endogenous BRUCE to the midbody ring depends on MKLP1 (Figure 8C), one can speculate that BRUCE-C might contain a specific interaction domain with midbody ring components.

Figure 18 continued
(E) The midbody ring-targeting domain of BRUCE interacts with MKLP1. HEK 293T cells were either transfected with empty vector or GFP-FLAG-BRUCE-C. Lysates were subjected to anti-FLAG IP and analyzed by anti-MKLP1 WB.
(F) Exogenously expressed BRUCE fragment containing the midbody ring-targeting domain competes with endogenous BRUCE for midbody ring binding via MKLP1. HEK293T cells were transfected with increasing amounts of GFP-BRUCE-C and decreasing amounts of GFP. Lysates (inputs are shown in the left panel) were subjected to immunoprecipitation (IP) with rabbit IgGs (control) or anti-MKLP-1 antibodies, and precipitated proteins were analyzed by Western blots. Competition on the single-cell level is shown for HeLa cells by immunofluorescence (endogenous, full-length BRUCE, red; GFP-BRUCE-C, green; DNA stained with DAPI). The arrowhead marks the midbody ring (scale bar = 10 μm).

Indeed, MKLP1 co-precipitates with full-length, endogenous BRUCE (Figure 18D, upper panel) and also with BRUCE-C (Figure 18D, lower panel). Interestingly, BRUCE-C selectively binds the faster migrating variant, MKLP1, but not CHO1, a larger variant caused by alternative splicing that additionally possesses an actin-interacting tail (Figure 18E). As both isoforms are present at the midbody (Kuriyama et al., 2002), this finding argues for different functions of these two variants during late stages of cytokinesis.

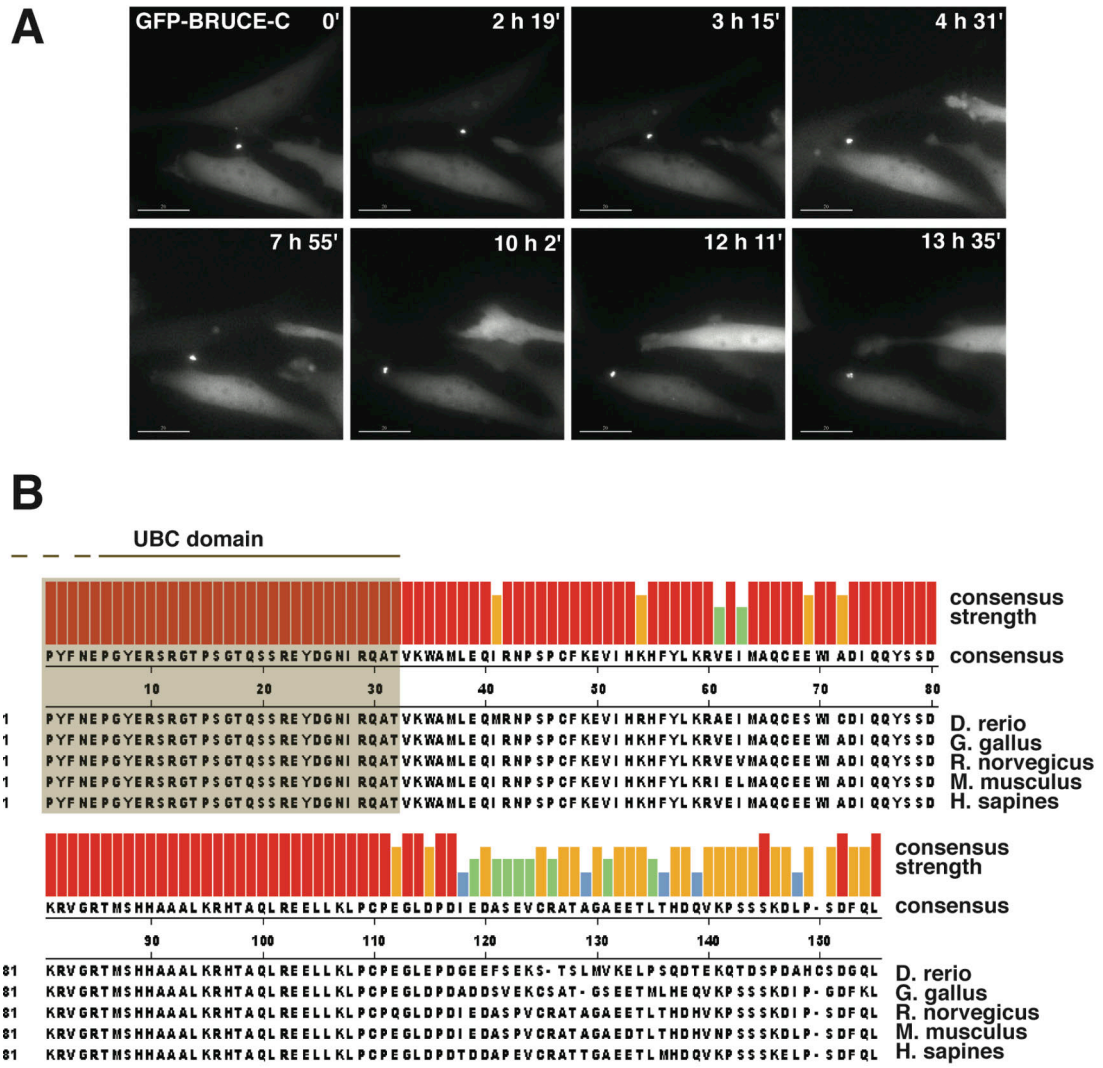

Figure 19. Midbody rings stained by BRUCE-C are taken up by one cell.
(A) The midbody ring is taken up by one cell after abscission. HeLa cells were transfected with GFP-BRUCE-C and images were taken by time lapse video microscopy (scale bar = 20 μm). (B) The C-terminus of BRUCE is highly conserved among vertebrates. Fish, chicken, rodent and human protein sequences are depicted showing high similarities, notably also outside the UBC domain.

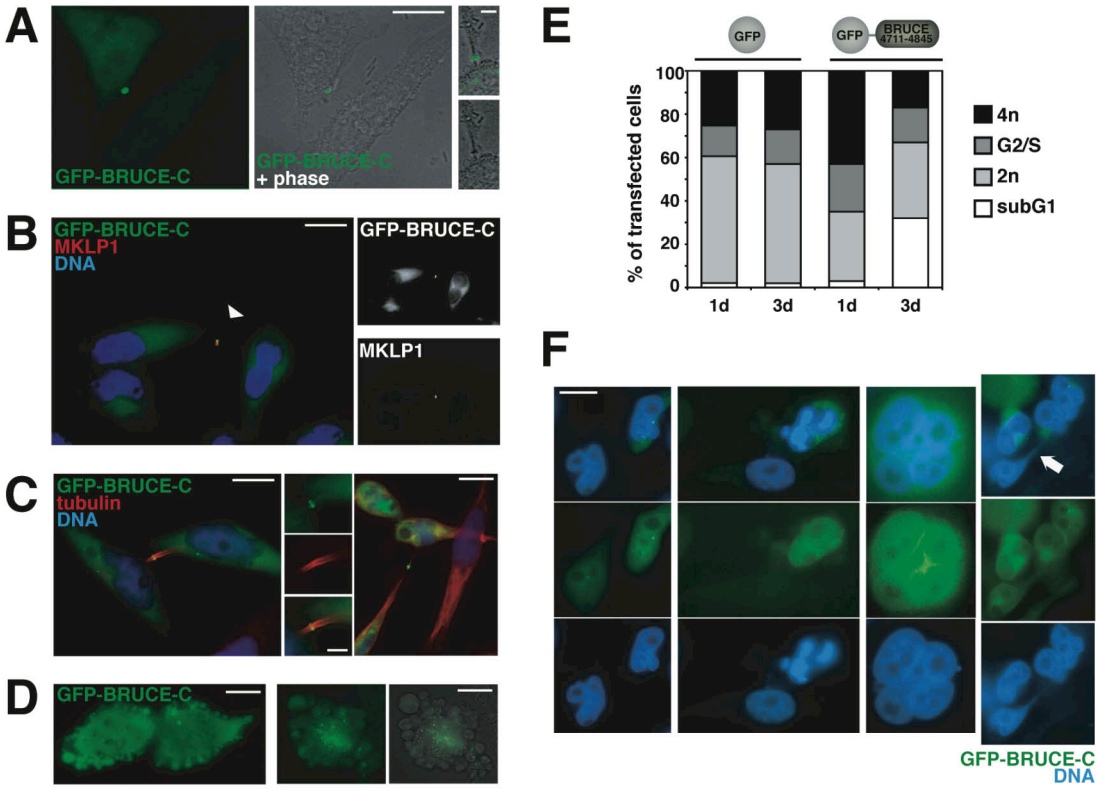

Figure 20. BRUCE-C localization and overexpression in HeLa cells.
(A) The midbody ring moves to the plasma membrane of one cell after completed cytokinesis. HeLa cells were transfected with GFP-BRUCE-C (green) and fixed after 12 h. Fluorescence and phase images are shown (scale bar = 20 μm). Right: Enlargement of the intercellular bridge shows localization of GFP-BRUCE-C on the phase-dense midbody ring (scale bar = 2.5 μm).
(B) BRUCE-C co-localizes with MKLP1. HeLa cells were transfected with GFP-BRUCE-C (green), fixed after 20 h and stained with anti-MKLP1 (red) and DAPI (blue) (scale bar = 10 μm). The large picture shows the merged images of the small pictures on the right.
(C) BRUCE-C expression does not alter the appearance of midbody microtubules but induces elongation of the intercellular bridge. HeLa cells were transfected with GFP-BRUCE-C (green), fixed after 20 h and stained with anti-α-tubulin (red) and DAPI (blue) (scale bar = 10 μm, and 2.5 μm in clippings). The three central images are enlargements of the left panel.
(D) HeLa cells undergo cytokinesis-associated apoptosis upon GFP-BRUCE-C expression. HeLa cells were transfected with GFP-BRUCE-C (green) and fixed after 40 h. Fluorescence and phase images are shown (scale bar = 15 μm).
(E) Prolonged expression of BRUCE-C leads to binucleation and apoptosis. HeLa cells were transfected either with GFP or GFP-BRUCE-C, stained with propidium iodide 1 and 3 days after transfection and DNA content was analyzed by flow cytometry gating for transfected cells.
(F) Pleiotropic mitotic phenotypes are associated with GFP-BRUCE-C overexpression. HeLa cells were transfected with GFP-BRUCE-C (green), fixed after 40 and 60 h and stained with DAPI (blue) (scale bar = 10 μm, and 2.5 μm in clippings). Arrowheads mark apoptotic and fragmented nuclei (second panel from top) and a DNA-bridge (lowest panel).

Notably, the C-terminal tail of BRUCE (BRUCE-C) is highly conserved from flies to vertebrates (Figure 19B), suggesting that the midbody targeting domain (MTD) and the interaction with MKLP1 are features of all BRUCE family members. As BRUCE-C at moderate expression levels binds exclusively to the midbody ring, it is feasible to speculate whether this construct could probably act as a dominant-negative tool specifically to monitor the function of BRUCE at this location. Indeed, overexpression of BRUCE-C can displace endogenous BRUCE from MKLP1 and the midbody ring (Figure 18F). Moderate overexpression of BRUCE-

C leads to aberrant cytokinesis and binucleation (Figure 20F). Notably, prolonged expression of BRUCE-C for three days, finally leads to apoptosis (Figure 20D), indicating that the apoptotic signal is probably triggered by the absence of BRUCE from the midbody ring. FACS analysis of cells overexpressing BRUCE-C supports the notion that cells most likely convert into binucleate structures first and then undergo apoptosis (Figure 20E).

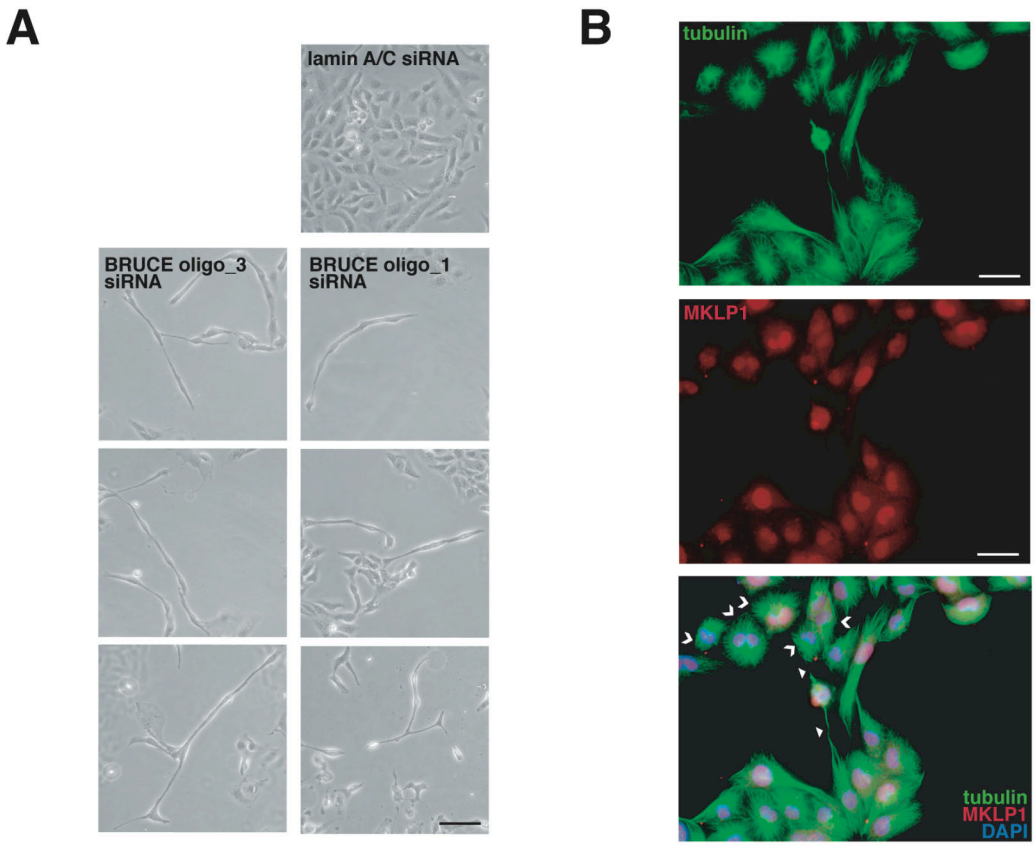

Figure 21. Two independent siRNAs targeting BRUCE give rise to the same phenotype.
(A) Syncytial growth after BRUCE depletion by two independent siRNA duplexes. U2OS cells were transfected with the indicated siRNAs at a final concentration of 100 nM. Representative brightfield images are shown (scale bar = 25 μm).
(B) Abscission failure in mitosis. U2OS cells were transfected with BRUCE siRNA oligo_1 at a final concentration of 100 nM and fixed after 3 days. Cells were stained with anti-α-tubulin (green), anti-MKLP1 (red) and DAPI (blue) (scale bar = 25 μm). Open arrowheads mark binucleate cells; closed arrows mark a cell in prometaphase that is still connected to two other cells.

4.5 BRUCE depletion causes defective abscission and cytokinesis-associated apoptosis

Depleting cultured cells of BRUCE was previously shown to reduce cell viability (Ren et al., 2005). To delineate the underlying mechanism, different siRNAs targeting BRUCE were designed (see Materials and Methods and Figure 21A). siRNA delivery by electroporation in U2OS cells leads to undetectable protein levels of BRUCE three days after transfection (Figure 22A).

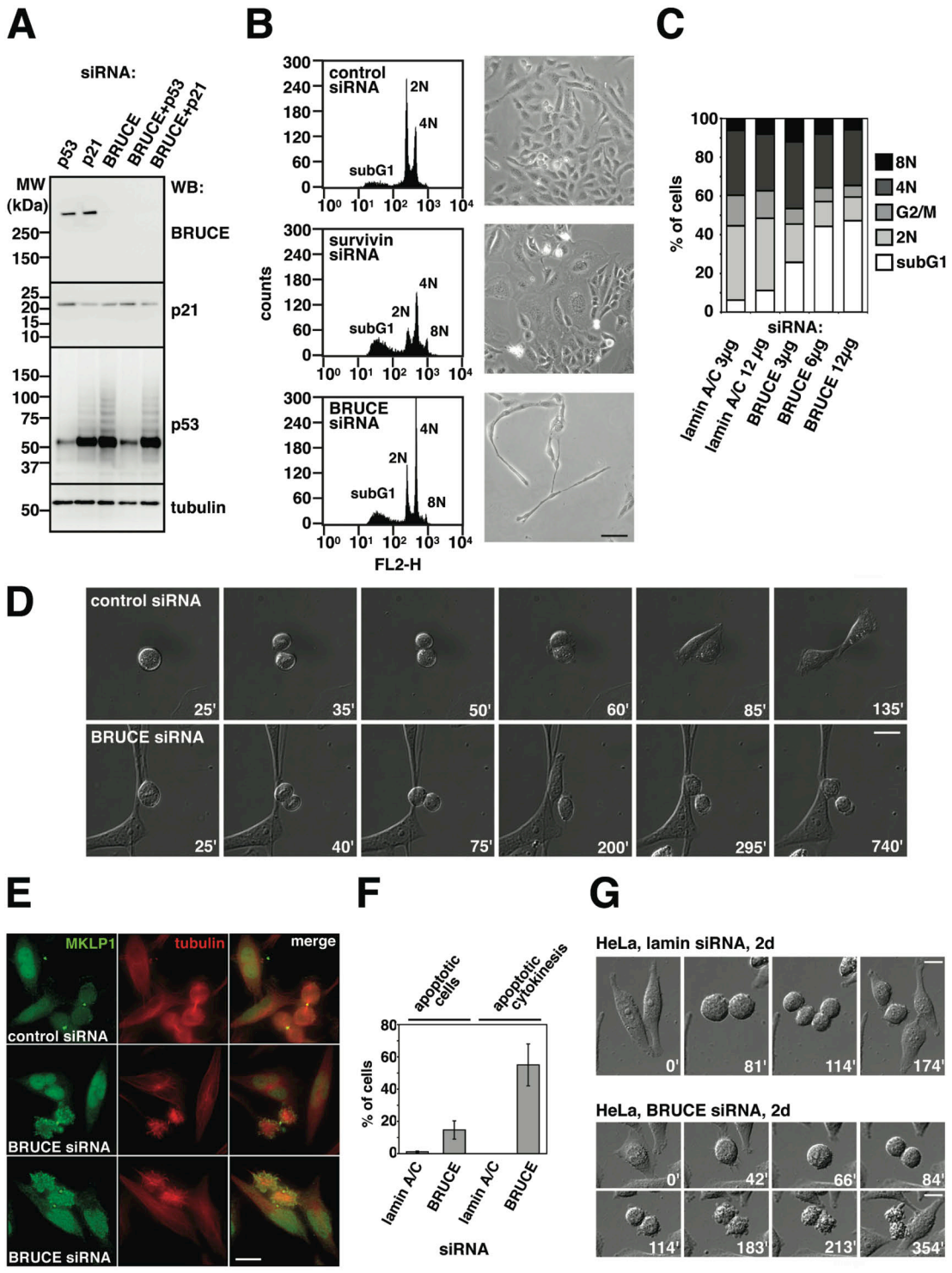

Figure 22. BRUCE depletion causes cytokinesis defects and cytokinesis-associated apoptosis.
(A) BRUCE depletion in U2OS cells has only minor consequences for p53 levels. Lysates of cells transfected with the indicated siRNAs were analyzed by Western blots with the indicated antibodies.
(B) BRUCE depletion in U2OS cells induces syncytia-like structures. Cells were treated with siRNAs for 3 days as shown in Figure 1C targeting lamin A/C, survivin, or BRUCE. After 3 days of incubation, a representative area of cells was photographed (scale bar = 20 μm), cells were harvested and prepared for propidium iodide staining, and the DNA content of cells was analyzed by flow cytometry.
(C) Cell cycle distribution after treatment with increasing concentrations of siRNA. Cells were treated with siRNA as in (A). The graph represents the cell cycle distribution as obtained by flow cytometry of the DNA content.

Monitoring of cells depleted of BRUCE shows strikingly elongated structures with interconnected cells as revealed by flow cytometry (Figure 22B and 22C). In contrast to survivin depletion, no cells with giant nuclei can be observed, arguing for a different mode of failure in cell division. Higher concentrations of siRNA and prolonged incubation show a loss of the normal diploid 2N population (Figure 22C) and an increased sub-G1 population, indicative of syncytia-like cells finally undergoing apoptosis. Moreover, reminiscent of centriolin depletion (Gromley et al., 2003), some apparently not completely detached cells fuse again or undergo mitosis while still interconnected (Figure 21B and see below). However, in contrast to the results obtained by Ren and coworkers (Ren et al., 2005), in the experiments shown here (Figure 22A), no increase in p53 levels was detected. Furthermore, p53 downstream targets like p21 also show no up-regulation, suggesting that apoptosis in these cells is not an immediate response to BRUCE depletion but a later corollary.

Live cell video microscopy reveals that BRUCE-depleted cells form a normal cleavage furrow, but do not complete cytokinesis even after hours. Some cells do not even regain their normal flattened appearance (Figure 22D). As mentioned above, cytokinesis structures are slightly different in HeLa cells that develop long intercellular connections. When HeLa cells are depleted of BRUCE, they undergo apoptosis, but, intriguingly, only during attempted cytokinesis (Figure 22E-G). After the formation of the midbody ring, almost 60% of the cells are apoptotic (Figure 22F). Note that cells in interphase are not undergoing apoptosis while the dividing cell shows membrane blebbing as early as 30 minutes after furrowing (Figure 22G). This suggests a mechanism by which apoptosis is triggered *via* cues that originate at the midbody in the absence of BRUCE.

4.6 BRUCE is required for membrane delivery to the midbody ring

As the experiments shown above demonstrated that BRUCE-C binding to the midbody ring acts in a dominant-negative fashion, membrane trafficking during cytokinesis was investigated making use of this tool.

Figure 22 continued
(D) Defective cytokinesis after BRUCE depletion. siRNA-treated U2OS cells were observed by differential interference contrast (DIC) microscopy. The images represent stills of movies at representative time points (scale bar = 20 μm).
(E) HeLa cells depleted of BRUCE undergo cytokinesis-associated apoptosis. HeLa cells were treated with siRNAs for two days as in (A), fixed, and stained with anti-MKLP1 (green) and anti-α-tubulin (red) (scale bar = 15 μm).
(F) Quantification of (E) with apoptotic cells relative to total cells and apoptotic cytokinesis versus total cells in cytokinesis (error bars represent ±SD of two independent experiments).
(G) Stills with DIC live-cell microscopy of HeLa cells treated with lamin siRNA (top) or BRUCE siRNA (bottom) for 2 days. Note that cells depleted for BRUCE undergo apoptosis after attempted cytokinesis (scale bar = 15 μm).

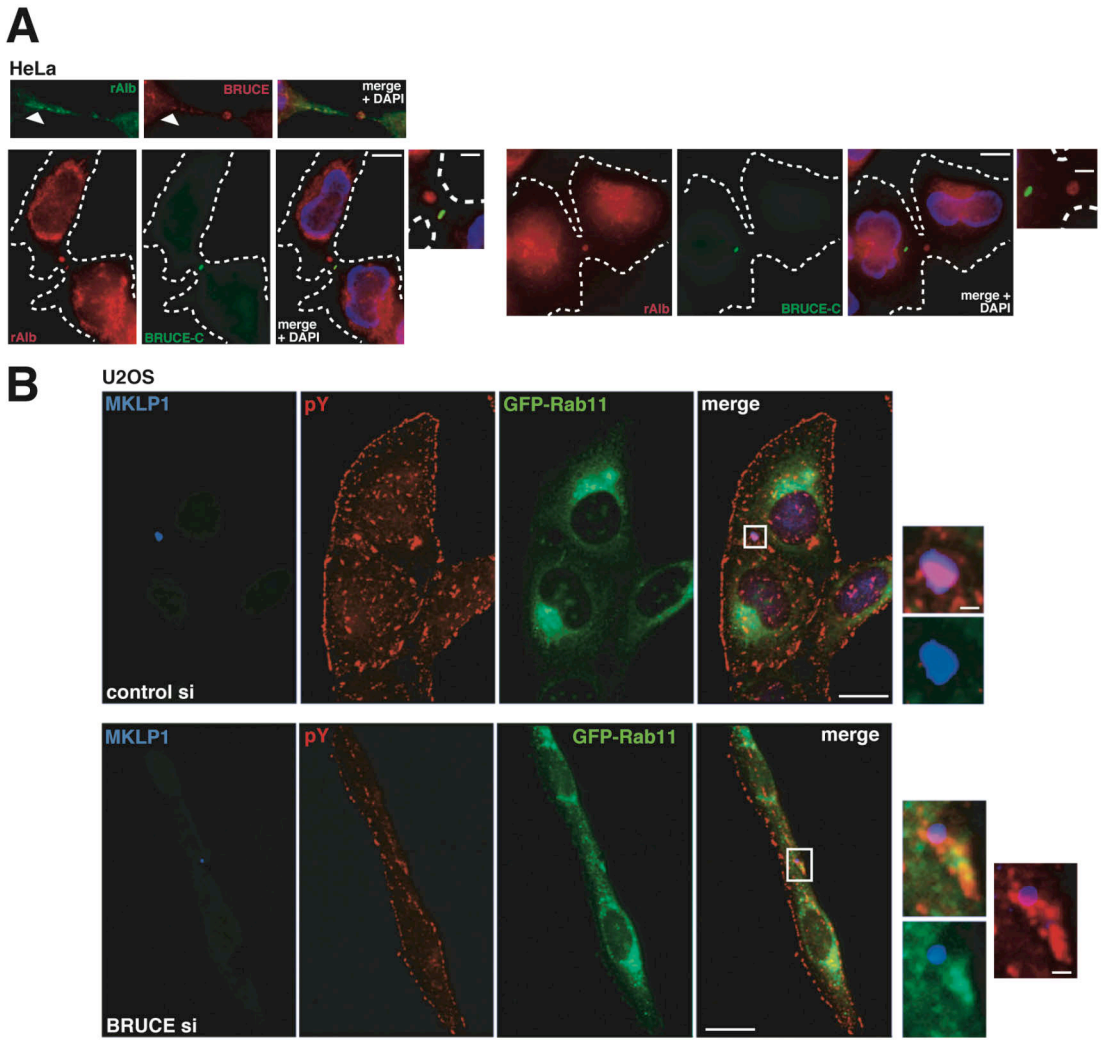

Figure 23. BRUCE functions in membrane delivery to the midbody ring.
(A) Expression of BRUCE-C leads to secretory vesicle accumulation in close vicinity to the midbody ring. Top: Enlarged midbody region of a HeLa cell stably expressing albumin (green) and stained for endogenous BRUCE (red). Bottom: Similar to above, but cells were transfected with GFP-BRUCE-C (green), fixed and stained. Two representative cells in cytokinesis are shown with the enlarged midbody region on the right (scale bar = 10 μm, scale bar of clippings = 2 μm). (B) Recycling endosomes accumulate close to the midbody ring in BRUCE-depleted cells. U2OS cells stably expressing GFP-Rab11 (green) were treated with 100 nM siRNAs for three days, were subsequently fixed and stained for MKLP1 (blue) and phospho-tyrosine (pY, red) with enlarged views of the midbody ring on the right (scale bar = 15 μm, scale bar of clippings = 1 μm).

In order to delineate the possible cause for aberrant cytokinesis in cells expressing BRUCE-C, HeLa cells stably expressing tagged albumin – as introduced above (see Figure 8) – were used. Secretory vesicles can only be found in the intercellular bridge in the case of untransfected cells but not in cells transfected with BRUCE-C. Cells expressing BRUCE-C show ball-like accumulations of vesicles in proximity to the intercellular bridge, interestingly, only on one side, speaking for failed membrane delivery as the cause of aberrant cytokinesis (Figure 23A).

To draw a generalized conclusion whether complete loss of BRUCE also leads to problems in membrane targeting, U2OS cells stably expressing GFP-Rab11 were treated with control siRNA or siRNA targeting BRUCE, respectively. In control cells that just completed cytokinesis (Figure 23B, upper panel), Rab11 readily adopts an interphase localization pattern and phospho-tyrosine staining is found on the midbody as it has recently been described (Kasahara et al., 2007). In contrast, BRUCE-depleted cells show an accumulation of Rab11- as well as phospho-tyrosine-positive material in close proximity to one side of the midbody (Figure 23B, lower panel), indicative of a failure in not only targeting membranes but also kinases recently found to be essential for the completion of cytokinesis. Notably, appearance of Src and ERK on the midbody have been described to be dependent on Rab11 (Kasahara et al., 2007), therefore, an indirect effect on these factors as a consequence of the defects in Rab11-endosomes cannot be ruled out.

4.7 Midbodies and midbody rings are platforms for ubiquitylation

Since it has already been demonstrated that BRUCE possesses ubiquitin ligase activity (Bartke et al., 2004; Hauser et al., 1998), it could be asked whether the midbody ring might be a site of ubiquitylation. Contrary to the current belief (Pines and Lindon, 2005), a distinct pattern of localization for ubiquitin can be observed during cytokinesis using a cell line that stably expresses a GFP-ubiquitin fusion protein (Figure 24A). Concomitant with the formation of the midbody ring in late telophase, ubiquitin is concentrated symmetrically on the distal tips of midzone microtubules omitting the midbody ring and persists until these microtubules constrict to form the midbody. Hereafter, ubiquitin is undetectable on the midbody but, surprisingly, reappears after 10-15 min on the midbody ring. Notably, inhibition of proteasomes with the inhibitor MG132 reveals that the dynamic relocalization of ubiquitin to the midbody ring depends on active protein degradation (Figure 24B).

This behavior of ubiquitin during cytokinesis unappreciated so far demanded closer investigation by fluorescent recovery after photobleaching (FRAP) experiments in order to better understand ubiquitin dynamics at this site. FRAP reveals that ubiquitin on the midbody ring during cytokinesis shows vastly reduced recovery as compared to e.g. cytosolic ubiquitin in the same cell or on midbody microtubules (Figure 25A, left panel and data not shown). To demonstrate that this is not simply due to the longer distance of the midbody ring from the general ubiquitin pool in the cell, midbody rings already taken up by one daughter cell were analyzed (Figure 25A, right panel). Ubiquitin on these rings shows essentially no recovery, concluding that ubiquitin on the midbody ring is of a substantially different dynamic nature than any other cellular pool of ubiquitin.

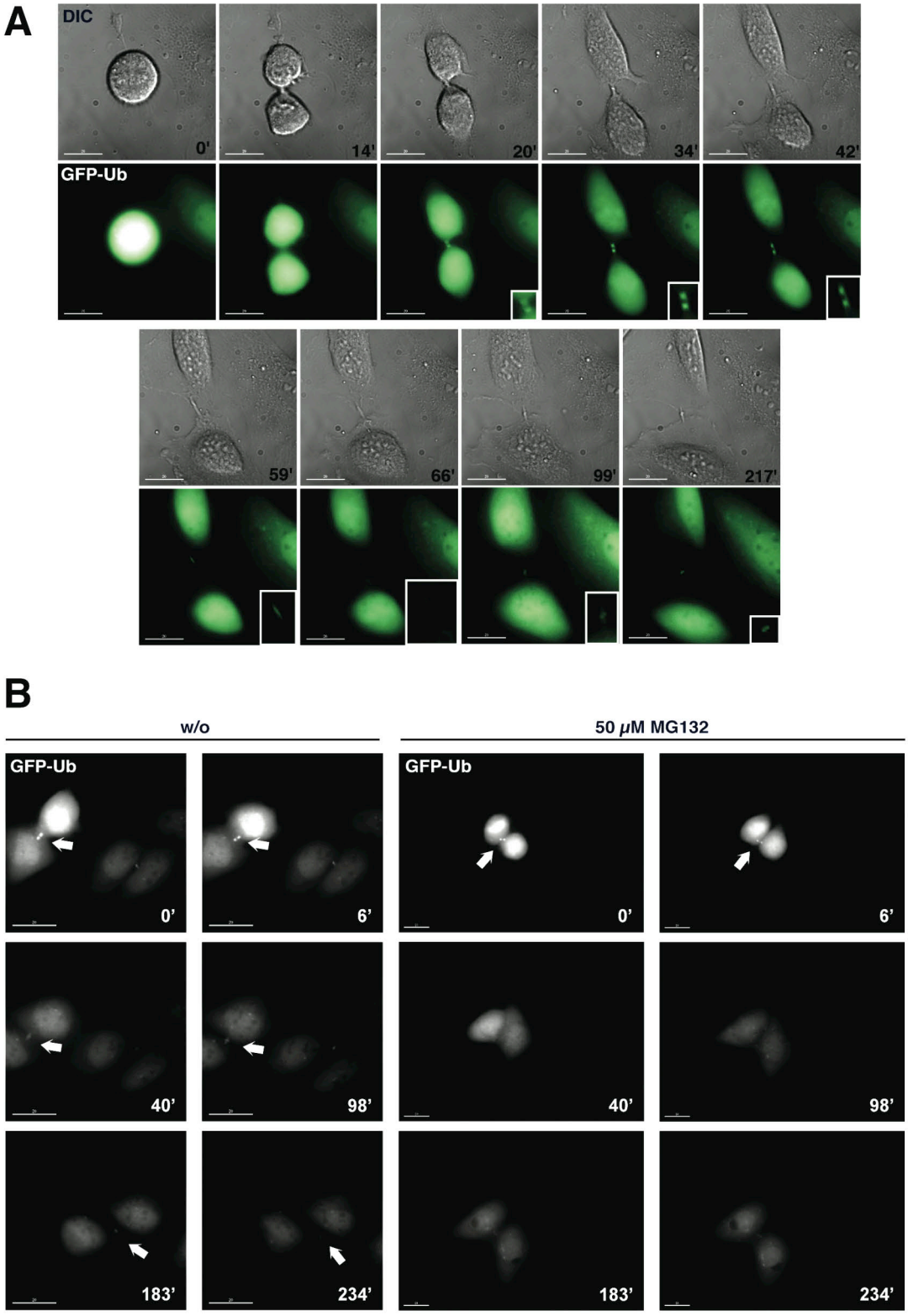

Figure 24. Ubiquitylation on the midbody and on the midbody ring.
(A) Ubiquitin (Ub) is concentrated on midbody microtubules and reappears on the midbody ring after midbody constriction. U2OS cells stably expressing GFP-tagged ubiquitin (GFP-Ub) were analyzed by time-lapse video microscopy. A representative cell is shown with the movie stills starting in pro-metaphase and ending shortly before abscission (scale bars = 20 μm).
(B) Proteasome inhibition prevents ubiquitylation at the midbody ring. U2OS cells stably expressing GFP-tagged ubiquitin (GFP-Ub) were analyzed by time-lapse video microscopy. Cells were either left untreated or 50 μM MG132 was applied right after anaphase onset. Representative cells are shown with the movie stills starting in late anaphase and ending shortly before abscission (scale bars = 20 μm). The arrows point to midbody/midbody ring localized ubiquitin.

This suggests that ubiquitin has a high turnover at the midbody through active ubiquitylation and de-ubiquitylation of proteins near the midbody microtubules. In striking contrast, ubiquitin on midbody ring components, can barely be replaced, once this modification has occurred. The local ubiquitylation activity is thus probably turned off at this stage.

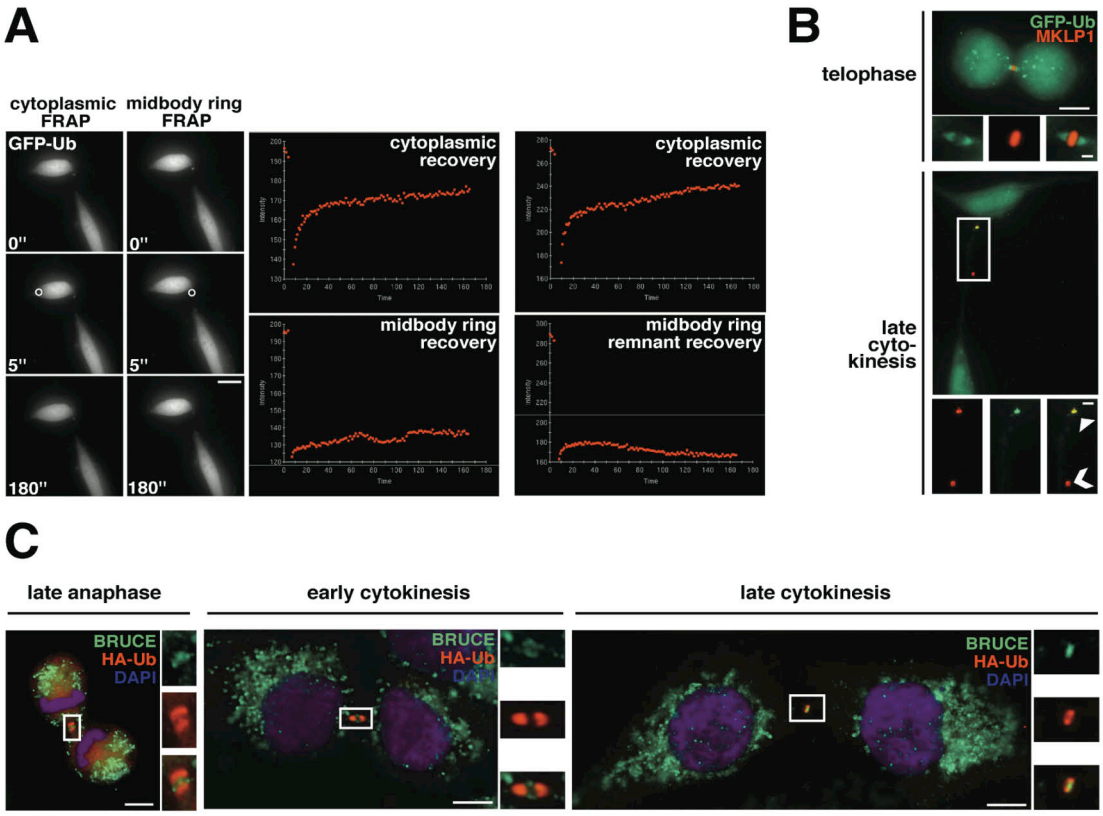

Figure 25. Timing and dynamics of ubiquitylation on the midbody ring.
(A) Ubiquitin at the midbody ring shows almost no exchange with the cellular ubiquitin pool. U2OS cells as in (A) were used for FRAP experiments. Left: A cell with ubiquitin on the midbody ring was bleached in the cytoplasm or at the midbody ring. The recovery of the fluorescence signal is shown on the right. Right: A cell with a midbody ring remnant in the plane of the plasma membrane was either bleached in the cytoplasm or at the midbody ring remnant. Only fluorescence recovery curves are shown (scale bars = 20 μm).
(B) Ubiquitin is lost from midbody ring remnants when cells acquired an active midbody ring. HeLa cells were transfected with GFP-Ub (green). Top panels show fixed cells in telophase with anti-MKLP1 staining (red). Lower panels show a cell in late cytokinesis with a putative active midbody ring and a remnant, both lying in the intercellular bridge. Note that the midbody ring remnant (open arrowhead) is not labeled with ubiquitin (scale bars = 10 μm and 2 μm for enlarged areas).
(C) Association of BRUCE with ubiquitin at the midbody ring. U2OS cells were transiently transfected with HA-epitope tagged ubiquitin (HA-Ub, red). Cells were fixed and stained with anti-BRUCE (green) and DAPI (blue) (scale bar = 10 μm). The framed areas are shown enlarged.

Relocalization of ubiquitin during cytokinesis is similar in HeLa cells (Figure 25B, top panel). Cells of both cell lines often harbor, besides the midbody ring engaged in cytokinesis, one or rarely two additional rings, which most likely represent remnants from previous divisions. Intriguingly, only the putative active midbody ring in the intercellular bridge is

decorated with ubiquitin whereas the midbody ring remnants apparently gradually loose the modification (Figure 25B, lower panel). This finding is in agreement with the FRAP data (Figure 25A), showing that ubiquitylation of the midbody ring occurs only once during cytokinesis, before the onset of abscission.

Notably, BRUCE and ubiquitin are closely associated during cell division and colocalize at the midbody ring during late cytokinesis (Figure 25C), suggesting that at least some of the detected ubiquitylation may be mediated by BRUCE (see Discussion). This allows to reason that BRUCE is most likely not implicated in degradative ubiquitylation due to the stability of midbody ring localized ubiquitin and its extremely low exchange rate.

4.8 Evidence for the de-ubiquitylating enzyme UBPY/USP8 being implicated in cytokinesis

Recent data (Wu et al., 2004) describe a complex containing BRUCE and the de-ubiquitylating enzyme USP8/UBPY, probably bridged by the RING-finger ubiquitin ligase Nrdp1/FLRF. BRUCE itself might be present as an oligomer in this complex (Bartke et al., 2004). It was therefore tested whether de-ubiquitylating activity might influence midbody-localized ubiquitin. Using a catalytically inactive form of UBPY ($UBPY^{C>A}$) that serves as a substrate trap (Alwan and van Leeuwen, 2007), an interaction with both BRUCE and MKLP1 can be detected (Figure 26A). Furthermore, $UBPY^{C>A}$ is localized on the midbody ring (Figure 27B), suggesting that ubiquitylation and de-ubiquitylation activities may work as a switchboard at this site. Hence, one can also ask whether BRUCE and MKLP1 are targets for UBPY-mediated de-ubiquitylation and whether interference with this process leads to problems in cytokinesis.

Intriguingly, BRUCE itself is ubiquitylated at its C-terminal domain (data not shown) and its ubiquitylation is enhanced when Nrdp1 is overexpressed, and lost when UBPY is overexpressed (Figure 26B). Using a denaturing purification protocol, it is also possible to demonstrate that MKLP1 is modified by mono-/oligo- but not multi-ubiquitylation and that this modification is strongly reduced when UBPY is overexpressed (Figure 26C). An increase of modified forms of MKLP1 by overexpression of $UBPY^{C>A}$ further argues for it acting as a de-ubiquitylating enzyme on the midbody ring and probably also argues that de-ubiquitylation rather than ubiquitylation activity might be limiting and important for regulation. In fact, HeLa cells transfected with $UBPY^{C>A}$ show more than 30% binucleated cells and, additionally, a mislocalization of MKLP1 to the cytoplasm in interphase whereas MKLP1 normally localizes to the nucleus at this cell cycle state (Figure 26D). This phenotype is reminiscent of an MKLP1 knockdown, suggesting that UBPY-mediated de-ubiquitylation of MKLP1 may trigger nuclear import, which appears to be needed for normal cytokinesis (Liu and Erikson, 2007).

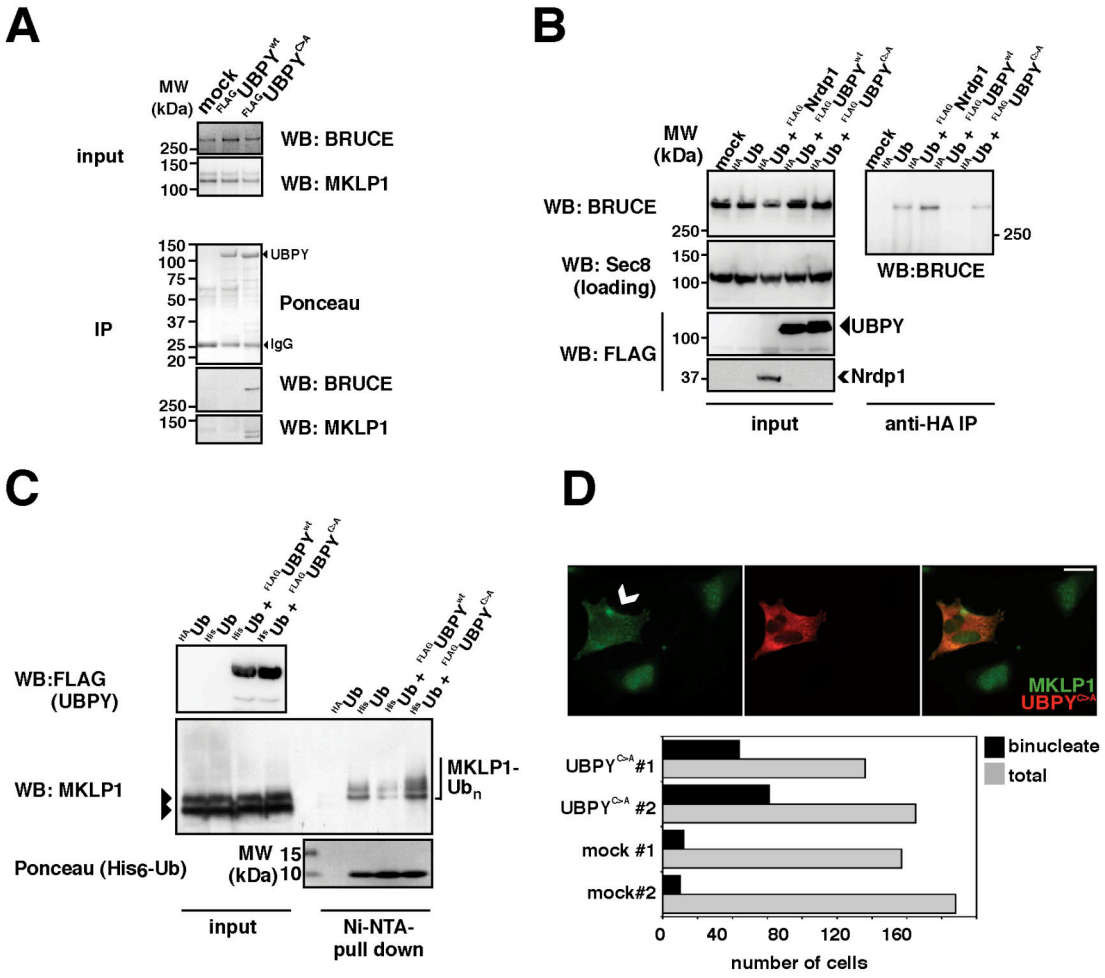

Figure 26. UBPY interacts with and de-modifies both BRUCE and MKLP1.
(A) Both BRUCE and MKLP1 interact with UBPY. HEK293T cells were transfected with empty vector or FLAG-epitope tagged UBPY and its catalytically inactive mutant (C>A). Cells were lysed and proteins were immunoprecipitated (IP) with anti-FLAG and analyzed by Western blots (WB).
(B) BRUCE is de-ubiquitylated by UBPY. HEK 293T cells were transfected with empty vector and HA-tagged ubiquitin (^{HA}Ub) in combination with FLAG-tagged UBPY wild-type and mutant proteins (^{FLAG}UBPY, ^{FLAG}UBPY$^{C>A}$) and FLAG-tagged Nrdp1 (^{FLAG}Nrdp1). Lysates were prepared and subjected to anti-HA immunoprecipitation, and both lysates (Input) and immunoprecipitated material (IP) were analyzed by Western blots (WB).
(C) MKLP1 is ubiquitylated in cells and is de-ubiquitylated by UBPY. HEK 293T cells were transfected with ^{HA}Ub or His$_6$-epitope tagged ubiquitin (His$_6$-Ub) in combination with ^{FLAG}UBPY and ^{FLAG}UBPY$^{C>A}$. Lysates were subjected to denaturing Ni-NTA pull down and analyzed by Western blots (WB).
(H) Overexpression of catalytically inactive UBPY leads to MKLP1 mislocalization and binucleation of cells. HeLa cells were transfected with empty vector (mock) or ^{FLAG}UBPY$^{C>A}$. Left: Cells were fixed and stained with anti-MKLP1 (green) and anti-FLAG (red) antibodies. The open arrowhead marks a transfected cell (scale bar = 15 μm). Right: Quantification of binucleate versus total cells (two independent experiments labeled #1 and #2, respectively).

Furthermore, in cells overexpressing UBPY$^{C>A}$ it is frequently observed that the tubular endosomal compartment where BRUCE localizes is highly compacted in the pericentrosomal area and that peripheral tubules that are still found in cells overexpressing wild type UBPY are almost completely lost in the case of the substrate trap mutant (Figure 27A). This indicates

that, besides functions in cytokinesis, UBPY also serves to regulate the appearance and probably also the mobility of tubular recycling endosomes. Preventing de-ubiquitylation of proteins on their surface therefore seems to inhibit the budding of carriers into the cell periphery.

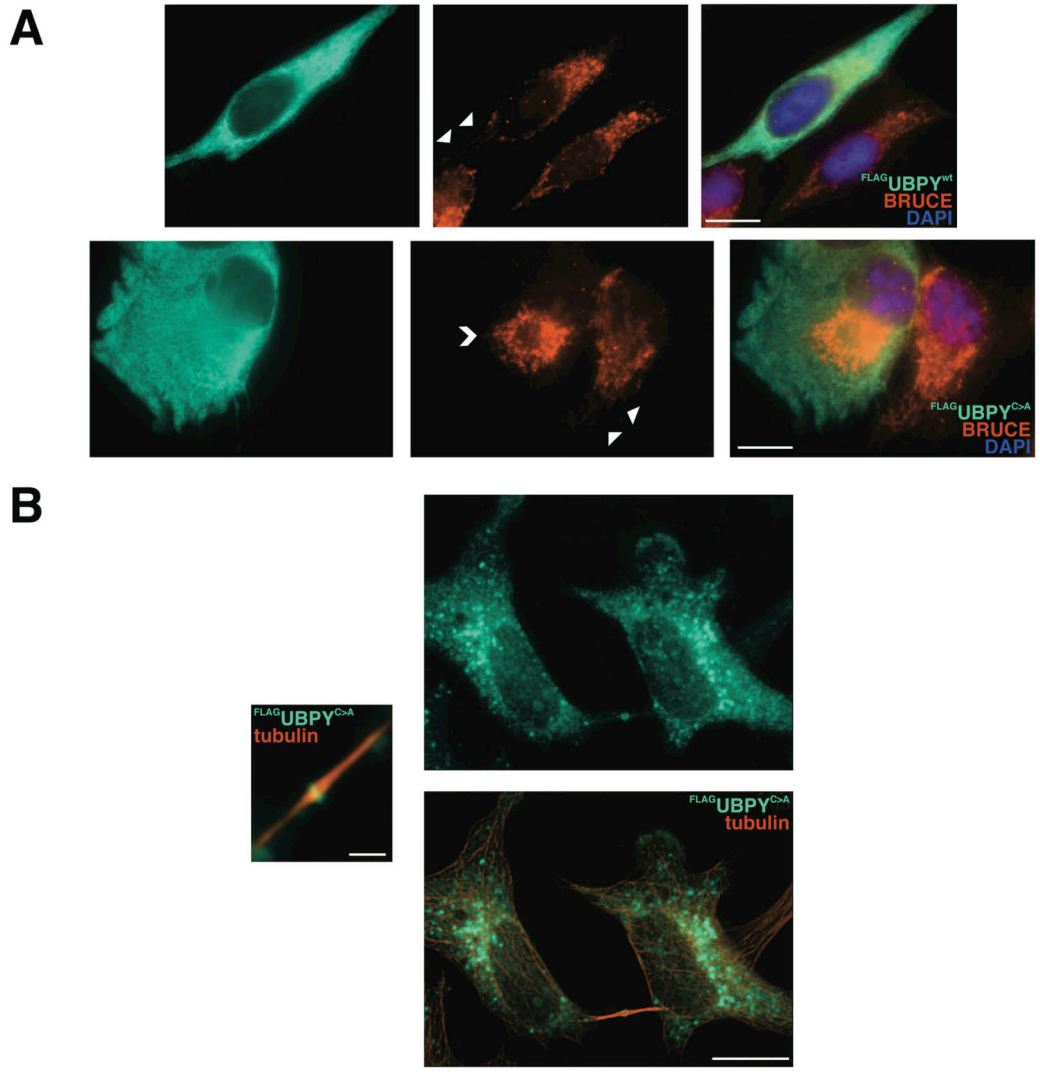

Figure 27. Catalytically inactive UBPY perturbs tubular endosome morphology and localizes to the midbody ring.
(A) Peripheral BRUCE tubular endosomes are lost in cells overexpressing UBPY$^{C>A}$. HeLa cells were transfected with either wild-type ^{FLAG}UBPY or the catalytically inactive form ^{FLAG}UBPY$^{C>A}$. Cells were fixed and stained with anti-FLAG and anti-BRUCE antibodies and DAPI to visualize DNA (scale bars = 10 μm). Note the peripheral tubules marked with closed arrowheads and the cell with higly compacted BRUCE staining in the case of UBPY$^{C>A}$ transfection (marked by an open arrowhead).
(B) Catalytically inactive UBPY localizes to the midbody ring. HeLa cells were transfected with ^{FLAG}UBPY$^{C>A}$, and cells were fixed and stained with anti-FLAG (green) and anti-α-tubulin (red) antibodies (scale bars = 10 μm and 2.5 μm in the clipping).

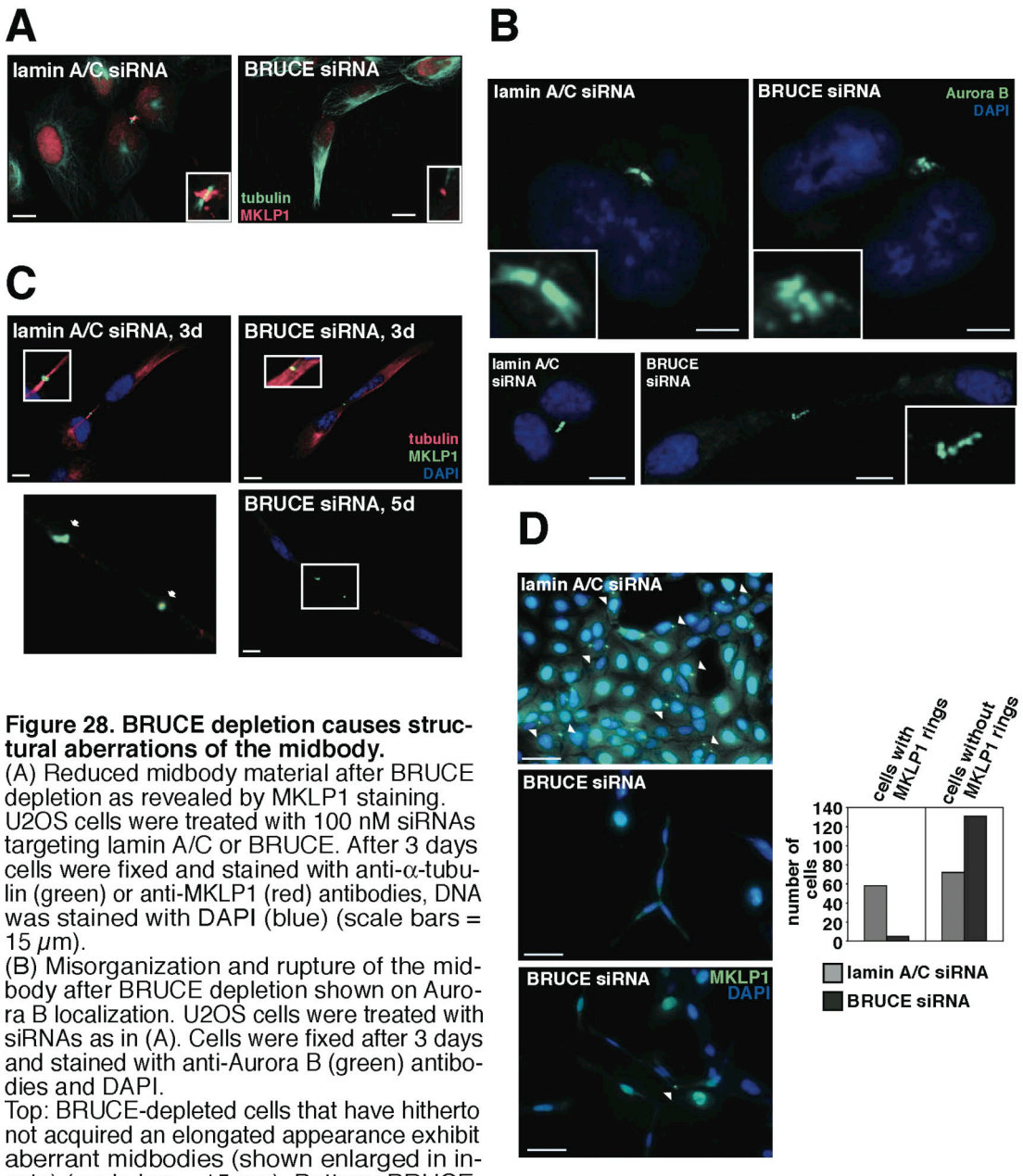

Figure 28. BRUCE depletion causes structural aberrations of the midbody.
(A) Reduced midbody material after BRUCE depletion as revealed by MKLP1 staining. U2OS cells were treated with 100 nM siRNAs targeting lamin A/C or BRUCE. After 3 days cells were fixed and stained with anti-α-tubulin (green) or anti-MKLP1 (red) antibodies, DNA was stained with DAPI (blue) (scale bars = 15 μm).
(B) Misorganization and rupture of the midbody after BRUCE depletion shown on Aurora B localization. U2OS cells were treated with siRNAs as in (A). Cells were fixed after 3 days and stained with anti-Aurora B (green) antibodies and DAPI.
Top: BRUCE-depleted cells that have hitherto not acquired an elongated appearance exhibit aberrant midbodies (shown enlarged in insets) (scale bar = 15 μm). Bottom: BRUCE-depleted cells that resemble syncytia contain fragmented Aurora B-positive material (scale bars = 20 μm).
(C) Midbody ring rupture in BRUCE-depleted cells as indicated by MKLP1 localization. The experiment was performed as in (B) and cells were fixed either after 3 or 5 days, stained for MKLP1 (green), α-tubulin (red), or DNA with DAPI (blue). After 5 days of siRNA treatment, syncytial cells arose with aberrant midbody rings (arrowheads) (scale bars = 10 μm).
(D) Growth retardation and loss of midbody rings after BRUCE depletion. Experiment was performed as in (B), cells were fixed after 5 days and stained with anti-MKLP1 (green) and DAPI. Arrowheads point to MKLP1-stained midbody rings. Right: Quantification of the phenotype observed in immunofluorescence images (scale bars = 30 μm).

4.9 BRUCE is required for midbody integrity, midbody ring formation, and midbody-localized ubiquitin

Prompted by the striking physical and functional connection of BRUCE with the midbody and the midbody ring, it seemed likely that BRUCE itself is crucial for the organization of these

structures. Indeed, significantly reduced MKLP1-positive midbody material can be found in BRUCE-depleted cells (Figure 28A and 28C and see also Figure 23B).

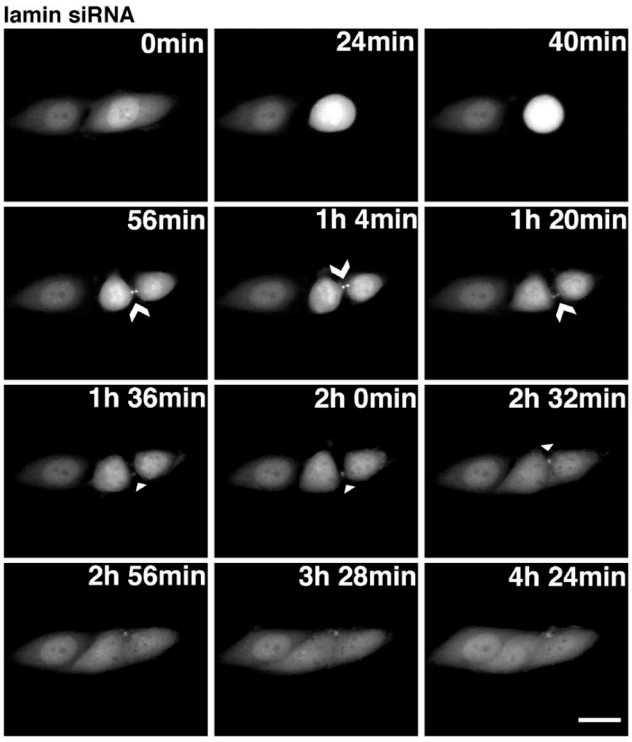

Figure 29. Concentration of ubiquitin at the midbody and midbody ring is lost in BRUCE-depleted cells. U2OS cells stably expressing GFP-ubiquitin were analyzed by time-lapse video microscopy. Stills from representative movies are shown. Cells were treated with 100 nM siRNA targeting lamin A/C (upper panels) or with siRNA targeting BRUCE (lower panels), respectively.
Note that in the case of lamin siRNA both the midbody and the midbody ring are decorated with GFP-ubiquitin (marked by an open arrowhead.) Furthermore, in the case of BRUCE siRNA two cell divisions are shown in the movie sequence. During the second division (starting at about 10h 56min), one cell from the first division is dragged into the cell lying top right then performing a joint mitosis. During the BRUCE siRNA sequence no obvious staining of the midbody by ubiquitin is observable (scale bars = 15 μm).

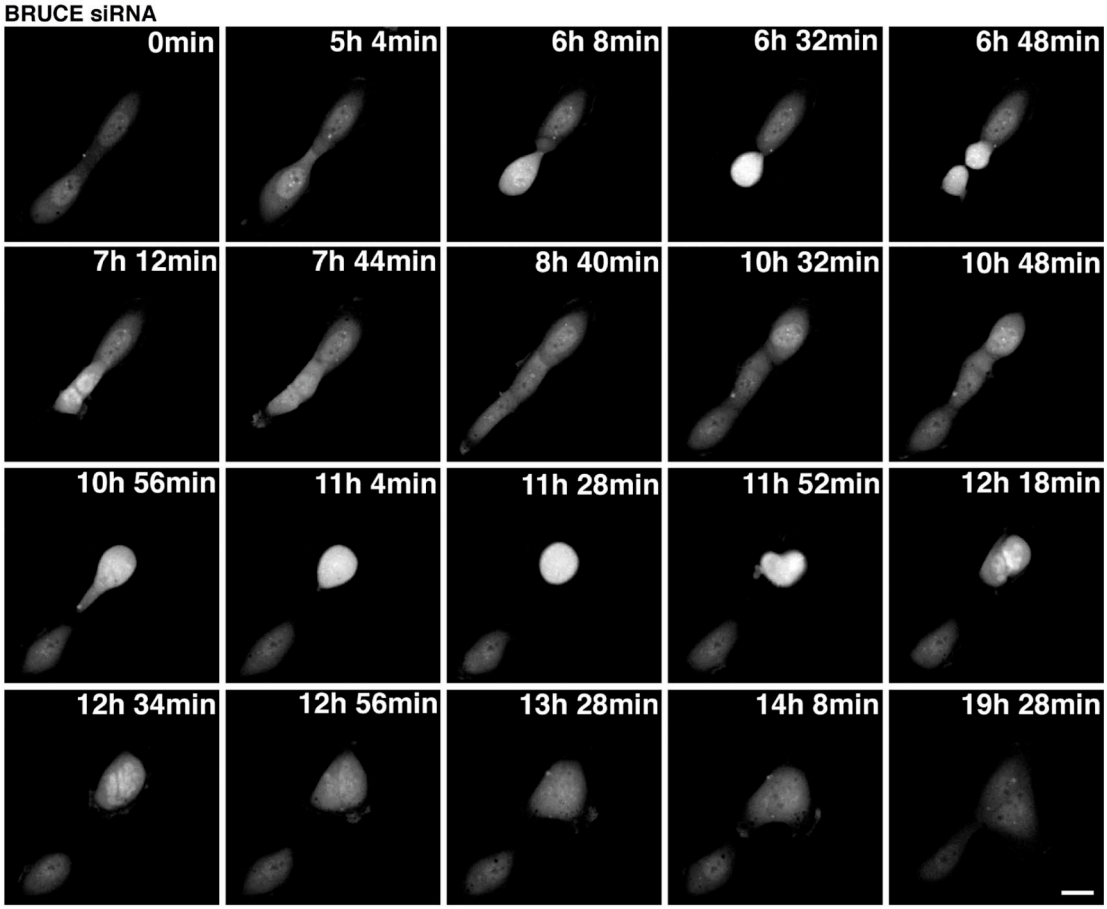

Additionally, a gradual effect on the midbody structure upon continued BRUCE depletion is detectable. Depletion for no more than three days leads to moderately misorganized midbodies with unfocused Aurora B staining (Figure 28B, top panel) and unconstricted microtubules (Figure 28C, top panel). However, BRUCE depletion for five days results in syncytia-like cells, which contain severely malformed midbodies, as visualized by Aurora B or MKLP1 staining (Figure 28B and 28C lower panels). Finally, most cells fail to form their midbody rings altogether and remnants do not persist, and those few cells that retain their midbody rings (less than 10%), have hitherto not adopted a syncytia-like appearance (Figure 28D).

Furthermore, it was investigated if localization of ubiquitin to midbody microtubules and the midbody ring is affected when cells are depleted of BRUCE. Cells treated with control siRNA showed the ubiquitin localization pattern described above (Figure 29, upper panels). In contrast, cells depleted for BRUCE neither showed a distinct staining of ubiquitin at midbody microtubules nor a detectable staining at the midbody ring (Figure 29, lower panels). These results suggest that BRUCE is not only required for normal vesicle targeting to the site of abscission, but also for the integrity of the midbody and the midbody ring, as well as for their striking ubiquitin modification.

Surprisingly, cells were found that fused with an adjacent cell and undergo a joint mitosis, a scenario not reported so far, but resembling divisions in syncytial networks described for centriolin depletion (Gromley et al., 2003). This clearly indicates that syncitia-like cells that are seemingly separate are in fact still interconnected.

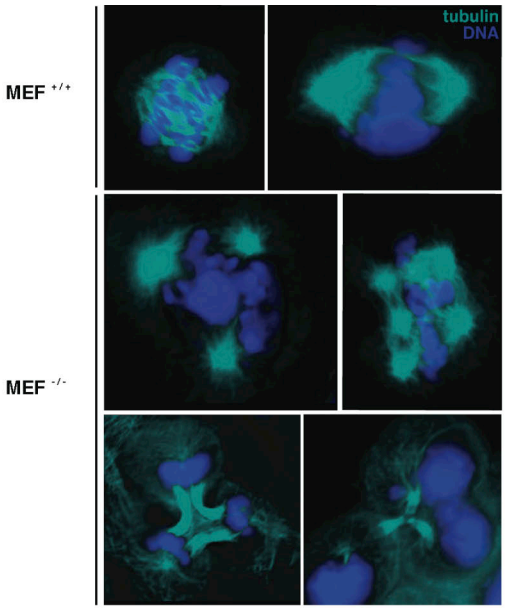

Figure 30. Mouse embryonic fibroblasts (MEFs) derived from BRUCE knockout embryos show aberrant cell divisions.
MEFs of BRUCE$^{-/-}$ embryos (MEF$^{-/-}$) and of wild type littermates (MEF$^{+/+}$) that spontaneously immortalized by a 3T3 protocol were used in this experiment. Cells were fixed and stained with anti-α-tubulin antibodies (green) and DNA was counterstained with DAPI (blue).
The lower panels show two cases of multipolar mitosis and two cases of cytokinesis involving three cells.

4.10 BRUCE appears also to be important for cytokinesis regulation in mice

Remarkably, aberrant mitotic and cytokinetic structures, like multipolar spindles and tripolar cytokinesis, were also observed in spontaneously immortalized BRUCE$^{-/-}$ MEFs (Figure 30). This argues for a loss of fidelity in cell division after loss of BRUCE expression on the one hand and for an accommodation to the genetic instability caused by these erroneous divisions on the other hand. Interestingly, the loss of BRUCE seems to be overcome by the loss of expression of other factors like e.g. p53 or p21 leading to a transformation-like state of the immortalized cells (see Discussion).

To prove that BRUCE is also involved in cytokinetic structures in tissues from live animals, mouse testis sections were stained for BRUCE (Figure 31). Spermatogenesis takes place in mouse testicular seminipherous tubules. This process involves the differentiation of the otherwise transient intercellular bridge of somatic cells or cells in culture and its midbody ring into a stable specialized structure, the ring canal. These ring canals provide a permanent connection of sperm precursor cells to allow communication of the syncytium and exchange of cytoplasmic contents. Notably, BRUCE is found to be a constituent of this developmentally regulated organelle (Figure 31). This argues for a broader involvement of BRUCE in processes in which cytokinetic structures fulfill specialized functions.

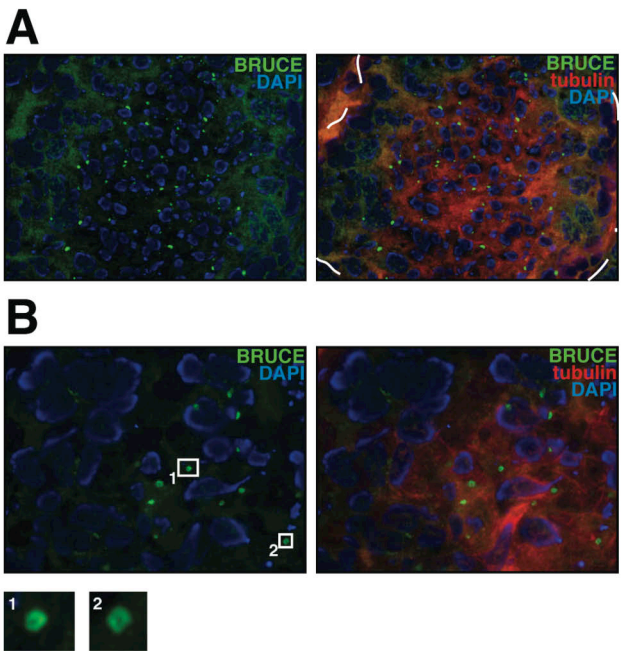

Figure 31. BRUCE is a component of ring canals in mouse testis.
(A) BRUCE is concentrated in testicular ring canals. Fixed cryosections of mouse testis (BioCat) were rehydrated and stained with anti-α-tubulin (red) and anti-BRUCE (green) antibodies and DAPI to stain DNA (blue). An almost complete seminipherous tubule is shown. The white line indicates the basal lamina of the seminipherous tubule.
(B) A magnification of the interior of a seminipherous tubule with cells in later stages of spermatogenesis is shown with staining as in (A). The boxes outlined in white are shown enlarged at the bottom. Here, individual ring canals are shown in an orientation that allows to visualize their donut-like shape.

5 Discussion

Ever since the early pioneering years of cell cycle research, cytokinesis remained a fascinating process because of its startling mechanical behavior. The two most perceptible processes of cytokinesis in animal cells, the contraction of the cleavage furrow and the physical separation of the daughter cells by abscission, are now recognized as two functionally and mechanistically different steps (Shuster and Burgess, 2002). The organizing principle for abscission is represented by the midbody, which is the target site for membrane delivery and membrane fusion, the driving forces of abscission. In particular the unique midbody ring, located at the midpoint of the intercellular bridge that connects the two prospective daughter cells, has emerged as the crucial structural element that guides the final steps of cytokinesis. This rigid and unvaryingly sized structure, originally described by Flemming as 'Zentralkörper' (thus sometimes called 'Flemming body'; Flemming, 1891), emerges in telophase and survives in one daughter cell in most cases often until the next division.

This study demonstrates that BRUCE, an unconventional baculovirus inhibitor of apoptosis repeat protein (BIRP) and multifunctional peripheral membrane protein with ubiquitin ligase activity, is an important regulator in cytokinesis. BRUCE coordinates processes at the midbody ring that are elementary for proper abscission. The functional integrity of the midbody, its formation, and membrane delivery to the site of abscission depend on the presence of BRUCE. Moreover, the discovery of a unique and highly dynamic localization pattern of ubiquitin conjugates at the midbody during cytokinesis reveals a so far unrecognized role of the ubiquitin proteasome system in regulating final stages of cell division. Additionally, this study demonstrates that BRUCE depletion disrupts ubiquitin localization at the midbody.

5.1 BRUCE, a BIRP with a highly dynamic behavior during the cell cycle

Recent studies have emphasized that animal cell cytokinesis is driven primarily by homotypically and heterotypically fusing endosomes and that a general requirement for exocytosis exists in any cytokinesis-related process (Finger and White, 2002; Albertson et al., 2005; Baluska et al., 2006). This study has shown that BRUCE follows the flow of vesicular traffic during cytokinesis. In interphase cells, BRUCE localizes to the TGN and tubular/recycling endosomes, but during cytokinesis, a fraction travels to the midzone where it arrives specifically at the midbody. Notably, BRUCE associates with the midbody ring concomitant with its appearance in telophase, travels into one daughter cell with the midbody ring after completed abscission, and remains bound to the discarded midbody ring all along until a new ring is formed during the next cell division.

It is conjectured that the dynamic relocalization of BRUCE is almost exclusively driven by the movement of organelle-bound BRUCE along microtubules. The majority of these organelles where BRUCE localizes are essentially large pleiomorphic traffic intermediates linked to Rab8 and Rab11 and probably Rab13 GTPases (Figures 13 to 15) (Peränen et al., 1996; Urbé et al., 1993; Yamamoto et al., 2003). Besides small round vesicles that are also essential for protein traffic in cells, large pleiomorphic traffic carriers seem to move the bulk of secretory cargo by *en bloc* extrusion and cleavage of large membranes (Polishchuk et al., 2003; Luini et al., 2005). These carriers emerge from the TGN, the penultimate compartment along the pathway for most secreted proteins. Formation and movement of these carriers depend on protein kinase D, dynamin, microtubules, kinesin motor proteins and the exocyst complex (Ghanekar and Lowe, 2005; Kreitzer et al., 2000; Polishchuk et al., 2003; Ponnambalam and Baldwin, 2003). Interestingly, interactions of BRUCE with several components of TGN to plasma membrane carriers were observed, like subunits of the exocyst membrane targeting complex, microtubules, and Rab8 and Rab11 GTPases (Figures 13 and 15). Additionally, transport carriers containing albumin or VSVG also stained positively for BRUCE and pleiomorphic traffic intermediates containing BRUCE were found exclusively collinear with microtubules (Figures 13 and 14). This allows the conclusion that in interphase cells BRUCE is a component of TGN to plasma membrane transport units moving on microtubules. During exocytic transport, BRUCE might act in different steps of trafficking, e.g. by affecting the ubiquitylation status of transport factors. However, it seems unlikely that BRUCE is implicated in fusion steps at the plasma membrane because it is found on peripheral carriers but never reaches the plasma membrane itself (Figure 8E).

For BRUCE partially localizes to both centrosomes and the TGN (Figure 9), it is tempting to speculate that cues originating from microtubule organizing centers (MTOCs) regulate trafficking of BRUCE-containing carriers. Two types of MTOCs are described so far. The well-characterized centrosomes which tether microtubule minus ends *via* γ-tubulin ring complexes and, only recently discovered, the TGN with tethering occuring *via* the peripheral membrane protein GCC185 and the microtubule binding protein CLASP (Bornens, 2002; Efimov et al., 2007). Strikingly, under conditions of artificially amplified centrosomes by treatment of U2OS cells with hydroxyurea, this study shows that BRUCE localizes around one centrosome even if this centrosome moves into the cell periphery or in cellular protrusions (Figure 9C). This clearly demonstrates that centrosomes act as key regulators for the tubular endosomes BRUCE is localized to.

During the relocalization events from endosomes to midbodies, BRUCE associates with numerous trafficking components and also mitotic regulators. An association of BRUCE

with kinases regulating mitotic events (Cdk1, Plk1, and Mek1) is shown in this study (Figure 10). Notably, both Plk1 and the active form of Cdk1 in complex with cyclin B are localized to centrosomes (Tsvetkov et al., 2003; Jackman et al., 2003) and both kinases are additionally involved in phosphorylating proteins on the Golgi apparatus to allow unlinking of Golgi stacks in early prophase (Colanzi and Corda, 2007). Phosphorylation of BRUCE by Cdk1 should occur early during mitosis as Cdk1 represents the kinase that drives cells through mitosis. As a general mechanism, Plk1 can localize to specific sites within cells where Cdk-mediated phosphorylation provides a structural mechanism for targeting the Plk1 kinase domain to its substrates (Elia et al., 2003). Co-localization of BRUCE and Plk1 can be observed on spindle poles and on the midbody arguing for an interaction at later stages of mitosis.

Considering the sequential Cdk1-Plk1 action, one can speculate that the mobile behavior of BRUCE is most likely regulated by a stepwise phosphorylation as was recently shown for two proteins required for cytokinesis. Both the peripheral Golgi lipid transfer protein Nir2 (Litvak et al., 2004) and the centrosomal protein Cep55 (Fabbro et al., 2005) undergo a priming phosphorylation by Cdk1 which in turn creates a docking site for Plk1. Preventing phosphorylation in either protein caused cytokinesis defects. It is therefore likely that a similar mechanism of phosphorylation-mediated relocalization might also apply for BRUCE as it contains a (S/T)PX(K/R) Cdk1 phosphorylation consensus site (VASTPPR at amino acids 3914-3920), several putative (D/E)XST(I/L/F/W/M/V/A) Plk1 sites (e.g. at amino acids 3967-3970 and 3990-3993 and therefore close to the Cdk1 site), and physically interacts with both Cdk1 and Plk1.

Additionally, BRUCE interacts with a third kinase, Mek1 (mitogen-activated protein kinase and Erk kinase 1) (Figure 10). Mitogens induce the sequential activation of the mitogen-activated protein kinase (MAPK) network kinases Raf1, Mek1, Erk2 and Rsk *via* the small GTPase Ras (Chang et al., 2003). Besides this conventional MAPK signaling, Mek1 is also involved in regulating membrane traffic and Golgi morphology. Organelle bound Mek1/Erk was shown to be required for bidirectional transport of melanosomes (Deacon et al., 2005). This finding was substantiated by a recent report that showed that a complex of Mek1, MP1 (Mek1 partner 1) and a scaffolding protein related to MP1, p14, regulates endosomal traffic during tissue homeostasis (Teis et al., 2006). In addition, Raf1-dependent activation of Mek1 and its presence on the Golgi apparatus at the G2/M transition is required for Golgi complex fragmentation (Colanzi et al., 2003; Feinstein and Linstedt, 2007). This might argue for a role of Mek1 in detaching BRUCE from sites of interphase localization or in a general regulation of BRUCE in endosomal traffic. The identification of phosphorylation sites in BRUCE and the delineation of contributions of individual kinases to BRUCE's modifications should therefore be

a future objective. Hence, it should be determined which phosphorylation events are needed for a constitutive contribution of BRUCE to vesicular trafficking, and which are specific to cell-cycle transitions enabling BRUCE to translocate to the midbody ring.

It should be pointed out that there is evidence for a second link of BRUCE to MAPK signaling. Recently, it was demonstrated that signaling from non-receptor tyrosine kinases of the Src family is needed for completion of cytokinesis (Kasahara et al., 2007). In this case, the signal is transduced from Src *via* Mek1 and Erk to the midbody where high levels of tyrosine phosphorylation were detected. Furthermore, Kasahara et al. found that Erk translocation to the midbody in turn was dependent on proper Rab11 function. In addition to these findings, data presented in Figure 23 show that phospho-tyrosine modification does not reach the midbody ring if cells are depleted of BRUCE. An explanation for the loss of phospho-tyrosine signals at the midbody after BRUCE depletion might be that also Rab11 endosomes do not reach the midbody and associated MAPKs do not reach this site, either (Figure 23). It could be envisioned that BRUCE might act as an organellar scaffolding factor to guide the Mek/Erk module to the midbody ring on tubular endosomes. Scaffold proteins in general contribute to the specificity of Mek/Erk pathways in mammalian cells (Sacks, 2006). These include KSR (kinase suppressor of Ras), β-arrestin, MEK partner-1 (MP1, see above), Sef and IQGAP1 (which is most likely also involved in cytokinesis). By organizing signaling complexes these scaffolds target Mek/Erk to specific substrates and facilitate communication with other pathways, thereby mediating diverse functions. BRUCE could generate a midbody ring based platform that allows crosstalk between MAPK signaling and vesicular traffic or ubiquitylation to drive completion of cytokinesis.

5.2 BRUCE is needed for proper cell division

This study demonstrates that BRUCE-depletion in cultured mammalian cells resulted in cytokinesis failure (Figures 21 and 22). The appearance of syncytial cells after BRUCE depletion in U2OS cells was partially reminiscent of the phenotype described for centriolin depletion (Gromley et al., 2003). In fact, besides syncytial cells that could still undergo mitosis, ‘innocent-bystander’ mitosis can be observed as well meaning that a cell that undergoes mitosis drags a neighboring cell into this process (Figure 29). This clearly demonstrates that the structures observed after transfection of cells with BRUCE siRNA are interconnected syncytia and not just simply cells in tight contact. To allow dragging of neighboring cells into a joint mitosis it has to be assumed that cells can communicate most likely *via* connections bridging the cytoplasms that allow diffusion of a soluble signal, most likely emerging only from one cell. Additionally, this signal has to diffuse into the other cell in order to signal mitosis. The

fact that mitosis does not spread over the whole syncytium might be explained by a concentration gradient of the mitosis-inducing agent that only affects neighboring cells. Proper sealing of the intercellular bridge in cytokinesis therefore assures that mitotic and probably other soluble signals (e.g. apoptotic) cannot spread into other cells. It is not clear yet whether the cell that is dragged into a joint mitosis also replicates DNA prior to the fusion with the neighboring cell. In normal cells, probably right after constriction of the midbody, diffusion between daughter cells is no longer possible as demonstrated in this study by the fact that endosomes from one cell cannot traverse the midbody into the other daughter cell (Figure 17).

Furthermore, cells with aneuploid DNA content are the outcome of divisions of a hexa- or octoploid cell-fusion, as could be seen by FACS analysis (Figure 22). After prolonged BRUCE depletion the syncytia and aneuploid cells they contain finally undergo apoptosis.

Remarkably, aberrant mitotic and cytokinetic structures like multipolar spindles and tripolar cytokinesis are also found in spontaneously immortalized BRUCE$^{-/-}$ MEFs (Figure 30), arguing for problems in cytokinesis in the knockout animals as well as for an adaptation to the instability caused by these erroneous divisions. Adaptation in the knockout embryos probably takes place e.g. by switching to complementary factors like centriolin that can also mediate membrane targeting at the midbody ring. The involvement of BRUCE in cytokinesis and membrane traffic would explain the embryonic lethality without obvious signs of apoptosis observed for BRUCE$^{-/-}$ mice (see below). Taking into account that knockout animals for other inhibitor of apoptosis proteins like XIAP$^{-/-}$ mice (Harlin et al., 2001) and NAIP$^{-/-}$ mice (Holcik et al., 2000) are perfectly viable, favors the idea that inhibition of unwanted apoptosis during development is probably not the main function of IAP proteins or that functions of IAPs are overlapping.

Additionally, the signs of apoptosis that were found in BRUCE gene trap mice (Ren et al., 2005; Hitz et al., 2005; see Introduction) can be explained by a dominant-negative effect of the BRUCE fragments still expressed in these mice. Due to the lack of the C-terminal part of BRUCE, which in the study presented here was shown to mediate targeting of BRUCE to the midbody ring (Figures 18 to 20), BRUCE truncations can still bind to factors needed for cytokinesis but might sequester them away from the site where they are needed. In this case complementary factors, would not be sufficient to protect cells from detrimental consequences as BRUCE truncations can function as competitors for other proteins needed during cytokinesis that would else bind to compensating factors.

5.3 Involvement of BRUCE and survivin in cytokinesis-coupled apoptosis

The unique pattern of cell cycle specific localization in the midzone and on the midbody suggests a resemblance of BRUCE with the chromosomal passenger protein survivin which harbors a BIR domain that is more similar to that of BRUCE than to BIR domains in any other inhibitor of apoptosis protein. In addition to their physical interaction, BRUCE is able to mono-ubiquitylate survivin *in vitro* arguing for a regulatory or priming ubiquitylation for the degradation of survivin later on in cytokinesis (Figure 11). Alternatively, ubiquitylation of survivin might allow for a dynamic association/dissociation from the midzone/midbody similar to the dynamic behavior of survivin on centromeres that is also regulated by cycles of ubiquitylation and de-ubiquitylation (Vong et al., 2005)

It seems likely that mixed IAP-IAP complexes play a broader role in apoptosis regulation than previously thought. Besides the complex of BRUCE and survivin a mixed IAP-IAP complex of survivin and XIAP can promote increased XIAP stability against ubiquitylation and allows synergistic inhibition of apoptosis (Dohi et al., 2004). The cytokinesis-associated apoptosis phenotype described in the study presented here for HeLa cells (Figure 22) can probably be connected to an observation that showed activation of caspase-9 on the midbody and subsequent apoptosis in HeLa cells that expressed a mutant form of survivin which is not phosphorylatable by Cdk1 and in consequence fails to stably bind caspase-9 (O'Connor et al., 2000). Therefore, a mixed BRUCE-survivin complex is probably required for regulation of apoptosis on the midbody. Crystal structures of XIAP – an IAP protein with three BIR domains in tandem – with caspase-3 and -7 revealed that not the BIR domains themselves bind to the caspase's active site but linker sequences in-between BIR domains (Chai et al., 2001; Huang et al., 2001; Riedl et al., 2001). It might thus be argued that a complex of BRUCE with survivin could represent a variation on the BRUCE oligomeric complexes needed for caspase inhibition (Bartke et al., 2004). In these complexes, BIR domains might arrange in a way that would generate similar linkers needed for firm inhibition of caspases. Furthermore, it would be interesting to investigate whether IAPs like BRUCE or XIAP can compete for other components of the chromosomal passenger complex for survivin binding. This would allow a switch in the function of survivin, e.g. at sites of high IAP concentrations, from a role in centromere/microtubule dynamics to apoptosis regulation (Jeyaprakash et al., 2007).

The cytokinesis-coupled apoptosis found in HeLa cells after BRUCE depletion (Figure 22) and the resemblance to the phenotype shown for the non-phosphorylatable survivin raise the question whether a cytokinesis checkpoint might exist. Such a checkpoint would either arrest cells in the state of failed cytokinesis or would trigger apoptosis when cells sense an erroneous cytokinesis. Making use of different manipulations that allow either a spindle

checkpoint override or block in cytokinesis completion, several reports demonstrated that cells containing active p53 arrested in the following G1 phase of the cell cycle with a tetraploid genome (Hirano and Kurimura, 1974; Cross et al., 1995; Minn et al., 1996; Lanni and Jacks, 1998; Andreassen et al., 2001; Meraldi et al., 2002). The notion was therefore that mammalian somatic cells inherit a 'tetraploidy checkpoint' that arrests cells after failed cytokinesis, which would thereby prevent aneuploidy and carcinogenesis (Margolis et al., 2003; Stukenberg, 2004). However, this idea became less likely as it was demonstrated that multinucleate hepatocytes can proliferate and are not arrested finally (Fausto and Campbell, 2003). Furthermore, it was shown that cells harboring functional p53 can still undergo further rounds of mitosis and cytokinesis even if they start replicating from a tetraploid state (Uetake and Sluder, 2004). It was thus suggested that cleavage failure in living organisms alone is either not happening or not sufficient to cause problems by itself. There are also several reports on tetraploid humans that can survive up to 26 months after birth (Lafer and Neu, 1988; Lopez Pajares et al., 1990; Guc-Scekic et al., 2002).

Other cases of apoptosis during cell division are unlikely to be important for a cytokinesis checkpoint because they are triggered much earlier in mitosis. DNA damage checkpoints (Castedo et al., 2004) and the spindle assembly checkpoint (Vogel et al., 2007) that signal *via* the checkpoint kinase Chk1/2 or *via* Polo-like kinases, respectively, can trigger apoptosis during metaphase or at anaphase onset, a process known as mitotic catastrophe (Castedo et al., 2002). Mitotic catastrophe is a p53 independent mechanism but involves the activation of caspase-2 and subsequent activation of the executioner caspase-3 (Castedo et al., 2004). Under certain conditions the spindle assembly checkpoint can also trigger a p73-dependent and caspase-independent mitotic cell death (Niikura et al., 2007).

Nonetheless, cells that harbor functional p53 can arrest after a failed cytokinesis in the following G1 phase (Uetake and Sluder, 2004; Wong and Stearns, 2005) and these binucleate cells developed hallmarks of senescence (Wong and Stearns, 2005). Strikingly, mouse embryonic fibroblasts isolated from BRUCE$^{-/-}$ embryos showed largely increased signs of senescence already after the second passage in culture indicative of an arrest after failed mitosis (Lotz, 2004). The function of BRUCE in cytokinesis in cell divisions of living organisms in particular might therefore be reflected by a G1 arrest and concomitant senescence which could lead to impaired differentiation and reduced growth rather than apoptosis. This was in fact observed for BRUCE$^{-/-}$ embryos where trophoblast cells of the placenta showed hallmarks of senescence but not of apoptosis (Lotz, 2004). Taken together, phenotypes found in tissue culture cells described in this study and in BRUCE$^{-/-}$ mice fit to a more global role of BRUCE in the regulation of cell division in cells that are not challenged by pro-apoptotic stimuli. It is not

excluded that developmental scenarios exist in which transient caspase-activation is needed for cell fate determination, which could also involve BRUCE. However, the general existence of a cytokinesis checkpoint is unlikely for several of the above mentioned reasons. *Nota bene* that BRUCE depletion in other cell types than HeLa did not induce cytokinesis-associated apoptosis but variable failures in cytokinesis. Nonetheless, it is likely that a specifically cytokinesis-associated apoptosis might be restricted to certain cell types that require specialized IAPs or a balanced ratio of different IAPs during cytokinesis like e.g. HeLa cells (Crnkovic-Mertens et al., 2006).

5.4 Cell type specific mechanisms of cytokinesis and stable intercellular connections during development

As shown in this study, depletion of BRUCE in U2OS cells results in the loss of midbody rings after approximately 4-5 days as visualized by MKLP1-staining (Figure 28). It is therefore likely that BRUCE plays a role in the formation or integrity of the midbody ring. After three days of BRUCE siRNA treatment, cells furrowed normally but contained largely reduced midbody rings with midbody microtubules also lying outside of the midbody ring. Hence, BRUCE does not seem to play a role in furrow formation, actomyosin ring constriction, or midzone establishment. Instead, it seems likely that BRUCE itself might act as a scaffold to recruit other proteins to the midbody ring or to allow their firm association with the midbody ring. Thus, the loss of midbody rings could indicate either a faster turnover of their constituents or an inefficient formation. From the data presented here the latter seems more likely – taking into account the fact that midbody microtubule bundling is also reduced.

When depleting BRUCE from hTERT-RPE1 cells, in addition to HeLa and U2OS cells, cells that complete cytokinesis but still harbor midbodies in cellular protrusions can be observed. Hence, the problem in abscission is apparently overcome by stretching the intercellular bridge until rupture. In consequence, the midbody is retracted in one cell and is found in a protrusion formerly constituting part of the intercellular channel. hTERT-RPE1 cells are very motile on standard cell culture ware and daughter cells are often found interconnected by extremely elongated intercellular channels, which would allow a rupture-like mechanism. In this scenario, the resulting hole in the plasma membrane would be minimal and could probably be sealed by constitutive secretion to the plasma membrane. Several other reports also described cells that apparently separated by rupture of the midbody (Mullins and Biesele, 1977; Golsteyn et al., 1994) or where midbodies could be discarded even after cytokinesis was already completed (Dubreuil et al., 2007).

The differences in phenotypes observed in U2OS, hTERT-RPE1 and HeLa cells indicate that different cell types try to overcome problems in abscission using different mechanisms like elongation of the intercellular bridge and syncytia-like growth, midbody rupture, or cytokinesis-coupled apoptosis, respectively.

Notably, cells in which myosin II is inhibited can still undergo cytokinesis, which is contractile ring independent but depends on strong adhesion (e.g. growth on fibronectin coated cell culture dishes) and on polar traction forces (Kanada et al., 2005). Additionally, in *Dictyostelium* so-called midwife cells can help in cytokinesis by severing the myosin II knockout daughter cells that would otherwise fail to undergo cytokinesis (Uyeda end Nagasaki, 2004). These findings clearly demonstrate that cells even without a contractile ring can undergo normal cell division when the physical or cellular environment is appropriate. Several genes in fact relevant for cytokinesis might therefore not score in genome wide screens due to weak phenotypes or due to suppression of phenotypes by rescuing pathways or inappropriate experimental conditions (Somma et al., 2002; Echard et a., 2004). When testing the phenotype of BRUCE depletion in U2OS cells on different substrates (fibronectin, collagen) no rescue was observed. Elongated syncytia still formed, which indicates that cells try to separate by polar traction forces but, in contrast to furrowing problems, a failure in abscission cannot be overcome by simply pulling daughter cells to opposite directions.

Although tissue culture cells studied here should, in general, divide in a symmetric fashion, the inheritance of the midbody remnant by only one of the daughter cells would generate asymmetry. Non-polarized transformed cells in culture are thus probably not ideally suited to investigate the consequences of asymmetric midbody remnant inheritance. Investigation of these cells did not reveal any evidence for differences in cell fate *post* cytokinesis completion. Furthermore, there were no hints suchlike observed in this study. However, a recent study demonstrated that dividing stem cells have developed mechanisms to avoid the generation of asymmetry by extrusion of the midbody remnant (Dubreuil et al., 2007). These cells need to preserve their naïve state in order to allow the maintenance of an undifferentiated cellular reservoir during development or tissue regeneration. It would hence be interesting to study the fate of the midbody remnant during stem cell or developmentally demanded asymmetric divisions to delineate whether loss or inheritance of midbody remnants is accompanied by a switch in cell fate.

Interestingly, the midbody is also used to allow a symmetric partitioning of cell fate determinants. Anchoring of vesicles associated with the spindle machinery at the midbody was recently found to allow equal segregation of a cell fate determinant into daughter cells (Bökel et al., 2006). A similar mechanism must take place on midbody microtubules as these

constitute the symmetric part and release of bound vesicles likely precedes membrane transport to the midbody that drives abscission.

The symmetric features of the midbody are also utilized in developmental scenarios where midbodies are differentiated into stable intercellular bridges. These are found mostly in germ line cells (Robinson and Cooley, 1996). In mammalian and avian oogonia, stable connections allow coordinated entry into mitosis and/or atresia. In spermatocytes and spermatids they enable genetically segregated haploid spermatids to share diploid gene products after meiosis and to mediate rapid transfer of signals or nutrients. Spermatocytes/spermatids might be especially sensitive to stochastic gene expression. Stable bridges in-between cells apparently eliminate heterogeneity so that relatively uniform gametes can develop (Guo and Zheng, 2004). Strikingly, during the generation of BRUCE knockout mice, difficulties in mating of a male chimeric animal with wild type females were observed (Pyrowolakis, 2000). It was concluded that the animal was most likely sterile and therefore progeny was generated by *in vitro* fertilization. Following up on this finding, this study shows that BRUCE is a component of the stable intercellular bridges during spermatogenesis (Figure 31). It can therefore be speculated that a loss of BRUCE might lead to problems in spermatogenesis, which would explain the male sterility.

A recent report described factors required for the formation and maturation of testis ring canals (Greenbaum et al., 2007). The authors identify a novel component, Tex14 – a putative testis-specific kinase – that is needed to allow transition from midbodies to ring canals (Greenbaum et al., 2006). Midbody maturation involves the removal of the actomyosin ring and microtubules after arrested cytokinesis. Subsequently, an outer ring of septins assembles on the primary inner midbody ring consisting of MKLP1 and MgcRacGAP. During later stages the inner ring expands from 1.5 to about 3 μm and the outer septin ring is gradually lost (Greenbaum et al., 2007). This study describes that BRUCE localizes to stable intercellular bridges in mouse testis. BRUCE might therefore be a good candidate for maintaining the differentiated state of the bridge as it is still found on expanded mature intercellular bridges and is a constituent of the inner midbody ring that is not lost during this differentiation process.

5.5 Membrane delivery during cytokinesis

This study demonstrates that tubular endosomal membranes transform into vesicular pools that are concentrated on the fanning out ends of midbody microtubules in cytokinesis. Along with these vesicles BRUCE travels to the midbody ring where part of it is already localized constitutively (Figures 8 and 15). Similar to recycling endosomes, it seems likely that tubular endosomes, normally needed for protrusion formation, might acquire specialized functions in

cytokinesis which are possibly mediated through BRUCE (Figure 15 and 17). Interaction of BRUCE with integral midbody components *via* its C-terminus and with the vesicle targeting machinery *via* its N-terminus allow to classify BRUCE as a linking factor (see model in Figure 32C). The giant middle part of BRUCE, which seems devoid of any recognizable domains, might function to accommodate interactions especially in the crowded environment of the midbody. In unperturbed cells, no obvious asymmetry is detectable during membrane delivery to the intercellular bridge. But strikingly, interfering with BRUCE function by either depletion or expressing the isolated midbody targeting domain, that is not able to bind to the exocyst or Rab8/11 GTPases, reveales an intrinsic asymmetric feature of abscission. Under these conditions, secretory cargo as well as recycling endosomes accumulate in close proximity to the midbody ring. Furthermore, it seems that MAPK signaling modules do not reach the midbody ring, either, highlighting the role of vesicular transport for kinase signaling. The asymmetric aspect of membrane transport is thus probably masked by a second bulk pathway of secretion towards the midbody ring, which does not serve to seal the intercellular channel but rather provides new material for the extending plasma membrane. Additionally, this suggests that the midbody does not only serve as the structure for delivery of vesicles needed for sealing the intercellular channel but might mediate targeted membrane insertion in cells that require more extensive plasma membrane remodeling than e.g. HeLa cells. In this respect, the finding that Rab8 endosomes are also transported along midbody microtubules in U2OS cells points to a role of this compartment in regaining the flattened appearance of cells after mitosis (Figure 15, 17 and 32) in addition to other pathways of membrane addition from intracellular pools, like blebbing (Byers and Abramson, 1968; Boucrot and Kirchhausen, 2007).

The movement of vesicles in the intercellular bridge could explain the drastic rapid movements of the midbody ring, especially as observed in HeLa cells (Figures 18 and 19). These movements could represent the consequences of the migration of thickenings or waves through the intercellular channel described almost 40 years ago (Byers and Abramson, 1968). The authors of this report observed asymmetry in the way that during later stages of cytokinesis waves emerged only on one side of the midbody. Rupture of the bridge took place just adjacent to the cell receiving these latter waves. Following the movements of the midbody ring in HeLa and U2OS cells it is also shown in the study presented here that prior to abscission the midbody ring contacts the cell that would later on take it up (Figure 19 and 20). It might therefore be concluded that vesicle movements fuel the translocation of the midbody ring inside the intercellular bridge and that directionality of these movements determines the fate of the midbody ring. Directionality of transport in turn might be governed by cues originating from centrosomes that are the only polarized organelles at this stage of cell

division. Besides its role in cytokinesis, targeted membrane insertion is required for a large number of other cellular processes. This study demonstrates that BRUCE also translocates to sites of membrane insertion during neuronal differentiation (Figure 16). Interestingly, this process involves another component that is a core component of the midbody ring, MKLP1 (Kobayashi, 2002). MKLP1 is needed to form both podocyte processes and neuronal dendrites. Strikingly, their elongation is supported by Rab8-regulated basolateral-type membrane transport. This represents strong evidence for a general involvement of Rab8/BRUCE-positive endosomes in membrane transport to sites that require extensive plasma membrane remodeling.

In summary, BRUCE represents a multifunctional scaffold that allows integration of signals from several regulators of vesicular trafficking to enable it to participate in numerous processes of targeted membrane insertion like neuronal differentiation, migration, and cytokinesis.

5.6 Ubiquitin dynamics during cytokinesis

At the time the actomyosin ring has constricted most, ubiquitin is found heavily concentrated on the plus-end tips of midbody microtubules (Figure 24 and 25). It is therefore tempting to speculate that, at this point, most cell cycle regulators that remained after mitotic exit (e.g. Aurora B, survivin, Plk1 etc.) are in fact degraded at that site thus creating compartmentalized protein degradation. Membrane traffic to the midbody ring possibly starts first after the actomyosin ring has dissolved and most degradation ceased. This could speak for a mechanism in which regulatory proteins that translocate to the midbody and need to be degraded there might impose a physical barrier that does not allow vesicular traffic. Bulk degradation of proteins on midbody microtubules during early cytokinesis would later on allow membrane flow to the midbody ring and could therefore act both as a timer and as an irreversible element that generates directionality of the transition. Interestingly, ubiquitylation on midbody microtubules and on the midbody ring are separate events as proteasome inhibition of cells in early cytokinesis prevents both cytokinesis and localization of ubiquitin to the midbody ring (Figure 24).

In the 15-30 min time-window following ubiquitylation on microtubule plus-end tips virtually no ubiquitin is detectable on the midbody. With a gradual increase, ubiquitin is then exclusively found on the midbody ring. Surprisingly, this pool of ubiquitin is completely different in nature, as it virtually shows no exchange with the cytoplasmic ubiquitin pool (Figure 25). At least part of it might be brought there e.g. by BRUCE which possesses ubiquitin ligase activity. As ubiquitin on the midbody ring seems very static, modification at this site does apparently

not lead to proteolysis but rather triggers downstream processes by recruitment of ubiquitin-binding proteins. Ubiquitin on the midbody ring could of course also represent auto-ubiquitylated E2/E3 enzymes. This auto-ubiquitylation might be a consequence of the loss of substrates at that site and due to the high local concentration of E2s/E3s. Auto-ubiquitylation could then be accompanied by inactivation of E2s/E3s to result in a negative feedback. This negative feedback would support a current model claiming that irreversible cell cycle transitions cannot be attributed to a single molecule or reaction but that they originate from reaction networks (Novak et al., 2007). Systems-level interaction in this model creates a switch in the rates of two states that are coupled *via* an irreversible transition and a feedback mechanism that allows bi-stability. It is thus conjectured that modification of the midbody ring triggers a process that leads to irreversibility of the final step in cytokinesis.

Such a secondary effect after midbody ring ubiquitylation might be mediated by ubiquitin binding proteins. Recent reports (Carlton and Martin-Serrano, 2007; Morita et al., 2007) clearly demonstrated a role for the ESCRT machinery in cytokinesis. Recruitment of ESCRT components has been shown to be mediated by interaction with Cep55, ROCK and probably IQGAP1 (see Introduction). In addition, the localization of ubiquitin to the midbody ring could allow direct binding e.g. of Tsg101 in ESCRT-I and other ubiquitin-binding ESCRT components (Hrs in ESCRT-0, Vps36 in ESCRT-II) thereby extending the Cep55-dependent mechanism by which ESCRT components are recruited to the midbody ring (Carlton and Martin-Serrano, 2007; Morita et al., 2007). Moreover, ubiquitin might also contribute to the regulation of the activity of the ESCRT proteins. It therefore seems possible to speculate on a requirement for ubiquitin during ESCRT-mediated resolution of membrane tubules also in cytokinesis.

Data presented here pointing to a direct function of the de-ubiquitylating enzyme UBPY in cytokinesis can be considered a direct link of ubiquitin-modification, vesicle transport, and ESCRT machineries (Figures 26 and 27). One reason to assume this is that UBPY also harbors a MIT-domain enabling it to bind to several ESCRT-III CHMP-proteins (Row et al., 2007) thereby placing it at a late stage of MVB biogenesis. The involvement of UBPY in the regulation of cytokinesis could also explain previous data that implicated UBPY in cell cycle regulation (Naviglio et al., 1998). Interestingly, UBPY function seems to be restricted to certain cell cycle stages. UBPY was found to be phosphorylated at serine 680 thereby recruiting the phospho-binding proteins 14-3-3ε, γ, and ζ which, in turn, inhibit the de-ubiquitylating activity of UBPY (Mizuno et al., 2007). After M-phase, the phosphorylation on serine 680 decreases and inhibition by 14-3-3 is diminished concomitantly. Subsequently, during mitosis, UBPY activity increases allowing it to act on ubiquitylated proteins later on in mitosis, e.g. MKLP1, as is

shown in this study (Figure 26). The failure in MKLP1 de-ubiquitylation in the case of over-expression of a catalytically inactive form of UBPY might therefore directly reflect the failure in cytokinesis observed. Furthermore, mislocalization of MKLP1 to the cytoplasm in interphase cells would allow to speculate on problems in re-import of MKLP1 into the nucleus as cause for the cytokinesis failure. Ubiquitylation of MKLP1 might mask a nuclear localization signal (NLS) from recognition similar to the Aurora B mediated phosphorylation inside the NLS (Neef et al., 2006). The constitutive ubiquitylation in fact phenocopied the deletion mutant of MKLP1 that lacked the NLS (Liu and Erikson, 2007).

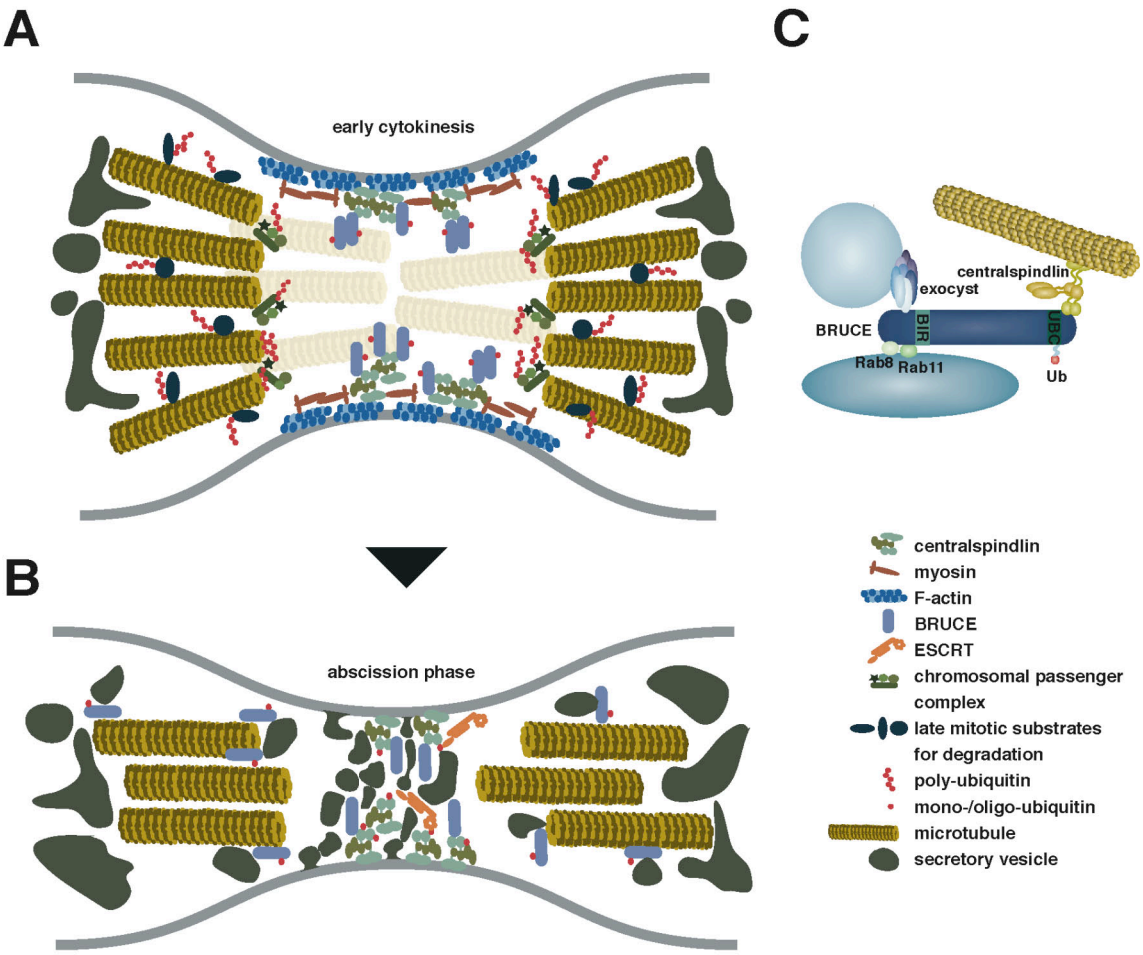

Figure 32. Model of membrane traffic and ubiquitylation in cytokinesis.
(A) Intercellular bridge in early cytokinesis. After actomyosin ring constriction a MKLP1-based ring forms that also contains BRUCE. High ubiquitylation activity is found on midbody microtubules omitting the midbody ring. This leads to the degradation of late mitotic substrates.
(B) Intercellular bridge after constriction. Microtubule bundling coincides with the loss of ubiquitylation on the midbody and leads to a static ubiquitylation of midbody ring components. Ubiquitin on the midbody ring might recruit ESCRT components as downstream effectors or might represent auto-ubiquitylated ubiquitin conjugating enzymes/ligases.
(C) Scaffolding function of BRUCE at the midbody ring. BRUCE represents a linker of membrane targeting and integral midbody ring components and might also transfer ubiquitin to the midbody ring.

Surprisingly, although UBPY and therefore de-ubiquitylating activity associated with the midbody ring, ubiquitin on the ring was not removed (Figure 25). The protection of midbody remnant bound ubiquitin from de-ubiquitylation might be achieved by enclosure of the midbody ring during abscission in a membrane-caged structure. Degradation of the remnant could therefore be similar to the one, which occurs inside multivesicular bodies. Hence, remnant clearance would be a cell cycle independent event, which resembles more to lysosomal degradation. This might explain why ubiquitin is found stably associating with the remnant and only slowly vanishing as it is gradually degraded inside a lysosome-like structure. This notion is also supported by the fact that interfering with the AAA-ATPase Vps4 leads to an arrest-like state in late cytokinesis (Morita et al., 2007). Furthermore, ubiquitylation of the midbody ring in addition to a possible impact on the ESCRT machinery might induce a switch in Rab proteins that are recruited to it. Notably, Rab7, a marker of lysosomes and autophagosomes (Feng et al., 1995; Eskelinen, 2005), was found in a proteomic study of the midbody inventory (Skop et al., 2004). Interestingly, there is a putative link to the ESCRT machinery *via* a protein called RILP that can interact with the Vps22 and Vps36 components of the ESCRT-II complex and Rab7 (Wang and Hong, 2006; Progida et al., 2007). Furthermore, subunits of ESCRT-I, -II and -III, as well as their regulatory ATPase Vps4 and the endosomal PI3P 5-kinase Fab1, all are required for autophagy (Rusten et al., 2007). A cell cycle independent compartmentalized lysosomal pathway for midbody remnant degradation would explain why in slowly proliferating cells only few midbody remnants could be observed, while fast replicating cells can harbor more than one such remnant. Additionally, a pathway suchlike could ensure that signaling from the remnant is prevented and thus the asymmetric inheritance, too, would not cause any cellular alterations.

Taken together, the data presented here show that the midbody ring represents a structure on which processes leading to the final separation of daughter cells converge. BRUCE as an integrative molecular platform is implicated in formation and proper function of the midbody ring in respect to the maintenance of its architecture, ubiquitin modification of its constituents, and vesicle targeting (Figure 32). Ubiquitin dynamics at the midbody reveal a spatially and temporally highly regulated process of posttranslational modifications that ensure proper cytokinesis. Studying its inventory and regulation might lead to the understanding of inherent asymmetric features during cytokinesis like inheritance of the midbody ring by only one cell or unidirectional membrane flow. Future objectives are thus to understand the movements of the midbody ring and whether these originate from vesicular trafficking, as well as to investigate whether ubiquitylation of the midbody ring itself can trigger abscission, and, finally, to find out what might be the crucial substrates for ubiquitylation on the midbody ring.

6 Materials and Experimental Methods

6.1 Cloning and protein expression in *E. coli*

E. coli strains used for cloning and protein expression

BL21 (DE3)	*E. coli* B F^- *dcm ompT* $hsdS(r_{B-}\ m_{B-})$ gal λ(DE3)
BL21 Codon Plus (DE3) – RIL	*E. coli* B F^- *ompT* $hsdS(r_{B-}\ m_{B-})$ *dcm*+ Tet^r gal λ(DE3) endA Hte [*argU ileY leuW* Cam^r]
XL1-Blue MR	*Δ(mcrA)183 Δ(mcrCB-hsdSMR-mrr)173 endA1 supE44 thi-1 recA1 gyrA96 relA1 lac*

E. coli cells were grown in LB or on LB plates (1% bacto-tryptone, 0.5% yeast extract, 1% NaCl, 1.5% agarose) supplemented with 50 µg/ml Ampicillin or 30 µg/ml Kanamycin at 37°C. Density of liquid cultures was determined by measuring the absorption at 600 nm wavelength with a standard spectrophotometer (Eppendorf).

Plasmids for protein expression in *E. Coli*

Plasmids of the pET (pET21b(+), pET24b(+) and pET28a/b/c(+), Novagen) and of the pGEX (pGEX2TK, pGEX4T1/2/3 and pGEX5X1, Amersham) vector series were used.

Preparation of chemically competent bacteria

To obtain highly competent cells a method from Inoue et al. (1990) was used. This protocol differs from other procedures in that the bacterial culture is grown at 18°C rather than the conventional 37°C.
Bacteria from frozen stock or single colonies from plates were used to inoculate a starter culture of 25 ml of SOB (2% bacto-tryptone, 0.5% yeast extract, 0.05% NaCl and after solutes have dissolved addition of 1% 250 mM KCl and 5 N NaOH *ad* pH 7.0) that was shaken at 37°C for 4-6 h. In the evening three flasks with 500 ml of SOB were inoculated with 1, 2 and 5 ml of the starter culture, respectively, and shaken at 18°C. When the OD_{600nm} reached 0.55 the next morning the culture vessel was transferred to an ice-water bath for 10 min. Cells were harvested by centrifugation at 2500 g for 10 min at 4°C. The supernatant was discarded and any remaining drops of medium removed using a vacuum aspirator. Cells were resuspended in 100 ml of pre-chilled Inoue transformation buffer (55 mM $MnCl_2$, 15 mM $CaCl_2$, 250 mM KCl, 10 mM PIPES [pH 6.7]) and again harvested by centrifugation. Thereafter cells were resuspended in 40 ml of Inoue buffer and 3 ml of DMSO were added by swirling the resuspension. The mixture was incubated on ice for 10 min. Aliquots of 100 µl were dispensed into pre-chilled thin-wall PCR tubes, frozen in liquid nitrogen and afterwards stored at –80°C until needed.

Plasmid DNA transformation in *E. coli*

Competent cells (in thin-wall or round-bottom tubes) were thawn on ice and 1.7 µl 10% β-mercaptoethanol was added to 100 µl of bacterial cell suspension and incubated on ice for 10 min. After addition of 1-4 µl of dissolved DNA the suspension was again incubated on ice for another 10-30 min. Cells were then heat-pulsed for 1 min at 42°C in a water bath and transferred back on ice for 1 min. 1 ml of SOB medium supplemented with 20 mM glucose was added and the suspension shaken for 30-60 min at 37°C. Hereafter cells were streaked on LB plates with the appropriate antibiotic.

Isolation of plasmid DNA

Plasmid DNA was isolated by alkaline lysis and binding to anion-exchange matrices using kits from Qiagen, Macherey&Nagel and Bioneer. For plasmid mini preparations (yielding 5-20 µg DNA), 4 ml of overnight cultures were used. For preparative purposes and to obtain DNA for transfection of mammalian cells overnight cultures of 250 ml and 1.5 l (in case of BRUCE constructs) were used. Manufacturers' protocols were slightly modified by centrifuging potassium-SDS complexes at 2500 g for 15 min at room temperature and by precipitating DNA after elution in a 10:7:1 ratio of elution buffer : isopropanol : 3 M Na-acetate [pH 5.2] at 3500 g for 30 min at 4°C. This 10:7:1 ratio mixture was also applied for general precipitation of DNA from aqueous solutions.
Alternatively DNA was purified using a PEG precipitation protocol. After alkaline lysis (0.2 M NaOH, 1% SDS) and precipitation of SDS-protein complexes (3 M KOAc, 1.18 M formic acid), DNA was precipitated and resuspended in 50 mM glucose, 25 mM Tris [pH 8.0], 10 mM EDTA and RNase was added *ad* 20 µg/ml and incubated 20 min at RT. After another round of alkaline lysis and precipitation the supernatant was extracted using phenol/chloroform. Hereafter, DNA was precipitated by addition of 1/4 volume 10 M NH_4OAc and 2 volumes ethanol and centrifugation at 10000 g (4°C). The pellet was resuspended in 2 ml TE and 0.8 ml of PEG solution were added (30% PEG 8000, 1.6 M NaCl). The suspension was incubated overnight at 4°C, pelleted the other day, the pellet resuspended, dissolved and precipitated with isopropanol and then finally resuspended in an appropriate volume of TE or dH_2O. DNA was quantified with a Nanodrop device (peqlab) with 1 $OD_{260\ nm}$ = 50 µg DNA.

Phenol/chloroform extraction of DNA

Extraction was performed using a 25:24:1 mixture of phenol : chloroform : isoamyl-alcohol (Roth). DNA from the aqueous phase was precipitated using isopropanol.

Enzymatic manipulation of DNA

Site specific restriction endonucleases were used in the appropriate buffers (all NEB). Usually 0.5-5 µg of DNA were digested with 1-10 U of enzyme for 1-3 h in a total volume of 20 µl. In the case of plasmid DNA 1 U calf intestinal phosphatase (CIP, NEB) was added 1-2 h after restriction digestion started. PCR products were digested overnight with 5-20 U enzyme in a total volume of 60 µl. Digested DNA was subjected to agarose gel electrophoresis, bands were visualized by ethidium bromide staining, cut out and subsequently purified from the gel slice using standard extraction kits (Qiagen, Macherey&Nagel). To fill in 3' recessed ends to allow blunt-end cloning of inserts, the large fragment of DNA polymerase I was used (NEB). DNA was dissolved in any restriction enzyme buffer and supplemented with 33 µM dNTPs. About 1 U of Klenow was added per µg of DNA and the reaction incubated for 15 min at 25°C. The reaction was stopped by addition of 10 mM EDTA and heating at 75°C for 10 min.

DNA ligation

Ligation of cohesive or blunt end DNA was carried out using Quick Ligase (NEB). Approximately 50-100 ng of vector was incubated with a 3- to 10-fold molar excess of insert in a total volume of 20 µl also comprising 1 µl of Quick Ligase. Samples were incubated for 5-60 min and subsequently transformed into chemically competent bacteria.

Gel electrophoresis of DNA

Agarose gel electrophoresis was performed with Tris-borate buffered solutions (0.5-fold TBE: 45 mM Tris-borate, 1 mM EDTA [pH 8.0]). DNA was mixed with loading buffer (5-fold

concentrated: 25% glycerol, 0.25% SDS, 25 mM EDTA [pH 8.0], Orange G in H_2O) and the mixtures transferred into the slots of the gel (1-2% agarose in TBE, mixed with 0.005% ethidium bromide after dissolution of the agarose). Electrophoresis was performed in minigels for 30-60 min at 5-15 V/cm.

DNA sequencing

DNA sequencing was carried out by a modified Sanger dideoxy terminator cycle sequencing chemistry using the DYEnamic ET Terminator Cycle Sequencing Kit (Amersham) with 0.1 – 1 μg DNA and 10 pmol primers, the ABI BigDye kit version 3.1, on a ABI 3730 48-capillary sequencer and 36 cm capillaries which was operated by the MPI of Biochemistry Core Facility.

Polymerase chain reaction (PCR)

PCR was performed according to standard protocols. Amplification was performed using Pfu Turbo (Stratagene) or Vent DNA polymerases (NEB) in a total volume of 50 μl. Amplification was carried out with 30 cycles of melting (95°C for 30 s), annealing (55°C for 30 s) and amplification (72°C for 60 s per 1 kb of DNA).

DNA mutagenesis

To generate point mutants, primers were designed that flanked the site to be mutated with 10-15 nt overhangs on either side. The melting temperature of the primer was calculated by T_m = 81.5 + [0.41(GC)] – [675/N] - [% of mismatch]. PCR amplification was performed using Pfu Turbo (Stratagene) or Vent DNA polymerases (NEB) in a total volume of 50 μl. Amplification was carried out with 18 cycles of melting (95°C for 30 s), annealing (T_m - 5°C for 60 s) and amplification (68°C for 60 s per 1 kb of DNA). PCR products were subsequently digested with 10 U DpnI for 1-3 h, heat inactivated and transformed into bacteria.

RT-PCR

To amplify sequences from mRNA an One-Step RT-PCR kit was used (Qiagen) according to the manufacturer's recommendations.

Generation of siRNAs from T7 transcribed cDNAs by digestion with Dicer

To generate siRNAs, primers were designed that amplify 300-600 bp of a cDNA of interest. Both sense and antisense primers contained a 5' T7 phage promoter extension (TAATACGACTCACTATAGG) that allows amplification of sense and antisense RNA in the same reaction by T7 RNA polymerase (T7 RiboMAX Express, Promega). dsRNA was then purified using RNeasy mini kit (Qiagen), quantified (1 $OD_{260\ nm}$ = 40 μg RNA) and purified dsRNA digested with 1 U recombinant Dicer (Stratagene) per μg of RNA for 18-20 h at 37°C. Dicer products were purified using a modification of the RNeasy kit protocol by Andreina Byrd and Carsten Watzl (Institut für Immunologie, Universität Heidelberg). Briefly, 1% ß-mercapoethanol was added to buffer RLT (RLT-β) and an 100 μl of RLT-β added to 100 μl of the Dicer reaction. Hereafter 100 μl of isopropanol were added, loaded on a RNeasy spin column and the mixture centrifuged (14000 g, 30 s, RT). In this step small dsRNA does not bind to the matrix and ends up in the flow through. The flow through was recovered and mixed with 200 μl of isopropanol and again loaded on a spin column and centrifuged. Here also small dsRNA binds to the matrix. Subsequent steps are equivalent to the manufacturer's protocol.

6.2 Protein biochemistry

Determination of protein concentrations in aqueous solutions

In most cases the Bradford assay was used to determine protein concentrations. To obtain a Bradford solution Coomassie Blue G (100 mg) was dissolved in 50 ml of methanol. The solution was added to 100 ml of 85% H_3PO_4, and diluted to 200 ml with water. Concentrations were determined in an $OD_{590\ nm}$ reading window of 0.1 to 2 using standard spectrophotometers (Eppendorf).

SDS-polyacrylamide gel electrophoresis

Proteins were resolved using either a Laemmli (Tris/glycine) gel system or a Bis-Tris-buffered gel system. For both systems gradient gels were prepared using a standard two-chamber mixer and a peristaltic pump.
Aqueous solutions of proteins or cleared cell lysates were mixed with 5-fold concentrated SDS sample buffer (312 mM Tris [pH 6.8], 50% glycerol, 10% SDS, 25% ß-mercaptoethanol and 0.01% bromophenolblue) boiled at 95°C for 5 min and transferred to the slots of the gel. Precision Plus Protein Standard (Biomol) was used as a marker for relative molecular size of proteins.
Tris/glycine gels were prepared as 4-20% gradient gels with 50 ml of the 4%-solution containing 6.7 ml 30% acrylamide/0.8% bisacrylamide, 12.5 ml 1.5 M Tris [pH 8.8], 500 µl 10% SDS and 29.8 ml dH_2O; and 50 ml of the 20%-solution containing 7.5 g sucrose, 33.3 ml 30% acrylamid/0.8% bisacrylamid, 12.5 ml 1.5 M Tris [pH 8.8], 500 µl 10% SDS. To start polymerization 1% v/v of a 10% APS solution and 0.1% v/v TEMED were added. After the separating gradient gel had solidified, a 3.75% stacking gel was poured on top with 10 ml containing 1.25 ml 30% acrylamid/0.8% bisacrylamid, 2.5 ml 0.5 M Tris [pH 6.8], 6 ml dH_2O, 100µl 10% SDS. To start polymerization 1% v/v of a 10% APS solution and 0.1% v/v TEMED were added. Gel electrophoresis was carried out in a buffer containing 50 mM Tris, 384 mM glycine and 0.1% SDS. Electrophoresis was performed with the current not exceeding 3.5 mA/cm.
Bis-Tris gels were prepared as 4-17.5% gradient gels with 50 ml of the 4%-solution containing 36.11 ml dH_2O, 7.25 ml 7-fold Bis-Tris/HCl concentrate (2.5 M Bis-Tris, 1.5 M HCl), 6.64 ml 30% acrylamid/0.8% bisacrylamid and 50 ml of the 17.5%-solution containing 9.8 ml dH_2O, 3.75 ml 65% sucrose solution, 7.25 ml 7-fold Bis-Tris/HCl concentrate, 29.1 ml 30% acrylamid/0.8% bisacrylamid. To start polymerization 1% v/v of a 10% APS solution and 0.1% v/v TEMED were added. Gels were poured without stacking gels and electrophoresis was carried out with MOPS running buffer prepared from a 20-fold concentrate (1 M MOPS, 1 M Tris, 69.3 mM SDS, 20.5 mM EDTA). Electrophoresis was performed with the current not exceeding 3.5 mA/cm.
Gels that were not used for immunoblotting were stained with 0.1% Coomassie Brilliant Blue R-250 dissolved in 25% methanol, 10% acetic acid. Gels were destained (25% methanol/8% acetic acid) until sufficient contrast was obtained.

Immunoblot

Proteins resolved by SDS-PAGE were transferred onto PVDF membranes (Millipore) using a tankblot device (Hoefer). Transfer was carried out in a cold room or using a water-cooling for 4-5 h in transfer buffer (25 mM Tris, 192 mM Glycin, 0.01% SDS and 20% methanol) with a constant current of 400 mA. Prior to antibody hybridisation the membrane was taken out of the blotting device, stained with Ponceau S, destained and washed with TBST (25 mM Tris [pH 7.5], 137 mM NaCl, 2.6 mM KCl, 0.05% Tween-20). Afterwards membranes were blocked using 5% w/v skim milk powder in TBST (1 h, RT) on a rotating platform (50-100 rpm).

Primary and secondary antibody were hybridized in 5% w/v skim milk powder in TBST for 1-3 h or overnight followed by extensive washing of the membrane with TBST after each hybridization step (3-5 times, 5 min, RT). Secondary HRP-conjugated antibodies were used in combination with chemi-luminiscence detection (ECL-Plus/ECL-Advanced Westernblot Detection Kit, Amersham) on conventional films (Kodak) or CCD cameras (Fuji). Alternatively self-prepared solutions for chemiluminescence detection were used. For this purpose, a 90 mM stock solution of coumaric acid and a 250 mM stock solution of luminol (both in DMSO) were prepared. For detection the blot membrane was coated with a solution prepared from 2.6 µl of 35% H_2O_2, 25 µl of the coumaric acid stock solution and 50 µl of the luminol stock solution added to 10 ml of 100 mM Tris [pH 8.5].
To reprobe blots, membranes were stripped by incubation of the membrane in stripping buffer (63.5 mM Tris [pH 6.8], 2% SDS, 100 mM ß-mercaptoethanol) for 30 min at 65°C.

Preparation of cell lysates

Lysates from cultured mammalian cells were prepared by either scraping cells from plates using a rubber policeman (for HeLa and U2OS cells) or by pipetting (HEK cells). Cells were then centrifuged (300 g, 3 min, RT) and washed in PBS. (Occasionally, cell pellets were stored at –20°C.) Pellets were resuspended in 2-5 pellet volumes of IP buffer (50 mM HEPES [pH 7.2], 150 mM NaCl, 2 mM EDTA, 0.1% NP-40) supplemented with 1 mM PMSF, Complete protease inhibitors (Roche) and additionally 1 mM NEM if ubiquitylation should be preserved. Suspensions were incubated on ice for 30 min. Debris was removed by centrifugation (10 min, 16000g, 4°C). Hereafter an appropriate amount of the supernatant representing the cell lysate was mixed with SDS loading buffer.
Alternatively – to prevent BRUCE binding to factors released from ruptured mitochondria – a lysis buffer was used that allows preservation of mitochondria (20 mM HEPES [pH 7.2], 10 mM KCl, 1.5 mM $MgCl_2$, 1 mM EDTA, 250 mM sucrose, 0.05% digitonin, 1 mM PMSF and Complete protease inhibitors).

Protein affinity-purifications and co-immunoprecipitations

To 500-1000 µl of cell lysate (5-10 mg total protein) 5-10 µg of antibody or alternatively 25-40 µl of antibody-agarose slurry was added (for HA, myc and FLAG). Coupled antibodies were incubated for 1-3 h in cell lysates (4°C) on a rotating wheel. In the case of non-coupled antibodies the mixture was incubated for 1 h (4°C) and subsequently 25-40 µl of protein G- or protein A-agarose (Amersham) were added and incubation continued for another 2 h. Afterwards beads were washed five times with IP buffer and bound proteins eluted by either boiling the beads in SDS loading buffer or by addition of antigenic peptides (0.1 mg/ml FLAG-peptide).

In vitro ubiquitylation

In vitro ubiquitylation reactions were performed by incubating 10 µM ubiquitin (bovine ubiquitin, SIGMA), 100 nM recombinant E1, 10-100 µM of the respective substrate protein and ≈ 1 µM WT or mutant ^{FLAG}BRUCE in a final volume of 30-50 µl ubiquitylation buffer (10 mM HEPES [pH 7.4], 5 mM $MgCl_2$, 5 mM ATP, 0.1 mM DTT) at 30°C for 1 h. Alternatively $^{32/33}$P-γ-ATP-labeled ubiquitin was prepared and reactions were analyzed by autoradiography.
To label ubiquitin a GST-ubiquitin construct was expressed and purified from *E. coli* that contains a thrombin cleavage site downstream of the GST that is followed by a canonical PKA phosphorylation site. Phosphorylation was performed in phosphorylation buffer (25 mM Tris [pH 7.5], 50 mM NaCl, 10 mM $MgCl_2$) using 50 µl of glutathione beads (Amersham), 50 µg of the fusion protein, 1 µl of a PKA solution (catalytic subunit, SIGMA, dissolved at 10 U final

concentration in 40 mM DTT) and 2 µl $^{32/33}$P-γ-ATP (at 10 µCi/µl) on ice for 1 h. Afterwards beads were washed 4 times with phosphorylation buffer and proteins were cleaved off the matrix using thrombin (30°C, 1 h). The supernatant was removed using a thin needle. Thrombin was inactivated by incubation at 75°C for 30 min. As a second alternative an ATP-regenerating system was used instead of 5 mM ATP in the ubiquitylation buffer. This system comprised 2 mM ATP, 10 mM creatine phosphate, 0.6 U/ml creatine phosphokinase and 0.6 U/ml inorganic pyrophosphatase.

In vitro phosphorylation

Phosphorylations were performed using immunopurified proteins. 2 µg of each protein were incubated with 10 µCi $^{32/33}$P-γ-ATP at 30°C for 30 min. Proteins were resolved using SDS-PAGE, gels were Coomassie-stained (see above) fixed (25% methanol, 10% acetic acid, 2% glycerol), dried and exposed using BioMax films (Kodak). To preserve phosphorylations 20 mM NaF and 200 µM Na_3VO_4 were added during lysis and purification.

Expression and purification of recombinant proteins from *E. coli*

GST- as well as His_6-fusion proteins were expressed in *E. coli* BL21(DE3)/RIL. Cultures were inoculated and shaken at 37°C in LB with the appropriate antibiotic. When $OD_{600\ nm}$ reached 0.4-0.7, cultures were induced by adding 1 mM IPTG and further shaken either 3-5 h at 37°C or overnight at RT. In the case of expression problems, 2-fold TY medium (16 g tryptone, 10 g yeast extract, 5 g NaCl, ad 1 l dH_2O and adjusted to pH 7.0 with NaOH) was used instead of LB.

In the case of GST-fusion proteins, cells were pelleted (6000 g, 10 min, 4°C) and resuspended in 5-10 pellet volumes of lysis buffer (20 mM Tris [pH 7.5], 150 mM NaCl, 2 mM EDTA, 1 mM PMSF, 1mM DTT, 1 mg/ml lysozyme per g of pellet) and incubated on ice for 30 min. DNA was sheared by sonification (Sonopuls HD2200, Bandelin). Lysates were centrifuged (30 min, 20000g, 4°C) to remove unbroken cells and debris. The supernatant was applied to a glutathione-sepharose column (Amersham). The column was washed with 25 column volumes GST washing buffer 1 (20 mM Tris [pH 7.5], 500 mM NaCl, 2 mM EDTA, 1% Triton-X-100, 1mM DTT), 10 column volumes of GST washing buffer 2 (20 mM Tris [pH 7.5], 150 mM NaCl, 2 mM EDTA, 0.1% Triton-X-100, 1mM DTT) and 10 column volumes of GST washing buffer 3 (20 mM Tris pH 7.5, 150 mM NaCl, 2 mM EDTA und 1mM DTT). Bound proteins were eluted with 5 column volumes GST elution buffer (10 mM Tris [pH 8.0], 10 mM glutathione), dialyzed against appropriate buffers, concentrated and 10% glycerol was added prior to freezing in liquid nitrogen.

In the case of His_6-fusion proteins, pellets were resuspended in Ni-NTA buffer (50 mM NaH_2PO_4 [pH 8.0], 300 mM NaCl, 20 mM imidazole, 2 mM PMSF, Complete protease inhibitors (Roche), 1 mg/ml lysozyme per g of pellet) and incubated on ice for 30 min. Cleared lysates were applied to Ni-NTA agarose columns (Qiagen), columns washed with 50 column volumes of Ni-NTA buffer and bound proteins eluted using 5 column volumes of Ni-NTA elution buffer (50 mM NaH_2PO_4 [pH 8.0], 150 mM NaCl, 250 mM imidazole).

To further purify fusion proteins, a second purification step of anion exchange chromatography was occasionally added. Proteins were dialysed against ResourceQ buffer (50 mM Tris [pH 7.5], 80 mM NaCl, 0.1 mM EDTA) and applied to a ResourceQ column (Amersham) using a FPLC system (Pharmacia). Proteins were eluted by gradually elevating NaCl concentration (80 mM to 1 M). Fractions containing the respective protein were pooled, dialyzed and frozen as described above.

Covalent coupling of proteins to CNBr sepharose

Pre-activated CNBr sepharose 4 Fast Flow (GE Healthcare) was resuspended in 1 mM HCl for 30 min. The gel was transferred to a Buchner funnel and washed with 15 gel volumes of cold 1 mM HCl and afterwards with coupling buffer (0.5 M NaCl, 0.1 M $NaHCO_3$ [pH 8.3]). The protein to be coupled to the beads was also dialyzed against coupling buffer. The washed gel and the protein solution were mixed and incubated either overnight at 4°C or for 3-4 h at room temperature. After coupling the supernatant was removed and any uncoupled sites were blocked by incubation with 1 M ethanolamine [pH 9.0] for 2 h at room temperature. To remove ethanolamine, the gel was washed extensively using PBS. Gels were stored at 4°C and 0.1% azide was added to allow for prolonged storage.

Preparation of ubiquitin activating enzyme E1

A CNBr-sepharose column coupled with ubiquitin was prepared as described above. In parallel His_6-Uba1 was expressed in bacteria and purified via Ni-NTA chromatography. The ubiquitin column was then equilibrated with 10 column volumes equilibration buffer (50 mM Tris [pH 7.2], 2 mM ATP, 5 mM $MgCl_2$, 0.2 mM DTT), the prepurified E1 in equilibration buffer applied and the column washed with 10 column volumes each of equilibration buffer, KCl buffer (50 mM Tris [pH 7.2], 1 mM KCl), and wash buffer (50 mM Tris [pH 7.2]). E1 was eluted in five fractions of 2 ml with DTT elution buffer (50 mM Tris [pH 7.2], 10 mM DTT). The column was cleaned, washed and prepared for storage by applying 10 column volumes each of pH 9 wash buffer (50 mM Tris [pH 9.0], 2 mM DTT), regeneration buffer (50 mM Tris [pH 9.0], 1 M KCl), and storage buffer (50 mM Tris [pH 7.2], 0.02% NaN_3).

TCA precipitation of proteins

Proteins in solution were precipitated by addition of an equal volume of 10% TCA and incubation on ice for 10 min. Precipitated material was pelleted by centrifugation (16000 g, 4°C, 10 min). Pellets were washed with acetone (-20°C), dried and resuspended in SDS loading buffer.

Denaturating Ni-NTA precipitation

Transiently transfected HEK 293T cells were harvested and pellets washed once in PBS. Cells were lysed in 6M guanidine-HCl, 0.1 M NaH_2PO_4, 0.1% Tween 20, 0.01 M Tris [pH 8.0]. To shear DNA, lysates were briefly sonicated. An aliquot of the lysate was kept for TCA precipitation. The remaining lysate was incubated with Ni-NTA agarose beads (Qiagen) for 3-5 h. Beads were washed 5 times with 8 M urea, 0.1 M NaH_2PO_4, 0.1% Tween 20, 0.01 M Tris [pH 8.0], and twice with PBS, 0.01% Tween 20. TCA precipitates and beads were boiled in loading buffer and subjected to SDS-PAGE and immunoblotting.

Antibodies

Antibodies used in this study were mouse monoclonal anti-BRUCE (clone 4), anti-MKLP1 (clone 24), anti-Cdk1 (clone 1), anti-p230 trans Golgi (clone 15), anti-GGA3 (clone 8), anti-Rab8 (clone 4), anti Rab-11 (clone 47, all BD Biosciences), anti-α-tubulin (clone B-7), anti-γ-tubulin (clone C-11), anti-Plk-1 (clone F-8), anti-HA (clone F-7), anti-GFP (clone B-2), anti-phosphotyrosine (clone PY99), anti-survivin (clone D8), anti-lamin A/C (clone 636), anti-c-Myc (clone 9E10), anti-p21 (clone 187), anti-p53 (clone DO-1), anti-MEK1 (clone H-8, all Santa Cruz), anti-Aurora B (Biozol), anti-rSec6 (clone 9H5), anti-rSec8 (clone 14G1, both abcam), anti-FLAG (clone M2, SIGMA), goat polyclonal anti-Rab11, rabbit polyclonal anti-MKLP1 (both Santa Cruz), anti-FLAG (SIGMA), polyclonal sheep anti-TGN46 (AbD Serotec). FITC, TRITC, AMCA and Cy3-labeled secondary sheep/rat anti-mouse, donkey anti-rabbit antibodies were

from Jackson ImmunoResearch. Antisera recognizing BRUCE N- and C-termini were generated by immunizing rabbits with His_6-fusion proteins as shown in Figure 7 (see also Hauser et al., 1998 and Bartke et al., 2004). For standard applications antibodies were diluted 1:750 to 1:2000 for immunoblot analysis and 1:50 to 1:200 for immunofluorescence detection.

6.3 Cell biology

Cell lines

HEK 293	tumorigenic human epithelial kidney cell line, hypotriploid with a modal chromosome number of 64, contains the left end segment of the adenovirus 5 genome from nts 1 to 4344 which is integrated into chromosome 19 (19q13.2)
HEK 293T	a highly transfectable derivative of the 293 cell line into which the temperature sensitive allele for SV40 T-antigen was inserted
HeLa	human epithelial cervix adenocarnoma, HeLa cells have been reported to contain human papilloma virus 18 (HPV-18) sequences
HeLa S3	HeLa S3 is a clonal derivative of the parent HeLa line. S3 was cloned in 1955 by T.T. Puck, P.I. Marcus, and S.J. Cieciura. This line can be adapted to grow in suspension.
U2OS	human osteosarcoma, chromosomally highly altered, with chromosome counts in the hyper-triploid range
PC12	derived from transplantable rat adrenal gland pheochromo-cytoma, the cells respond reversibly to NGF by induction of the neuronal phenotype
hTERT-RPE1	human retinal pigment epithelial cell line (Clontech) that stably expresses telomerase, normal diploid genotype, non-tumorigenic

Plasmids for protein expression in mammalian cells

Plasmids of the pCMV-Tag2/3/4 (Stratagene) and pcDNA3.1/pcDNA3.1-Myc-His (Invitrogen) series as well as pCI/pCI-Neo (Promega), pEGFP-F, pEGFP/CFP/ YFP, and pDsRed-monomer vectors (Clontech) were used.
Cloning of BRUCE and engineering of mutants and truncations was described previously (Bartke et al., 2004). BRUCE cDNAs were expressed from pCI (Promega) or pCMV2 (Stratagene) as were FLAG-tagged cDNAs of luciferase, BRUCE 1-522 and BRUCE 1-648.
GFP-BRUCE-C (amino acids 4711-4845) was cloned into pEGFP-C1 (Clontech) using an internal XhoI site (bp 14135) in the full length cDNA and an PCR-introduced BamHI site downstream of the stop codon. Nrdp1 was amplified from HeLa mRNA using primers that generate an N-terminal FLAG-epitope tag and cloned into pCI (Promega). GFP-Rab8 was a gift of J. Peranen (Hattula and Peranen, 2000), GFP-Rab11 was obtained from M. Zerial (Sönnichsen et al., 2000), GFP-ubiquitin was a gift of N. Dantuma (Dantuma et al., 2006), HA-epitope tagged rat albumin was a gift of D. LeBel (Daull et al., 2004) and FLAG-epitope tagged UBPY and its mutant were from H. Alwan (Alwan and van Leeuwen, 2007). His_6- and HA-epitope tagged ubiquitin were described previously (Treier et al., 1994).

siRNA sequences and transfection of siRNA

siRNA sequences were designed using rules previously described (Jagla et al., 2005). siRNAs were 19- or 21-mer duplexes (MWG) with 3' TT-overhangs. siRNA duplexes targeting BRUCE in human cells were oligo_1 CUCAGGAGAGUACUGCUCA, oligo_2 GAACCAGAA GGACUUACUC, oligo_3 (as in Ren et al. 2005) GUUUCAAAGCAGGAUGAUG, siRNA targeting lamin A/C CUGGACUUCCAGAAGAACA, p53 (Warburton et al., 2005) GGACAUACC

AGCUUAGAUU, p21 GUCAGAACCGGCTGGGGAU, survivin (Lens et al., 2003) GAGGCUG GCUUCAUCCACU and MKLP1 (Liu et al., 2004) GGGCUUUCCUGAUCAAGAGUG.

Propagation of mammalian tissue culture cells

MEF, hTERT-RPE1, U2OS, HeLa and HEK 293/T cells were maintained at 37°C, 7.5% CO_2 in DMEM (SIGMA) supplemented with 10% FCS (referred to as normal culture medium). To a 15 cm dish 20 ml of culture medium were added, to a 10 cm dish 10 ml, and to a 6-well cavity 3 ml.

Preparation of large scale suspension cultures for cell cycle arrests

HeLa S3 cells were grown on standard cell culture plastic dishes until 75% confluence was reached. Cells were then dislodged by trypsin treatment and transferred into spinner flasks (Bellco). Cells were arrested by incubation with either 100 ng/ml nocodazole (arresting cells in prometaphase), 1 mM taxol (arresting cells at G2/M) or 5 mM hydroxyurea (arresting cells at G1) for 16 h.

Transfections

Transient transfections were performed in 10 cm dishes (HEK 293T) or 6-well plates (HeLa, U2OS, hTERT-RPE1) using calcium phosphate or lipofection protocols. Furthermore U2OS cells were also transfected by electroporation using the Nucleofector kit (Amaxa).
For standard calcium phosphate transfections (HEK 293T) 2 x 10^6 cells were seeded in a 10 cm dish one day before transfection. Transfection mixes were prepared in 2 ml Eppendorf tubes comprising 12-15 μg plasmid DNA adjusted to 450 μl with dH_2O. To this solution 50 μl of a 2.5 M $CaCl_2$-solution were added drop wise and the mix was agitated vigorously. Hereafter 500 μl of 2-fold HBS solution (16.012 g NaCl, 0.744 g KCl, 9.532 g HEPES, 0.248 g Na_2HPO_4 ad 1 l dH_2O and adjusted to pH 7.05 with NaOH) were added dropwise and the mix again agitated vigorously. The transfection mixture was incubated for 3 min at RT and added to the cells. Cells were then incubated for 5 h with the transfection mix under normal culture conditions and the medium was hereafter replaced with fresh medium. After an additional 30-50 h of incubation, cells were harvested.
To transfect HeLa cells, a modification of the standard calcium phosphate protocol was used. After seeding 1.5 x 10^5 cells per 6-well cavity the day prior to transfection, the normal culture medium was exchanged for transfection medium (DMEM supplemented with 10% heat inactivated horse serum, 2.5 μg/ml 25-hydroxy-cholesterol) right before the transfection. The transfection solution was prepared as described above apart from using a BES buffered solution instead of the HBS buffered one (2-fold BES solution: 50 mM BES [pH 6.95], 280 mM NaCl und 1.5 mM Na_2HPO_4). Only 300 μl of the total 1000 μl of transfection mix were added to one cavity of a 6-well plate. Cells were then incubated for not more than 4 h with the transfection mix under normal culture conditions and the medium was hereafter replaced with fresh normal culture medium. After an additional 12-30 h of incubation, cells were harvested.
Nota bene that the pH of HBS/BES solutions has to be experimentally adjusted to allow high transfection rates.
U2OS and hTERT-RPE1 cells used for siRNA experiments were transfected by electroporation. A confluent plate of cells was split 1:2 the day before transfection. On the day of transfection cells were dislodged by trypsination and 1 x 10^6 cells per transfection were pelleted by centrifugation. The supernatant was removed and the pellet resuspended in 100 μl Amaxa nucleofector solution V per transfection. siRNA duplexes obtained from MWG were transfected at a final concentration of 100 nM. The cell suspension and the siRNAs were mixed in the electroporation cuvette and the nucleofector device with a preset program (U2OS, ATCC) used for applying the electroporation pulse. After transfection 1 x 10^6 U2OS

cells were seeded in either 10 cm dishes or 1 x 10^5 cells in 35 mm dishes. Cells used in immunofluorescence microscopy were seeded on glass coverslips (Roth).
Additionally HeLa and U2OS cells were frequently also transfected by lipofection. 1 x 10^5 cells were seeded in a cavity of a 6-well plate the day before transfection. To transfect plasmid DNA, 3 µg of the respective DNA were added to 200 µl of OptiMEM medium (Invitrogen) and at the same time 3 µl of lipofectamine 2000 (Invitrogen) were added to a separate vial also containing 200 µl of OptiMEM medium. Both solutions were incubated for not more than 5 min and then united, mixed and incubated for another 15 min. This mix was added to cells and cells were incubated for up to 4 h with the transfection mixture. Subsequently cell culture medium was replaced with normal culture medium and cells were harvested 12-30 h after transfection.
To transfect siRNAs, 3 µg of the respective dsRNAs were added to 200 µl of OptiMEM medium (Invitrogen) and at the same time 3 µl of oligofectamine (Invitrogen) were added to a separate vial also containing 200 µl of OptiMEM medium. Both solutions were incubated for not more than 5 min and then united, mixed and incubated for another 15 min. During this incubation the cell culture medium was replaced with OptiMEM. The transfection mix was then added to cells and cells were incubated for up to 4 h with the transfection mixture. Subsequently, cell culture medium was replaced with normal culture medium and cells were harvested 30-50 h after transfection.

Generation of stable cell lines

HeLa cells stably expressing HA-rAlb and U2OS cells stably expressing GFP-Rab8, GFP-Rab11 and GFP-ubiquitin were generated by transfecting cells in a 6-well format using lipofection. One day after transfection cells were replated in 15 cm dishes and 750-1000 µg/ml G418 (SIGMA) were added to the normal culture medium. Afterwards medium was exchanged every 2-4 d and cells were cultivated until visible colonies appeared (which took approximately 3-4 weeks). Then either a polyclonal cell line was generated by simply trypsinizing all clones and replating. Alternatively colonies were screened for expression of the protein of interest and single colonies were picked from the plate using trypsin-soaked cloning discs and these were then transferred to the cavities of a 12-well plate and expanded.

Flow cytometry

To obtain DNA histograms by propidium iodide staining cells were harvested by either scraping or trypsination, centrifuged and the pellets washed with PBS. Cell pellets were then resuspended in 300 µl PBS and while mildly agitating the suspension 700 µl of –20°C ethanol were added drop wise. Cell suspensions were then incubated for at least 4 h at 4°C. Thereafter, cells were pelleted, washed with PBS, resuspended in staining solution (100 µg/ml propidium iodide, 200 µg/ml RNase A in PBS) and incubated for 30-60 min in the dark. Cell cycle profiles were obtained using a FACSCalibur system and CELLQuest analysis software (Becton Dickinson). Transfection status of cells was checked by assessing the GFP signal either through co-transfection of a membrane anchored GFP-variant (EGFP-F, which contains the Ras prenylation signal) or by the signal of the GFP-fusion protein of interest.

Immunofluorescence and live cell video microscopy

Immunofluorescence was performed according to standard protocols after fixation in methanol. Cells were carefully washed with PBS and PBS was removed via vacuum aspiration. Cells were then placed in a -20°C freezer and precooled methanol was added (-20°C, 3 min). After incubation methanol was removed by aspiration and the cells were dried for 3-5 min. Rewetting was performed using TBST followed by blocking with TBST supplemented with 2% BSA (1 h, RT, mild shaking). Coverslips (24 x 24 mm, Roth) were then

placed on Parafilm (Pechiney) in a humidified chamber. On each coverslip a 1:50 to 1:200 dilution of primary antibody in TBST + 2% BSA was pipetted. Coverslips were incubated for 1-2 h and then washed three times in TBST (3 min each, RT). After incubation with secondary antibody in a procedure corresponding to that with the primary, cover slips were mounted using glycerol-based mounting medium (0.5% p-phenylenediamine, 20 mM Tris [pH 8.8], 90% glycerol – the p-phenylenediamine is dissolved by bubbling nitrogen into the mixture for 3-4 h).
Mouse testis was obtained as frozen tissue slices on glass support (BioChain). Slices were rehydrated in TBST and processed for immunofluorescence as described above.
Images were acquired on a Leica DM RXA microscope equipped with a Hamatsu ORCA-ER camera. Image acquisition and deconvolution of images was carried out using Openlab software. Confocal laser scanning microscopy was performed with a Leica TCS SP2 confocal scanning microscope. For fluorescence live cell video microscopy and photobleaching experiments, U2OS cells were cultured in 35 mm μ-dishes with No. 1.5 bottom (ibidi). Live cell video microscopy and FRAP were carried out on an AppliedPrecision DeltaVision RT system equipped with a quantifiable laser module. After photobleaching of the GFP fluorescence with 25-50% laser intensity images were obtained every second during a time frame of 3 min. Fluorescence intensities were measured and quantified and images processed using SoftWorx software (AppliedPrecision). For live cell video microscopy DIC or phase and fluorescence images were taken every 1-5 min over a time frame of 10 to 48 h.

Neuronal differentiation of PC-12 cells

PC-12 cells were maintained in RPMI 1640 (Invitrogen) supplemented with 10% fetal bovine serum and 5% horse serum at 37°C, 7.5% CO_2. Cells were resuspended using a glass pipette with narrow opening that was prepared by melting the opening with the flame of a Bunsen burner. For differentiation cells were grown in RPMI 1640 supplemented with 1% horse serum and 100 ng/ml NGF (NGF-7S, SIGMA) for three days and processed for immunofluorescence microscopy.

Mouse embryonic fibroblasts

MEFs were generated from E11.5 to E14.5 embryos by shearing the embryo in a 18/19G needle in 5 ml DMEM + 10% FCS + 100 U/ml penicillin/streptomycin. Embryo fragments were plated, incubated for 1 day and adhering cells and embryonic bodies trypsinized. After sedimentation of embryonic bodies the fibroblast-rich supernatent was plated. Immortalization was carried out using a so-called 3T3 protocol. Every three days 3 x 10^5 cells were replated on a 6 cm dish. During growth crisis cells were not replated, instead only the medium was exchanged.

6.4 Software

Resources of the National Center for Biotechnology Information (NCBI) were used for data base searching and retrieval of sequences. Analysis of DNA and proteins was carried out using DNA Star package (DNA Star). Texts, graphs and tables were prepared using Excel and Word (Microsoft), images were prepared using Photoshop and Illustrator (Adobe). Gels and films were scanned on a Duoscan T1200 (AGFA) and on a Scan Maker i900 (Mikrotek).

7 References

Abaza, A., Soleilhac, J. M., Westendorf, J., Piel, M., Crevel, I., Roux, A. and Pirollet, F. (2003). M phase phosphoprotein 1 is a human plus-end-directed kinesin-related protein required for cytokinesis. J Biol Chem 278, 27844-52.

Adams, R. R., Tavares, A. A., Salzberg, A., Bellen, H. J. and Glover, D. M. (1998). pavarotti encodes a kinesin-like protein required to organize the central spindle and contractile ring for cytokinesis. Genes Dev 12, 1483-94.

Albertson, R., Riggs, B. and Sullivan, W. (2005). Membrane traffic: a driving force in cytokinesis. Trends Cell Biol 15, 92-101.

Altan-Bonnet, N., Phair, R. D., Polishchuk, R. S., Weigert, R. and Lippincott-Schwartz, J. (2003). A role for Arf1 in mitotic Golgi disassembly, chromosome segregation, and cytokinesis. Proc Natl Acad Sci U S A 100, 13314-9.

Alwan, H. A. and van Leeuwen, J. E. (2007). UBPY-mediated epidermal growth factor receptor (EGFR) de-ubiquitination promotes EGFR degradation. J Biol Chem 282, 1658-69.

Amerik, A. Y. and Hochstrasser, M. (2004). Mechanism and function of deubiquitinating enzymes. Biochim Biophys Acta 1695, 189-207.

Andreassen, P. R., Lohez, O. D., Lacroix, F. B. and Margolis, R. L. (2001). Tetraploid state induces p53-dependent arrest of nontransformed mammalian cells in G1. Mol Biol Cell 12, 1315-28.

Arama, E., Agapite, J. and Steller, H. (2003). Caspase activity and a specific cytochrome C are required for sperm differentiation in Drosophila. Dev Cell 4, 687-97.

Baluska, F., Menzel, D. and Barlow, P. W. (2006). Cytokinesis in plant and animal cells: endosomes 'shut the door'. Dev Biol 294, 1-10.

Ban, K. H., Torres, J. Z., Miller, J. J., Mikhailov, A., Nachury, M. V., Tung, J. J., Rieder, C. L. and Jackson, P. K. (2007). The END network couples spindle pole assembly to inhibition of the anaphase-promoting complex/cyclosome in early mitosis. Dev Cell 13, 29-42.

Banks, D. P., Plescia, J., Altieri, D. C., Chen, J., Rosenberg, S. H., Zhang, H. and Ng, S. C. (2000). Survivin does not inhibit caspase-3 activity. Blood 96, 4002-3.

Bardroff, M. (1997). Charakterisierung eines neuartigen Proteins der Maus mit Homologie zu Ubiquitin-Konjugationsenzymen und Apoptose-Inhibitoren. In Fakultät für Chemie und Pharmazie. Eberhard-Karls-Universität Tübingen.

Barr, F. A., Sillje, H. H. and Nigg, E. A. (2004). Polo-like kinases and the orchestration of cell division. Nat Rev Mol Cell Biol 5, 429-40.

Bartke, T. (2004). Charakterisierung von BRUCE als antiapoptotisches IAP. In Fakultät für Biologie. Ludwig-Maximilians-Universität München.

Bartke, T., Pohl, C., Pyrowolakis, G. and Jentsch, S. (2004). Dual role of BRUCE as an antiapoptotic IAP and a chimeric E2/E3 ubiquitin ligase. Mol Cell 14, 801-11.

Batchelder, E. L., Thomas-Virnig, C. L., Hardin, J. D. and White, J. G. (2007). Cytokinesis is not controlled by calmodulin or myosin light chain kinase in the Caenorhabditis elegans early embryo. FEBS Lett 581, 4337-41.

Belar, K. (1929a). Beiträge zur Kausalanalyse der Mitose. II. Untersuchungen an der Spermatocyte von Chorthippus (Stenbothrus) lineatus. Wilhelm Roux Archiv Entw Mechanik 118, 359-484.

Belar, K. (1929b). Mitotic spindle, analyzed by Dr. Belar in Lecture. Pasadena,USA: Dept Biol CalTech.

Birkenfeld, J., Nalbant, P., Bohl, B. P., Pertz, O., Hahn, K. M. and Bokoch, G. M. (2007). GEF-H1 modulates localized RhoA activation during cytokinesis under the control of mitotic kinases. Dev Cell 12, 699-712.

Bluemink, J. G. and de Laat, S. W. (1973). New membrane formation during cytokinesis in normal and cytochalasin B-treated eggs of Xenopus laevis. I. Electron microscope observations. J Cell Biol 59, 89-108.

Bogard, N., Lan, L., Xu, J. and Cohen, R. S. (2007). Rab11 maintains connections between germline stem cells and niche cells in the Drosophila ovary. Development 134, 3413-8.

Bokel, C., Schwabedissen, A., Entchev, E., Renaud, O. and Gonzalez-Gaitan, M. (2006). Sara endosomes and the maintenance of Dpp signaling levels across mitosis. Science 314, 1135-9.

Bornens, M. (2002). Centrosome composition and microtubule anchoring mechanisms. Curr Opin Cell Biol 14, 25-34.

Bosl, W. J. and Li, R. (2005). Mitotic-exit control as an evolved complex system. Cell 121, 325-33.

Boucrot, E. and Kirchhausen, T. (2007). Endosomal recycling controls plasma membrane area during mitosis. Proc Natl Acad Sci U S A 104, 7939-44.

Bray, D. and White, J. G. (1988). Cortical flow in animal cells. Science 239, 883-8.

Brennan, I. M., Peters, U., Kapoor, T. M. and Straight, A. F. (2007). Polo-like kinase controls vertebrate spindle elongation and cytokinesis. PLoS ONE 2, e409.

Bringmann, H. and Hyman, A. A. (2005). A cytokinesis furrow is positioned by two consecutive signals. Nature 436, 731-4.

Burkard, M. E., Randall, C. L., Larochelle, S., Zhang, C., Shokat, K. M., Fisher, R. P. and Jallepalli, P. V. (2007). Chemical genetics reveals the requirement for Polo-like kinase 1 activity in positioning RhoA and triggering cytokinesis in human cells. Proc Natl Acad Sci U S A 104, 4383-8.

Byers, B. and Abramson, D. H. (1968). Cytokinesis in HeLa: post-telophase delay and microtubule-associated motility. Protoplasma 66, 413-35.

Canman, J. C., Hoffman, D. B. and Salmon, E. D. (2000). The role of pre- and post-anaphase microtubules in the cytokinesis phase of the cell cycle. Curr Biol 10, 611-4.

Carlton, J. G. and Martin-Serrano, J. (2007). Parallels between cytokinesis and retroviral budding: a role for the ESCRT machinery. Science 316, 1908-12.

Casanova, J. E., Wang, X., Kumar, R., Bhartur, S. G., Navarre, J., Woodrum, J. E., Altschuler, Y., Ray, G. S. and Goldenring, J. R. (1999). Association of Rab25 and Rab11a with the apical recycling system of polarized Madin-Darby canine kidney cells. Mol Biol Cell 10, 47-61.

Castedo, M., Perfettini, J. L., Roumier, T., Andreau, K., Medema, R. and Kroemer, G. (2004). Cell death by mitotic catastrophe: a molecular definition. Oncogene 23, 2825-37.

Castedo, M., Perfettini, J. L., Roumier, T. and Kroemer, G. (2002). Cyclin-dependent kinase-1: linking apoptosis to cell cycle and mitotic catastrophe. Cell Death Differ 9, 1287-93.

Castro, A., Arlot-Bonnemains, Y., Vigneron, S., Labbe, J. C., Prigent, C. and Lorca, T. (2002). APC/Fizzy-Related targets Aurora-A kinase for proteolysis. EMBO Rep 3, 457-62.

Chai, J., Shiozaki, E., Srinivasula, S. M., Wu, Q., Datta, P., Alnemri, E. S. and Shi, Y. (2001). Structural basis of caspase-7 inhibition by XIAP. Cell 104, 769-80.

Chan, Y. L., Suzuki, K. and Wool, I. G. (1995). The carboxyl extensions of two rat ubiquitin fusion proteins are ribosomal proteins S27a and L40. Biochem Biophys Res Commun 215, 682-90.

Chang, F., Steelman, L. S., Shelton, J. G., Lee, J. T., Navolanic, P. M., Blalock, W. L., Franklin, R. and McCubrey, J. A. (2003). Regulation of cell cycle progression and apoptosis by the Ras/Raf/MEK/ERK pathway (Review). Int J Oncol 22, 469-80.

Chavrier, P., Vingron, M., Sander, C., Simons, K. and Zerial, M. (1990). Molecular cloning of YPT1/SEC4-related cDNAs from an epithelial cell line. Mol Cell Biol 10, 6578-85.

Chen, Q., Lakshmikanth, G. S., Spudich, J. A. and De Lozanne, A. (2007). The localization of inner centromeric protein (INCENP) at the cleavage furrow is dependent on Kif12 and involves interactions of the N terminus of INCENP with the actin cytoskeleton. Mol Biol Cell 18, 3366-74.

Chen, X. W., Inoue, M., Hsu, S. C. and Saltiel, A. R. (2006). RalA-exocyst-dependent recycling endosome trafficking is required for the completion of cytokinesis. J Biol Chem 281, 38609-16.

Chen, Y. A. and Scheller, R. H. (2001). SNARE-mediated membrane fusion. Nat Rev Mol Cell Biol 2, 98-106.

Chen, Z., Naito, M., Hori, S., Mashima, T., Yamori, T. and Tsuruo, T. (1999). A human IAP-family gene, apollon, expressed in human brain cancer cells. Biochem Biophys Res Commun 264, 847-54.

Chiu, Y. H., Sun, Q. and Chen, Z. J. J. (2007). E1-L2 activates both ubiquitin and FAT10. Molecular Cell 27, 1014-1023.

Ciechanover, A., Elias, S., Heller, H. and Hershko, A. (1982). "Covalent affinity" purification of ubiquitin-activating enzyme. J Biol Chem 257, 2537-42.

Clague, M. J. and Urbe, S. (2006). Endocytosis: the DUB version. Trends Cell Biol 16, 551-9.

Colanzi, A. and Corda, D. (2007). Mitosis controls the Golgi and the Golgi controls mitosis. Curr Opin Cell Biol 19, 386-93.

Colanzi, A., Sutterlin, C. and Malhotra, V. (2003). RAF1-activated MEK1 is found on the Golgi apparatus in late prophase and is required for Golgi complex fragmentation in mitosis. J Cell Biol 161, 27-32.

Crnkovic-Mertens, I., Semzow, J., Hoppe-Seyler, F. and Butz, K. (2006). Isoform-specific silencing of the Livin gene by RNA interference defines Livin beta as key mediator of apoptosis inhibition in HeLa cells. J Mol Med 84, 232-40.

Cross, S. M., Sanchez, C. A., Morgan, C. A., Schimke, M. K., Ramel, S., Idzerda, R. L., Raskind, W. H. and Reid, B. J. (1995). A p53-dependent mouse spindle checkpoint. Science 267, 1353-6.

D'Avino, P. P., Archambault, V., Przewloka, M. R., Zhang, W., Lilley, K. S., Laue, E. and Glover, D. M. (2007). Recruitment of Polo kinase to the spindle midzone during cytokinesis requires the Feo/Klp3A complex. PLoS ONE 2, e572.

Dantuma, N. P., Groothuis, T. A., Salomons, F. A. and Neefjes, J. (2006). A dynamic ubiquitin equilibrium couples proteasomal activity to chromatin remodeling. J Cell Biol 173, 19-26.

Daull, P., Home, W. and LeBel, D. (2004). Characterization of the TGN exit routes in AtT20 cells using pancreatic amylase and serum albumin. Eur J Cell Biol 83, 121-30.

Deacon, S. W., Nascimento, A., Serpinskaya, A. S. and Gelfand, V. I. (2005). Regulation of bidirectional melanosome transport by organelle bound MAP kinase. Curr Biol 15, 459-63.

Di Fiore, B. and Pines, J. (2007). Emi1 is needed to couple DNA replication with mitosis but does not regulate activation of the mitotic APC/C. J Cell Biol 177, 425-37.

Diamonti, A. J., Guy, P. M., Ivanof, C., Wong, K., Sweeney, C. and Carraway, K. L., 3rd. (2002). An RBCC protein implicated in maintenance of steady-state neuregulin receptor levels. Proc Natl Acad Sci U S A 99, 2866-71.

Ditzel, M. and Meier, P. (2002). IAP degradation: decisive blow or altruistic sacrifice? Trends Cell Biol 12, 449-52.

Dohi, T., Okada, K., Xia, F., Wilford, C. E., Samuel, T., Welsh, K., Marusawa, H., Zou, H., Armstrong, R., Matsuzawa, S. et al. (2004). An IAP-IAP complex inhibits apoptosis. J Biol Chem 279, 34087-90.

Doxsey, S., McCollum, D. and Theurkauf, W. (2005). Centrosomes in cellular regulation. Annu Rev Cell Dev Biol 21, 411-34.

Doxsey, S. J. (2005). Molecular links between centrosome and midbody. Mol Cell 20, 170-2.

Dubreuil, V., Marzesco, A. M., Corbeil, D., Huttner, W. B. and Wilsch-Brauninger, M. (2007). Midbody and primary cilium of neural progenitors release extracellular membrane particles enriched in the stem cell marker prominin-1. J Cell Biol 176, 483-95.

Echard, A., Hickson, G. R., Foley, E. and O'Farrell, P. H. (2004). Terminal cytokinesis events uncovered after an RNAi screen. Curr Biol 14, 1685-93.

Efimov, A., Kharitonov, A., Efimova, N., Loncarek, J., Miller, P. M., Andreyeva, N., Gleeson, P., Galjart, N., Maia, A. R., McLeod, I. X. et al. (2007). Asymmetric CLASP-dependent nucleation of noncentrosomal microtubules at the trans-Golgi network. Dev Cell 12, 917-30.

Eggert, U. S., Mitchison, T. J. and Field, C. M. (2006). Animal cytokinesis: from parts list to mechanisms. Annu Rev Biochem 75, 543-66.

Elia, A. E., Cantley, L. C. and Yaffe, M. B. (2003). Proteomic screen finds pSer/pThr-binding domain localizing Plk1 to mitotic substrates. Science 299, 1228-31.

Eskelinen, E. L. (2005). Maturation of autophagic vacuoles in Mammalian cells. Autophagy 1, 1-10.

Fabbro, M., Zhou, B. B., Takahashi, M., Sarcevic, B., Lal, P., Graham, M. E., Gabrielli, B. G., Robinson, P. J., Nigg, E. A., Ono, Y. et al. (2005). Cdk1/Erk2- and Plk1-dependent phosphorylation of a centrosome protein, Cep55, is required for its recruitment to midbody and cytokinesis. Dev Cell 9, 477-88.

Fausto, N. and Campbell, J. S. (2003). The role of hepatocytes and oval cells in liver regeneration and repopulation. Mech Dev 120, 117-30.

Feinstein, T. N. and Linstedt, A. D. (2007). Mitogen-activated protein kinase kinase 1-dependent Golgi unlinking occurs in G2 phase and promotes the G2/M cell cycle transition. Mol Biol Cell 18, 594-604.

Feng, Y., Press, B. and Wandinger-Ness, A. (1995). Rab 7: an important regulator of late endocytic membrane traffic. J Cell Biol 131, 1435-52.

Field, C. M., Coughlin, M., Doberstein, S., Marty, T. and Sullivan, W. (2005). Characterization of anillin mutants reveals essential roles in septin localization and plasma membrane integrity. Development 132, 2849-60.

Fielding, A. B., Schonteich, E., Matheson, J., Wilson, G., Yu, X., Hickson, G. R., Srivastava, S., Baldwin, S. A., Prekeris, R. and Gould, G. W. (2005). Rab11-FIP3 and FIP4 interact with Arf6 and the exocyst to control membrane traffic in cytokinesis. Embo J 24, 3389-99.

Finger, F. P. and White, J. G. (2002). Fusion and fission: membrane trafficking in animal cytokinesis. Cell 108, 727-30.

Finley, D., Bartel, B. and Varshavsky, A. (1989). The tails of ubiquitin precursors are ribosomal proteins whose fusion to ubiquitin facilitates ribosome biogenesis. Nature 338, 394-401.

Flamand, A. (1970). Genetic Study of Vesicular Stomatitis Virus - Classification of Spontaneous Thermosensitive Mutants in Complementation Groups. Journal of General Virology 8, 187-&.

Flemming, W. (1891). Neue Beiträgezur Kenntnis der Zelle. Arc. Mikr. Anat. 37, 685-751.

Fraser, A. G., James, C., Evan, G. I. and Hengartner, M. O. (1999). Caenorhabditis elegans inhibitor of apoptosis protein (IAP) homologue BIR-1 plays a conserved role in cytokinesis. Curr Biol 9, 292-301.

Gallione, C. J. and Rose, J. K. (1985). A Single Amino-Acid Substitution in a Hydrophobic Domain Causes Temperature-Sensitive Cell-Surface Transport of a Mutant Viral Glycoprotein. Journal of Virology 54, 374-382.

Garrus, J. E., von Schwedler, U. K., Pornillos, O. W., Morham, S. G., Zavitz, K. H., Wang, H. E., Wettstein, D. A., Stray, K. M., Cote, M., Rich, R. L. et al. (2001). Tsg101 and the vacuolar protein sorting pathway are essential for HIV-1 budding. Cell 107, 55-65.

Ghanekar, Y. and Lowe, M. (2005). Protein kinase D: activation for Golgi carrier formation. Trends Cell Biol 15, 511-4.

Giet, R. and Glover, D. M. (2001). Drosophila aurora B kinase is required for histone H3 phosphorylation and condensin recruitment during chromosome condensation and to organize the central spindle during cytokinesis. J Cell Biol 152, 669-82.

Gillingham, A. K. and Munro, S. (2007). The Small G Proteins of the Arf Family and Their Regulators. Annu Rev Cell Dev Biol.

Glotzer, M. (2001). Animal cell cytokinesis. Annu Rev Cell Dev Biol 17, 351-86.

Glotzer, M., Murray, A. W. and Kirschner, M. W. (1991). Cyclin is degraded by the ubiquitin pathway. Nature 349, 132-8.

Golsteyn, R. M., Schultz, S. J., Bartek, J., Ziemiecki, A., Ried, T. and Nigg, E. A. (1994). Cell cycle analysis and chromosomal localization of human Plk1, a putative homologue of the mitotic kinases Drosophila polo and Saccharomyces cerevisiae Cdc5. J Cell Sci 107 (Pt 6), 1509-17.

Goody, R. S., Rak, A. and Alexandrov, K. (2005). The structural and mechanistic basis for recycling of Rab proteins between membrane compartments. Cell Mol Life Sci 62, 1657-70.

Greenbaum, M. P., Ma, L. and Matzuk, M. M. (2007). Conversion of midbodies into germ cell intercellular bridges. Dev Biol 305, 389-96.

Greenbaum, M. P., Yan, W., Wu, M. H., Lin, Y. N., Agno, J. E., Sharma, M., Braun, R. E., Rajkovic, A. and Matzuk, M. M. (2006). TEX14 is essential for intercellular bridges and fertility in male mice. Proc Natl Acad Sci U S A 103, 4982-7.

Grenfell, S. J., Trausch-Azar, J. S., Handley-Gearhart, P. M., Ciechanover, A. and Schwartz, A. L. (1994). Nuclear localization of the ubiquitin-activating enzyme, E1, is cell-cycle-dependent. Biochem J 300 (Pt 3), 701-8.

Grigoriev, I., Splinter, D., Keijzer, N., Wulf, P. S., Demmers, J., Ohtsuka, T., Modesti, M., Maly, I. V., Grosveld, F., Hoogenraad, C. C. et al. (2007). Rab6 regulates transport and targeting of exocytotic carriers. Dev Cell 13, 305-14.

Gromley, A., Jurczyk, A., Sillibourne, J., Halilovic, E., Mogensen, M., Groisman, I., Blomberg, M. and Doxsey, S. (2003). A novel human protein of the maternal centriole is required for the final stages of cytokinesis and entry into S phase. J Cell Biol 161, 535-45.

Gromley, A., Yeaman, C., Rosa, J., Redick, S., Chen, C. T., Mirabelle, S., Guha, M., Sillibourne, J. and Doxsey, S. J. (2005). Centriolin anchoring of exocyst and SNARE complexes at the midbody is required for secretory-vesicle-mediated abscission. Cell 123, 75-87.

Gruneberg, U., Neef, R., Honda, R., Nigg, E. A. and Barr, F. A. (2004). Relocation of Aurora B from centromeres to the central spindle at the metaphase to anaphase transition requires MKlp2. J Cell Biol 166, 167-72.

Gruneberg, U., Neef, R., Li, X., Chan, E. H., Chalamalasetty, R. B., Nigg, E. A. and Barr, F. A. (2006). KIF14 and citron kinase act together to promote efficient cytokinesis. J Cell Biol 172, 363-72.

Guc-Scekic, M., Milasin, J., Stevanovic, M., Stojanov, L. J. and Djordjevic, M. (2002). Tetraploidy in a 26-month-old girl (cytogenetic and molecular studies). Clin Genet 61, 62-5.

Guo, G. Q. and Zheng, G. C. (2004). Hypotheses for the functions of intercellular bridges in male germ cell development and its cellular mechanisms. J Theor Biol 229, 139-46.

Guse, A., Mishima, M. and Glotzer, M. (2005). Phosphorylation of ZEN-4/MKLP1 by aurora B regulates completion of cytokinesis. Curr Biol 15, 778-86.

Haas, A. L., Warms, J. V., Hershko, A. and Rose, I. A. (1982). Ubiquitin-activating enzyme. Mechanism and role in protein-ubiquitin conjugation. J Biol Chem 257, 2543-8.

Haas, A. L., Warms, J. V. and Rose, I. A. (1983). Ubiquitin adenylate: structure and role in ubiquitin activation. Biochemistry 22, 4388-94.

Hales, C. M., Vaerman, J. P. and Goldenring, J. R. (2002). Rab11 family interacting protein 2 associates with Myosin Vb and regulates plasma membrane recycling. J Biol Chem 277, 50415-21.

Hansen, D. V., Loktev, A. V., Ban, K. H. and Jackson, P. K. (2004). Plk1 regulates activation of the anaphase promoting complex by phosphorylating and triggering SCFbetaTrCP-dependent destruction of the APC Inhibitor Emi1. Mol Biol Cell 15, 5623-34.

Hao, Y., Sekine, K., Kawabata, A., Nakamura, H., Ishioka, T., Ohata, H., Katayama, R., Hashimoto, C., Zhang, X., Noda, T. et al. (2004). Apollon ubiquitinates SMAC and caspase-9, and has an essential cytoprotection function. Nat Cell Biol 6, 849-60.

Harlin, H., Reffey, S. B., Duckett, C. S., Lindsten, T. and Thompson, C. B. (2001). Characterization of XIAP-deficient mice. Mol Cell Biol 21, 3604-8.

Hattula, K. and Peranen, J. (2000). FIP-2, a coiled-coil protein, links Huntingtin to Rab8 and modulates cellular morphogenesis. Curr Biol 10, 1603-6.

Hauser, H. (1992). Charakterisierung von UbcM1, einem Vertreter einer neuen Klasse von Ubiquitin-Konjugationsenzmyen in Vertebraten. In Fakultät für Chemie und Pharmazie. Eberhard-Karls-Universität Tübingen.

Hauser, H. P., Bardroff, M., Pyrowolakis, G. and Jentsch, S. (1998). A giant ubiquitin-conjugating enzyme related to IAP apoptosis inhibitors. J Cell Biol 141, 1415-22.

Hershko, A., Heller, H., Eytan, E. and Reiss, Y. (1986). The protein substrate binding site of the ubiquitin-protein ligase system. J Biol Chem 261, 11992-9.

Hicke, L., Schubert, H. L. and Hill, C. P. (2005). Ubiquitin-binding domains. Nat Rev Mol Cell Biol 6, 610-21.

Hickson, G. R., Matheson, J., Riggs, B., Maier, V. H., Fielding, A. B., Prekeris, R., Sullivan, W., Barr, F. A. and Gould, G. W. (2003). Arfophilins are dual Arf/Rab 11 binding proteins that regulate recycling endosome distribution and are related to Drosophila nuclear fallout. Mol Biol Cell 14, 2908-20.

Hill, E., Clarke, M. and Barr, F. A. (2000). The Rab6-binding kinesin, Rab6-KIFL, is required for cytokinesis. Embo J 19, 5711-9.

Hinds, M. G., Norton, R. S., Vaux, D. L. and Day, C. L. (1999). Solution structure of a baculoviral inhibitor of apoptosis (IAP) repeat. Nat Struct Biol 6, 648-51.

Hirano, A. and Kurimura, T. (1974). Virally transformed cells and cytochalasin B. I. The effect of cytochalasin B on cytokinesis, karyokinesis and DNA synthesis in cells. Exp Cell Res 89, 111-20.

Hitz, C., Vogt-Weisenhorn, D., Ruiz, P., Wurst, W. and Floss, T. (2005). Progressive loss of the spongiotrophoblast layer of Birc6/Bruce mutants results in embryonic lethality. Genesis 42, 91-103.

Holcik, M., Thompson, C. S., Yaraghi, Z., Lefebvre, C. A., MacKenzie, A. E. and Korneluk, R. G. (2000). The hippocampal neurons of neuronal apoptosis inhibitory protein 1 (NAIP1)-deleted mice display increased vulnerability to kainic acid-induced injury. Proc Natl Acad Sci U S A 97, 2286-90.

Hopkins, C. R. (1983). Intracellular Routing of Transferrin and Transferrin Receptors in Epidermoid Carcinoma A431-Cells. Cell 35, 321-330.

Hsu, S. C., Hazuka, C. D., Roth, R., Foletti, D. L., Heuser, J. and Scheller, R. H. (1998). Subunit composition, protein interactions, and structures of the mammalian brain sec6/8 complex and septin filaments. Neuron 20, 1111-22.

Hsu, S. C., TerBush, D., Abraham, M. and Guo, W. (2004). The exocyst complex in polarized exocytosis. Int Rev Cytol 233, 243-65.

Huang, Y., Park, Y. C., Rich, R. L., Segal, D., Myszka, D. G. and Wu, H. (2001). Structural basis of caspase inhibition by XIAP: differential roles of the linker versus the BIR domain. Cell 104, 781-90.

Huber, L. A., Pimplikar, S., Parton, R. G., Virta, H., Zerial, M. and Simons, K. (1993). Rab8, a small GTPase involved in vesicular traffic between the TGN and the basolateral plasma membrane. J Cell Biol 123, 35-45.

Hunter, T. (2007). The age of crosstalk: phosphorylation, ubiquitination, and beyond. Mol Cell 28, 730-8.

Hurley, J. H. and Emr, S. D. (2006). The ESCRT complexes: structure and mechanism of a membrane-trafficking network. Annu Rev Biophys Biomol Struct 35, 277-98.

Hurley, J. H., Lee, S. and Prag, G. (2006). Ubiquitin-binding domains. Biochem J 399, 361-72.

Inoue, S. (1953). [Polarization optical studies of the mitotic spindle. I. The demonstration of spindle fibers in living cells.]. Chromosoma 5, 487-500.

Jackman, M., Lindon, C., Nigg, E. A. and Pines, J. (2003). Active cyclin B1-Cdk1 first appears on centrosomes in prophase. Nat Cell Biol 5, 143-8.

Jagla, B., Aulner, N., Kelly, P. D., Song, D., Volchuk, A., Zatorski, A., Shum, D., Mayer, T., De Angelis, D. A., Ouerfelli, O. et al. (2005). Sequence characteristics of functional siRNAs. Rna 11, 864-72.

Jentsch, S. (1992). The ubiquitin-conjugation system. Annu Rev Genet 26, 179-207.

Jeyaprakash, A. A., Klein, U. R., Lindner, D., Ebert, J., Nigg, E. A. and Conti, E. (2007). Structure of a Survivin-Borealin-INCENP Core Complex Reveals How Chromosomal Passengers Travel Together. Cell 131, 271-85.

Jiang, W., Jimenez, G., Wells, N. J., Hope, T. J., Wahl, G. M., Hunter, T. and Fukunaga, R. (1998). PRC1: a human mitotic spindle-associated CDK substrate protein required for cytokinesis. Mol Cell 2, 877-85.

Jin, J., Li, X., Gygi, S. P. and Harper, J. W. (2007). Dual E1 activation systems for ubiquitin differentially regulate E2 enzyme charging. Nature 447, 1135-8.

Julian, M., Tollon, Y., Lajoie-Mazenc, I., Moisand, A., Mazarguil, H., Puget, A. and Wright, M. (1993). gamma-Tubulin participates in the formation of the midbody during cytokinesis in mammalian cells. J Cell Sci 105 (Pt 1), 145-56.

Kaiser, P. and Fon, E. A. (2007). Expanding horizons at Big Sky. Symposium on ubiquitin and signaling. EMBO Rep 8, 817-22.

Kanada, M., Nagasaki, A. and Uyeda, T. Q. (2005). Adhesion-dependent and contractile ring-independent equatorial furrowing during cytokinesis in mammalian cells. Mol Biol Cell 16, 3865-72.

Kasahara, K., Nakayama, Y., Nakazato, Y., Ikeda, K., Kuga, T. and Yamaguchi, N. (2007). Src signaling regulates completion of abscission in cytokinesis through ERK/MAPK activation at the midbody. J Biol Chem 282, 5327-39.

Kerscher, O., Felberbaum, R. and Hochstrasser, M. (2006). Modification of proteins by ubiquitin and ubiquitin-like proteins. Annu Rev Cell Dev Biol 22, 159-80.

Kobayashi, N. (2002). Mechanism of the process formation; podocytes vs. neurons. Microsc Res Tech 57, 217-23.

Koegl, M., Hoppe, T., Schlenker, S., Ulrich, H. D., Mayer, T. U. and Jentsch, S. (1999). A novel ubiquitination factor, E4, is involved in multiubiquitin chain assembly. Cell 96, 635-44.

Komaba, S., Hamao, H., Murata-Hori, M. and Hosoya, H. (2001). Identification of myosin II kinase from sea urchin eggs as protein kinase CK2. Gene 275, 141-8.

Komatsu, S., Murai, N., Totsukawa, G., Abe, M., Akasaka, K., Shimada, H. and Hosoya, H. (1997a). Identification of MAPKAPK homolog (MAPKAPK-4) as a myosin II regulatory light-chain kinase in sea urchin egg extracts. Arch Biochem Biophys 343, 55-62.

Komatsu, S., Murata-Hori, M., Totsukawa, G., Murai, N., Fujimoto, H., Mabuchi, I. and Hosoya, H. (1997b). Identification of p34cdc2 kinase from sea urchin Hemicentrotus pulcherrimus and its involvement in the phosphorylation of myosin II regulatory light chain in the metaphase extract. Gene 198, 359-65.

Kosako, H., Yoshida, T., Matsumura, F., Ishizaki, T., Narumiya, S. and Inagaki, M. (2000). Rho-kinase/ROCK is involved in cytokinesis through the phosphorylation of myosin light chain and not ezrin/radixin/moesin proteins at the cleavage furrow. Oncogene 19, 6059-64.

Kouranti, I., Sachse, M., Arouche, N., Goud, B. and Echard, A. (2006). Rab35 regulates an endocytic recycling pathway essential for the terminal steps of cytokinesis. Curr Biol 16, 1719-25.

Krapp, A., Gulli, M. P. and Simanis, V. (2004). SIN and the art of splitting the fission yeast cell. Curr Biol 14, R722-30.

Kreitzer, G., Marmorstein, A., Okamoto, P., Vallee, R. and Rodriguez-Boulan, E. (2000). Kinesin and dynamin are required for post-Golgi transport of a plasma-membrane protein. Nat Cell Biol 2, 125-7.

Kunitoku, N., Sasayama, T., Marumoto, T., Zhang, D., Honda, S., Kobayashi, O., Hatakeyama, K., Ushio, Y., Saya, H. and Hirota, T. (2003). CENP-A phosphorylation by Aurora-A in prophase is required for enrichment of Aurora-B at inner centromeres and for kinetochore function. Dev Cell 5, 853-64.

Kurasawa, Y. and Todokoro, K. (1999). Identification of human APC10/Doc1 as a subunit of anaphase promoting complex. Oncogene 18, 5131-7.

Kuriyama, R., Gustus, C., Terada, Y., Uetake, Y. and Matuliene, J. (2002). CHO1, a mammalian kinesin-like protein, interacts with F-actin and is involved in the terminal phase of cytokinesis. J Cell Biol 156, 783-90.

Lafer, C. Z. and Neu, R. L. (1988). A liveborn infant with tetraploidy. Am J Med Genet 31, 375-8.

Lanni, J. S. and Jacks, T. (1998). Characterization of the p53-dependent postmitotic checkpoint following spindle disruption. Mol Cell Biol 18, 1055-64.

Lecuit, T. and Wieschaus, E. (2000). Polarized insertion of new membrane from a cytoplasmic reservoir during cleavage of the Drosophila embryo. J Cell Biol 150, 849-60.

Lee, K. S., Yuan, Y. L., Kuriyama, R. and Erikson, R. L. (1995). Plk is an M-phase-specific protein kinase and interacts with a kinesin-like protein, CHO1/MKLP-1. Mol Cell Biol 15, 7143-51.

Lee, O. K., Frese, K. K., James, J. S., Chadda, D., Chen, Z. H., Javier, R. T. and Cho, K. O. (2003). Discs-Large and Strabismus are functionally linked to plasma membrane formation. Nat Cell Biol 5, 987-93.

Lens, S. M., Wolthuis, R. M., Klompmaker, R., Kauw, J., Agami, R., Brummelkamp, T., Kops, G. and Medema, R. H. (2003). Survivin is required for a sustained spindle checkpoint arrest in response to lack of tension. Embo J 22, 2934-47.

Li, F., Ackermann, E. J., Bennett, C. F., Rothermel, A. L., Plescia, J., Tognin, S., Villa, A., Marchisio, P. C. and Altieri, D. C. (1999). Pleiotropic cell-division defects and apoptosis induced by interference with survivin function. Nat Cell Biol 1, 461-6.

Lindon, C. and Pines, J. (2004). Ordered proteolysis in anaphase inactivates Plk1 to contribute to proper mitotic exit in human cells. J Cell Biol 164, 233-41.

Lindsay, A. J. and McCaffrey, M. W. (2002). Rab11-FIP2 functions in transferrin recycling and associates with endosomal membranes via its COOH-terminal domain. J Biol Chem 277, 27193-9.

Litvak, V., Argov, R., Dahan, N., Ramachandran, S., Amarilio, R., Shainskaya, A. and Lev, S. (2004). Mitotic phosphorylation of the peripheral Golgi protein Nir2 by Cdk1 provides a docking mechanism for Plk1 and affects cytokinesis completion. Mol Cell 14, 319-30.

Liu, D., Zhang, N., Du, J., Cai, X., Zhu, M., Jin, C., Dou, Z., Feng, C., Yang, Y., Liu, L. et al. (2006). Interaction of Skp1 with CENP-E at the midbody is essential for cytokinesis. Biochem Biophys Res Commun 345, 394-402.

Liu, X. and Erikson, R. L. (2007). The nuclear localization signal of mitotic kinesin-like protein Mklp-1: effect on Mklp-1 function during cytokinesis. Biochem Biophys Res Commun 353, 960-4.

Liu, X., Zhou, T., Kuriyama, R. and Erikson, R. L. (2004). Molecular interactions of Polo-like-kinase 1 with the mitotic kinesin-like protein CHO1/MKLP-1. J Cell Sci 117, 3233-46.

Lombardi, D., Soldati, T., Riederer, M. A., Goda, Y., Zerial, M. and Pfeffer, S. R. (1993). Rab9 functions in transport between late endosomes and the trans Golgi network. Embo J 12, 677-82.

Lopez Pajares, I., Delicado, A., Diaz de Bustamante, A., Pellicer, A., Pinel, I., Pardo, M. and Martin, M. (1990). Tetraploidy in a liveborn infant. J Med Genet 27, 782-3.

Lotz, K. (2004). Funktionelle Charakterisierung des IAP-verwandten, Ubiquitin-konjugierenden Enzyms BRUCE in vivo durch die phänotypische Analyse eines Maus-Knockout-Modells. In Fakultät für Biologie. Ludwig-Maximilians-Universität München.

Lotz, K., Pyrowolakis, G. and Jentsch, S. (2004). BRUCE, a giant E2/E3 ubiquitin ligase and inhibitor of apoptosis protein of the trans-Golgi network, is required for normal placenta development and mouse survival. Mol Cell Biol 24, 9339-50.

Low, S. H., Li, X., Miura, M., Kudo, N., Quinones, B. and Weimbs, T. (2003). Syntaxin 2 and endobrevin are required for the terminal step of cytokinesis in mammalian cells. Dev Cell 4, 753-9.

Luini, A., Ragnini-Wilson, A., Polishchuck, R. S. and De Matteis, M. A. (2005). Large pleiomorphic traffic intermediates in the secretory pathway. Curr Opin Cell Biol 17, 353-61.

Machesky, L. M. (1998). Cytokinesis: IQGAPs find a function. Curr Biol 8, R202-5.

Machida, Y. J. and Dutta, A. (2007). The APC/C inhibitor, Emi1, is essential for prevention of rereplication. Genes Dev 21, 184-94.

Maddox, A. S., Lewellyn, L., Desai, A. and Oegema, K. (2007). Anillin and the septins promote asymmetric ingression of the cytokinetic furrow. Dev Cell 12, 827-35.

Margolis, R. L., Lohez, O. D. and Andreassen, P. R. (2003). G1 tetraploidy checkpoint and the suppression of tumorigenesis. J Cell Biochem 88, 673-83.

Matheson, J., Yu, X., Fielding, A. B. and Gould, G. W. (2005). Membrane traffic in cytokinesis. Biochem Soc Trans 33, 1290-4.

Matuliene, J. and Kuriyama, R. (2002). Kinesin-like protein CHO1 is required for the formation of midbody matrix and the completion of cytokinesis in mammalian cells. Mol Biol Cell 13, 1832-45.

Mazumdar, A. and Mazumdar, M. (2002). How one becomes many: blastoderm cellularization in Drosophila melanogaster. Bioessays 24, 1012-22.

Meraldi, P., Honda, R. and Nigg, E. A. (2002). Aurora-A overexpression reveals tetraploidization as a major route to centrosome amplification in p53-/- cells. Embo J 21, 483-92.

Meraldi, P., Lukas, J., Fry, A. M., Bartek, J. and Nigg, E. A. (1999). Centrosome duplication in mammalian somatic cells requires E2F and Cdk2-cyclin A. Nat Cell Biol 1, 88-93.

Minn, A. J., Boise, L. H. and Thompson, C. B. (1996). Expression of Bcl-xL and loss of p53 can cooperate to overcome a cell cycle checkpoint induced by mitotic spindle damage. Genes Dev 10, 2621-31.

Mishima, M., Kaitna, S. and Glotzer, M. (2002). Central spindle assembly and cytokinesis require a kinesin-like protein/RhoGAP complex with microtubule bundling activity. Dev Cell 2, 41-54.

Mizuno, E., Kitamura, N. and Komada, M. (2007). 14-3-3-dependent inhibition of the deubiquitinating activity of UBPY and its cancellation in the M phase. Exp Cell Res 313, 3624-34.

Mollinari, C., Kleman, J. P., Jiang, W., Schoehn, G., Hunter, T. and Margolis, R. L. (2002). PRC1 is a microtubule binding and bundling protein essential to maintain the mitotic spindle midzone. J Cell Biol 157, 1175-86.

Morita, E., Sandrin, V., Chung, H. Y., Morham, S. G., Gygi, S. P., Rodesch, C. K. and Sundquist, W. I. (2007). Human ESCRT and ALIX proteins interact with proteins of the midbody and function in cytokinesis. Embo J 26, 4215-27.

Moshe, Y., Boulaire, J., Pagano, M. and Hershko, A. (2004). Role of Polo-like kinase in the degradation of early mitotic inhibitor 1, a regulator of the anaphase promoting complex/cyclosome. Proc Natl Acad Sci U S A 101, 7937-42.

Mullins, J. M. and Biesele, J. J. (1977). Terminal phase of cytokinesis in D-98s cells. J Cell Biol 73, 672-84.

Murata-Hori, M., Fukuta, Y., Ueda, K., Iwasaki, T. and Hosoya, H. (2001). HeLa ZIP kinase induces diphosphorylation of myosin II regulatory light chain and reorganization of actin filaments in nonmuscle cells. Oncogene 20, 8175-83.

Murata-Hori, M., Fumoto, K., Fukuta, Y., Iwasaki, T., Kikuchi, A., Tatsuka, M. and Hosoya, H. (2000). Myosin II regulatory light chain as a novel substrate for AIM-1, an aurora/Ipl1p-related kinase from rat. J Biochem (Tokyo) 128, 903-7.

Naito, Y., Okada, M. and Yagisawa, H. (2006). Phospholipase C isoforms are localized at the cleavage furrow during cytokinesis. J Biochem (Tokyo) 140, 785-91.

Naviglio, S., Mattecucci, C., Matoskova, B., Nagase, T., Nomura, N., Di Fiore, P. P. and Draetta, G. F. (1998). UBPY: a growth-regulated human ubiquitin isopeptidase. Embo J 17, 3241-50.

Neef, R., Gruneberg, U., Kopajtich, R., Li, X., Nigg, E. A., Sillje, H. and Barr, F. A. (2007). Choice of Plk1 docking partners during mitosis and cytokinesis is controlled by the activation state of Cdk1. Nat Cell Biol 9, 436-44.

Neef, R., Klein, U. R., Kopajtich, R. and Barr, F. A. (2006). Cooperation between mitotic kinesins controls the late stages of cytokinesis. Curr Biol 16, 301-7.

Neef, R., Preisinger, C., Sutcliffe, J., Kopajtich, R., Nigg, E. A., Mayer, T. U. and Barr, F. A. (2003). Phosphorylation of mitotic kinesin-like protein 2 by polo-like kinase 1 is required for cytokinesis. J Cell Biol 162, 863-75.

Nickerson, D. P., Russell, M. R. and Odorizzi, G. (2007). A concentric circle model of multivesicular body cargo sorting. EMBO Rep 8, 644-50.

Niendorf, S., Oksche, A., Kisser, A., Lohler, J., Prinz, M., Schorle, H., Feller, S., Lewitzky, M., Horak, I. and Knobeloch, K. P. (2007). Essential role of ubiquitin-specific protease 8 for receptor tyrosine kinase stability and endocytic trafficking in vivo. Mol Cell Biol 27, 5029-39.

Nigg, E. A. (2001). Mitotic kinases as regulators of cell division and its checkpoints. Nat Rev Mol Cell Biol 2, 21-32.

Niikura, Y., Dixit, A., Scott, R., Perkins, G. and Kitagawa, K. (2007). BUB1 mediation of caspase-independent mitotic death determines cell fate. J Cell Biol 178, 283-96.

Niiya, F., Xie, X., Lee, K. S., Inoue, H. and Miki, T. (2005). Inhibition of cyclin-dependent kinase 1 induces cytokinesis without chromosome segregation in an ECT2 and MgcRacGAP-dependent manner. J Biol Chem 280, 36502-9.

Nislow, C., Lombillo, V. A., Kuriyama, R. and McIntosh, J. R. (1992). A plus-end-directed motor enzyme that moves antiparallel microtubules in vitro localizes to the interzone of mitotic spindles. Nature 359, 543-7.

Nislow, C., Sellitto, C., Kuriyama, R. and McIntosh, J. R. (1990). A monoclonal antibody to a mitotic microtubule-associated protein blocks mitotic progression. J Cell Biol 111, 511-22.

Norden, C., Mendoza, M., Dobbelaere, J., Kotwaliwale, C. V., Biggins, S. and Barral, Y. (2006). The NoCut pathway links completion of cytokinesis to spindle midzone function to prevent chromosome breakage. Cell 125, 85-98.

Novak, B., Tyson, J. J., Gyorffy, B. and Csikasz-Nagy, A. (2007). Irreversible cell-cycle transitions are due to systems-level feedback. Nat Cell Biol 9, 724-8.

Novick, P., Ferro, S. and Schekman, R. (1981). Order of events in the yeast secretory pathway. Cell 25, 461-9.

Novick, P., Field, C. and Schekman, R. (1980). Identification of 23 complementation groups required for post-translational events in the yeast secretory pathway. Cell 21, 205-15.

O'Connor, D. S., Grossman, D., Plescia, J., Li, F., Zhang, H., Villa, A., Tognin, S., Marchisio, P. C. and Altieri, D. C. (2000). Regulation of apoptosis at cell division by p34cdc2 phosphorylation of survivin. Proc Natl Acad Sci U S A 97, 13103-7.

Otegui, M. S., Verbrugghe, K. J. and Skop, A. R. (2005). Midbodies and phragmoplasts: analogous structures involved in cytokinesis. Trends Cell Biol 15, 404-13.

Papoulas, O., Hays, T. S. and Sisson, J. C. (2005). The golgin Lava lamp mediates dynein-based Golgi movements during Drosophila cellularization. Nat Cell Biol 7, 612-8.

Pelissier, A., Chauvin, J. P. and Lecuit, T. (2003). Trafficking through Rab11 endosomes is required for cellularization during Drosophila embryogenesis. Curr Biol 13, 1848-57.

Pelzer, C., Kassner, I., Matentzoglu, K., Singh, R. K., Wollscheid, H. P., Scheffner, M., Schmidtke, G. and Groettrup, M. (2007). UBE1L2, a novel E1 enzyme specific for ubiquitin. J Biol Chem 282, 23010-4.

Peng, J., Schwartz, D., Elias, J. E., Thoreen, C. C., Cheng, D., Marsischky, G., Roelofs, J., Finley, D. and Gygi, S. P. (2003). A proteomics approach to understanding protein ubiquitination. Nat Biotechnol 21, 921-6.

Peranen, J., Auvinen, P., Virta, H., Wepf, R. and Simons, K. (1996). Rab8 promotes polarized membrane transport through reorganization of actin and microtubules in fibroblasts. J Cell Biol 135, 153-67.

Peters, J. M. (2006). The anaphase promoting complex/cyclosome: a machine designed to destroy. Nat Rev Mol Cell Biol 7, 644-56.

Petronczki, M., Glotzer, M., Kraut, N. and Peters, J. M. (2007). Polo-like kinase 1 triggers the initiation of cytokinesis in human cells by promoting recruitment of the RhoGEF Ect2 to the central spindle. Dev Cell 12, 713-25.

Pickart, C. M. (2001). Mechanisms underlying ubiquitination. Annu Rev Biochem 70, 503-33.

Pickart, C. M. and Fushman, D. (2004). Polyubiquitin chains: polymeric protein signals. Curr Opin Chem Biol 8, 610-6.

Pickart, C. M. and Rose, I. A. (1985). Ubiquitin carboxyl-terminal hydrolase acts on ubiquitin carboxyl-terminal amides. J Biol Chem 260, 7903-10.

Piekny, A., Werner, M. and Glotzer, M. (2005). Cytokinesis: welcome to the Rho zone. Trends Cell Biol 15, 651-8.

Piel, M., Nordberg, J., Euteneuer, U. and Bornens, M. (2001). Centrosome-dependent exit of cytokinesis in animal cells. Science 291, 1550-3.

Pines, J. (2006). Mitosis: a matter of getting rid of the right protein at the right time. Trends Cell Biol 16, 55-63.

Pines, J. and Lindon, C. (2005). Proteolysis: anytime, any place, anywhere? Nat Cell Biol 7, 731-5.

Polishchuk, E. V., Di Pentima, A., Luini, A. and Polishchuk, R. S. (2003). Mechanism of constitutive export from the golgi: bulk flow via the formation, protrusion, and en bloc cleavage of large trans-golgi network tubular domains. Mol Biol Cell 14, 4470-85.

Ponnambalam, S. and Baldwin, S. A. (2003). Constitutive protein secretion from the trans-Golgi network to the plasma membrane. Mol Membr Biol 20, 129-39.

Potapova, T. A., Daum, J. R., Pittman, B. D., Hudson, J. R., Jones, T. N., Satinover, D. L., Stukenberg, P. T. and Gorbsky, G. J. (2006). The reversibility of mitotic exit in vertebrate cells. Nature 440, 954-8.

Powers, J., Bossinger, O., Rose, D., Strome, S. and Saxton, W. (1998). A nematode kinesin required for cleavage furrow advancement. Curr Biol 8, 1133-6.

Prekeris, R., Davies, J. M. and Scheller, R. H. (2001). Identification of a novel Rab11/25 binding domain present in Eferin and Rip proteins. J Biol Chem 276, 38966-70.

Prekeris, R., Klumperman, J. and Scheller, R. H. (2000). A Rab11/Rip11 protein complex regulates apical membrane trafficking via recycling endosomes. Mol Cell 6, 1437-48.

Progida, C., Malerod, L., Stuffers, S., Brech, A., Bucci, C. and Stenmark, H. (2007). RILP is required for the proper morphology and function of late endosomes. J Cell Sci 120, 3729-37.

Pyrowolakis, G. (2000). Funktion des BRUCE-Ubiquitin-Konjugationsenzyms in vitro und in vivo und Identifizierung von HUB, einem neuartigen Protein-Modifikationssystem mit Verwandtschaft zum Ubiquitin-System. In Naturwissenschaftlich-Mathematische Gesamtfakultät. Ruprecht-Karls-Universität Heidelberg.

Qiu, X. B. and Goldberg, A. L. (2002). Nrdp1/FLRF is a ubiquitin ligase promoting ubiquitination and degradation of the epidermal growth factor receptor family member, ErbB3. Proc Natl Acad Sci U S A 99, 14843-8.

Qiu, X. B., Markant, S. L., Yuan, J. and Goldberg, A. L. (2004). Nrdp1-mediated degradation of the gigantic IAP, BRUCE, is a novel pathway for triggering apoptosis. Embo J 23, 800-10.

Raich, W. B., Moran, A. N., Rothman, J. H. and Hardin, J. (1998). Cytokinesis and midzone microtubule organization in Caenorhabditis elegans require the kinesin-like protein ZEN-4. Mol Biol Cell 9, 2037-49.

Rangasamy, D., Berven, L., Ridgway, P. and Tremethick, D. J. (2003). Pericentric heterochromatin becomes enriched with H2A.Z during early mammalian development. Embo J 22, 1599-607.

Rappaport, R. (1975). Establishment and organization of the cleavage mechanism. Soc Gen Physiol Ser 30, 287-304.

Rappaport, R. (1996). Cytokinesis in Animal Cells. Cambridge,UK: Cambridge University Press.

Rappaport, R. and Rappaport, B. N. (1993). Duration of division-related events in cleaving sand dollar eggs. Dev Biol 158, 265-73.

Reed, J. C. and Bischoff, J. R. (2000). BIRinging chromosomes through cell division--and survivin' the experience. Cell 102, 545-8.

Ren, J., Shi, M., Liu, R., Yang, Q. H., Johnson, T., Skarnes, W. C. and Du, C. (2005). The Birc6 (Bruce) gene regulates p53 and the mitochondrial pathway of apoptosis and is essential for mouse embryonic development. Proc Natl Acad Sci U S A 102, 565-70.

Richly, H., Rape, M., Braun, S., Rumpf, S., Hoege, C. and Jentsch, S. (2005). A series of ubiquitin binding factors connects CDC48/p97 to substrate multiubiquitylation and proteasomal targeting. Cell 120, 73-84.

Riedl, S. J., Renatus, M., Schwarzenbacher, R., Zhou, Q., Sun, C., Fesik, S. W., Liddington, R. C. and Salvesen, G. S. (2001). Structural basis for the inhibition of caspase-3 by XIAP. Cell 104, 791-800.

Riggs, B., Fasulo, B., Royou, A., Mische, S., Cao, J., Hays, T. S. and Sullivan, W. (2007). The concentration of Nuf, a Rab11 effector, at the microtubule-organizing center is cell cycle regulated, dynein-dependent, and coincides with furrow formation. Mol Biol Cell 18, 3313-22.

Robbins, E. and Gonatas, N. K. (1964). The Ultrastructure of a Mammalian Cell During the Mitotic Cycle. J Cell Biol 21, 429-63.

Robinson, D. N. and Cooley, L. (1996). Stable intercellular bridges in development: the cytoskeleton lining the tunnel. Trends Cell Biol 6, 474-9.

Rosa, J., Canovas, P., Islam, A., Altieri, D. C. and Doxsey, S. J. (2006). Survivin modulates microtubule dynamics and nucleation throughout the cell cycle. Mol Biol Cell 17, 1483-93.

Rose, I. A. and Warms, J. V. (1983). An enzyme with ubiquitin carboxy-terminal esterase activity from reticulocytes. Biochemistry 22, 4234-7.

Row, P. E., Liu, H., Hayes, S., Welchman, R., Charalabous, P., Hofmann, K., Clague, M. J., Sanderson, C. M. and Urbe, S. (2007). The MIT Domain of UBPY Constitutes a CHMP Binding and Endosomal Localization Signal Required for Efficient Epidermal Growth Factor Receptor Degradation. J Biol Chem 282, 30929-37.

Row, P. E., Prior, I. A., McCullough, J., Clague, M. J. and Urbe, S. (2006). The ubiquitin isopeptidase UBPY regulates endosomal ubiquitin dynamics and is essential for receptor down-regulation. J Biol Chem 281, 12618-24.

Ruchaud, S., Carmena, M. and Earnshaw, W. C. (2007). Chromosomal passengers: conducting cell division. Nat Rev Mol Cell Biol 8, 798-812.

Rusten, T. E. V., T.; Lindmo, K.; Rodahl, L.M.W.; Nezis, I.P.; Sem-Jacobsen, C.; Wendler, F.; Vincent, J-P.; Brech, A.; Bilder, D.; Stenmark, H. (2007). Escrts and Fab1 regulate distinct steps of autophagy. Current Biology.

Sacks, D. B. (2006). The role of scaffold proteins in MEK/ERK signalling. Biochem Soc Trans 34, 833-6.

Salvesen, G. S. and Duckett, C. S. (2002). IAP proteins: blocking the road to death's door. Nat Rev Mol Cell Biol 3, 401-10.

Samuel, T., Okada, K., Hyer, M., Welsh, K., Zapata, J. M. and Reed, J. C. (2005). cIAP1 Localizes to the nuclear compartment and modulates the cell cycle. Cancer Res 65, 210-8.

Savoian, M. S., Khodjakov, A. and Rieder, C. L. (1999). Unilateral and wandering furrows during mitosis in vertebrates: implications for the mechanism of cytokinesis. Cell Biol Int 23, 805-12.

Schmidt, K. and Nichols, B. J. (2004). A barrier to lateral diffusion in the cleavage furrow of dividing mammalian cells. Current Biology 14, 1002-1006.

Semple, C. A. (2003). The comparative proteomics of ubiquitination in mouse. Genome Res 13, 1389-94.

Sharp, D. J., Kuriyama, R., Essner, R. and Baas, P. W. (1997). Expression of a minus-end-directed motor protein induces Sf9 cells to form axon-like processes with uniform microtubule polarity orientation. J Cell Sci 110 (Pt 19), 2373-80.

Shu, H. B., Li, Z., Palacios, M. J., Li, Q. and Joshi, H. C. (1995). A transient association of gamma-tubulin at the midbody is required for the completion of cytokinesis during the mammalian cell division. J Cell Sci 108 (Pt 9), 2955-62.

Shuster, C. B. and Burgess, D. R. (2002). Targeted new membrane addition in the cleavage furrow is a late, separate event in cytokinesis. Proc Natl Acad Sci U S A 99, 3633-8.

Sisson, J. C., Field, C., Ventura, R., Royou, A. and Sullivan, W. (2000). Lava lamp, a novel peripheral golgi protein, is required for Drosophila melanogaster cellularization. J Cell Biol 151, 905-18.

Skop, A. R., Liu, H., Yates, J., 3rd, Meyer, B. J. and Heald, R. (2004). Dissection of the mammalian midbody proteome reveals conserved cytokinesis mechanisms. Science 305, 61-6.

Soares, L., Seroogy, C., Skrenta, H., Anandasabapathy, N., Lovelace, P., Chung, C. D., Engleman, E. and Fathman, C. G. (2004). Two isoforms of otubain 1 regulate T cell anergy via GRAIL. Nat Immunol 5, 45-54.

Somma, M. P., Fasulo, B., Cenci, G., Cundari, E. and Gatti, M. (2002). Molecular dissection of cytokinesis by RNA interference in Drosophila cultured cells. Mol Biol Cell 13, 2448-60.

Song, Z., Yao, X. and Wu, M. (2003). Direct interaction between survivin and Smac/DIABLO is essential for the anti-apoptotic activity of survivin during taxol-induced apoptosis. J Biol Chem 278, 23130-40.

Sonnichsen, B., De Renzis, S., Nielsen, E., Rietdorf, J. and Zerial, M. (2000). Distinct membrane domains on endosomes in the recycling pathway visualized by multicolor imaging of Rab4, Rab5, and Rab11. J Cell Biol 149, 901-14.

Spitzer, C., Schellmann, S., Sabovljevic, A., Shahriari, M., Keshavaiah, C., Bechtold, N., Herzog, M., Muller, S., Hanisch, F. G. and Hulskamp, M. (2006). The Arabidopsis elch mutant reveals functions of an ESCRT component in cytokinesis. Development 133, 4679-89.

Strack, B., Calistri, A., Craig, S., Popova, E. and Gottlinger, H. G. (2003). AIP1/ALIX is a binding partner for HIV-1 p6 and EIAV p9 functioning in virus budding. Cell 114, 689-99.

Straight, A. F., Cheung, A., Limouze, J., Chen, I., Westwood, N. J., Sellers, J. R. and Mitchison, T. J. (2003). Dissecting temporal and spatial control of cytokinesis with a myosin II Inhibitor. Science 299, 1743-7.

Straight, A. F. and Field, C. M. (2000). Microtubules, membranes and cytokinesis. Curr Biol 10, R760-70.

Strickland, L. I. and Burgess, D. R. (2004). Pathways for membrane trafficking during cytokinesis. Trends Cell Biol 14, 115-8.

Stukenberg, P. T. (2004). Triggering p53 after cytokinesis failure. J Cell Biol 165, 607-8.

Suizu, F., Fukuta, Y., Ueda, K., Iwasaki, T., Tokumitsu, H. and Hosoya, H. (2002). Characterization of Ca2+/calmodulin-dependent protein kinase I as a myosin II regulatory light chain kinase in vitro and in vivo. Biochem J 367, 335-45.

Sumara, I., Quadroni, M., Frei, C., Olma, M. H., Sumara, G., Ricci, R. and Peter, M. (2007). A Cul3-based E3 ligase removes Aurora B from mitotic chromosomes, regulating mitotic progression and completion of cytokinesis in human cells. Dev Cell 12, 887-900.

Tagwerker, C., Flick, K., Cui, M., Guerrero, C., Dou, Y., Auer, B., Baldi, P., Huang, L. and Kaiser, P. (2006). A tandem affinity tag for two-step purification under fully denaturing conditions: application in ubiquitin profiling and protein complex identification combined with in vivocross-linking. Mol Cell Proteomics 5, 737-48.

Teis, D., Taub, N., Kurzbauer, R., Hilber, D., de Araujo, M. E., Erlacher, M., Offterdinger, M., Villunger, A., Geley, S., Bohn, G. et al. (2006). p14-MP1-MEK1 signaling regulates endosomal traffic and cellular proliferation during tissue homeostasis. J Cell Biol 175, 861-8.

TerBush, D. R., Maurice, T., Roth, D. and Novick, P. (1996). The Exocyst is a multiprotein complex required for exocytosis in Saccharomyces cerevisiae. Embo J 15, 6483-94.

Thrower, J. S., Hoffman, L., Rechsteiner, M. and Pickart, C. M. (2000). Recognition of the polyubiquitin proteolytic signal. Embo J 19, 94-102.

Treier, M., Staszewski, L. M. and Bohmann, D. (1994). Ubiquitin-dependent c-Jun degradation in vivo is mediated by the delta domain. Cell 78, 787-98.

Tsvetkov, L., Xu, X., Li, J. and Stern, D. F. (2003). Polo-like kinase 1 and Chk2 interact and co-localize to centrosomes and the midbody. J Biol Chem 278, 8468-75.

Uetake, Y. and Sluder, G. (2004). Cell cycle progression after cleavage failure: mammalian somatic cells do not possess a "tetraploidy checkpoint". J Cell Biol 165, 609-15.

Urbe, S., Huber, L. A., Zerial, M., Tooze, S. A. and Parton, R. G. (1993). Rab11, a small GTPase associated with both constitutive and regulated secretory pathways in PC12 cells. FEBS Lett 334, 175-82.

Uren, A. G., Beilharz, T., O'Connell, M. J., Bugg, S. J., van Driel, R., Vaux, D. L. and Lithgow, T. (1999). Role for yeast inhibitor of apoptosis (IAP)-like proteins in cell division. Proc Natl Acad Sci U S A 96, 10170-5.

Uyeda, T. Q. and Nagasaki, A. (2004). Variations on a theme: the many modes of cytokinesis. Curr Opin Cell Biol 16, 55-60.

Vega, I. E. and Hsu, S. C. (2001). The exocyst complex associates with microtubules to mediate vesicle targeting and neurite outgrowth. J Neurosci 21, 3839-48.

Verhagen, A. M., Coulson, E. J. and Vaux, D. L. (2001). Inhibitor of apoptosis proteins and their relatives: IAPs and other BIRPs. Genome Biol 2, REVIEWS3009.

Vernooy, S. Y., Chow, V., Su, J., Verbrugghe, K., Yang, J., Cole, S., Olson, M. R. and Hay, B. A. (2002). Drosophila Bruce can potently suppress Rpr- and Grim-dependent but not Hid-dependent cell death. Curr Biol 12, 1164-8.

Visintin, R., Stegmeier, F. and Amon, A. (2003). The role of the polo kinase Cdc5 in controlling Cdc14 localization. Mol Biol Cell 14, 4486-98.

Vogel, C., Hager, C. and Bastians, H. (2007). Mechanisms of mitotic cell death induced by chemotherapy-mediated G2 checkpoint abrogation. Cancer Res 67, 339-45.

Vong, Q. P., Cao, K., Li, H. Y., Iglesias, P. A. and Zheng, Y. (2005). Chromosome alignment and segregation regulated by ubiquitination of survivin. Science 310, 1499-504.

Wang, T. and Hong, W. (2006). RILP interacts with VPS22 and VPS36 of ESCRT-II and regulates their membrane recruitment. Biochem Biophys Res Commun 350, 413-23.

Warburton, H. E., Brady, M., Vlatkovic, N., Linehan, W. M., Parsons, K. and Boyd, M. T. (2005). p53 regulation and function in renal cell carcinoma. Cancer Res 65, 6498-503.

Werner, M., Munro, E. and Glotzer, M. (2007). Astral signals spatially bias cortical myosin recruitment to break symmetry and promote cytokinesis. Curr Biol 17, 1286-97.

Wheatley, S. P., Hinchcliffe, E. H., Glotzer, M., Hyman, A. A., Sluder, G. and Wang, Y. (1997). CDK1 inactivation regulates anaphase spindle dynamics and cytokinesis in vivo. J Cell Biol 138, 385-93.

Williams, R. L. and Urbe, S. (2007). The emerging shape of the ESCRT machinery. Nat Rev Mol Cell Biol 8, 355-68.

Wilson, G. M., Fielding, A. B., Simon, G. C., Yu, X., Andrews, P. D., Hames, R. S., Frey, A. M., Peden, A. A., Gould, G. W. and Prekeris, R. (2005). The FIP3-Rab11 protein complex regulates recycling endosome targeting to the cleavage furrow during late cytokinesis. Mol Biol Cell 16, 849-60.

Wojcik, C., Paweletz, N. and Schroeter, D. (1995). Localization of proteasomal antigens during different phases of the cell cycle in HeLa cells. Eur J Cell Biol 68, 191-8.

Wong, C. and Stearns, T. (2005). Mammalian cells lack checkpoints for tetraploidy, aberrant centrosome number, and cytokinesis failure. BMC Cell Biol 6, 6.

Wu, X., Yen, L., Irwin, L., Sweeney, C. and Carraway, K. L., 3rd. (2004). Stabilization of the E3 ubiquitin ligase Nrdp1 by the deubiquitinating enzyme USP8. Mol Cell Biol 24, 7748-57.

Xu, P. and Peng, J. (2006). Dissecting the ubiquitin pathway by mass spectrometry. Biochim Biophys Acta 1764, 1940-7.

Yamamoto, Y., Nishimura, N., Morimoto, S., Kitamura, H., Manabe, S., Kanayama, H. O., Kagawa, S. and Sasaki, T. (2003). Distinct roles of Rab3B and Rab13 in the polarized transport of apical, basolateral, and tight junctional membrane proteins to the plasma membrane. Biochem Biophys Res Commun 308, 270-5.

Yamashiro, S., Totsukawa, G., Yamakita, Y., Sasaki, Y., Madaule, P., Ishizaki, T., Narumiya, S. and Matsumura, F. (2003). Citron kinase, a Rho-dependent kinase, induces di-phosphorylation of regulatory light chain of myosin II. Mol Biol Cell 14, 1745-56.

Yoshida, S., Kono, K., Lowery, D. M., Bartolini, S., Yaffe, M. B., Ohya, Y. and Pellman, D. (2006). Polo-like kinase Cdc5 controls the local activation of Rho1 to promote cytokinesis. Science 313, 108-11.

Yu, X., Prekeris, R. and Gould, G. W. (2007). Role of endosomal Rab GTPases in cytokinesis. Eur J Cell Biol 86, 25-35.

Yuce, O., Piekny, A. and Glotzer, M. (2005). An ECT2-centralspindlin complex regulates the localization and function of RhoA. J Cell Biol 170, 571-82.

Zeitlin, S. G., Shelby, R. D. and Sullivan, K. F. (2001). CENP-A is phosphorylated by Aurora B kinase and plays an unexpected role in completion of cytokinesis. J Cell Biol 155, 1147-57.

Zerial, M. and McBride, H. (2001). Rab proteins as membrane organizers. Nat Rev Mol Cell Biol 2, 107-17.

Zhao, J., Tenev, T., Martins, L. M., Downward, J. and Lemoine, N. R. (2000). The ubiquitin-proteasome pathway regulates survivin degradation in a cell cycle-dependent manner. J Cell Sci 113 Pt 23, 4363-71.

Zhao, W. M. and Fang, G. (2005). Anillin is a substrate of anaphase-promoting complex/cyclosome (APC/C) that controls spatial contractility of myosin during late cytokinesis. J Biol Chem 280, 33516-24.

Zhao, W. M., Seki, A. and Fang, G. (2006). Cep55, a microtubule-bundling protein, associates with centralspindlin to control the midbody integrity and cell abscission during cytokinesis. Mol Biol Cell 17, 3881-96.

Zhu, C. and Jiang, W. (2005). Cell cycle-dependent translocation of PRC1 on the spindle by Kif4 is essential for midzone formation and cytokinesis. Proc Natl Acad Sci U S A 102, 343-8.

Zhu, C., Zhao, J., Bibikova, M., Leverson, J. D., Bossy-Wetzel, E., Fan, J. B., Abraham, R. T. and Jiang, W. (2005). Functional analysis of human microtubule-based motor proteins, the kinesins and dyneins, in mitosis/cytokinesis using RNA interference. Mol Biol Cell 16, 3187-99.

8 Abbreviations

AMCA	aminomethylcoumarin
APC/C	anaphase promoting complex/cyclosome
APS	ammonium peroxodisulphate
Arl	Arf-like
Arf	ADP-ribosylation factor
ATP	adenosine triphosphate
BES	N,N-Bis(2-hydroxyethyl)-2-aminoethansulfonate
BFA	Brefeldin A
BIR	baculovirus inhibitor of apoptosis repeat
BIRP	BIR domain-containing protein
BRUCE	BIR repeat-containing ubiquitin-conjugating enzyme
BSA	bovine serum albumin
BTB	Bric-a-brac/Tramtrack/Broad complex
Bub	budding uninhibited by benzimidazoles
C-	carboxy-
CD	cluster of differentiation
Cdc	cell division cycle
Cdh1	Cdc20 homolog 1
Cdk	cell cycle dependent kinase
cDNA	complementary DNA
CENP	centromere protein
Cep	centrosomal protein
CPC	chromosomal passenger complex
cIAP1	cellular inhibitor of apoptosis protein 1 (MIHB, HIAP-1)
cIAP2	cellular inhibitor of apoptosis protein 2 (MIHC, HIAP-2)
Cul	cullin
Cy3	carbocyanin 3
d	day
DAPI	4',6-diamidino-2-phenylindole
DIABLO	direct IAP-binding protein with low pI (Smac)
DIC	differential interference contrast
DMEM	Dulbecco/Vogt modified Eagle's minimal essential medium
DMSO	dimethylsulfoxide
DNA	deoxyribonucleic acid
DNase	deoxyribonuclease
dNTPs	desoxyribonucleotides
DTT	dithiothreitol
ECL	enhanced chemiluminescence
ECT2	epithelial cell transforming sequence 2 oncogene
EDTA	ethylendiamintetraacetat
EGFP-F	enhanced GFP (farnesylated)
Emi	early mitotic inhibitor
ER	endoplasmic reticulum
ErbB	erythroblastic leukemia viral oncogene homolog B
Erk	extracellular signal-regulated kinase
ESCRT	endosomal sorting complex required for transport
FACS	fluorescence activated cell sorter
FCS	fetal calf serum
FEAR	Cdc14 early anaphase release
FIP	Rab11 family interacting protein

FITC	fluorescein isothiocyanate
FLRF	fetal liver RING-finger
FPLC	fast protein liquid chromatography
FRAP	fluorescence recovery after photobleaching
GAP	GTPase activating protein
GDI	GDP dissociation inhibitor
GDP	guanosine diphosphate
GEF	guanine nucleotide exchange factor
GFP	green fluorescent protein
GLUE	gram-like ubiquitin binding in EAP45
GST	glutathion S-transferase
GTP	guanosine triphosphate
h	hour
H	histone
HA	hemagglutinin
HBS	HEPES buffered saline
HECT	homologous to E6-AP carboxy terminus
HEPES	N-(2-hydroxyethyl)-piperazin-N'-(2-ethansulfonate)
HPV	human papilloma virus
Hid	head involution defective
Hrs	hepatocyte growth factor-regulated tyrosine kinase substrate
HtrA2	high-temperature requirement (Omi)
IAP	inhibitor of apoptosis protein
IBM	IAP binding motif
IgG	immunoglobulin G
IκB	inhibitor of nuclear factor κB
INCENP	inner centromere protein
IP	immunoprecipitation
IPTG	isopropyl-ß-D-thiogalactopyranoside
kb	kilobases
kDa	kilo Dalton
KIF	kinesin superfamily protein
LATS	large tumor suppressor
M	molar
mAb	monoclonal antibody
Mad	mitotic arrest deficient
MAP	microtubule-associated protein
MAPK	mitogen activated protein kinase
MCAK	mitotic centromere-associated kinesin
MEF	mouse embryonic fibroblast
Mek	mitogen activated protein kinase/ERK kinase
MEN	mitotic exit network
min	minute
MKLP	mitotic kinesin like protein
MOPS	3-(N-morpholino)-propane sulfonate
mRNA	messenger RNA
MT	microtubule
MVB	multivesicular body
N-	amino-
NAIP	neuronal apoptosis inhibitory protein
NFκB	nuclear factor κB
NGF	neuronal growth factor

Ni-NTA	nickel-nitrilo triacetate
NLS	nuclear localization sequence
NP-40	Nonidet P-40
Nrdp1	neuregulin receptor degradation protein 1
Nuf	nuclear fallout
OD	optical density
OTU	ovarian tumor
pAb	polyclonal antibody
PBS	phospate buffered saline
PCR	polymerase chain reaction
PEG	polyethylene glycol
PIP	phosphatidyl inositol phosphate
PIPES	piperazin-N,N'-bis(2-ethansulfonsäure)
Plk	Polo-like kinase
PMSF	phenylmethylsulphonylfluoride
PRC1	protein required for cytokinesis 1
Rab	Ras-related protein
RING	really interesting new gene
RNA	ribonucleic acid
RNase	ribonuclease
RNAi	RNA-Interference
ROCK	Rho-associated protein kinase
rpm	revolutions per minute
RT	room temperature, reverse transcriptase
S	sedimentation coefficient (Svedberg)
s	second
SCF	Skp1-Cullin-F-box complex
shRNA	short hairpin RNA
SDS	sodium dodecylsulphate
SDS-PAGE	SDS-Polyacrylamid-Gelelektrophorese
SIN	septation initiation network
siRNA	small interfering RNA
Smac	second mitochondria-derived activator of caspases (DIABLO)
SNARE	soluble N-ethyl maleimide sensitive factor attachment receptor
SPB	spindle pole body
STAM	signal transducing adaptor molecule
SV40	simian virus 40
TBS	Tris-buffered saline
TBST	Tris-buffered saline
TCA	trichloroactetic acid
TE	Tris-EDTA buffer
TEMED	N,N,N',N'-Tetramethyl ethylene diamine
TGN	*trans* Golgi network
TNF	tumor necrosis factor
ßTrCP	beta-transducin repeat containing
Tris	Tris-(hydroxymethyl)-aminomethan
TRITC	tetramethylrhodamine isothiocyanate
Tsg	tumor susceptibility gene
U	units
Ub	ubiquitin
UBC	ubiquitin-conjugating enzyme
UBP/USP	ubiquitin specific protease

UCH	ubiquitin C-terminal hydrolase
UEV	ubiquitin-E2 variant
UIM	ubiquitin interacting motif
UPS	ubiquitin-proteasome system
VAMP	vesicle-associated membrane protein
Vps	vacuolar protein sorting
VSVG	vesicular stomatitis virus glycoprotein
WB	Western blot/Immunoblot
WT	wild type
XIAP	X-linked inhibitor of apoptosis protein (MIHA, hILP)

9 Acknowledgements

I would like to sincerely thank my research advisor, Stefan Jentsch, for his continuous support and his trust in my work. I have been fortunate to have an advisor who gave me the freedom to explore on my own, and at the same time patiently allowed me to build on new experiments when my previous steps faltered. Stefan's insightful comments were thought-provoking and helped me focus my ideas. His openness and kindness create a great working atmosphere that will be hard to find elsewhere.

I gratefully acknowledge all the members of my committee who have given their time to read this manuscript and I thank them for their readiness to participate in the viva voce.

I owe much thanks and sincere gratitude to all members of the lab for their insightful comments, help and for making the lab a pleasant place. My heartfelt thanks to Tim, Kenji and Dirk for their good moods and for spending a cheerful time in and outside the lab together. I greatly value Shravan for his level-headed nature and for being a circumspect lab colleague. Tim and Shravan, I wish much luck and success with their rebellious Hub1. Special thanks must also be given to Ulla and 'Kempe' for their care about a plethora of things.

I am especially indebted to my former lab colleague Till who continually offered me his support and practical advice already during my Diploma project and also in the first months of my thesis work. Till was an ideal mentor who was always motivated by his technical perfection paired with the most respectable perseverance.

Moreover, I would like to thank Anca, Olaf, Shravan and Tim for ciritically reading drafts of the manuscript.

I also wish to express my thanks to my brother for his interest in and his different and pragmatic view on my work.

My parents have helped me keep my live in proper perspective and balance through these difficult years. Their tramendous support and care helped me overcome setbacks and appreciate the world outside the Petri dish. My profuse gratitude goes to their compassionate care and love and I deeply appreciate their perpetual belief in me.

Finally, I am immensely thankful to Sibylle because only together with her live with all its obstacles makes sense.

10 Curriculum vitae

Adresse	Christian Pohl Schleissheimer Strasse 271 80809 München
Geburtsdatum	5. August 1976
Geburtsort	Heidenheim an der Brenz
Nationalität	Deutsch

2003 - 2008	Doktorarbeit am Max-Planck-Institut für Biochemie, Martinsried unter Anleitung von Prof. Stefan Jentsch Titel der Arbeit: “Coordination of late stages of cytokinesis by the inhibitor of apoptosis protein BRUCE”.
Februar 2003	Diplom Biochemiker (Universität Tübingen)
2002 - 2003	Diplomarbeit unter Anleitung von Prof. Wolfgang Voelter, Eberhard-Karls Universität Tübingen Titel der Arbeit: “Charakterisierung der proteolytischen Prozessierung des IAP-verwandten Proteins BRUCE durch Caspasen”. (In Kooperation mit Prof. Stefan Jentsch, Max-Planck-Institut für Biochemie).
2001 - 2002	Austauschstudent an der Ludwig-Maximilians Universität München.
1998 - 2003	Student der Biochemie, Eberhard-Karls Universität Tübingen
1997-1998	Wehrdienst beim Heeresmusikkorps 10, Ulm
Juni 1996	Abitur
1993-1996	Hellenstein-Gymnasium, Heidenheim
1987-1993	Progymnasium, Herberchtingen
1983-1987	Wartbergschule, Herbrechtingen

Cell

Final Stages of Cytokinesis and Midbody Ring Formation Are Controlled by BRUCE

Christian Pohl[1] and Stefan Jentsch[1,*]
[1]Department of Molecular Cell Biology, Max Planck Institute of Biochemistry, Am Klopferspitz 18, 82152 Martinsried, Germany
*Correspondence: jentsch@biochem.mpg.de
DOI 10.1016/j.cell.2008.01.012

SUMMARY

Cytokinesis involves the formation of a cleavage furrow, followed by abscission, the cutting of the midbody channel, the final bridge between dividing cells. Recently, the midbody ring became known as central for abscission, but its regulation remains enigmatic. Here, we identify BRUCE, a 528 kDa multifunctional protein, which processes ubiquitin-conjugating activity, as a major regulator of abscission. During cytokinesis, BRUCE moves from the vesicular system to the midbody ring and serves as a platform for the membrane delivery machinery and mitotic regulators. Depletion of BRUCE in cell cultures causes defective abscission and cytokinesis-associated apoptosis, accompanied by a block of vesicular targeting and defective formation of the midbody and the midbody ring. Notably, ubiquitin relocalizes from midbody microtubules to the midbody ring during cytokinesis, and depletion of BRUCE disrupts this process. We propose that BRUCE coordinates multiple steps required for abscission and that ubiquitylation may be a crucial trigger.

INTRODUCTION

Cytokinesis is the concluding step of cell division by which the prospective daughter cells separate their cytoplasmic volumes. This process starts by contraction of a plasma-membrane-anchored actomyosin ring, leading to the formation of a cleavage furrow (Eggert et al., 2006). By the end of furrowing, the dividing cells are connected by a narrow, tubular intercellular bridge, which contains the midbody consisting of tightly bundled antiparallel microtubules, which embrace a phase-dense circular structure called midbody ring (or occasionally Flemming body). At the final stage of cytokinesis, in a process termed abscission, this bridge is cleaved, and two daughter cells are formed.

At the midbody, several cytokinesis-coupled events converge, including degradation of cell cycle regulators, cytoskeleton rearrangements, membrane traffic, and plasma membrane remodeling. Recent reports demonstrate a direct involvement of the traffic-regulating GTPases Arf1, Arf6 and Rab11 in cytokinesis (Albertson et al., 2005). Arf6 and Rab11 are coupled to the exocyst complex, which seems crucial for the proper targeting of vesicles to the site of abscission. Interestingly, some types of vesicles seem to arrive at the midbody ring chiefly from only one of the prospective daughter cells (Gromley et al., 2005), suggesting an intrinsic asymmetric element in cytokinesis. The factors that control targeting to the midbody and guide midbody ring assembly are largely unknown, but one protein required for exocyst targeting to the midbody ring was recently identified as centriolin, which also binds to the maternal centriole (Gromley et al., 2003, 2005).

Previous studies revealed an emerging role of ubiquitylation and proteasomal activity in regulating cytokinesis (Pines and Lindon, 2005). Notably, ubiquitin-activating enzyme E1 and the proteasome are concentrated on midbodies (Grenfell et al., 1994; Wojcik et al., 1995), and both proteolytic and non-proteolytic functions of ubiquitin seem to play a role. Chromosomal passenger proteins, the kinase Aurora B and the baculovirus inhibitor of apoptosis repeat (BIR)-containing protein survivin, as well as the Polo-like kinase Plk1 (Lindon and Pines, 2004) are degraded just before or during cytokinesis (Lindon and Pines, 2004; Sumara et al., 2007). Proteasome inhibition after anaphase onset results in incomplete cytokinesis (Straight et al., 2003), and, interestingly, combined inhibition of Cdk1 and proteasomes can revert late cytokinesis to an apparent preanaphase state (Potapova et al., 2006). A non-proteolytic role of ubiquitin in cytokinesis is suggested by the fact that the ubiquitin-controlled endosomal sorting complex required for transport (ESCRT) is necessary for abscission (Carlton and Martin-Serrano, 2007).

Proteins harboring a BIR domain (BIRPs) are primarily known for their function to protect cells against apoptosis by their activity to inhibit caspases and proapoptotic factors through binding and ubiquitin-dependent degradation (Verhagen et al., 2001). However, BIRPs like survivin and cIAP1 are also crucial for cell cycle events and cytokinesis (Li et al., 1999; Samuel et al., 2005). Here, we report that another conserved BIRP, the 528 kDa protein BRUCE (also known as Apollon or BIRC6), is a crucial regulator for the final stages of cytokinesis. BRUCE is a multifunctional protein owing to the presence of different functional domains and multiple binding partners (Bartke et al., 2004; Hauser et al., 1998). Close to its amino (N)-terminus, BRUCE harbors a single BIR domain, which most closely resembles the BIR of survivin. BRUCE can inhibit caspases through this domain,

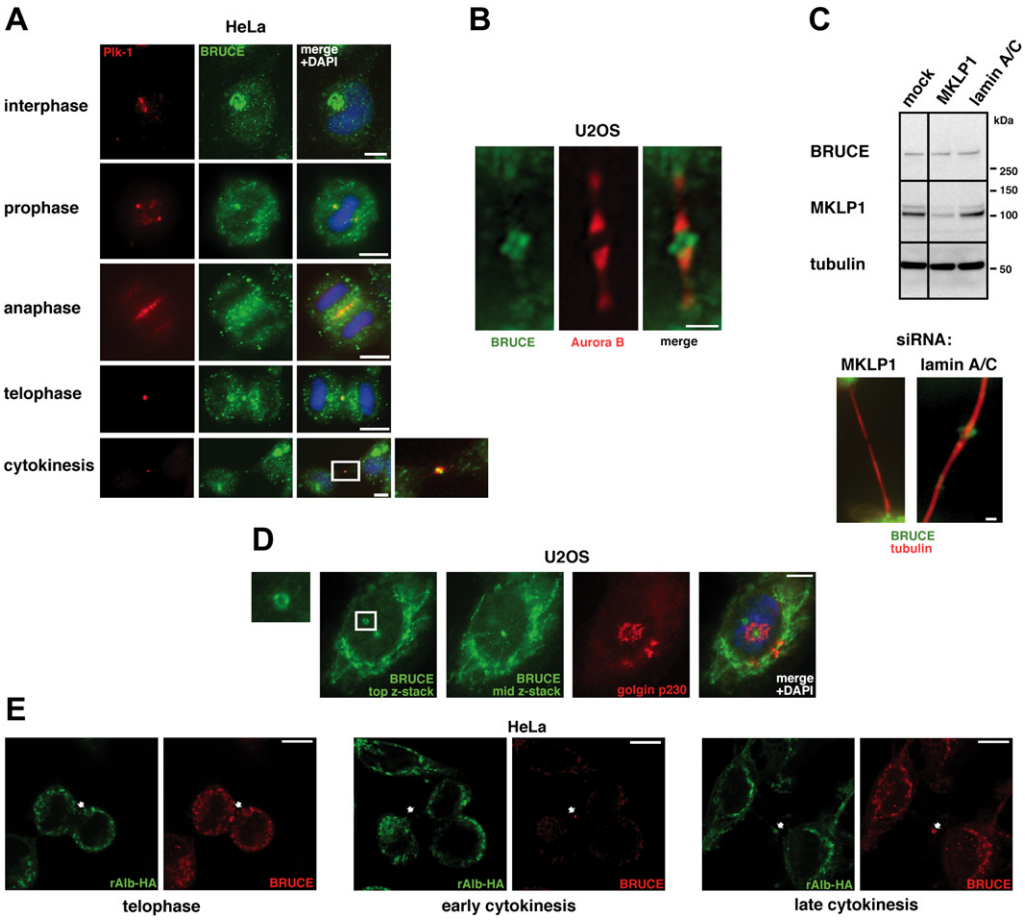

Figure 1. BRUCE Shows a Cell Cycle-Dependent Localization

(A) BRUCE localizes to mitotic structures. Immunofluorescence (IF) of HeLa cells stained with anti-Plk-1 (red) and anti-BRUCE (green) and DAPI to visualize DNA. The box outlined in yellow shows the enlarged midbody region of the cytokinesis merge. The scale bar represents 10 μm.

(B) BRUCE localizes to the midbody ring of U2OS cells. The midbody region is shown with anti-Aurora B (red) and anti-BRUCE (green) staining. The scale bar represents 1 μm.

(C) Localization of BRUCE to the midbody ring depends on MKLP1. Top: lysates from siRNA-transfected HeLa cells were analyzed by BRUCE, MKLP1, and α-tubulin immunoblotting. Bottom: midbodies of siRNA-treated cells are shown stained with anti-α-tubulin (red) and anti-BRUCE (green). The scale bar represents 1 μm.

(D) BRUCE is found on midbody ring remnants. U2OS cells were stained with anti-BRUCE (green) and anti-golgin p230 (red), and DAPI (blue). The scale bar represents 10 μm. The top z-stack on the left shows a midbody ring remnant in the plane of the plasma membrane (shown enlarged on the left).

(E) Relationship between BRUCE and constitutive secretory cargo. HeLa cells stably expressing HA-albumin are shown in different cell cycle stages with anti-HA (green) and anti-BRUCE (red) staining. The scale bar represents 10 μm. The arrow shows the position of the midbody ring.

and has antiapoptotic potential (Bartke et al., 2004). However, its antiapoptotic function may be particularly relevant for the trans-Golgi network (TGN) and vesicular structures where it mainly localizes (Hauser et al., 1998). Near its carboxy (C)-terminal end, BRUCE carries a ubiquitin-conjugating (UBC) domain, which endows the protein with a hybrid E2/E3 ubiquitin ligase activity (Bartke et al., 2004; Hauser et al., 1998). In vitro, BRUCE primarily mono- or oligo-ubiquitylates proteins, suggesting that its main role is non-proteolytic (Bartke et al., 2004). BRUCE-knockout mice usually die perinatally due to impaired placental development that can be attributed to insufficient differentiation (Lotz et al., 2004), and depletion of BRUCE in cultured cells sensitizes against apoptotic stimuli and finally leads to cell death (Hao et al., 2004; Ren et al., 2005).

In this report we show that BRUCE is an important novel player of cytokinesis and important for abscission. We demonstrate that BRUCE localizes to the midbody ring during cytokinesis, where it binds mitotic regulators and components of the vesicle targeting machinery. Microscopic studies and live-cell imaging with wild-type and BRUCE-depleted cells, and of cells that express a dominant-negative version, revealed that BRUCE is involved in the correct delivery of membrane vesicles to the site of abscission and for the integrity of the midbody, in particular the midbody ring. We further discovered a remarkable dynamic relocalization of ubiquitin from the midbody to the midbody ring, show that both BRUCE and MKLP1 are ubiquitylated and that UBPY serves as their deubiquitylating enzyme. Our work suggests that this giant protein, through its multiple activities,

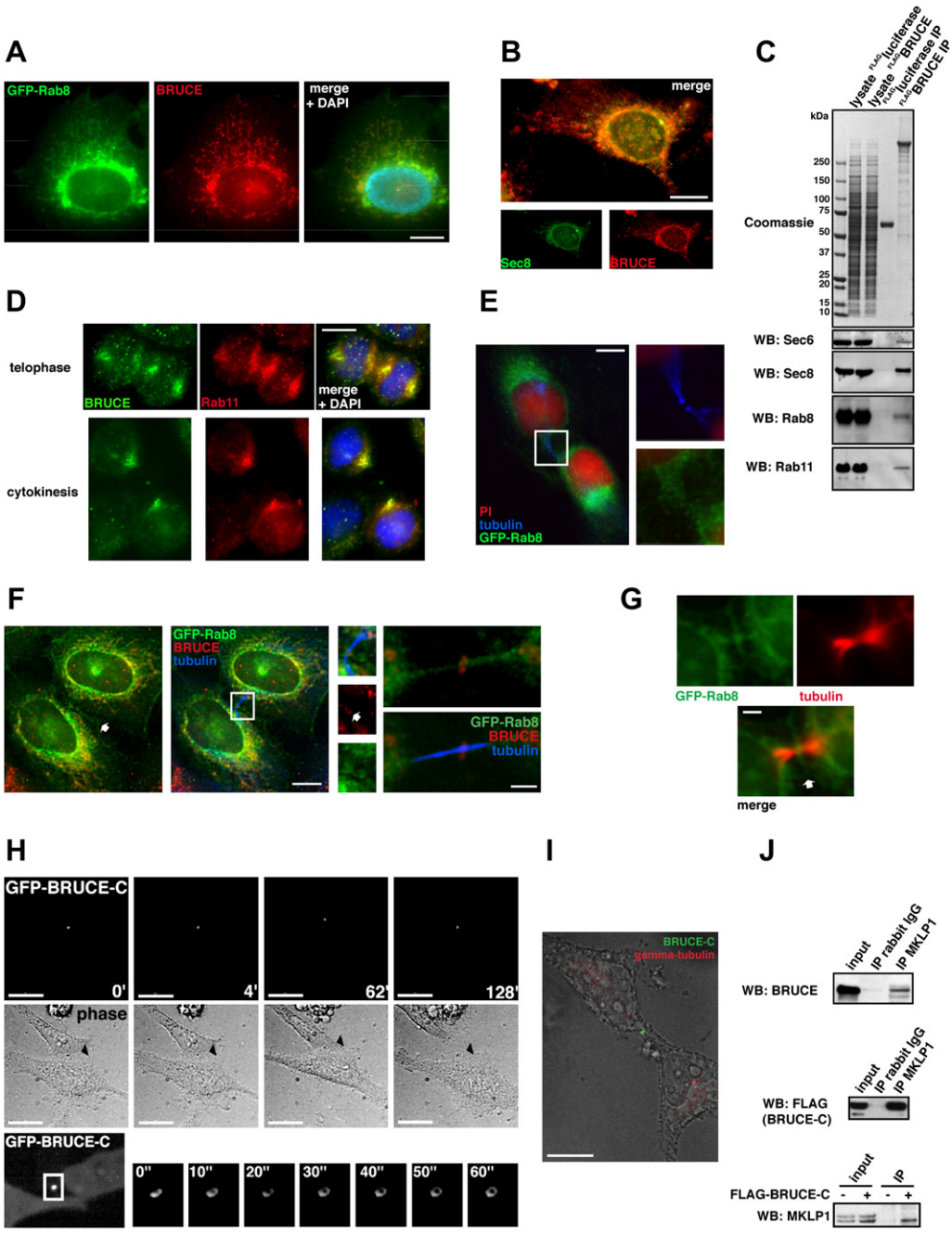

Figure 2. BRUCE Is a Component of Tubular Endosomes, Interacts with Membrane Targeting Factors, and Contains a Midbody Ring-Targeting Domain

(A) BRUCE localizes to Rab8 tubular endosomes in interphase cells. U2OS cells stably expressing GFP-Rab8 (green) were fixed and stained with anti-BRUCE (red) and DAPI (blue). The scale bar represents 10 μm.

(B) BRUCE colocalizes with the exocyst component Sec8 in a perinuclear compartment. Fixed U2OS cells; anti-BRUCE (red), anti-Sec8 (green). The scale bar represents 15 μm.

(C) BRUCE copurifies with exocyst components Sec6, Sec8, and endosomal GTPases Rab8, Rab11. HEK293T cells were transfected with either FLAG-epitope tagged luciferase or BRUCE. Cells were lysed and FLAG-fusion proteins purified. Bound material was eluted with FLAG peptide and analyzed by western blots (WB).

(D) Colocalization of BRUCE with Rab11 recycling endosomes in cytokinesis. Fixed HeLa cells; anti-Rab11 (red), anti-BRUCE (green), and DAPI (blue). The scale bar represents 15 μm.

(E) Rab8 tubular endosomes are found in the midbody region. Fixed U2OS cells; anti-tubulin (blue), and propidium iodide DNA staining (red). The scale bar represents 10 μm.

crucially coordinates several events that conclude cytokinesis, and additionally uncovers a previously unrecognized role of ubiquitin in this process.

RESULTS

BRUCE Localizes to the Midbody Ring and Associates with Mitotic Regulators

BRUCE is a cytosolic protein, which is peripherally associated with endomembranes (Hauser et al., 1998). By using three different polyclonal antibodies directed against N- or C-terminal regions of BRUCE (Bartke et al., 2004; Hauser et al., 1998) (Figure S1 available online) we found in both HeLa and U2OS cells that BRUCE relocalizes considerably during the cell cycle. It concentrates in a pericentriolar compartment in interphase, moves partially to spindle poles in metaphase, and finally localizes to the spindle midzone and the midbody in telophase and during cytokinesis (Figure 1A and Figure S2). On the midbody, BRUCE localizes in a characteristic ring-like arrangement that is embraced by Aurora B and microtubules (Figures 1B and 1C), indicating that BRUCE is associated with the midbody ring (Gromley et al., 2005). By using siRNAs targeting MKLP1, a mitotic kinesin essential for the formation of the midbody matrix (Matuliene and Kuriyama, 2002), we observed in midbody forming cells a complete loss of BRUCE at the midbody (Figure 1C). In untreated cells, BRUCE localized to the midbody ring as soon as this structure first appeared in telophase, and BRUCE persisted on the ring even after its uptake by one of the daughter cells after completion of abscission (Figures 1D and 1E). To investigate membrane traffic and to trace vesicles containing constitutively secreted cargo, we constructed a HeLa cell line expressing HA-epitope tagged albumin. Localization of secretory vesicles on the midbody ring was visible only in late cytokinesis when the intercellular bridge had constricted to about 1μm in diameter, whereas BRUCE, as an apparent firm resident of the midbody ring, localized to the midbody ring much earlier, concurrently when it had been formed (Figure 1E).

Given its highly dynamic localization pattern during cell division, we searched for binding partners and asked whether BRUCE might be a target for mitotic phosphorylation. Indeed, we found that BRUCE was particularly phosphorylated in S-phase extracts (data not shown) and that immunopurified BRUCE was also phosphorylated by copurified factors (Figure S3A). By immunopurification (IP) of FLAG-tagged BRUCE, or immunoprecipitation of endogenous BRUCE, we found BRUCE associated with the mitotic kinases Cdk1, MEK1, and Plk-1 (Figures S3B–S3G) and also α-tubulin (data not shown). Moreover, overexpressed BRUCE could immunoprecipitate endogenous survivin, and vice versa, indicating that these two BIRPs may cooperate at the midzone or the midbody, where both proteins were found (Figures S3H and S3I).

BRUCE Is a Component of Tubular and Recycling Endosomes and Associates with the Exocyst

To characterize BRUCE localization further, we assayed for colocalization with markers of the vesicular system. We found only partial colocalization with the TGN markers golgin p230 and TGN38 (Figure S2B and Hauser et al., 1998). However, we observed substantial colocalization with GFP-tagged versions of the endosomal GTPases Rab8 and Rab11, even with Rab8-positive, peripheral tubular endosomes (Figure 2A and Figure S4A) and with the exocyst subunit Sec8 (Figure 2B). Importantly, Rab8 and Rab11, as well as the exocyst subunits Sec6 and Sec8, physically associate with BRUCE, as demonstrated by immunoprecipitations (Figure 2C and Figures S4B and S4C). Similar to the mitotic kinases (Figure S3B), the binding site for the exocyst seems to lie within the N-terminal region of BRUCE (Figure S4D) and thus involves a different region in BRUCE than for midbody ring interaction (see below). Notably, similar to exocyst subunit Exo70 (Vega and Hsu, 2001), BRUCE also relocalizes to growth cones in neuronally differentiated cells (Figure S4E), strongly indicating that BRUCE is firmly connected to the exocyst and plays a more general role in targeted membrane delivery.

Rab11 and Rab8-Endosomes Are Sources of Membrane Material in Cytokinesis and the Midbody Ring Acts as a Barrier

Next, we asked whether vesicles containing BRUCE participate in cytokinesis. We could confirm previous observations (Fielding et al., 2005) that suggested a role for recycling Rab11-endosomes in cytokinesis. Two pools of Rab11-endosomes were found on both sides of the intercellular bridge during cytokinesis, and a small fraction also seemed to reach the midbody ring (Figure 2D). However, in contrast to a recent report on HeLa cells (Yu et al., 2007), we found in engineered U2OS cells also GFP-Rab8 staining at the midbody (Figures 2E and 2F) and also at the newly formed plasma membrane at the contact site of dividing cells (Figure 2G). Indeed, live-cell imaging suggests that Rab8-endosomes are delivered to the midbody ring and that this supplied material then diffuses at the plasma membrane laterally (data not shown). Remarkably, by using photobleaching experiments, we found that Rab8-endosomes are unable to move freely from one perspective daughter cell to the

(F and G) Rab8 is found at the midbody ring and at the newly formed plasma membrane between dividing cells. Fixed U2OS cells; arrowheads indicate the site of the newly formed plasma membrane. The scale bars represent, respectively, (F) 10 μm and (G) 2 μm. The smaller figures are enlargements of the framed areas. The position of the midbody ring is indicated by an arrow.

(H) The C terminus of BRUCE represents a midbody ring-targeting domain. GFP fused to the C terminus of BRUCE (amino acids 4711–4845, GFP-BRUCE-C) is localized to the midbody ring. The movie stills (of Movie S5) show GFP-BRUCE-C on the midbody ring of HeLa cells. The scale bar represents 15 μm.

(I) Localization of BRUCE-C relative to centrosomes. HeLa cells transfected with GFP-BRUCE-C (green) were stained with anti-γ-tubulin (red). The image shows a merge with the bright-field channel. The scale bar represents 15 μm.

(J) The midbody ring-targeting domain of BRUCE interacts with MKLP1. Top: lysates of HEK293T cells were immunoprecipitated (IP) with either rabbit IgGs or anti-MKLP1 antibodies and analyzed by anti-BRUCE WB. Middle: HEK293T cells transfected with GFP-FLAG-BRUCE-C were lysed and proteins immunoprecipitated with rabbit IgG (control) or anti-MKLP1 IgGs. Input and precipitates (IP) were analyzed by anti-FLAG blots (WB) detecting BRUCE-C. Bottom: HEK293T cells were either transfected with empty vector or GFP-FLAG-BRUCE-C. Lysates were subjected to anti-FLAG IP and analyzed by anti-MKLP1 WB.

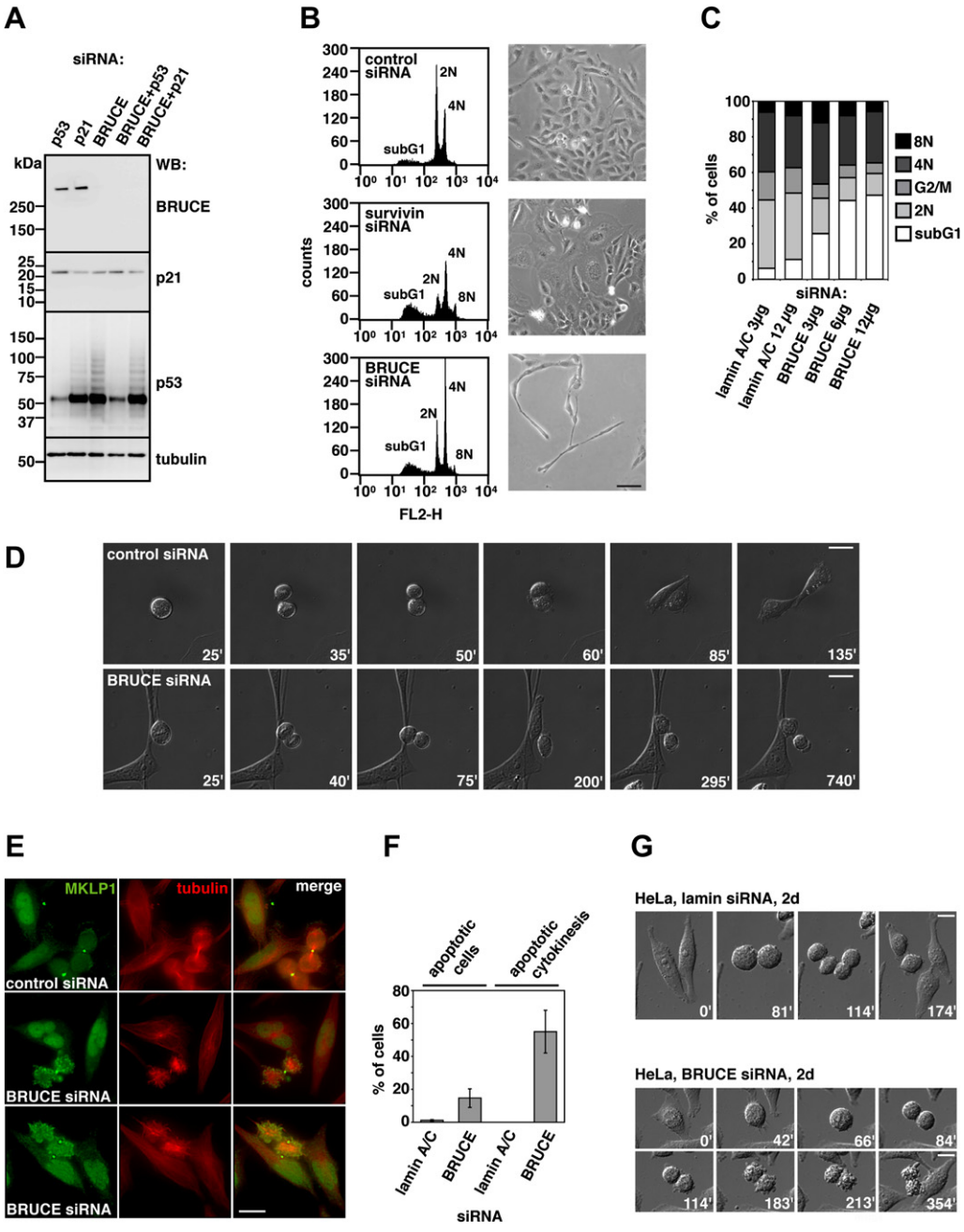

Figure 3. BRUCE Depletion Causes Cytokinesis Defects and Cytokinesis-Associated Apoptosis

(A) BRUCE depletion in U2OS cells has only minor consequences for p53 levels. Lysates of cells transfected with the indicated siRNAs were analyzed by western blots with the indicated antibodies.

(B) BRUCE depletion in U2OS cells induces syncytia-like structures. Cells were treated with siRNAs for 3 days as shown in Figure 1C targeting lamin A/C, survivin, or BRUCE. After 3 days of incubation, a representative area of cells was photographed (scale bar represents 20 μm), cells were harvested and prepared for propidium iodide staining, and the DNA content of cells was analyzed by flow cytometry. The 4N peak is marked by an arrow.

(C) Cell cycle distribution after treatment with increasing concentrations of siRNA. Cells were treated with siRNA as in (A). The graph represents the cell cycle distribution as obtained by flow cytometry of the DNA content.

(D) Defective cytokinesis after BRUCE depletion. siRNA-treated U2OS cells were observed by differential interference contrast (DIC) microscopy. The images represent stills of movies at representative time points. The scale bar represents 20 μm.

(E) HeLa cells depleted of BRUCE undergo cytokinesis-associated apoptosis. HeLa cells were treated with siRNAs for 2 days as in (A), fixed, and stained with anti-MKLP1 (green) and anti-α-tubulin (red). The scale bar represents 15 μm.

(F) Quantification of (E) with apoptotic cells relative to total cells and apoptotic cytokinesis versus total cells in cytokinesis (error bars represent ± SD of two independent experiments).

other once the midbody ring has been assembled in telophase (Movies S1 and S2), which differs from the otherwise mobile behavior of these vesicles during interphase. This finding considerably substantiates the idea that midbody rings, in addition to acting as the site for membrane delivery, may play a role as a diffusion barrier in-between the two prospective daughter cells (Schmidt and Nichols, 2004). Apparently, this barrier does not only prevent intercellular exchange of plasma membrane-associated material as shown before (Schmidt and Nichols, 2004), but also of endosomal vesicles.

BRUCE Harbors a Midbody Ring-Targeting Domain

The distinctive and dynamic localization of BRUCE suggested the presence of dedicated targeting domains. By using truncation constructs we in fact noticed that the typical localization of BRUCE at sorting compartments requires its C-terminal region (Figure S4F). Surprisingly, when we constructed a GFP-fusion of the C-terminal 145 amino acids of BRUCE (termed BRUCE-C), this construct localized exclusively to the midbody ring (Figures 2H and 2I and Movie S3 and S4). Time-lapse video microscopy revealed that the BRUCE-C-labeled ring-like structure showed a degree of mobility and tilting characteristic for the midbody ring, and that it was taken up by one of the daughter cells after abscission (Figure 2H and Movie S5). As the localization of endogenous BRUCE to the midbody ring depends on MKLP1 (Figure 1C), we speculated that BRUCE-C might contain a specific interaction domain with midbody ring components. Indeed, we found MKLP1 coprecipitating with full-length, endogenous BRUCE (Figure 2J, top panel) and also with BRUCE-C (Figure 2J, middle panel). Interestingly, BRUCE-C selectively bound the faster migrating variant, MKLP1, but not CHO1, a larger variant caused by alternative splicing that additionally possesses an actin-interacting tail (Figure 2J, lower panel). As both isoforms are present at the midbody (Kuriyama et al., 2002), this finding argues for different functions of these two variants during late stages of cytokinesis. Notably, the C-terminal tail of BRUCE (BRUCE-C) is highly conserved from flies to vertebrates, suggesting that the identified midbody ring-targeting domain (MTD) and the interaction with MKLP1 are features of all BRUCE family members.

BRUCE Depletion Causes Defective Abscission and Cytokinesis-Associated Apoptosis

Depleting BRUCE from cultured cells was previously shown to reduce cell viability (Ren et al., 2005). To identify the basis of this phenotype, we designed different siRNAs targeting BRUCE (see Supplemental Experimental Procedures and Figure S5). Delivery of BRUCE-targeted siRNA by electroporation in U2OS cells depleted BRUCE to undetectable levels 3 days after transfection (Figure 3A). These cells acquired a striking elongated appearance and built up interconnected cells, but in contrast to survivin depletion, no cells with giant nuclei developed (Figure 3B and Figure S1C). Moreover, reminiscent of centriolin depletion (Gromley et al., 2003), some apparently not completely detached cells fused again together or underwent mitosis (data not shown and see below). Higher siRNA concentrations and longer incubation times resulted in a decrease in the amount of normal G1 phase (2N) cells (Figure 3C and data not shown) but a strong rise of a sub-G1 population, indicative of syncytia-like cells, which finally undergo apoptosis. However, different from the results by Ren and coworkers (Ren et al., 2005), no rise in the levels of p53 or of p53 targets like p21 were observed (Figure 3A), suggesting that apoptosis in these cells is not an immediate response to BRUCE depletion but a later corollary. Live-cell video microscopy showed that BRUCE-depleted cells form a normal cleavage furrow, but do not complete cytokinesis even after hours, and that some cells even did not regain their normal flattened appearance (Figure 3D). When we depleted BRUCE in HeLa cells, cells underwent apoptosis, but, intriguingly, only during attempted cytokinesis (Figures 3E–3G). After the formation of the midbody ring, almost 60% of the cells were apoptotic (Figure 3F), and membrane blebbing occurred already 30 min after furrowing (Figure 3G). This suggests a mechanism by which apoptosis is triggered by cues that originate at the midbody in the absence of BRUCE.

BRUCE Is Involved in Membrane Delivery to the Midbody Ring

Because BRUCE-C binds to the midbody ring so well, we wondered whether we could utilize it as a dominant-negative tool specifically to monitor the function of BRUCE at this location. Indeed, overexpression of BRUCE-C could displace endogenous BRUCE from MKLP1 and the midbody ring (Figure 4A) and led to aberrant cytokinesis and binucleation (Figures 4B and 4C). Notably, after prolonged expression of BRUCE-C for 3 days, apoptosis occurred (Figure S6), indicating that the apoptotic signal is in fact triggered by the absence of BRUCE from the midbody ring. When we analyzed HeLa cells that stably express tagged albumin, we found secretory vesicles within the intercellular bridge. Intriguingly, however, cells overexpressing BRUCE-C showed single balloon-like accumulations of cargo-containing vesicles in close proximity to the intercellular bridge, but only on one of its sides (Figure 4B). From these findings we conclude that the presence of BRUCE at the midbody is needed for normal delivery of vesicles to the site of abscission and that prolonged absence of BRUCE interferes with cytokinesis.

To corroborate BRUCE's role in vesicle traffic, we next addressed in U2OS cells that stably express GFP-Rab11 whether also siRNA-directed BRUCE depletion interferes with normal membrane targeting. When we examined control cells (transfected with a control siRNA) that had just completed cytokinesis (Figure 4D, upper panel), Rab11 had already adopted typical interphase localization and phosphotyrosine was found on the midbody as reported (Kasahara et al., 2007). In striking contrast, BRUCE-depleted cells accumulated Rab11-endosomes, as well as phosphotyrosine-positive material, in close proximity to one side of the midbody (Figure 4D, lower panel). This finding confirms our conclusion that BRUCE is needed for the targeting of vesicles to the midbody, and further suggests that BRUCE is

(G) Stills with DIC live-cell microscopy of HeLa cells treated with lamin siRNA (top) or BRUCE siRNA (bottom) for 2 days. Note that cells depleted for BRUCE undergo apoptosis after attempted cytokinesis. The scale bar represents 15 μm.

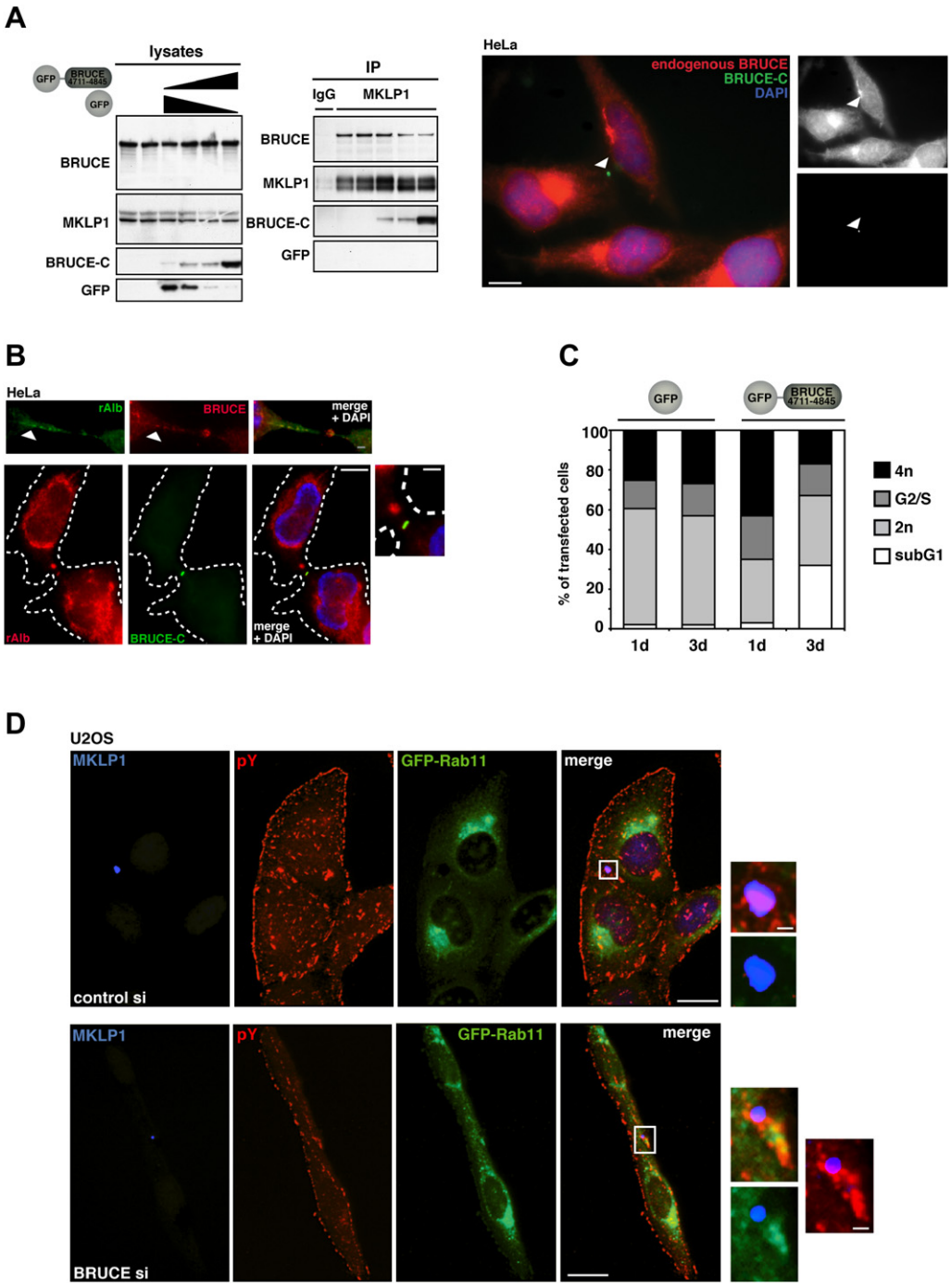

Figure 4. BRUCE Functions in Membrane Delivery to the Midbody Ring

(A) Exogenously expressed BRUCE fragment containing the midbody ring-targeting domain competes with endogenous BRUCE for midbody ring binding via MKLP1. HEK293T cells were transfected with increasing amounts of GFP-BRUCE-C and decreasing amounts of GFP. Lysates (inputs are shown in the left panel) were subjected to immunoprecipitation (IP) with rabbit IgGs (control) or anti-MKLP-1 antibodies, and precipitated proteins were analyzed by western blots. Competition on the single-cell level is shown for HeLa cells by immunofluorescence (endogenous, full-length BRUCE, red; GFP-BRUCE-C, green; DNA stained with DAPI). The arrowhead marks the midbody ring. The scale bar represents 10 μm.

(B) Expression of BRUCE-C leads to secretory vesicle accumulation in close vicinity to the midbody ring. Top: enlarged midbody region of a HeLa cell stably expressing albumin (green; cells as in Figure 1E) and stained for endogenous BRUCE (red). Bottom: similar to above, but cells were transfected with GFP-BRUCE-C (green), fixed, and stained. A representative cell in cytokinesis is shown with the enlarged midbody region on the right. The scale bar represents 10 μm; scale bar of clippings represents 2 μm.

crucial for the presence of tyrosine kinases at the midbody as well. Both functions might be linked, however, as sorting of Src and ERK to the midbody seems to depend on Rab11 (Kasahara et al., 2007).

Midbodies and Midbody Rings Are Platforms for Ubiquitylation

Since BRUCE possesses ubiquitin ligase activity (Bartke et al., 2004; Hauser et al., 1998), we next asked whether the midbody ring might be a site of ubiquitylation. Contrary to the current belief (Pines and Lindon, 2005), we could observe a dramatic relocalization of ubiquitin during cytokinesis (Figure 5A and Movie S6) using a cell line that stably expresses a GFP-ubiquitin fusion protein that can form conjugates in vivo (Dantuma et al., 2006). Parallel to the formation of the midbody ring in late telophase, ubiquitin is first concentrated on midzone microtubules but not on the midbody ring. However, once the microtubules start to constrict to form the midbody, the bulk of ubiquitin vanishes rapidly from this area, but after a brief period of absence, reappears concentrated on the midbody ring.

Motivated by this so far unrecognized behavior of ubiquitin, we performed fluorescent recovery after photobleaching (FRAP) experiments with U2OS cells to address the dynamics of this unusual process. In contrast to normal ubiquitin pools in the same cell in the cytosol or on midbody microtubules, ubiquitin on the midbody ring during cytokinesis showed a vastly reduced recovery (Figure 5B, left panels). Moreover, also midbody rings that had already been taken up by one daughter after completed cytokinesis showed virtually no recovery (Figure 5B, right panels). This suggests that ubiquitin has a high turnover at the midbody through active ubiquitylation and deubiquitylation of proteins near the midbody microtubules. In striking contrast, ubiquitin on midbody ring components, once this modification had occurred, can barely be replaced, suggesting that the local ubiquitylation activity is turned off at this stage. Notably, BRUCE and ubiquitin are closely associated during cell division and colocalize at the midbody ring during late cytokinesis (Figure 5C), suggesting that at least some of the detected ubiquitylation may be mediated by BRUCE (see Discussion).

Relocalization of ubiquitin during cytokinesis was similar in HeLa cells (Figure 5D, top panel), and cells of both cell lines often harbored besides the midbody ring engaged in cytokinesis one or rarely two additional rings, which most likely represent remnants from previous divisions. Intriguingly, only the putative active midbody ring in the intercellular bridge was decorated with ubiquitin whereas the midbody ring remnants had apparently gradually lost the modification (Figure 5D, lower panel). This finding is in agreement with our FRAP data (Figure 5B), showing that ubiquitylation of the midbody ring occurs only once during cytokinesis, before the onset of abscission.

BRUCE is known to homooligomerize (Bartke et al., 2004) and seems to associate in part with the deubiquitylating enzyme UBPY (alias USP8) and the RING-finger ubiquitin ligase Nrdp1 (alias FLRF) (Wu et al., 2004). We therefore asked whether deubiquitylating activity might influence midbody localized ubiquitin as well. By using a catalytically inactive form of UBPY ($UBPY^{C>A}$) that serves as a substrate trap (Alwan and van Leeuwen, 2007), we observed that it bound both BRUCE and MKLP1 (Figure 5E). Intriguingly, also $UBPY^{C>A}$ localizes to the midbody ring (Figure S7), suggesting that ubiquitylation and deubiquitylation activities may perhaps work as a switchboard at this site. BRUCE itself is ubiquitylated at its C-terminal domain (data not shown) and this modification is enhanced upon Nrdp1 overexpression, and conversely lost when UBPY is overexpressed (Figure 5F). Using a denaturing purification protocol that preserves ubiquitin modifications we also found that MKLP1 is modified by mono-/oligo- but not poly-ubiquitylation, and that this modification is strongly reduced if UBPY was overexpressed (Figure 5G). While BRUCE overexpression triggered no increase in MKLP1 ubiquitylation (data not shown), overexpression of the dominant-negative $UBPY^{C>A}$ version induced this modification (Figure 5G), suggesting that another ubiquitin ligase acts on MKLP1, or that deubiquitylation rather than ubiquitylation activity might be limiting and important for regulation. In fact, more than 30% of HeLa cells transfected with $UBPY^{C>A}$ exhibited cytokinesis defects linked with binucleation and mislocalized MKLP1 from its normal interphase localization in the nucleus to the cytoplasm (Figure 5H). This phenotype is reminiscent of an MKLP1 knockdown, suggesting that perhaps UBPY-mediated deubiquitylation of MKLP1 may trigger nuclear import, which appears to be needed for normal cytokinesis (Liu and Erikson, 2007).

BRUCE Is Crucial for Midbody Integrity, Midbody Ring Formation, and Midbody-Localized Ubiquitin

Prompted by the striking physical and functional connection of BRUCE with the midbody and the midbody ring, we next asked whether BRUCE itself is crucial for the organization of these structures. Indeed, we observed significantly reduced MKLP1-positive midbody material in BRUCE-depleted cells (Figure 6A and see also Figure 4D). Additionally, we detected a gradual effect on the midbody structure upon continued BRUCE depletion. Depletion for no more than three days led to moderately misorganized midbodies with unfocused Aurora B staining (Figure 6B, top panel) and unconstricted microtubules (Figure 6C, top panel). However, BRUCE depletion for five days resulted in syncytia-like cells, which contained severely malformed midbodies, as visualized by Aurora B or MKLP1 staining (Figures 6B and 6C lower panels). In the end, most cells failed to form their midbody rings altogether and no remnants persisted, and those few cells that retained their midbody rings (less than 10%), had hitherto not adopted a syncytia-like appearance (Figures 6D and 6E). We also explored whether BRUCE depletion affects the distribution of ubiquitin at the midbody.

(C) Prolonged expression of BRUCE-C leads to binucleation and apoptosis. HeLa cells were transfected either with GFP or GFP-BRUCE-C, stained with propidium iodide 1 and 3 days after transfection and DNA content was analyzed by flow cytometry gating for transfected cells.

(D) Recycling endosomes accumulate close to the midbody ring in BRUCE-depleted cells. U2OS cells stably expressing GFP-Rab11 (green) were treated with siRNAs as in Figure 1C fixed and stained for MKLP1 (blue) and phosphotyrosine (pY, red) with enlarged views of the midbody ring on the right. The scale bar represents 15 μm; scale bar of clippings represents 1 μm.

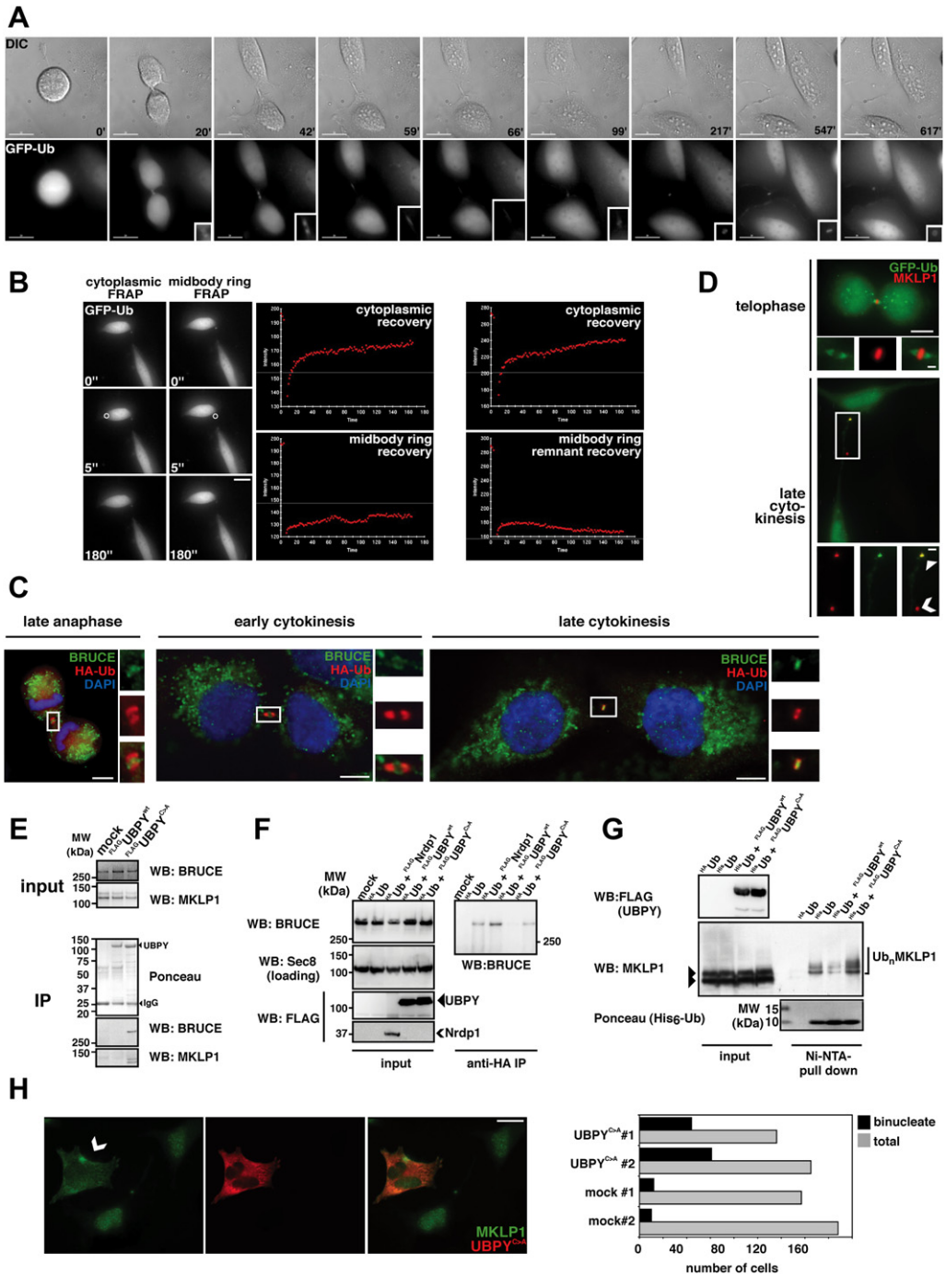

Figure 5. Ubiquitylation on the Midbody Ring

(A) Ubiquitin (Ub) is concentrated on midbody microtubules and reappears on the midbody ring after midbody constriction. U2OS cells stably expressing GFP-tagged ubiquitin (GFP-Ub) were analyzed by time-lapse video microscopy. A representative cell is shown with the movie stills (of Movie S6) starting in prometaphase and ending shortly before abscission. The scale bar represents 20 μm.

(B) Ubiquitin at the midbody ring shows almost no exchange with the cellular ubiquitin pool. U2OS cells as in (A) were used for FRAP experiments. Left: a cell with ubiquitin on the midbody ring was bleached in the cytoplasm or at the midbody ring. The recovery of the fluorescence signal is shown on the right. Right: a cell with a midbody ring remnant in the plane of the plasma membrane was either bleached in the cytoplasm or at the midbody ring remnant. Only fluorescence recovery curves are shown. The scale bar represents 20 μm.

(C) Association of BRUCE with ubiquitin at the midbody ring. U2OS cells were transiently transfected with HA-epitope tagged ubiquitin (HA-Ub, red). Cells were fixed and stained with anti-BRUCE (green) and DAPI (blue). The scale bar represents 10 μm. The framed areas are shown enlarged.

Indeed, in contrast to cells treated with a control siRNA (Figure 6F, upper panel, and Movie S7), cells depleted for BRUCE neither showed a distinct ubiquitin staining at midbody microtubules nor at the surviving midbody rings (Figure 6F, lower panel and Movie S8). These results suggest that BRUCE is not only crucial for normal vesicle targeting to the site of abscission, but also for the integrity of the midbody and the midbody ring, and its striking ubiquitin modification.

DISCUSSION

The two most perceptible processes of cytokinesis of animal cells, the contraction of the cleavage furrow and the physical separation of the daughter cells by abscission, are now recognized as two functionally and mechanistically different steps. Central to abscission is the midbody, which is the target site for membrane delivery and membrane fusion, the driving forces of abscission. In particular the unique midbody ring, located at the midpoint of the intercellular bridge, has drawn attention recently as it seems to be the key structural element that guides the events that lead to abscission. This rigid and unvaryingly sized structure, originally described by Flemming as "Zentralkörper" (Flemming, 1891), thus sometimes called "Flemming body," materializes in telophase and survives in one daughter cell often until the next division.

In this report, we identified BRUCE as a constant companion of the midbody ring and found that its normal assembly requires BRUCE. Moreover, we found that BRUCE is crucial for membrane delivery to the cleavage site and for normal abscission.

Membrane Dynamics

Recent studies have emphasized the decisive role of plasma membrane reorganization during abscission (Albertson et al., 2005). This process requires vesicle-mediated transport and the incorporation of additional membrane to the site of abscission by hetero- and homotypic membrane fusion events. As shown previously for (Rab11-positive) recycling endosomes, our data suggest that also (Rab8-positive) tubular endosomes significantly contribute to membrane dynamics during cytokinesis (Figure 2G). Previous studies suggested that membrane delivery to the midbody occurs largely asymmetric, i.e., only from one of the prospective daughter cells. However, when we monitored cargo delivery or endosomal sorting in unperturbed U2OS cells (which may require more membrane reshaping than HeLa cells) we failed to detect any marked asymmetry of membrane delivery to the intercellular bridge. However, upon interfering with BRUCE function by either BRUCE depletion or overexpression of the dominant-negative BRUCE-C variant (that does not bind the exocyst or Rab8/11 GTPases) cells strikingly accumulated large vesicular structures close to only one side of the midbody ring. Thus abscission has indeed an intrinsic asymmetric contribution, and BRUCE appears to be crucial for normal vesicle targeting. In fact, BRUCE seems well equipped to function as a midbody targeting factor for vesicles as it binds via its N-terminal region to the exocyst and endosomal components and via its C-terminal targeting domain to the midbody ring.

BRUCE and the Midbody Ring

Our studies suggest an intimate relationship between BRUCE and the midbody ring. In interphase cells, BRUCE localizes to the TGN and endosomes, but during cytokinesis, a fraction moves to the midzone where it specifically arrives at the midbody ring. Notably, BRUCE associates with the midbody ring concomitantly with its appearance in telophase, travels after completed abscission with the midbody ring into one daughter cell, and remains bound to the discarded midbody ring all along until a new ring is formed during the next cell division (Figure 1A and 5D). Most importantly, BRUCE depletion prevents normal midbody ring formation, suggesting that its activity may indeed be required for proper ring assembly.

The midbody ring appears to mediate at least two functions. First, it seems to play a role as the docking site for vesicles, which supply the plasma membrane with new material at the site of abscission. As detailed above, BRUCE is crucial for this process. Second, perhaps similar to the septin ring of yeast (Faty et al., 2002), the midbody ring seems to function as a diffusion barrier. Previous studies indicated that the midbody ring prevents plasma membrane diffusion across the intercellular bridge (Schmidt and Nichols, 2004). Our FRAP experiments extend these findings as they indicate that also Rab8-endosomes are unable to transverse the ring from one prospective daughter cell to the other. Therefore, the midbody ring may represent the first physical barrier that disunites the daughter cells. As observed before (Gromley et al., 2005), perhaps fueled by asymmetric membrane delivery, the midbody ring is pushed to one daughter cell where it is eventually dissolved. As BRUCE follows the same path, even the final fate of the midbody ring appears to be allied with BRUCE.

(D) Ubiquitin is lost from midbody ring remnants when cells acquired an active midbody ring. HeLa cells were transfected with GFP-Ub (green). Top panels show fixed cells in telophase with anti-MKLP1 staining (red). Lower panels show a cell in late cytokinesis with a putative active midbody ring and a remnant, both lying in the intercellular bridge. Note that the midbody ring remnant (open arrowhead) is not labeled with ubiquitin. The scale bar represents 10 μm and 2 μm (for enlarged areas).

(E) Both BRUCE and MKLP1 interact with UBPY. HEK293T cells were transfected with empty vector or FLAG-epitope tagged UBPY and its catalytically inactive mutant (C > A). Cells were lysed and proteins were immunoprecipitated (IP) with anti-FLAG and analyzed by western blots (WB).

(F) BRUCE is deubiquitylated by UBPY. HEK293T cells were transfected with empty vector and HA-tagged ubiquitin (^{HA}Ub) in combination with FLAG-tagged UBPY wild-type and mutant proteins (^{FLAG}UBPY, ^{FLAG}UBPY$^{(C > A)}$) and FLAG-tagged Nrdp1 (^{FLAG}Nrdp1). Lysates were prepared and subjected to anti-HA immunoprecipitation, and both lysates (Input) and immunoprecipitated material (IP) were analyzed by western blots (WB).

(G) MKLP1 is ubiquitylated in cells and is deubiquitylated by UBPY. HEK293T cells were transfected with ^{HA}Ub or His_6-epitope tagged ubiquitin (His6-Ub) in combination with ^{FLAG}UBPY and ^{FLAG}UBPY$^{(C > A)}$. Lysates were subjected to denaturing Ni-NTA pull down and analyzed by western blots (WB).

(H) Overexpression of catalytically inactive UBPY leads to MKLP1 mislocalization and binucleation of cells. HeLa cells were transfected with empty vector (mock) or ^{FLAG}UBPY$^{(C > A)}$. Left: cells were fixed and stained with anti-MKLP1 (green) and anti-FLAG (red) antibodies. The open arrowhead marks a transfected cell. The scale bar represents 15 μm. Right: quantification of binucleate versus total cells (two independent experiments labeled #1 and #2, respectively).

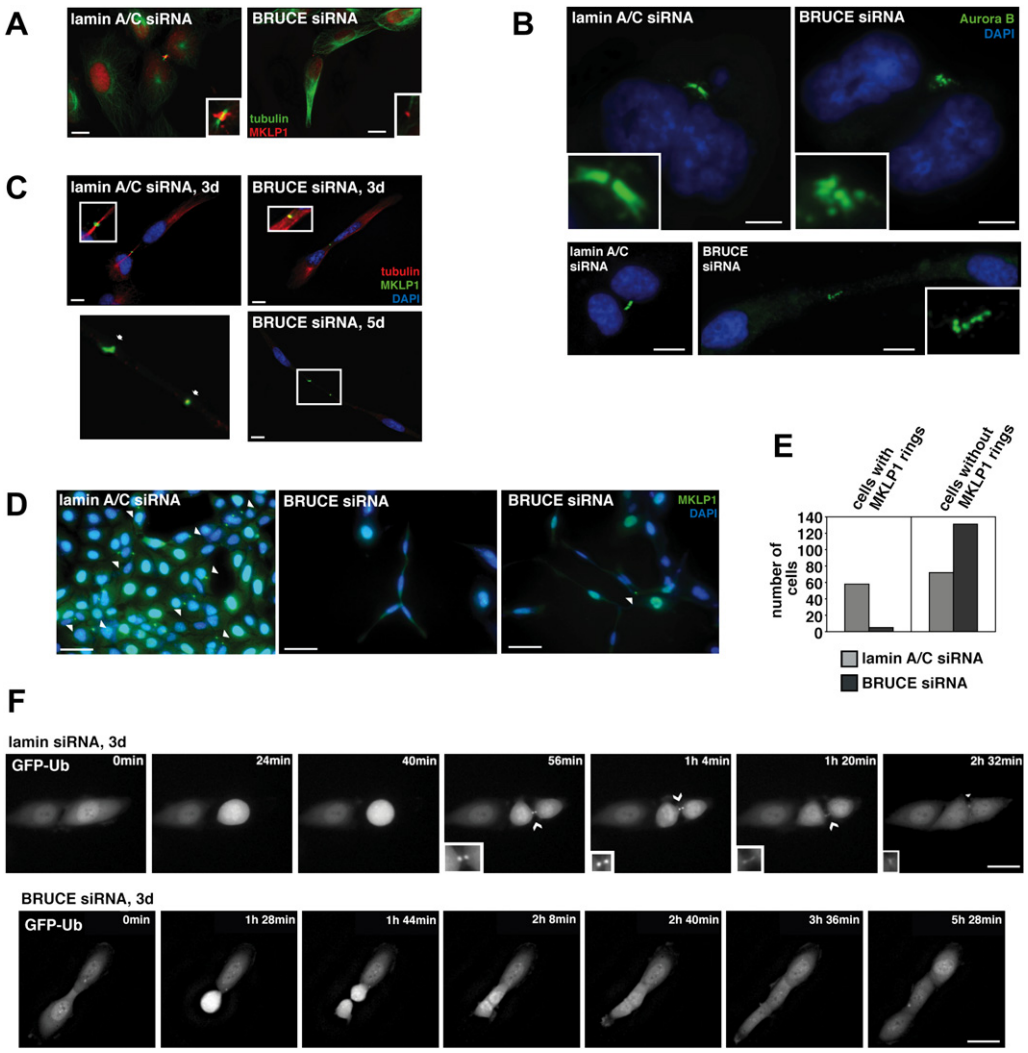

Figure 6. BRUCE Depletion Causes Structural Aberrations of the Midbody and Ubiquitin Mislocalization

(A) Reduced midbody material after BRUCE depletion as revealed by MKLP1 staining. U2OS cells were treated with siRNAs targeting lamin A/C or BRUCE as in Figure 1B. After 3 days, cells were fixed and stained with anti-α-tubulin (green) or anti-MKLP1 (red) antibodies. The scale bar represents 15 μm.

(B) Misorganization and rupture of the midbody after BRUCE depletion. U2OS cells were treated with siRNAs as in (A). Cells were fixed after 3 days and stained with anti-Aurora B (green) antibodies and DAPI. Top: BRUCE-depleted cells that have hitherto not acquired an elongated appearance exhibit aberrant midbodies (shown enlarged in insets) (scale bar ≅ 15 μm). Bottom: BRUCE-depleted cells that resemble syncytia contain fragmented Aurora B-positive material. The scale bar represents 20 μm.

(C) Midbody ring rupture in BRUCE-depleted cells as indicated by MKLP1 localization. The experiment was performed as in (B), and cells were fixed either after 3 or 5 days, stained for MKLP1 (green), α-tubulin (red), or DNA with DAPI (blue). After 5 days of siRNA treatment, syncytial cells arose with aberrant midbody rings (arrowheads). The scale bar represents 10 μm.

(D) Growth retardation and loss of midbody rings after BRUCE depletion. Experiment was performed as in (B); cells were fixed after 5 days and stained with anti-MKLP1 (green) and DAPI. Arrowheads point to MKLP1-stained midbody rings.

(E) Quantification of (D). The scale bar represents 30 μm.

(F) Concentration of ubiquitin at the midbody is lost in BRUCE-depleted cells. U2OS cells stably expressing GFP-Ub (see Figure 5A) were analyzed by time-lapse video microscopy. Stills are from Movie S8. The scale bar represents 15 μm.

BRUCE Is Crucial for Faithful Cell Division

A further consequence of BRUCE depletion is the appearance of syncytial cells and sometimes a reunion followed by mitosis of apparently incompletely separated cells (Movie S8). Syncytial cells also form upon centriolin depletion (Gromley et al., 2005), suggesting that perhaps BRUCE and centriolin, a protein of unknown biochemical activity, fulfill related or coupled functions in cytokinesis. Although *BRUCE*$^{-/-}$ embryos survive embryogenesis and usually die only shortly before birth, we also noticed a delay in cell cycle progression of mouse embryonic fibroblasts (MEFs) isolated from *BRUCE*$^{-/-}$ embryos (Lotz et al., 2004) and aberrant divisions characterized by multipolar spindles

and tripolar cytokinesis in spontaneously immortalized *BRUCE*$^{-/-}$ MEFs (unpublished data). This suggests that cells may adapt to a loss of BRUCE activity, however, with the predisposition (perhaps depending on the cell type) of erroneous cell divisions. Intriguingly, BRUCE depletion in HeLa cells induces apoptosis precisely at the time of attempted abscission (Figure 3G). Since we also observed apoptosis upon prolonged expression of BRUCE-C, which displaces endogenous BRUCE from the midbody ring (Figure S6D), the apoptotic cue seems to materialize specifically when BRUCE is absent from this structure. As BRUCE possesses antiapoptotic activity and binds caspases (Bartke et al., 2004), it seems reasonable to assume that the observed cell death may be a direct consequence of the lack of BRUCE activity at the midbody ring. Notably, BRUCE also physically associates with survivin, which also localizes to the midbody, and BRUCE is able to ubiquitylate this BIRP in vitro (Figure S3 and data not shown). It thus seems attractive to speculate that perhaps BRUCE and survivin normally collaborate, and that BRUCE depletion alters the local antiapoptotic activity with possible consequences for caspase activation (O'Connor et al., 2000).

Ubiquitin Dynamics During Cytokinesis

In this study we discovered a unique and highly dynamic localization pattern of ubiquitin conjugates at the midbody during cytokinesis. At the time when the actomyosin ring has maximally constricted, ubiquitin is unusually concentrated in two large foci symmetrically localized near both plus-end tips of midbody microtubules (Figure 5A). This almost compartmentalized compaction may be indicative of a concentration of ubiquitylation/deubiquitylation activities and extensive protein turnover at these sites. It seems attractive to speculate that substrates may include mitotic regulators or components of the vesicular sorting machinery. Strikingly, in the succeeding 15–30 min interval, ubiquitin disappeared from the midbody to undetectable levels, but reappears firmly associated with the midbody ring. Ubiquitylation of the midbody ring seems to occur only once during cytokinesis and appears to be stable until abscission is completed, as indicated by our photobleaching experiments. Furthermore, this modification appears to be largely mono-ubiquitin as indicated by the fact that conjugates of GFP-ubiquitin, in which the ubiquitin domain lacks lysine residues (GFP-ubiquitin-K_0), enriched normally at the midbody ring but not at the midbody flanks (Figure S8). Together these data suggest that midbody ring (mono) ubiquitylation may serve structural or regulatory functions rather than promoting proteasomal proteolysis.

As BRUCE is tightly connected to the midbody ring and required for its integrity, it seems reasonable to speculate that its ubiquitin ligase activity may contribute to these ubiquitylation events. However, ubiquitylation is also required for protein sorting via the ESCRT pathway, which plays a role in cytokinesis (Carlton and Martin-Serrano, 2007; Morita et al., 2007). In fact, the BRUCE-associated deubiquitylating enzyme UBPY harbors a so-called MIT-domain that mediates association with proteins of the ESCRTIII complex (Row et al., 2007). Moreover, disassembly of the ESCRTIII complex is thought to be catalyzed by Vps4, an AAA-ATPase that seems to play a crucial role at late stages of cytokinesis (Morita et al., 2007). Whatever the crucial ubiquitylation targets are, the unique combination of multiple activities in a single large protein suggests that BRUCE may coordinate cytokinesis events perhaps in a stepwise fashion. Strikingly, after completed cytokinesis, midbody ring-localized BRUCE is discarded into only one of the two daughter cells as well, possibly representing the final manifestation of the apparent built-in asymmetry of cytokinesis.

EXPERIMENTAL PROCEDURES

Plasmids and siRNA

Cloning of *BRUCE* and engineering of mutants and truncations was described previously (Bartke et al., 2004; Hauser et al., 1998). *BRUCE* cDNAs were expressed from pCI (Promega) or *pCMV2* vectors (Stratagene) as was FLAG-tagged cDNA of luciferase. GFP-BRUCE-C (amino acids 4711–4845) was cloned into pEGFP-CI (Clontech) using an internal *Xho*I site (bp 14135). Nrdp1 was amplified from HeLa mRNA using primers that generate an N-terminal FLAG-epitope tag and cloned into pCI. GFP-Rab8 was a gift of J. Peränen, GFP-Rab11 was obtained from M. Zerial, GFP-ubiquitin and GFP-ubiquitin-K_0 were gifts of N. Dantuma, HA-epitope-tagged rat albumin was a gift of D. LeBel and FLAG-epitope-tagged UBPY and its mutant were from H. Alwan.

Antibodies

A detailed list of antibodies can be found in the Supplemental Experimental Procedures.

Cell Culture and Transfections

U2OS, HeLa, and HEK293T cells were maintained at 37°C, 7.5% CO_2 in DMEM (SIGMA) supplemented with 10% FCS. Transient transfections were performed in 10 cm dishes (293T) or 6-well plates (HeLa) using calcium phosphate or lipofection protocols, as described previously (Bartke et al., 2004). U2OS cells were transfected by electroporation using AMAXA Nucleofector kit according to the manufacturer's recommendations. siRNA duplexes were obtained from MWG and were transfected at a final concentration of 100 nM. siRNA sequences are listed in supplemental material and methods. HeLa cells stably expressing HA-rAlb and U2OS cells stably expressing GFP-Rab8, GFP-Rab11 and GFP-ubiquitin were generated by selecting cells with 750 μg/ml G418 (SIGMA) after lipofection for 3–4 weeks.

Flow Cytometry

DNA histograms were obtained by flow cytometry of PI-stained ethanol-fixed cells using standard protocols, a FACSCalibur system and CELLQuest analysis software (Becton Dickinson).

Coimmunoprecipitations and Immunoblot Analysis

Immunoprecipitations, purification of FLAG-fusion proteins, and immunoblot analysis were carried out as described previously (Bartke et al., 2004).

Denaturating Ni-NTA Pull-Down

Transiently transfected HEK293T cells were harvested and pellets were washed once in PBS. Cells were lysed in 6 M guanidine-HCl, 0.1M NaH_2PO_4, 0.1% Tween-20, 0.01M Tris (pH 8.0). Lysates were briefly sonicated to shear DNA. An aliquot of the lysate was kept for TCA precipitation. The remaining lysate was incubated with Ni-NTA agarose beads (QIAGEN) for 3–5 hr. Beads were washed 5 times with 8 M urea, 0.1 M NaH_2PO_4, 0,1% Tween-20, 0.01M Tris (pH 8.0), and twice with PBS, 0.01% Tween-20. TCA precipitates and beads were boiled in loading buffer and subjected to SDS-PAGE and immunoblotting.

Immunofluorescence and Live-Cell Microscopy

Immunofluorescence was performed according to standard protocols after fixation in methanol (−20°C, 3 min). Images were acquired on a Leica DM RXA microscope equipped with a Hamatsu ORCA-ER camera. Image acquisition and deconvolution of images was carried out using Openlab software. For fluorescence live-cell video microscopy and photobleaching experiments,

U2OS cells were cultured in 35 mm μ-dishes with No. 1.5 bottom (Integrated BioDiagnostics). Confocal laser scanning microscopy was performed with a Leica TCS SP2 confocal scanning microscope. Live-cell video microscopy and FRAP were carried out on an AppliedPrecision DeltaVision RT system equipped with a quantifiable laser module. After photobleaching of the GFP fluorescence with 25%–50% laser intensity, images were obtained every second during a time frame of 3 min. Fluorescence intensities were measured and quantified and images processed using SoftWorx software (AppliedPrecision). For live-cell video microscopy, DIC or phase and fluorescence images were taken every 1–5 min over a time frame of 10–48 hr.

SUPPLEMENTAL DATA

Supplemental Data include Supplemental Experimental Procedures, Supplemental References, eight figures, and eight movies and can be found with this article online at http://www.cell.com/cgi/content/full/132/5/832/DC1/.

ACKNOWLEDGMENTS

We thank U. Cramer for technical assistance; T. Bartke, S. Mishra, and O. Stemmann for advice and comments on the manuscript; H. Alwan, N. Dantuma, D. LeBel, J. Peränen, and M. Zerial for materials. This work is supported (to S.J.) by the Max Planck Society, Munich Center of Integrated Protein Science, Rubicon EU Network of Excellence, and Fonds der Chemischen Industrie.

Received: October 9, 2007
Revised: December 17, 2007
Accepted: January 8, 2008
Published: March 6, 2008

REFERENCES

Albertson, R., Riggs, B., and Sullivan, W. (2005). Membrane traffic: a driving force in cytokinesis. Trends Cell Biol. *15*, 92–101.

Alwan, H.A., and van Leeuwen, J.E. (2007). UBPY-mediated epidermal growth factor receptor (EGFR) de-ubiquitination promotes EGFR degradation. J. Biol. Chem. *282*, 1658–1669.

Bartke, T., Pohl, C., Pyrowolakis, G., and Jentsch, S. (2004). Dual Role of BRUCE as an Antiapoptotic IAP and a Chimeric E2/E3 Ubiquitin Ligase. Mol. Cell *14*, 801–811.

Carlton, J.G., and Martin-Serrano, J. (2007). Parallels between cytokinesis and retroviral budding: a role for the ESCRT machinery. Science *316*, 1908–1912.

Dantuma, N.P., Groothuis, T.A., Salomons, F.A., and Neefjes, J. (2006). A dynamic ubiquitin equilibrium couples proteasomal activity to chromatin remodeling. J. Cell Biol. *173*, 19–26.

Eggert, U.S., Mitchison, T.J., and Field, C.M. (2006). Animal cytokinesis: from parts list to mechanisms. Annu. Rev. Biochem. *75*, 543–566.

Faty, M., Fink, M., and Barral, Y. (2002). Septins: a ring to part mother and daughter. Curr. Genet. *41*, 123–131.

Fielding, A.B., Schonteich, E., Matheson, J., Wilson, G., Yu, X., Hickson, G.R., Srivastava, S., Baldwin, S.A., Prekeris, R., and Gould, G.W. (2005). Rab11–FIP3 and FIP4 interact with Arf6 and the exocyst to control membrane traffic in cytokinesis. EMBO J. *24*, 3389–3399.

Flemming, W. (1891). Neue Beiträgezur Kenntnis der Zelle. Arc. Mikr. Anat. *37*, 685–751.

Grenfell, S.J., Trausch-Azar, J.S., Handley-Gearhart, P.M., Ciechanover, A., and Schwartz, A.L. (1994). Nuclear localization of the ubiquitin-activating enzyme, E1, is cell-cycle-dependent. Biochem. J. *300*, 701–708.

Gromley, A., Jurczyk, A., Sillibourne, J., Halilovic, E., Mogensen, M., Groisman, I., Blomberg, M., and Doxsey, S. (2003). A novel human protein of the maternal centriole is required for the final stages of cytokinesis and entry into S phase. J. Cell Biol. *161*, 535–545.

Gromley, A., Yeaman, C., Rosa, J., Redick, S., Chen, C.T., Mirabelle, S., Guha, M., Sillibourne, J., and Doxsey, S.J. (2005). Centriolin anchoring of exocyst and SNARE complexes at the midbody is required for secretory-vesicle-mediated abscission. Cell *123*, 75–87.

Hao, Y., Sekine, K., Kawabata, A., Nakamura, H., Ishioka, T., Ohata, H., Katayama, R., Hashimoto, C., Zhang, X., Noda, T., et al. (2004). Apollon ubiquitinates SMAC and caspase-9, and has an essential cytoprotection function. Nat. Cell Biol. *6*, 849–860.

Hauser, H.P., Bardroff, M., Pyrowolakis, G., and Jentsch, S. (1998). A giant ubiquitin-conjugating enzyme related to IAP apoptosis inhibitors. J. Cell Biol. *141*, 1415–1422.

Kasahara, K., Nakayama, Y., Nakazato, Y., Ikeda, K., Kuga, T., and Yamaguchi, N. (2007). Src signaling regulates completion of abscission in cytokinesis through ERK/MAPK activation at the midbody. J. Biol. Chem. *282*, 5327–5339.

Kuriyama, R., Gustus, C., Terada, Y., Uetake, Y., and Matuliene, J. (2002). CHO1, a mammalian kinesin-like protein, interacts with F-actin and is involved in the terminal phase of cytokinesis. J. Cell Biol. *156*, 783–790.

Li, F., Ackermann, E.J., Bennett, C.F., Rothermel, A.L., Plescia, J., Tognin, S., Villa, A., Marchisio, P.C., and Altieri, D.C. (1999). Pleiotropic cell-division defects and apoptosis induced by interference with survivin function. Nat. Cell Biol. *1*, 461–466.

Lindon, C., and Pines, J. (2004). Ordered proteolysis in anaphase inactivates Plk1 to contribute to proper mitotic exit in human cells. J. Cell Biol. *164*, 233–241.

Liu, X., and Erikson, R.L. (2007). The nuclear localization signal of mitotic kinesin-like protein Mklp-1: effect on Mklp-1 function during cytokinesis. Biochem. Biophys. Res. Commun. *353*, 960–964.

Lotz, K., Pyrowolakis, G., and Jentsch, S. (2004). BRUCE, a giant E2/E3 ubiquitin ligase and inhibitor of apoptosis protein of the trans-Golgi network, is required for normal placenta development and mouse survival. Mol. Cell. Biol. *24*, 9339–9350.

Matuliene, J., and Kuriyama, R. (2002). Kinesin-like protein CHO1 is required for the formation of midbody matrix and the completion of cytokinesis in mammalian cells. Mol. Biol. Cell *13*, 1832–1845.

Morita, E., Sandrin, V., Chung, H.Y., Morham, S.G., Gygi, S.P., Rodesch, C.K., and Sundquist, W.I. (2007). Human ESCRT and ALIX proteins interact with proteins of the midbody and function in cytokinesis. EMBO J. *26*, 4215–4227.

O'Connor, D.S., Grossman, D., Plescia, J., Li, F., Zhang, H., Villa, A., Tognin, S., Marchisio, P.C., and Altieri, D.C. (2000). Regulation of apoptosis at cell division by p34cdc2 phosphorylation of survivin. Proc. Natl. Acad. Sci. USA *97*, 13103–13107.

Pines, J., and Lindon, C. (2005). Proteolysis: anytime, any place, anywhere? Nat. Cell Biol. *7*, 731–735.

Potapova, T.A., Daum, J.R., Pittman, B.D., Hudson, J.R., Jones, T.N., Satinover, D.L., Stukenberg, P.T., and Gorbsky, G.J. (2006). The reversibility of mitotic exit in vertebrate cells. Nature *440*, 954–958.

Ren, J., Shi, M., Liu, R., Yang, Q.H., Johnson, T., Skarnes, W.C., and Du, C. (2005). The Birc6 (Bruce) gene regulates p53 and the mitochondrial pathway of apoptosis and is essential for mouse embryonic development. Proc. Natl. Acad. Sci. USA *102*, 565–570.

Row, P.E., Liu, H., Hayes, S., Welchman, R., Charalabous, P., Hofmann, K., Clague, M.J., Sanderson, C.M., and Urbe, S. (2007). The MIT domain of UBPY constitutes a CHMP binding and endosomal localisation signal required for efficient EGF receptor degradation. J. Biol. Chem. *282*, 30929–30937.

Samuel, T., Okada, K., Hyer, M., Welsh, K., Zapata, J.M., and Reed, J.C. (2005). cIAP1 Localizes to the nuclear compartment and modulates the cell cycle. Cancer Res. *65*, 210–218.

Schmidt, K., and Nichols, B.J. (2004). A barrier to lateral diffusion in the cleavage furrow of dividing mammalian cells. Curr. Biol. *14*, 1002–1006.

Straight, A.F., Cheung, A., Limouze, J., Chen, I., Westwood, N.J., Sellers, J.R., and Mitchison, T.J. (2003). Dissecting temporal and spatial control of cytokinesis with a myosin II Inhibitor. Science *299*, 1743–1747.

Sumara, I., Quadroni, M., Frei, C., Olma, M.H., Sumara, G., Ricci, R., and Peter, M. (2007). A Cul3-based E3 ligase removes Aurora B from mitotic chromosomes, regulating mitotic progression and completion of cytokinesis in human cells. Dev. Cell *12*, 887–900.

Vega, I.E., and Hsu, S.C. (2001). The exocyst complex associates with microtubules to mediate vesicle targeting and neurite outgrowth. J. Neurosci. *21*, 3839–3848.

Verhagen, A.M., Coulson, E.J., and Vaux, D.L. (2001). Inhibitor of apoptosis proteins and their relatives: IAPs and other BIRPs. Genome Biol. *2*, reviews3009.1–reviews3009.

Wojcik, C., Paweletz, N., and Schroeter, D. (1995). Localization of proteasomal antigens during different phases of the cell cycle in HeLa cells. Eur. J. Cell Biol. *68*, 191–198.

Wu, X., Yen, L., Irwin, L., Sweeney, C., and Carraway, K.L., 3rd. (2004). Stabilization of the E3 ubiquitin ligase Nrdp1 by the deubiquitinating enzyme USP8. Mol. Cell. Biol. *24*, 7748–7757.

Yu, X., Prekeris, R., and Gould, G.W. (2007). Role of endosomal Rab GTPases in cytokinesis. Eur. J. Cell Biol. *86*, 25–35.